PHYSIOLOGICALLY-BASED PHARMACOKINETICS IN CRITICALLY ILL CHILDREN

Kevin M. Watt

A dissertation submitted to the faculty of the University of North Carolina at Chapel Hill in partial fulfillment of the requirements for the degree of Doctor of Philosophy in the Department of Pharmaceutical Sciences in the UNC Eshelman School of Pharmacy

Chapel Hill
2016

Approved by:

Kim L.R. Brouwer

Dhiren Thakker

Julie Dumond

Michael Cohen-Wolkowiez

Daniel K. Benjamin, Jr.

ABSTRACT

Kevin M. Watt: Physiologically-based Pharmacokinetics in Critically Ill Children
(Under the direction of Kim L.R. Brouwer)

Extracorporeal membrane oxygenation (ECMO) is used to support cardiorespiratory failure in critically ill infants, children, and adults. In these vulnerable populations, the effect of ECMO on drug disposition leaves clinicians with uncertainty about dosing. The goal of this dissertation research was to develop a physiologically-based pharmacokinetic (PBPK) modeling approach that translated results from ex vivo ECMO studies to bedside dosing recommendations. To determine optimal dosing, the impact of the ECMO circuit on antifungal disposition was first assessed in isolation through *ex vivo* studies of three antifungal drugs. These experiments showed variable degrees of extraction by the ECMO circuit with micafungin highly extracted and fluconazole and amphotericin B deoxycholate with limited extraction. These results were then used to parameterize drug-specific ECMO compartments in the PBPK models. Model building followed an established workflow whereby a PBPK model was developed in adults and scaled to children. Once the Pediatric PBPK Model met acceptance criteria, an ECMO compartment was added to the Pediatric PBPK Model to form the ECMO PBPK Model. The fluconazole ECMO PBPK Model over-predicted exposure (1.13 fold error) but was within the pre-specified acceptance criteria of 0.7-1.3 fold error. PBPK-predicted

dosing recommendations showed good agreement with recommendations based on the Fluconazole ECMO PK Trial. The micafungin ECMO PBPK Model also over-predicted exposure (1.16 fold error), but, again, dosing recommendations were in close agreement with recommendations determined from the trial. The two clinical PK trials of fluconazole and micafungin in children on ECMO were performed in parallel with the PBPK model building. Both the Fluconazole and Micafungin ECMO PK Trials showed that exposure was significantly lower in children on ECMO compared to children not on ECMO. Although determining optimal dosing for these two commonly used drugs in children on ECMO was important, more importantly, the PBPK modeling developed in this dissertation demonstrated the utility of this approach to understand and quantify the physiologic alterations driving drug disposition in critically ill children. A more precise, refined, integrated approach for drug dosing in this pediatric sub-population will improve both the safety and efficacy of drug therapy in children supported with ECMO.

To my family, who enabled and provided guidance.

Thank you for your unwavering support and encouragement.

ACKNOWLEDGMENTS

I wish to acknowledge and thank all of my committee members (Drs. Kim Brouwer, Danny Benjamin, Dhiren Thakker, Julie Dumond, Jeff Barrett, and Micky Cohen-Wolkowiez) for providing me with guidance and support during my Ph.D. degree. I especially want to thank Dr. Brouwer for welcoming me into her lab, being enthusiastic about pediatric research, and tolerating my clinical schedule.

The PBPK modeling would not have been possible without the mentorship from Jeff Barrett, Andrea Edginton, Ping Zhao, and the folks at Bayer Technology Services, especially Tobias Kanacher, Martin Hobe, and Michael Sevestre. I especially want to single out Andrea Edginton for her help in developing the ECMO compartment and troubleshooting when the model did not work.

I want to thank the members of the Brouwer Lab, past and present, for their patience in explaining their interesting work and enthusiasm for ECMO: Nate Pfeifer, Brian Ferslew, Kyunghee Yang, Kathleen Köck, Jason Slizgi, Eleftheria Tsakalozou, Cen Guo, Izna Ali. I also need to acknowledge Arlo Brown, Kathy Maboll, and Anna Crollman for their help throughout.

Additionally I need to acknowledge many others that have taught me a great deal: Danny Gonzalez, Christoph Hornik, Dan Crona, Nicole Zane, Mary Paine, Heyward Hull, and Edmund Capparelli.

I wish to thank the Thrasher Research Fund for my Early Career Award and the NICHD at the National Institutes of Health for my Loan Repayment and K23 Career Development Awards.

Finally, I need to thank my family – Melissa, Jonah, and Sarah – for their patience and unwavering support. When I decided at age 39, while a pediatric critical care fellow, to pursue a PhD, Melissa told me I was crazy. While the jury is still out on that one, she has remained steadfast in her support even in the face of my busy clinical schedule, her own successful career, and the birth of our second child. I could not have done it without her.

TABLE OF CONTENTS

LIST OF TABLES

LIST OF FIGURES

LIST OF ABBREVIATIONS

AAG	Alpha-1-acid glycoprotein
ADME	Absorption, distribution, metabolism, elimination
AE	Adverse event
ALT	Alanine aminotransferase
AST	Aspartate aminotransferase
AUC	Area under the curve
C_{bc}	Concentration in blood cells
C_{in}	Concentration coming in
C_{last}	Last measured concentration
C_{max}	Maximum concentration
C_{min}	Minimum concentration
C_{out}	Concentration going out
C_{pls}	Concentration in plasma
CDH	Congenital diaphragmatic hernia
CHD	Congenital heart disease
CI	Confidence interval
CL	Clearance
CVVH	Continuous veno-venous hemofiltration
CVVHD	Continuous veno-venous hemodialysis
CYP	Cytochrome P450
ECMO	Extracorporeal membrane oxygenation
EDTA	Ethylenediaminetetraacetic acid
GFR	Glomerular filtration rate
Hct	Hematocrit

IDSA	Infectious Disease Society of America
IQR	Interquartile range
IV	Intravenous
k	Elimination rate constant
MecAsp	Meconium aspiration
MIC	Minimum inhibitory concentration
OATP	Organic anion-transporting polypeptide
OSF	Ontogeny scaling factor
PBPK	Physiologically-based pharmacokinetics
PD	Pharmacodynamics
PK	Pharmacokinetics
PNA	Postnatal age
PPHN	Persistent pulmonary hypertension
Q	Flow
SCR	Serum creatinine
t½	Half-life
T_{last}	Time at last measurement
t_{MIC}	Time above minimum inhibitory concentration
UGT	UDP-Glucuronosyltransferase
V	Volume of distribution
VA	Venoarterial
VPC	Visual predictive check
VV	Venovenous

CHAPTER 1. INTRODUCTION: ALTERED PHARMACOKINETICS DUE TO EXTRACORPOREAL LIFE SUPPORT

Extracorporeal membrane oxygenation (ECMO) is life-saving in patients with cardiorespiratory failure. ECMO is a cardiopulmonary bypass device that provides complete respiratory and cardiac support (Figure 1.1). Mechanically, blood is drained from the venous system, pumped through an artificial lung membrane, and then returned to either the venous or arterial circulation. ECMO was first used successfully in 1972 to support an adult with respiratory failure and three years later was used successfully in an infant.[1,2] Early controlled studies showed a clear mortality benefit in infants with respiratory failure, and ECMO is now standard of care in this population.[3-5] However, early trials of ECMO in adults showed no survival benefit over standard of care, and use in adults was limited until 2009.[6,7] In 2009, ECMO was used successfully as rescue therapy for adults with H1N1 influenza.[8,9] Multiple observational studies showed improved survival associated with ECMO support, and adult ECMO programs were scaled up worldwide.[10-16] While pediatric ECMO support has remained steady with ~2000 cases per year, ECMO use in adults has increased from <500 cases in 2008 to nearly 3000 cases in 2014.[17]

The ECMO Circuit

ECMO support comes in two forms: veno-venous (VV) and veno-arterial (VA). VV ECMO provides pulmonary support and VA ECMO provides both pulmonary and cardiac support. In VV ECMO, deoxygenated blood is drained from the venous system, pumped through the oxygenator where oxygen is added and carbon dioxide removed, and then returned to the venous system. From the venous circulation, this oxygenated blood then drains into the heart where native cardiac function distributes it to the arterial circulation. In VA ECMO, deoxygenated blood is also drained from the venous system and pumped through the oxygenator but returned to the arterial circulation, completely bypassing the heart and lungs. Oxygenated blood is distributed to the arterial circulation via non-pulsatile flow by the ECMO pump.

Regardless of whether the ECMO circuit is configured for VV or VA ECMO, the components are the same: tubing, pump, and oxygenator. In some cases a hemofilter is added to function as an artificial kidney. Most of the tubing used in ECMO circuits is polyvinylchloride (PVC). However, when blood comes into contact with an extrinsic surface such as PVC, various cellular mechanisms are activated that trigger clotting and inflammatory cascades.[18,19] To limit these interactions, different coatings have been applied to ECMO tubing, hemofilters, and oxygenators.[20-22] The Maquet Quadrox iD Oxygenator® used in the experiments in this dissertation has a proprietary coating (Bioline®) consisting of albumin adsorbed to the PVC and covered by covalently bound heparin.

ECMO oxygenators employ a gas-permeable membrane with a countercurrent gas mixture (sweep gas) flowing on one side of the membrane and the patient's blood on the other.[23] Gas diffuses down a concentration gradient with oxygen crossing the membrane into the blood and carbon dioxide diffusing from blood into the sweep gas. Early oxygenators had a silicone membrane, but high resistance to permeating gases necessitated a large surface area to ensure adequate oxygenation and ventilation. To enhance gas transfer, microporous hollow-fiber membranes were developed. However, these membranes were plagued by plasma leakage across the membrane that resulted in an oxygenator lifespan of 2-3 days. Oxygenators in use today employ a non-microporous, hollow-fiber, polymethylpentane membrane. These devices are low resistance, require much smaller surface area, do not suffer from plasma leakage, and have a lifespan measured in weeks. The type and amount of material to which the blood is exposed can have a substantial impact on drug interaction with the ECMO circuit.

Pharmacokinetic changes during ECMO support

While ECMO allows for the survival of a very critically ill subset of patients, it also presents new challenges related to their management. One of these challenges is understanding and appropriately compensating for the effect of ECMO on drug pharmacokinetics (PK). This topic has been studied since the late 1980's in neonates and isolated *ex vivo* ECMO circuits, and more recently, data from older children and adults have been published. In general, ECMO has been shown to impact PK in three primary ways, as discussed below.

Direct extraction by the circuit

Drug extraction by the ECMO circuit is a well-recognized contributor to PK alterations across all patient populations that depends on both the circuit component materials and the drug physicochemical properties. The interaction between the drug and the ECMO circuit has been studied primarily in *ex vivo* experiments in which drug is administered to isolated ECMO circuits.[24-33] Because there is no human attached to the circuit, any change in concentration over time is due to extraction by the circuit or drug degradation. In general, *ex vivo* studies have demonstrated increased extraction of highly lipophilic and protein bound drugs.[28,31,32]

However, the degree of extraction, even for the same drug, can be markedly affected by circuit materials. A study of fentanyl (LogP 4, protein binding 80%) in an ECMO circuit using a silicone membrane oxygenator showed >99% fentanyl loss in 180 minutes.[28] When the same experiment was repeated in a microporous, hollow-fiber polypropylene oxygenator, fentanyl loss was only 66% at 180 minutes.[28] Another study compared the effect of six different coatings on drug extraction by the PVC tubing by administering fentanyl to circuits constructed with only a pump and tubing (no oxygenator).[34,35] In the uncoated circuit, fentanyl loss at 120 minutes was 80%.[34] In the coated tubing, fentanyl loss at 120 minutes ranged from 40-75%.[35]

Drug extraction by the circuit is likely due to non-specific adsorption,[33-37] Adsorption is a function of 1) interactions between the drug and the material surface, 2) the maximal amount of binding per unit of surface area, and 3) the affinity of the drug for the surface. The process of adsorption is driven primarily by electrostatic and

hydrophobic interactions. Interactions with polymers such as those used in ECMO circuit equipment tend to be due to hydrophobic adsorption (i.e., hydrophobic drugs adsorb to hydrophobic alkyl groups on polymers). Electrostatic interactions tend to dominate when surface coatings are applied to ECMO circuit components. As noted above, surface coatings are applied to ECMO circuit components to minimize the inflammatory response triggered when blood comes into contact with a foreign material,[20-22] but coatings also can change the nature of interaction between the drug and material surface. When the drug and surface are oppositely charged, the degree of ionization driven by blood pH and drug pKa can influence the degree of adsorption.

The extent and irreversibility of adsorption depend on the number of binding sites on the material surface and the affinity of the drug for the surface. In the ECMO system data are conflicting as to whether binding is saturable. Two *ex vivo* studies have attempted to answer this question by comparing extraction in freshly primed circuits versus circuits that were used clinically and exposed to multiple drugs during their clinical use. Dagan et al. showed that morphine extraction in the freshly primed circuit was 36% after four hours but only 16% in a circuit that had been in clinical use for five days.[25] In contrast, Wildschut et al. showed no significant difference in morphine extraction at three hours between fresh and used circuits (76% vs 70%, respectively).[28] The higher absolute extraction of morphine in Wildschut et al. was likely due to differences in equipment and flow rates. While both studies used uncoated tubing with silicone membrane oxygenators, the oxygenators used by Wildschut et al. had twice the surface area of the oxygenators used by Dagan et al.[28,38] In addition, the blood flow rate was 10% higher in the Wildschut et al. study. The discrepancy in saturation between the

two studies is less clear, but may be related to one of three factors: 1) the dose of morphine administered to the circuit; 2) other drugs administered with morphine during the experiment, or 3) drugs administered to the used circuit while it was in use clinically. Dagan et al dosed morphine to achieve a concentration of 0.008 mg/L while Wildschut et al achieved an initial concentration over 200x higher (~1.7 mg/L). It is possible that the higher dose in the Wildschut et al study saturated binding sites for the new circuit as well as the old circuit. Secondly, both sets of experiments were designed to measure extraction of multiple drugs in a single circuit. The co-administered drugs were different between studies, and it is possible that co-administered drugs confounded the results by competing for binding sites. Finally, the drugs that were administered to the patient/circuit prior to the *ex vivo* experiment were neither controlled nor reported, and differences in clinical drug administration between the two studies could impact morphine extraction. More work is needed to determine if drug extraction by the ECMO circuit is saturable. Further, it is unknown whether extraction is reversible. While the volume of distribution (V) may be increased as drug is extracted, clearance (CL) may be decreased if drug is slowly released back into the systemic circulation.

Increased volume of distribution

ECMO support can increase V via multiple mechanisms: 1) drug extraction via direct interaction with the circuit as mentioned above; 2) hemodilution; and 3) physiologic changes related to ECMO support and critical illness. Hemodilution occurs due to the large volume of exogenous blood required to prime the circuit, frequent

transfusions of blood products, and administration of crystalloid to maintain circuit flows. Hemodilution has the largest effect on drugs whose distribution is limited to the plasma compartment (i.e. low V drugs). Drugs with a large V may be less impacted because drug extracted by the circuit may be replaced by drug stored in the tissue. The impact of hemodilution is likely inversely related to age. For a 3kg infant, the circuit prime volume (250-400mL) might exceed the infant's native blood volume (~250mL), while in a 70kg adolescent, the prime volume is ~8% of the child's blood volume (~5L). Ongoing hemolysis and the need to maintain hemostasis results in frequent transfusions of blood products, often totaling 6-8L over the course of an ECMO run.[39] Additionally, on occasion ECMO circuits fail and need to be replaced with a freshly primed circuit, which can further increase the amount of exogenous fluid administered.

The disease state can also impact V. Exposure to the ECMO circuit results in an inflammatory response.[18,19,40] Inflammation often results in capillary leak and edema, which can increase V.[18,41,42] In addition, patients on ECMO can have altered blood pH, which can affect a drug's ionization and distribution into tissues. Finally, the renin-angiotensin system in the kidney can be upregulated, possibly related to non-pulsatile blood flow seen in VA EMCO.[43] Upregulation of the renin-angiotensin system alters handling of fluids and can change the ratio of fluids in the body fluid compartments.

Our understanding of the impact of ECMO on V is limited by the fact that most studies were done in infants or an *ex vivo* system. Although *ex vivo* studies are useful in understanding how drugs interact with an ECMO circuit in isolation, direct translation of those results into humans is challenging. Translating results from infant studies is challenging because infants differ from older children and adults in important ways. In

addition to the different ratio of exogenous to native blood volume described above, infants have a higher proportion of body water and lower protein binding, both of which can impact V.[44-46] For these reasons, extrapolation of infant ECMO data to older children and adults must be done with caution.

Altered clearance

ECMO alters the PK of certain drugs by the effect it has on various organ systems. Renal dysfunction is common in patients on ECMO, occurring in >30% of ECMO patients.[17] Reasons for the renal dysfunction are not entirely clear but appear to be multifactorial. Hypoxia and poor organ perfusion prior to ECMO support likely contributes. Non-pulsatile blood flow seen with VA ECMO is associated with decreased glomerular filtration rate (GFR).[43] Of note, in VV ECMO where blood flow is pulsatile, the incidence of renal dysfunction (32%) is almost as high as that observed in VA ECMO (47%).[17] Altered renal function can substantially increase exposure of renally-cleared drugs and places patients at risk for toxicity. The effect is exacerbated if hemofiltration or dialysis are combined with ECMO support.[47]

The impact of ECMO on metabolic capacity is not well described. It is postulated that decreased regional flow to the liver could result in decreased metabolism of hepatically-cleared drugs, especially those where extraction is blood-flow dependent.[48] Further, ECMO causes inflammation and that inflammation tends to decrease the expression and function of drug metabolizing enzymes.[40,49] Of the enzymes that are relevant for this dissertation, the Cytochrome P450 (CYP) enzymes and UDP

glucuronosyltransferase 2B7 (UGT2B7) are down regulated, likely mediated by inflammatory cytokines.[50-53] On the other hand, rat models of liver disease show upregulation of arylsulfatase activity. [54,55] There are no data describing the impact of ECMO on drug transporters. Transporters also are impacted by inflammation, so it is reasonable to assume that ECMO could also impact disposition of drugs that rely on transporters.[56-58]

Because patients on ECMO are exposed to multiple drugs, it is important to understand the impact of ECMO support on drug PK. Such PK alterations are complex and challenging to investigate, arguing for a targeted approach based on the frequency of use of the drug, medical need, delayed clinical effect, and expected PK changes on ECMO. Some drugs have a readily apparent clinical effect and are easily titrated (e.g., epinephrine). Easily titratable drugs can be dosed clinically and dedicated PK studies are less necessary. However, many drugs have effects that are not easily measured. Antimicrobials are a good example, and multiple studies have been conducted to describe the effect of ECMO on the PK of antibiotics.[24,59-68] However, an important category of antimicrobial agents that have not been investigated extensively are the antifungal drugs.

Fungal infection on ECMO

Candida is the most common cause of ECMO-related nosocomial infection in adults and children and the second most common cause in neonates.[69] Incidence varies by center and rates as high as 10% have been reported.[69,70] *Candida* infections cause

substantial morbidity and mortality[70] and are difficult to eradicate due to the organism's ability to adhere to indwelling catheters. For this reason, routine management for candidiasis consists not only of antifungal agents but also removal of catheters.[71] Catheter removal for patients on ECMO is often impossible, because the ECMO cannulas connect the patient to the ECMO circuit. Therefore, therapy on ECMO relies on either prevention of invasive candidiasis or optimal therapeutic dosing in children with infection. Optimal dosing for prevention or treatment of candidiasis in children on ECMO is unknown due to the PK changes induced by the ECMO circuit.

Fluconazole and micafungin are first-line agents for prevention and treatment of candidiasis in children. [72,73] Amphotericin B deoxycholate is used less frequently because of its renal toxicity and safer alternatives, but remains a mainstay of treatment for serious invasive fungal infections. Each of these antifungal drugs has potential strengths and limitations in the ECMO system.[72-77] Fluconazole penetrates tissue well, and its hydrophilicity, neutral charge, and low binding to plasma proteins may protect it from adsorption by the ECMO circuit.[32,74] However, fluconazole is eliminated primarily by the kidneys, which may prolong its half-life and alter dosing in this patient population that frequently develops renal insufficiency.[74,78] Amphotericin B deoxycholate is a fungicidal against many clinically important species of fungi and undergoes renal clearance similar to fluconazole. Amphotericin is a slightly lipophilic (LogP 0.8) zwitterion that is 90% protein bound; it is unknown how these physicochemical properties will impact extraction by the ECMO circuit. Micafungin, an echinocandin, is active against both *Candida* spp. and *Aspergillus* spp., has few known drug-drug interactions, and most importantly has the ability to penetrate *Candida* biofilms.[73,79]

These biofilms can form in the different components of the ECMO circuit, which makes micafungin a promising antifungal drug in this setting. However, micafungin is more than 99% protein-bound and negatively charged at physiologic pH, which may result in high adsorption by the ECMO circuit and significantly decrease exposure.

Approaches to determining drug dosing on ECMO

Dosing recommendations are frequently derived by conducting PK trials and analyzing the data with traditional PK modeling and simulation. Traditional PK models (e.g., noncompartmental, compartmental, and population PK analyses) are built by fitting a model to drug concentration-time data from individuals or populations. This approach is well accepted by regulatory agencies and employs simplified models (e.g., 1-compartment model) with well-defined validation criteria. However, this approach is costly and time-consuming as it depends on collecting data from a trial, and care must be taken when extrapolating results to a population that is different from the population used to build the model. As an example, in this dissertation the results from a PK trial of fluconazole in 21 children on ECMO are reported. This study was performed under a Food and Drug Administration (FDA) investigational new drug (IND) application. Dosing recommendations submitted to the FDA were determined using nonlinear mixed effects population PK modeling. From the time of study design to FDA submission was six years for a single drug. Additionally, there is concern that if new ECMO technology is adopted in the future, the drug may interact differently with the new equipment. If true,

the dosing recommendations based on the old ECMO equipment would no longer be valid and a new trial would be necessary.

Physiologically-based pharmacokinetics (PBPK) offers an alternative modeling platform with greater flexibility, efficiency, and the ability to account for the complex physiology of critically ill children. PBPK models expand on traditional compartmental models by incorporating the key physiological, biochemical, and physicochemical determinants of drug disposition. The models are parameterized using a physiologic structure (Figure 1.2) with mathematical equations that describe the volume of the compartments, flows into and out of the compartments, and drug disposition within the compartments. These models can account for the effect that physiologic changes have on organ function (e.g., decreased renal perfusion) and provide a mechanistic understanding of drug disposition. Understanding the mechanism(s) of drug disposition enables more accurate dose predictions and optimization of trial design for different disease states.

In children on ECMO, an ECMO compartment can be added to the PBPK model to account for the effect of ECMO on drug disposition. The ECMO compartment is assigned a volume based on the volume of blood required to prime the ECMO circuit, and assigned an equal blood flow into and out of the compartment. Drug interaction (e.g. adsorption) within the ECMO compartment is informed by administering a drug of interest to an isolated *ex vivo* ECMO circuit. Drug extraction by the ECMO circuit can be described mathematically with a disposition function that is added to the ECMO compartment to predict dosing. While the model predictions will still need to be validated with PK data from children on ECMO, the number of children required will be less and

the trial design more efficient. Further, if ECMO technology changes, the *ex vivo* experiment can be repeated with the new circuit to understand whether the drug interaction is different. Based on the interaction with the new circuit, parameterization of the ECMO compartment can be updated in the PBPK model and new predictions of drug disposition can be generated. While the critically ill child, especially with extracorporeal support (e.g., ECMO, dialysis), represents an ideal population for the use of PBPK modeling, this approach has never been applied in this population.

The hypothesis of this proposal is that PBPK modeling can be combined with *ex vivo* ECMO experiments to mechanistically understand drug disposition and provide evidence-based dosing recommendations in children on ECMO.

Specific Aim 1: Evaluate the ECMO circuit extraction of three antifungal drugs *ex vivo*.

Hypothesis 1: Fluconazole and amphotericin B deoxycholate will undergo limited extraction due to their physicochemical properties (low lipophilicity, neutral or zwitterionic charge), while micafungin will be highly extracted because of its high degree of protein binding.

Specific Aim 2: Develop PBPK models of fluconazole and micafungin in critically ill children.

Hypothesis 2: PBPK models will predict drug exposure of fluconazole and micafungin as measured by area under the concentration time curve (AUC) within 0.7-1.3 fold of observed exposure in critically ill children and can be adapted to different physiologic states including ECMO.

Specific Aim 3: Prospectively evaluate through clinical trials PBPK models of fluconazole and micafungin in children on ECMO.

Hypothesis 3: Addition of the ECMO compartment into PBPK models will predict drug exposure of fluconazole and micafungin as measured by AUC within 0.7-1.3 fold of observed exposure in children on ECMO.

Figure 1.1. ECMO Circuit Schematic. An ECMO circuit has at least three components: tubing, pump, and oxygenator. Some circuits will also employ a hemofilter that can remove fluid and perform dialysis. *Ex vivo* ECMO experiments would replace the child in this schematic with a reservoir.

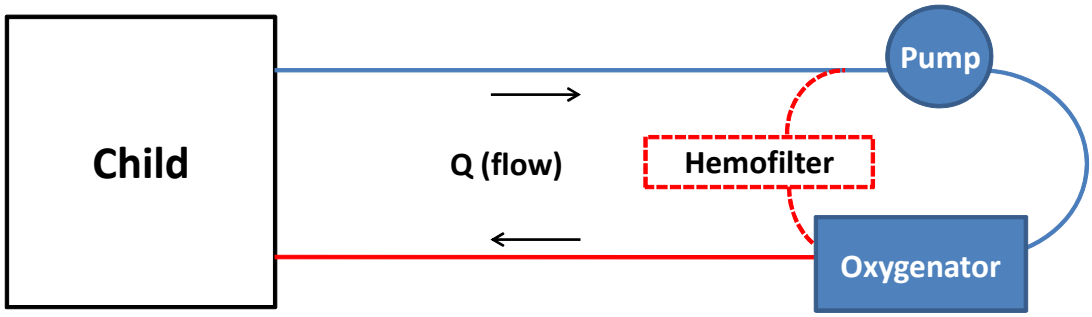

Figure 1.2. PBPK Model Structure. Each organ compartment is assigned a volume and flow based on the age, weight, and height of the individual or population. Drug-specific information such as physicochemical properties and clearance pathways determine drug disposition within each compartment. In children on ECMO, an ECMO compartment can be added.

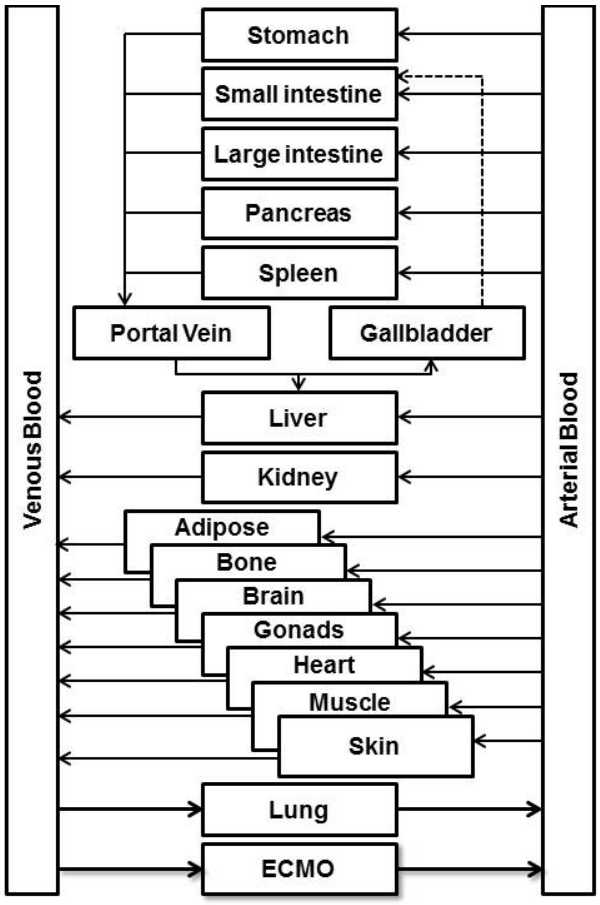

REFERENCES

1. Bartlett RH, Gazzaniga AB, Jefferies MR, Huxtable RF, Haiduc NJ, Fong SW. Extracorporeal membrane oxygenation (ECMO) cardiopulmonary support in infancy. Transactions - American Society for Artificial Internal Organs 1976;22:80-93.

2. Hill JD, O'Brien TG, Murray JJ, et al. Prolonged extracorporeal oxygenation for acute post-traumatic respiratory failure (shock-lung syndrome). Use of the Bramson membrane lung. N Engl J Med 1972;286:629-34.

3. Bartlett RH, Roloff DW, Cornell RG, Andrews AF, Dillon PW, Zwischenberger JB. Extracorporeal circulation in neonatal respiratory failure: a prospective randomized study. Pediatrics 1985;76:479-87.

4. O'Rourke PP, Crone RK, Vacanti JP, et al. Extracorporeal membrane oxygenation and conventional medical therapy in neonates with persistent pulmonary hypertension of the newborn: a prospective randomized study. Pediatrics 1989;84:957-63.

5. UK collaborative randomised trial of neonatal extracorporeal membrane oxygenation. UK Collaborative ECMO Trail Group. Lancet 1996;348:75-82.

6. Morris AH, Wallace CJ, Menlove RL, et al. Randomized clinical trial of pressure-controlled inverse ratio ventilation and extracorporeal CO2 removal for adult respiratory distress syndrome. American journal of respiratory and critical care medicine 1994;149:295-305.

7. Zapol WM, Snider MT, Hill JD, et al. Extracorporeal membrane oxygenation in severe acute respiratory failure. A randomized prospective study. JAMA 1979;242:2193-6.

8. Bessereau J, Chenaitia H, Michelet P, Roch A, Gariboldi V. Acute Respiratory Distress Syndrome following 2009 H1N1 virus pandemic: When ECMO come to the patient bedside. Annales francaises d'anesthesie et de reanimation.

9. Mitchell MD, Mikkelsen ME, Umscheid CA, Lee I, Fuchs BD, Halpern SD. A systematic review to inform institutional decisions about the use of extracorporeal membrane oxygenation during the H1N1 influenza pandemic. Crit Care Med 2010;38:1398-404.

10. Buckley E, Sidebotham D, McGeorge A, Roberts S, Allen SJ, Beca J. Extracorporeal membrane oxygenation for cardiorespiratory failure in four patients with pandemic H1N1 2009 influenza virus and secondary bacterial infection. Br J Anaesth;104:326-9.

11. Davies A, Jones D, Bailey M, et al. Extracorporeal Membrane Oxygenation for 2009 Influenza A(H1N1) Acute Respiratory Distress Syndrome. JAMA 2009;302:1888-95.

12. Firstenberg MS, Blais D, Louis LB, Stevenson KB, Sun B, Mangino JE. Extracorporeal membrane oxygenation for pandemic (H1N1) 2009. Emerg Infect Dis 2009;15:2059-60.

13. Grasselli G, Foti G, Patroniti N, et al. A case of ARDS associated with influenza A - H1N1 infection treated with extracorporeal respiratory support. Minerva Anestesiol 2009;75:741-5.

14. Kao TM, Wang CH, Chen YC, Ko WJ, Chang SC. The first case of severe novel H1N1 influenza successfully rescued by extracorporeal membrane oxygenation in Taiwan. Journal of the Formosan Medical Association 2009;108:894-8.

15. Kumar A, Zarychanski R, Pinto R, et al. Critically ill patients with 2009 influenza A(H1N1) infection in Canada. JAMA 2009;302:1872-9.

16. Peek GJ, Elbourne D, Mugford M, et al. Randomised controlled trial and parallel economic evaluation of conventional ventilatory support versus extracorporeal membrane oxygenation for severe adult respiratory failure (CESAR). Health Technol Assess 2010;14:1-46.

17. ELSO. ECLS Registry Report: International Summary; 2014 January 2015.

18. Butler J, Pathi VL, Paton RD, et al. Acute-phase responses to cardiopulmonary bypass in children weighing less than 10 kilograms. Ann Thorac Surg 1996;62:538-42.

19. Kozik DJ, Tweddell JS. Characterizing the inflammatory response to cardiopulmonary bypass in children. Ann Thorac Surg 2006;81:S2347-54.

20. Palatianos GM, Foroulis CN, Vassili MI, et al. A prospective, double-blind study on the efficacy of the bioline surface-heparinized extracorporeal perfusion circuit. Ann Thorac Surg 2003;76:129-35.

21. Tayama E, Hayashida N, Akasu K, et al. Biocompatibility of heparin-coated extracorporeal bypass circuits: new heparin bonded bioline system. Artificial organs 2000;24:618-23.

22. De Somer F, Francois K, van Oeveren W, et al. Phosphorylcholine coating of extracorporeal circuits provides natural protection against blood activation by the material surface. European journal of cardio-thoracic surgery : official journal of the European Association for Cardio-thoracic Surgery 2000;18:602-6.

23. Palanzo D, Qiu F, Baer L, Clark JB, Myers JL, Undar A. Evolution of the extracorporeal life support circuitry. Artificial organs 2010;34:869-73.

24. Bhatt-Mehta V, Johnson CE, Schumacher RE. Gentamicin pharmacokinetics in term neonates receiving extracorporeal membrane oxygenation. Pharmacotherapy 1992;12:28-32.

25. Dagan O, Klein J, Gruenwald C, Bohn D, Barker G, Koren G. Preliminary studies of the effects of extracorporeal membrane oxygenator on the disposition of common pediatric drugs. Ther Drug Monit 1993;15:263-6.

26. Mehta NM, Halwick DR, Dodson BL, Thompson JE, Arnold JH. Potential drug sequestration during extracorporeal membrane oxygenation: results from an ex vivo experiment. Intensive Care Med 2007;33:1018-24.

27. Mulla H, Lawson G, von Anrep C, et al. In vitro evaluation of sedative drug losses during extracorporeal membrane oxygenation. Perfusion 2000;15:21-6.

28. Wildschut ED, Ahsman MJ, Allegaert K, Mathot RA, Tibboel D. Determinants of drug absorption in different ECMO circuits. Intensive Care Med 2010;36:2109-16.

29. Koren G, Crean P, Klein J, Goresky G, Villamater J, MacLeod SM. Sequestration of fentanyl by the cardiopulmonary bypass (CPBP). Eur J Clin Pharmacol 1984;27:51-6.

30. Lemaitre F, Hasni N, Leprince P, et al. Propofol, midazolam, vancomycin and cyclosporine therapeutic drug monitoring in extracorporeal membrane oxygenation circuits primed with whole human blood. Crit Care 2015;19:40.

31. Shekar K, Roberts JA, McDonald CI, et al. Sequestration of drugs in the circuit may lead to therapeutic failure during extracorporeal membrane oxygenation. Crit Care 2012;16:R194.

32. Shekar K, Roberts JA, McDonald CI, et al. Protein-bound drugs are prone to sequestration in the extracorporeal membrane oxygenation circuit: results from an ex vivo study. Crit Care 2015;19:164.

33. Harthan AA, Buckley KW, Heger ML, Fortuna RS, Mays K. Medication adsorption into contemporary extracorporeal membrane oxygenator circuits. The journal of pediatric pharmacology and therapeutics : JPPT : the official journal of PPAG 2014;19:288-95.

34. Preston TJ, Hodge AB, Riley JB, Leib-Sargel C, Nicol KK. In vitro drug adsorption and plasma free hemoglobin levels associated with hollow fiber oxygenators in the extracorporeal life support (ECLS) circuit. The journal of extra-corporeal technology 2007;39:234-7.

35. Preston TJ, Ratliff TM, Gomez D, et al. Modified surface coatings and their effect on drug adsorption within the extracorporeal life support circuit. The journal of extra-corporeal technology 2010;42:199-202.

36. Palmgren JJ, Monkkonen J, Korjamo T, Hassinen A, Auriola S. Drug adsorption to plastic containers and retention of drugs in cultured cells under in vitro conditions. European journal of pharmaceutics and biopharmaceutics : official journal of Arbeitsgemeinschaft fur Pharmazeutische Verfahrenstechnik eV 2006;64:369-78.

37. Unger JK, Kuehlein G, Schroers A, Gerlach JC, Rossaint R. Adsorption of xenobiotics to plastic tubing incorporated into dynamic in vitro systems used in pharmacological research--limits and progress. Biomaterials 2001;22:2031-7.

38. Kolobow T, inventor Dow Corning, assignee. Artificial organ for membrane dialysis of biological fluids. USA. 1970.

39. Buck ML. Pharmacokinetic changes during extracorporeal membrane oxygenation: implications for drug therapy of neonates. Clin Pharmacokinet 2003;42:403-17.

40. B. MR, Timpa JG, Kurundkar AR, et al. Plasma concentrations of inflammatory cytokines rise rapidly during ECMO-related SIRS due to the release of preformed stores in the intestine. Lab Invest 2010;90:128-39.

41. Seghaye MC, Grabitz RG, Duchateau J, et al. Inflammatory reaction and capillary leak syndrome related to cardiopulmonary bypass in neonates undergoing cardiac operations. J Thorac Cardiovasc Surg 1996;112:687-97.

42. Anderson HL, 3rd, Coran AG, Drongowski RA, Ha HJ, Bartlett RH. Extracellular fluid and total body water changes in neonates undergoing extracorporeal membrane oxygenation. J Pediatr Surg 1992;27:1003-7; discussion 7-8.

43. Many M, Soroff HS, Birtwell WC, Giron F, Wise H, Deterling RA, Jr. The physiologic role of pulsatile and nonpulsatile blood flow. II. Effects on renal function. Arch Surg 1967;95:762-7.

44. Ehrnebo M, Agurell S, Jalling B, Boreus LO. Age differences in drug binding by plasma proteins: studies on human foetuses, neonates and adults. Eur J Clin Pharmacol 1971;3:189-93.

45. Friis-Hansen B. Water distribution in the foetus and newborn infant. Acta paediatrica Scandinavica Supplement 1983;305:7-11.

46. McNamara PJ, Alcorn J. Protein binding predictions in infants. AAPS pharmSci 2002;4:E4.

47. Shekar K, Fraser JF, Taccone FS, et al. The combined effects of extracorporeal membrane oxygenation and renal replacement therapy on meropenem pharmacokinetics: a matched cohort study. Crit Care 2014;18:565.

48. Mulla H, Lawson G, Firmin R, Upton DR. Drug Disposition During Extracorporeal Membrane Oxygenation (ECMO). Pediatric and Perinatal Drug Therapy 2001;4:109-20.

49. Morgan ET. Regulation of cytochromes P450 during inflammation and infection. Drug Metab Rev 1997;29:1129-88.

50. Abdel-Razzak Z, Loyer P, Fautrel A, et al. Cytokines down-regulate expression of major cytochrome P-450 enzymes in adult human hepatocytes in primary culture. Mol Pharmacol 1993;44:707-15.

51. Rivory LP, Slaviero KA, Clarke SJ. Hepatic cytochrome P450 3A drug metabolism is reduced in cancer patients who have an acute-phase response. British journal of cancer 2002;87:277-80.

52. Siewert E, Bort R, Kluge R, Heinrich PC, Castell J, Jover R. Hepatic cytochrome P450 down-regulation during aseptic inflammation in the mouse is interleukin 6 dependent. Hepatology 2000;32:49-55.

53. Richardson TA, Sherman M, Kalman D, Morgan ET. Expression of UDP-glucuronosyltransferase isoform mRNAs during inflammation and infection in mouse liver and kidney. Drug metabolism and disposition: the biological fate of chemicals 2006;34:351-3.

54. Dufour JF, Zimmermann A, Reichen J. Increased hepatic lysosomal activity in biliary cirrhosis originates from hepatocytes rather than from macrophages. Journal of hepatology 1994;20:524-30.

55. Ugazio G, Artizzu M, Pani P, Dianzani MU. The changes in some hydrolytic enzymes in carbon tetrachloride-induced fatty livers. The Biochemical journal 1964;90:109-16.

56. Cherrington NJ, Slitt AL, Li N, Klaassen CD. Lipopolysaccharide-mediated regulation of hepatic transporter mRNA levels in rats. Drug metabolism and disposition: the biological fate of chemicals 2004;32:734-41.

57. Piquette-Miller M, Pak A, Kim H, Anari R, Shahzamani A. Decreased expression and activity of P-glycoprotein in rat liver during acute inflammation. Pharm Res 1998;15:706-11.

58. Ueyama J, Nadai M, Kanazawa H, et al. Endotoxin from various gram-negative bacteria has differential effects on function of hepatic cytochrome P450 and drug transporters. Eur J Pharmacol 2005;510:127-34.

59. Ahsman MJ, Wildschut ED, Tibboel D, Mathot RA. Pharmacokinetics of cefotaxime and desacetylcefotaxime in infants during extracorporeal membrane oxygenation. Antimicrob Agents Chemother 2010;54:1734-41.

60. Amaker RD, DiPiro JT, Bhatia J. Pharmacokinetics of vancomycin in critically ill infants undergoing extracorporeal membrane oxygenation. Antimicrob Agents Chemother 1996;40:1139-42.

61. Buck ML. Vancomycin pharmacokinetics in neonates receiving extracorporeal membrane oxygenation. Pharmacotherapy 1998;18:1082-6.

62. Cohen P, Collart L, Prober CG, Fischer AF, Blaschke TF. Gentamicin pharmacokinetics in neonates undergoing extracorporal membrane oxygenation. Pediatr Infect Dis J 1990;9:562-6.

63. Donadello K, Roberts JA, Cristallini S, et al. Vancomycin population pharmacokinetics during extracorporeal membrane oxygenation therapy: a matched cohort study. Crit Care 2014;18:632.

64. Hoie EB, Swigart SA, Leuschen MP, et al. Vancomycin pharmacokinetics in infants undergoing extracorporeal membrane oxygenation. Clin Pharm 1990;9:711-5.

65. Mulla H, Pooboni S. Population pharmacokinetics of vancomycin in patients receiving extracorporeal membrane oxygenation. Br J Clin Pharmacol 2005;60:265-75.

66. Munzenberger PJ, Massoud N. Pharmacokinetics of gentamicin in neonatal patients supported with extracorporeal membrane oxygenation. ASAIO Trans 1991;37:16-8.

67. Southgate WM, DiPiro JT, Robertson AF. Pharmacokinetics of gentamicin in neonates on extracorporeal membrane oxygenation. Antimicrob Agents Chemother 1989;33:817-9.

68. Veinstein A, Debouverie O, Gregoire N, et al. Lack of effect of extracorporeal membrane oxygenation on tigecycline pharmacokinetics. J Antimicrob Chemother 2011.

69. Bizzarro MJ, Conrad SA, Kaufman DA, Rycus P. Infections acquired during extracorporeal membrane oxygenation in neonates, children, and adults. Pediatr Crit Care Med 2010.

70. Gardner AH, Prodhan P, Stovall SH, et al. Fungal infections and antifungal prophylaxis in pediatric cardiac extracorporeal life support. J Thorac Cardiovasc Surg 2011.

71. Eppes SC, Troutman JL, Gutman LT. Outcome of treatment of candidemia in children whose central catheters were removed or retained. Pediatr Infect Dis J 1989;8:99-104.

72. Pappas PG, Kauffman CA, Andes D, et al. Clinical practice guidelines for the management of candidiasis: 2009 update by the Infectious Diseases Society of America. Clin Infect Dis 2009;48:503-35.

73. EMA. Mycamine : EPAR - Product Information In: Agency EM, ed. Leiderdorp, The Netherlands: Astellas Pharma Europe B.V.; 2010.

74. FDA. Fluconazole Injection, USP Product Label. In: U.S. Dept. of Health and Human Services FaDA, ed.: Roerig, a division of Pfizer, Inc.; 2015.

75. Ikeda F, Wakai Y, Matsumoto S, et al. Efficacy of FK463, a new lipopeptide antifungal agent, in mouse models of disseminated candidiasis and aspergillosis. Antimicrob Agents Chemother 2000;44:614-8.

76. Tawara S, Ikeda F, Maki K, et al. In vitro activities of a new lipopeptide antifungal agent, FK463, against a variety of clinically important fungi. Antimicrob Agents Chemother 2000;44:57-62.

77. Kaneko Y, Ohno H, Fukazawa H, et al. Anti-Candida-biofilm activity of micafungin is attenuated by voriconazole but restored by pharmacological inhibition of Hsp90-related stress responses. Medical mycology : official publication of the International Society for Human and Animal Mycology 2010;48:606-12.

78. Brammer KW, Coates PE. Pharmacokinetics of fluconazole in pediatric patients. Eur J Clin Microbiol Infect Dis 1994;13:325-9.

79. Fiori B, Posteraro B, Torelli R, et al. In vitro activities of anidulafungin and other antifungal agents against biofilms formed by clinical isolates of different Candida and Aspergillus species. Antimicrob Agents Chemother 2011;55:3031-5.

CHAPTER 2. ANTIFUNGAL EXTRACTION BY THE EXTRACOPOREAL MEMBRANE OXYGENATION (ECMO) CIRCUIT *EX VIVO*

INTRODUCTION

Extracorporeal membrane oxygenation (ECMO) is a cardiopulmonary bypass device used to support patients with refractory respiratory and/or cardiac failure. Patients supported with ECMO are critically ill and, thus, exposed to multiple drugs. Optimal dosing of drugs in this setting is unknown because ECMO can alter drug pharmacokinetics (PK). Studies of antimicrobials (e.g., vancomycin,[1-4] gentamicin[5-8]) and sedatives (e.g., opiates,[9-12] benzodiazepines[13,14]) generally show an increased volume of distribution (V) and decreased clearance (CL). These alterations in PK are caused by multi-organ dysfunction, the large volume of exogenous blood required to prime the ECMO circuit, and drug extraction by the circuit.

Drug extraction by the ECMO circuit is thought to be due to non-specific binding by the components of the circuit.[15-19] While supported by ECMO, nearly all of a patient's blood is drained from the venous system via a large bore cannula and pumped through tubing to an artificial lung (oxygenator) before being returned to the patient. In some cases the ECMO circuit also contains a hemofilter that can provide hemofiltration or dialysis for patients with renal injury. As drugs transit the ECMO circuit they come in contact with the various components of the circuit (e.g., tubing, pump, oxygenator, hemofilter) and are vulnerable to extraction. The extent of drug extraction by the ECMO

circuit depends on the materials in the circuit and the physicochemical properties of the drug. Non-specific binding of drugs occurs via two primary mechanisms: 1) hydrophobic interactions and 2) ionic interactions.[20] Hydrophobic binding can occur between hydrophobic drugs and a hydrophobic surface, while ionic binding occurs when the drug and surface are oppositely charged. Non-specific binding of drugs can significantly decrease exposure and lead to therapeutic failure.

Circuit-drug interactions have been investigated using *ex vivo* ECMO experiments in which drug is administered to an isolated ECMO circuit.[13,15,21-29] Because there is no corporeal metabolism or elimination in this system, decreases in drug concentration are due to either extraction by the circuit or drug degradation. In general, highly lipophilic (e.g., fentanyl) and highly protein bound (e.g., caspofungin) drugs are extensively extracted by the circuit.[23,30] However, this relationship is not always predictable. Ciprofloxacin is lipophilic with low protein binding but not extracted, while meropenem is hydrophilic with low protein binding and extensively extracted.[22,23] This suggests that other factors such as ionic binding may play a role. Additionally, the site(s) of extraction within the circuit is not known.

In the present study, the extent of extraction by the ECMO circuit was determined for selected antifungal drugs in an *ex vivo* ECMO system. Antifungal drugs were chosen because fungal infections are common in children on ECMO and treatment depends on optimal dosing.[31] The contribution of each component of the ECMO circuit to overall extraction was determined by comparing extraction in three circuit configurations with different component combinations.

METHODS

Drug selection

Three antifungal drugs were selected for evaluation: fluconazole, micafungin, and amphotericin B dexoycholate. These drugs were selected based on their frequency of use in clinical practice and range of physicochemical properties (Table 2.1, Figure 2.1).

Circuit configuration

In order to determine the impact of each component on drug extraction, the experiment was designed with three circuit configurations (Figure 2.2). The Complete Circuit contained tubing, a pump, an oxygenator, and a hemofilter (Table 2.2). The Oxygenator Circuit was identical to the Complete Circuit except that the hemofilter was removed. The Pump Circuit was identical to the Oxygenator Circuit except that the oxygenator was removed. Any difference in extraction between the Complete and Oxygenator Circuits was due to the hemofilter. Similarly, any difference in extraction between the Oxygenator and Pump Circuits was due to the Oxygenator (Figure 2.2).

Circuit setup

Circuits were assembled according to the standard practice for Duke University Children's Hospital. Circuits were primed with a solution of 1 unit of packed red blood cells (~350mL), 0.5 unit of fresh frozen plasma (~175mL), and plasmalyte crystalloid (500mL). In addition, the following were added to each circuit to complete the prime

solution: heparin sulfate (0.1 units), sodium bicarbonate (30mEq), and calcium gluconate (6.5mg). Additional sodium bicarbonate and/or carbon dioxide were added to the system to maintain physiologic pH. To be consistent with standard practice at Duke, albumin was not routinely added to the circuit, and albumin concentrations were low (≤1.0 mg/dL). However, if a drug showed extraction in any of the circuit configurations, subsequent experiments were performed and human serum albumin was added to achieve two additional concentration levels: low-physiologic (2.2-2.8 mg/dL; typical for a child on ECMO) and physiologic (3.5-3.8 mg/dL). In order to examine the impact of albumin on extraction, extraction was compared between circuits with low, low-physiologic, and physiologic albumin concentrations.

Because there was no human connected to the circuit, the circuit was completed via a reservoir (plasmalyte IV bag). An ECMO heat exchanger was used to maintain a constant temperature of 36˚ C throughout the study. ECMO flow was set to 1L/min to simulate the clinical scenario for a 10kg child.

Control

In order to determine the amount of drug degradation over time, at least three clear, polyvinylchloride plastic tubes per drug were filled with 30mL of the prime solution drawn from the ECMO circuit. The prime solution was collected from the ECMO circuit after ≥5 minutes of circulation and before drug administration. The control tubes were tightly capped in a 36˚ C static, water bath.

Drug administration and sample collection

Drug was introduced into the circuit via a port downstream of the sampling port at time=0 and dosed to achieve a therapeutic concentration. Drug was dosed to achieve a comparable concentration in the control samples at time -5 minutes, sealed with a tight cap, and then gently mixed for 5 minutes until time=0. At time=0, the controls were returned to the water bath where they remained for the duration of the experiment, except at times of sample collection. Immediately prior to control sample collection, control tubes were removed from the water bath and gently inverted five times to ensure adequate mixing. In the initial set of experiments, samples were collected from the circuits and controls for 4 hours at the following time points: 1, 5, 15, and 30min, 1, 2, 3, and 4h. In order to better understand drug disposition over an entire dosing interval, subsequent experiments measured concentrations up to 24 hours by collecting additional samples at 8, 12, and 24h.

Analysis

Drug concentrations were measured using assays that were developed and validated according to FDA guidance.[32] Fluconazole concentrations were measured at OpAns Laboratory (Durham, NC) using HPLC/MS-MS. Plasma samples were acidified with formic acid and precipitated with acetonitrile. Samples were centrifuged and diluted with water containing 0.2% (v/v) acetic acid prior to injection into the HPLC system. Separation was achieved with a Poroshell 120 EC-C18 Column. Fluconazole was quantified using an electrospray ionization source in the positive mode and under the

following conditions: gas temperature 300ºC, gas flow 10 L/min, nebulizer pressure 50 psi, sheath gas temperature 345 ºC, sheath gas flow 11 L/min, capillary voltage 3500 V, nozzle voltage 500 V, Dynamic MRM scan type. The lower limit of quantification (LLOQ) was 0.01 mg/L with a calibration curve range of 0.01 to 10 mg/L. Intraday and interday precision (%CV) ranged from 1.4% to 8.5% and 2.8% to 5.8%, respectively. Micafungin concentrations were measured at the University of Texas Health System Fungal Testing Laboratory using HPLC with fluorescence detection. Plasma samples were acidified with phosphoric acid and precipitated with acetonitrile. Samples were centrifuged and diluted with 10mM ammonium acetate prior to injection into the HPLC system. Injection into the HPLC occurred under the following conditions: mobile phase with 10mM ammonium acetate/acetonitrile 60:40 v/v at a flow rate of 1.0 mL/min. Separation was achieved with a Phenomenex-Luna 5µ C18 Column. Micafungin was quantified by fluorescence. Fluorescence detector excitation and emission wavelengths were 273nm and 464nm, respectively. The LLOQ was 0.05 mg/L. The calibration curve ranged from 0.05 to 25 mg/L. Intraday precision ranged from 1.19% to 7.35% except at the LLOQ where the range was 12.0% to 21.6%. Interday precision ranged from 4.88% to 10.3%. Amphotericin B deoxycholate also was measured at the Fungal Testing Laboratory using HPLC. Plasma samples were deproteinated and precipitated with acetonitrile, centrifuged and injected into the HPLC system. Injection into the HPLC occurred under the following conditions: mobile phase with 0.01M TEMED buffer/acetonitrile 65:35 v/v at a flow rate of 0.8 mL/min. Separation was achieved with a Phenomenex Luna 5u C18(2) 150 X 4.6 mm column. UV detection was at 406nm. The LLOQ was 0.05 mg/L;

intraday and interday precision ranged from 0% to 11.8% and 3.23 to 5.65%, respectively.

Drug recovery in circuits and controls was calculated at each sample time using the following equation:

$$Recovery\ (\%) = \frac{C_t}{C_i} * 100$$

where C_t is the concentration at time *t* and C_i is the initial concentration measured at time=1 minute. Data are reported as the mean and 95% confidence interval.

Ethics

The Duke University Medical Center Institutional Review Board provided a waiver of review because the protocol met the definition of research not involving human subjects.

RESULTS

The total number of circuits studied, by configuration, are summarized for each drug in Table 2.3.

Fluconazole

Fluconazole was not extracted by the ECMO circuit (Figure 2.3.a). In three Complete Circuits, the mean (95% confidence interval) recovery of fluconazole was

97.8% (96.3, 99.3) at 4 hours. In the two Complete Circuits that were run for 24 hours, 95.2% (89.6, 100.9) of the initial concentration was recovered. When the hemofilter was removed to create the Oxygenator Circuit, 92.3% (83.1 101.5) of the initial fluconazole concentration was recovered at 4 hours (n=4). One Oxygenator Circuit was run for 24 hours and 98.4% of the initial concentration was recovered at 24 hours. When fluconazole was administered to the Pump Circuit (n=1), 105.8% was recovered after 4 hours. Because no extraction was observed in the Complete or Oxygenator Circuits, additional Pump Circuits were not run. In the control samples, 100.2% (95.5, 104.9) of the initial fluconazole concentration was recovered at 4 hours (n=4) and 100.6% (98.5, 102.8) at 24 hours (n=3).

Micafungin

In the Complete Circuit (n=10), micafungin recovery was low at 4h (46.3% [35.3, 57.3]). However, when the hemofilter was removed (Oxygenator Circuit, n=4), micafungin recovery at 4 hours was 91.1% (85.2, 97.0) (Figure 2.3.b). Similarly, in the Pump Circuit (n=1) and Control (n=4) 98.1% and 90.9% (86.8, 95.0), respectively, were recovered at 4 hours. By 24 hours, however, recovery of micafungin was low in the Complete (26.0% [15.0, 37.0]; n=9) and Oxygenator Circuits (42.6% [31.3, 53.9]; n=3) as well as in the Control samples (56.8% [49.2, 64.4]; n=3).

Micafungin extraction during the first 4 hours was dependent on albumin concentration (Figure 2.4). At low albumin concentrations (≤ 1.0 g/dL; n=4) in a Complete Circuit, 29.0% (19.7, 38.4) and 16.1% (1.7, 30.5) of the initial micafungin

concentrations were recovered at 4 and 24 hours, respectively. At low physiologic albumin concentrations (2.2-2.8 g/dL; n=3) recovery was 58.4% (53.5, 63.3) and 35.7% (24.7, 46.7) at 4 and 24 hours, respectively. Similarly, when albumin concentrations were in the normal range (3.5-3.8 g/dL; n=3), micafungin recovery was 57.2% (54.8, 59.5) and 26.1% (20.4, 31.9) at 4 and 24 hours, respectively.

Because the hemofilter was responsible for micafungin extraction in the first 4 hours, micafungin concentrations were measured in the hemofiltrate for one circuit to determine if micafungin passively crossed the hemofilter membrane (hemofilter was only in-line and not actively filtering). Concentrations in the hemofiltrate at 1min, 1h, 2h, and 24h were only 0.07, 0.06, 0.21 and 0.16 mg/L, respectively. Concentrations in the plasma samples from the ECMO circuit at the same times were 15.5, 13.1, 11.6, and 8.1 mg/L, respectively. Concentrations in the hemofiltrate were <2% of concentrations in the circuit suggesting that micafungin does not cross the hemofilter membrane.

Amphotericin

Three amphotericin B deoxycholate Complete Circuits and Controls were run for 24 hours. The three circuits showed virtually no loss of amphotericin at 4 hours or 12 hours, with recovery of 98.9% (88.7, 109.1) and 99.2% (88.5, 110.1), respectively (Figure 2.3.c). Results after 12 hours were unable to be reported because the circuits and controls developed substantial hemolysis after 12 hours. Hemolysis interferes with the amphotericin assay resulting in unreliable concentration measurements. Because amphotericin was not extracted in the Complete Circuit, extraction by the Oxygenator or

Pump Circuits would not be expected. Therefore, additional circuit configurations were not evaluated for amphotericin. Of note, the concentrations of amphotericin in the control samples increased over the first 4 hours so that recovery was 143.8% (137.5, 150.1) of the initial concentration. Between 4 hours and 12 hours concentrations remained constant with recovery of 145.3% (140.4, 150.3) at 12 hours.

DISCUSSION

ECMO can alter drug pharmacokinetics (PK) directly and indirectly through a variety of mechanisms. Direct effects include 1) increased volume of distribution due to the addition of the large volume of exogenous blood required to prime the ECMO circuit, 2) hemofiltration, which is common in patients on ECMO, and 3) extraction of drug by components of the circuit.[33] *Ex vivo* ECMO experiments such as those performed in this study provide insight into extraction via circuit-drug interactions. The degree of interaction with the ECMO circuit is drug-dependent and likely influenced by the physicochemical properties of the drug and circuit components (e.g., oxygenator, hemofilter).[23,30] Results of the present study demonstrate important differences in antifungal drug extraction by the ECMO circuit that can affect dosing recommendations in clinical practice.

Micafungin was highly extracted in the first 4 hours in a Complete Circuit but not in the other circuit configurations. This suggests that extraction was due to the hemofilter. Three possible mechanisms may explain extraction by the hemofilter: 1) diffusion across the hemofilter membrane; 2) areas of stasis in the hemofilter that

"trapped" the drug; or 3) direct adsorption by the hemofilter. Micafungin would not be expected to diffuse across the hemofilter membrane due to its high degree of protein binding (>99%) and the fact that the hemofilter was not actively filtering during the experiments. This was confirmed by collecting samples of hemofiltrate, which contained virtually undetectable concentrations of micafungin. Although areas of low flow can occur around the hemofilter, inconsistency in the degree of "trapping" and more variability in recovery would be expected if this were the mechanism. Adsorption by the hemofilter appears to be the most likely explanation. This is supported by greater extraction at low albumin concentrations suggesting that the unbound fraction is adsorbed by the hemofilter membrane. However, the polyethersulfone membrane used in these experiments was hydrophobic and had no net charge, making it less likely to interact with a hydrophilic anion such as micafungin. Further studies to understand the mechanism of drug loss to the hemofilter are needed.

These results are in contrast to studies of micafungin in continuous venovenous hemofiltration (CVVH) using similar hemofilters that showed no loss when micafungin concentrations were measured pre- and post-hemofilter.[34,35] However, several important differences were noted between our ECMO *ex vivo* system and the CVVH studies that could explain this apparent discrepancy: 1) the CVVH studies were PK trials in critically ill adults so other unmeasured factors inherent to clinical trials may have influenced drug concentrations; 2) flow rates were higher in the ECMO experiments compared to CVVH and for drugs where extraction is perfusion limited, increased flow results in higher extraction; and 3) the CVVH studies were actively filtering and by removing plasma water but not drug, micafungin was functionally concentrating in the

plasma. Differences in protein binding between the *in vivo* and *ex vivo* studies could also account for the differences. Albumin concentrations were higher in the *in vivo* CVVH studies. Because micafungin is highly protein bound, small changes in binding can substantially alter the amount of unbound drug available to be absorbed by the hemofilter.

More important than the hemofilter-related decrease in concentration over four hours was the observation that micafungin concentrations decreased over a 24 hour dosing interval in all circuit configurations and the controls. Non-specific binding to circuit materials should occur quickly (i.e., <4 hours).[16,18-20] The continued extraction of micafungin over 24 hours in both circuits and controls suggests that drug degradation or plasma metabolism may have occurred. Micafungin is known to degrade in light.[36] It is possible that light penetration of the ECMO tubing and control tubes caused sample degradation throughout the study. Clinically, ECMO circuits are exposed to light so that clinicians operating the circuit can monitor for clot accumulation in the components. As a result, a substantial amount of blood is exposed to light at any given time during ECMO support, and this may have important dosing implications for light-sensitive drugs. Alternatively, metabolism by plasma peptidases could result in continuous loss of micafungin. Although plasma metabolism is not described for micafungin, peptidases are a major elimination pathway for both caspofungin and anidulafungin, echinocandins with similar structure. Experiments are ongoing to determine the mechanism of continued drug loss. Regardless of the mechanism, the fact that mean micafungin recovery ranged from 26-57% at 24 hours suggests that micafungin dosing may need to be increased in patients on ECMO.

In the present study, fluconazole was not extracted by the ECMO circuit. The fluconazole results are consistent with a recent ECMO *ex vivo* study where fluconazole recovery at 24 hours in a system similar to the Oxygenator Circuit and Control used in this study were 96% and 102%, respectively.[23] Based on physicochemical properties, fluconazole would not be expected to interact with the ECMO circuit. It is only slightly lipophilic (LogP 0.4) and should not undergo extensive hydrophobic binding to polymers. The present findings also are supported by an ECMO *ex vivo* study that demonstrated minimal extraction of linezolid, a drug with similar physicochemical properties (LogP of 0.9, protein binding of 30%).[23] Additionally, fluconazole has a neutral charge at physiologic pH so it would not be expected to undergo extensive ionic binding.

Amphotericin B deoxycholate also was not extracted by the ECMO circuit. There are no prior studies of amphotericin in ECMO. Amphotericin is slightly lipophilic, similar to fluconazole, and would not be expected to undergo extensive hydrophobic binding. More importantly, amphotericin is a zwitterion. Zwitterions would not be expected to adsorb to hydrophobic or charged surfaces because they tend to be well hydrated with both positive and negative groups, but have no net charge. In fact, zwitterions have been used as a surface coating on polymers to prevent adsorption of drugs.[37] The increase in amphotericin concentrations in the control samples over the first four hours was unexpected. Hemolysis was observed in control and circuit samples and can cause elevations in plasma concentrations when drug that is sequestered in the red blood cell is released into the extracellular space. A study of amphotericin B lipid complex showed that the amphotericin blood:plasma ratio was 1.5:1.[38] This degree of partitioning is not

likely to explain the observed increase in concentration as most hemolysis occurred after four hours and a concomitant increase would have been expected in the circuit samples, as well. It is more likely that amphotericin did not distribute evenly in the control sample solution leading to sampling error. The deoxycholic acid component of amphotericin disperses very rapidly in plasma. *In vitro* studies show that amphotericin solubility is time dependent, and amphotericin is not completely solubilized even at one hour.[39] It is possible that the amphotericin precipitated and was concentrated near the bottom of the control tubes. If samples were not adequately mixed, this could result in increasing concentrations until solubilization was complete. This phenomenon would be less likely in the ECMO circuit because it was flowing continuously. More work is necessary to understand the disposition of amphotericin B deoxycholate in this system. Additionally, studies should be conducted to characterize the circuit interactions with other, more commonly used amphotericin forumulations (e.g. liposomal, lipid complexed) that may result in interaction with the ECMO circuit.

In summary, it is clear that a single physicochemical property (e.g., lipophilicity) is unable to predict which and to what extent drugs are extracted by the ECMO circuit. Even if older circuits with uncoated, hydrophobic polymers were used, differences in the materials and residuals in the matrix such as plasticizers would likely require an empiric correction factor to accurately describe the extent of adsorption.[20] The circuit-drug interactions are even more complicated when surface coatings are applied. Although surface coatings are added primarily to increase biocompatibility, the impact on adsorption can be substantial. Studies comparing the adsorption of drugs between tubing with different surface coatings showed significant differences in drug recovery

both between coated and uncoated materials, and also between the different types of surface coatings.[16,17] Many knowledge gaps remain. It is unknown if surface coatings on ECMO circuits change over time. Further, it is unknown to what extent endogenous materials (e.g., plasma proteins, platelets) compete for binding sites on circuit components. Future work should explore high-throughput systems to evaluate the interaction between ECMO circuit components and different drugs. Until that time, *ex vivo* experiments remain the best way to define specific circuit-drug interactions. The results from the present *ex vivo* experiments will be used to inform the ECMO compartment of the fluconazole and micafungin PBPK models and translate those circuit-drug interactions into dosing recommendations in children on ECMO.

Table 2.1. Antifungal drug physicochemical properties and clearance pathways

Antifungal	Charge	LogP	Plasma Protein Binding (%)[a]	Molecular Weight (g/mol)	Primary Metabolic Pathway
Amphotericin	Zwitterion	0.8	90	924	Renal
Fluconazole	Neutral	0.4	11%	306	Renal
Micafungin	Negative	-0.4	99%	1270	Hepatic

[a]Amphotericin binds to plasma lipoproteins, albumin, and alpha-1-acid glycoprotein.[40,41] Fluconazole binds primarily to alpha-1acid-glycoprotein.[42,43] Micafungin binds primarily to albumin.[44]

Table 2.2. ECMO circuit components

Component	Manufacturer	Model	Material
Oxygenator	Maquet	Adult/Pediatric Quadrox iD[a]	Polymethylpentane hollow fibers with Bioline[b] coating
Hemofilter	Sorin	DHF0.2	Polyethersulfone
Pump	Sorin	Revolution Centrifugal	Polycarbonate
Tubing	Sorin	Smart Tubing	Phosphorylcholine coated polyvinylchloride

[a] Adult and pediatric oxygenators only differed in surface area ($1.8m^2$ for adult and $0.8m^2$ for pediatric). Because the oxygenator was not responsible for clinically significant extraction, and no difference was observed between adult and pediatric oxygenator circuits, adult and pediatric oxygenators were assumed to be equivalent for the purposes of these experiments.

Table 2.3. Number of circuits by configuration and drug

Configuration	Fluconazole	Micafungin	Amphotericin
A. Complete Circuit (hemofilter, oxygenator, pump, tubing)	3[a]	10[d]	3[g]
B. Oxygenator Circuit (oxygenator, pump, tubing)	4[b]	4[e]	-
C. Pump Circuit (pump, tubing)	1	1	-
D. Control	4[c]	4[f]	3[g]

[a] 1 circuit run for 4 hours; 2 circuits run for 24 hours

[b] 3 circuits run for 4 hours; 1 circuit run for 24 hours

[c] 4 controls sampled for 4 hours; 3 controls sampled for 24 hours

[d] 10 circuits stratified by albumin level (g/dL): low (≤ 1; N=4), low physiologic (2.2-2.8; N=3); physiologic (3.5-3.8; N=3). 1 circuit run for 4 hours (low albumin); 9 circuits run for 24 hours

[e] 2 circuits run for 4 hours; 2 circuits run for 24 hours

[f] 1 control sampled for 4 hours; 3 controls sampled for 24 hours

[g] All 3 circuits and controls sampled for 24 hours

Figure 2.1. Molecular Structure of Antifungals

Fluconazole[45]

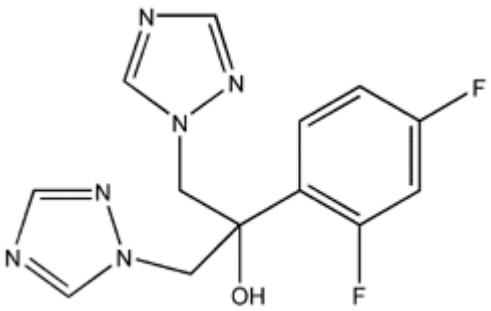

Micafungin[46]

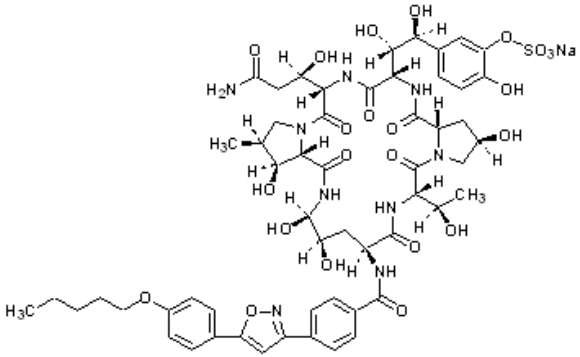

Amphotericin B deoxycholate[47]

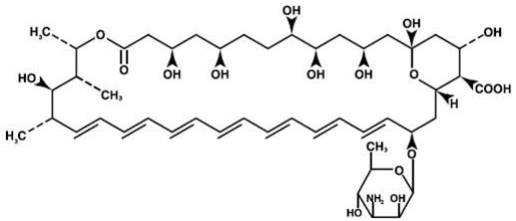

Figure 2.2. ECMO circuit configurations. A. Complete Circuit; B. Oxygenator Circuit; C. Pump Circuit

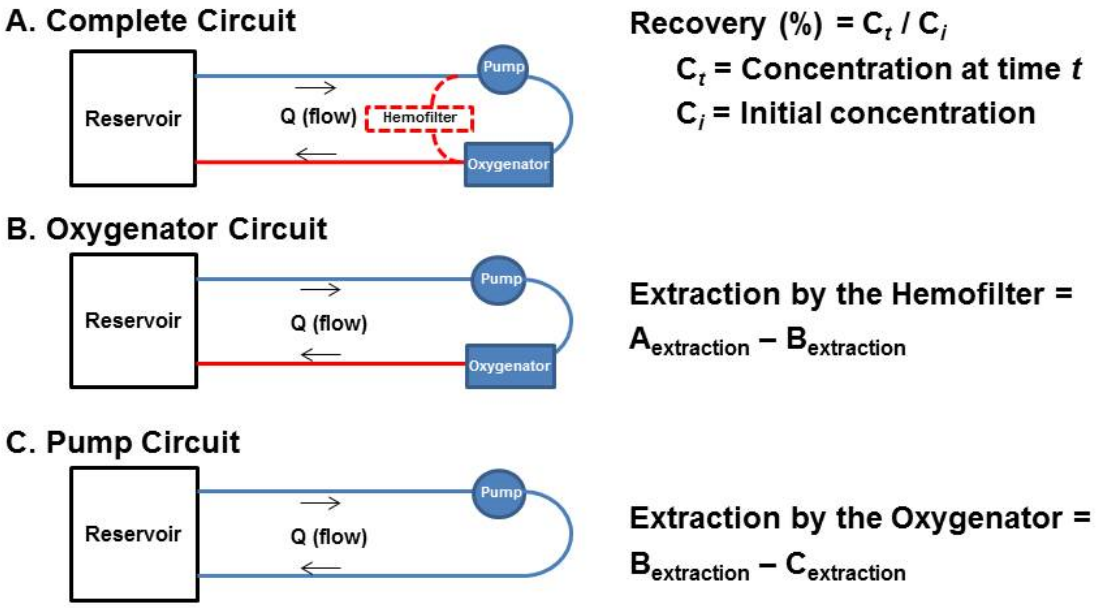

Figure 2.3. Recovery (mean [95% confidence interval]) by circuit configuration for each drug.

A Fluconazole – 4h

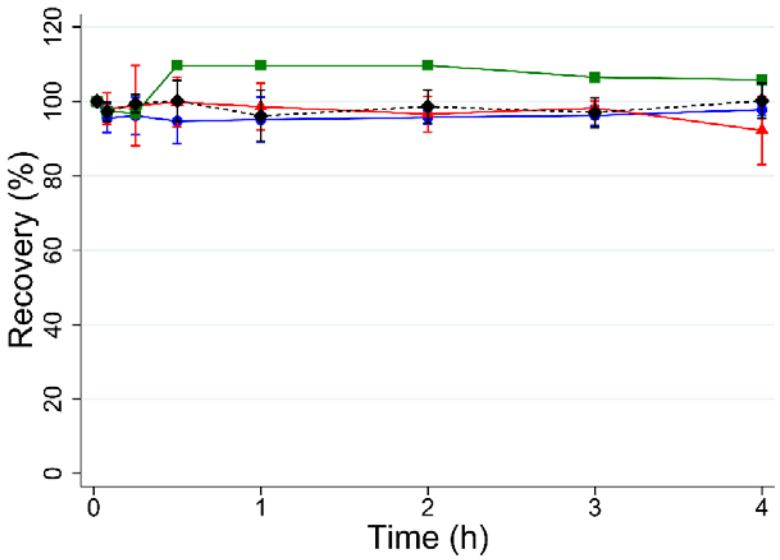

Fluconazole – 24h

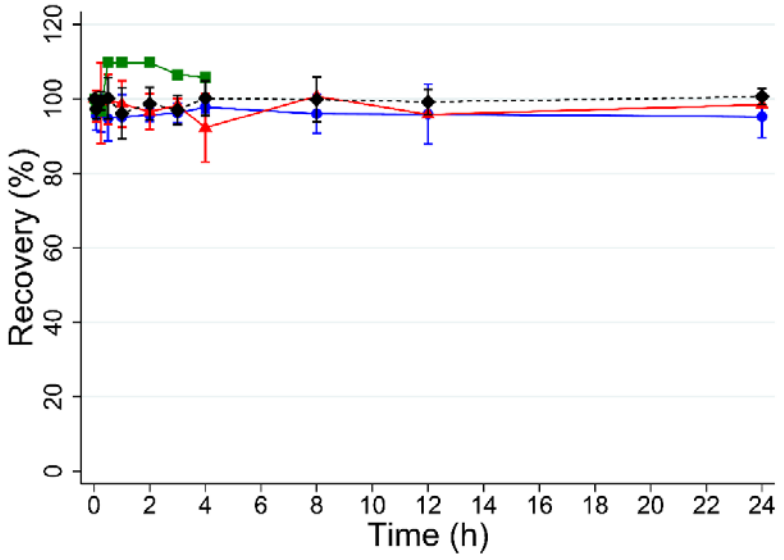

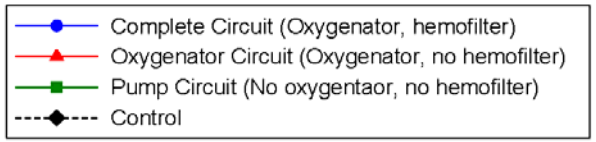

B Micafungin – 4h

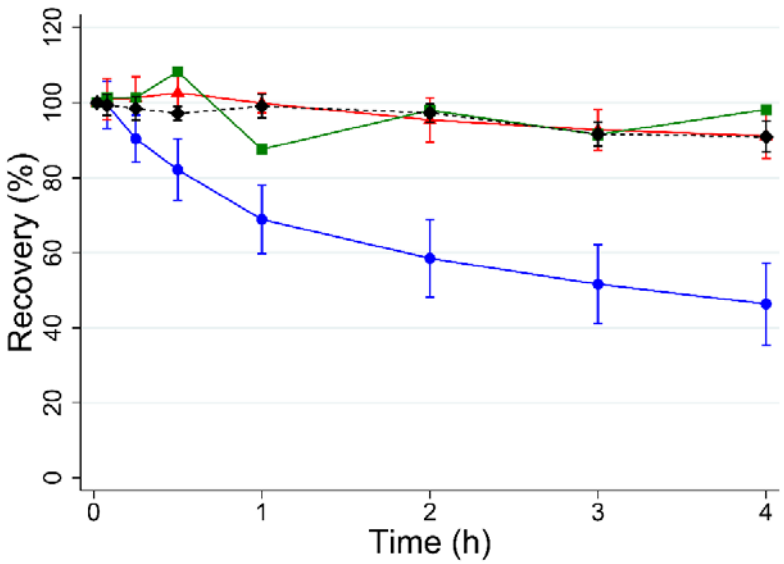

Micafungin – 24h

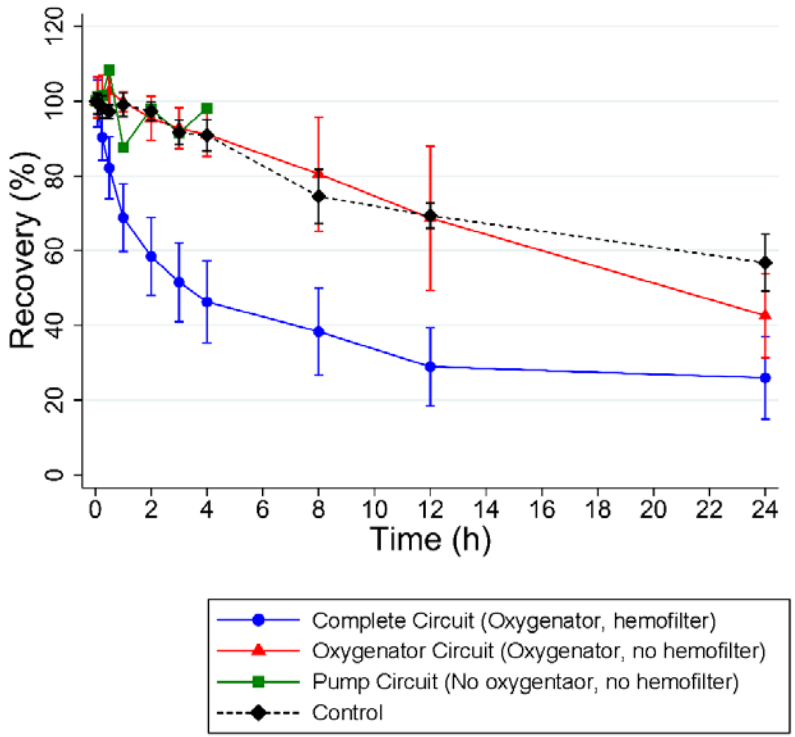

C Amphotericin B deoxycholate – 4h

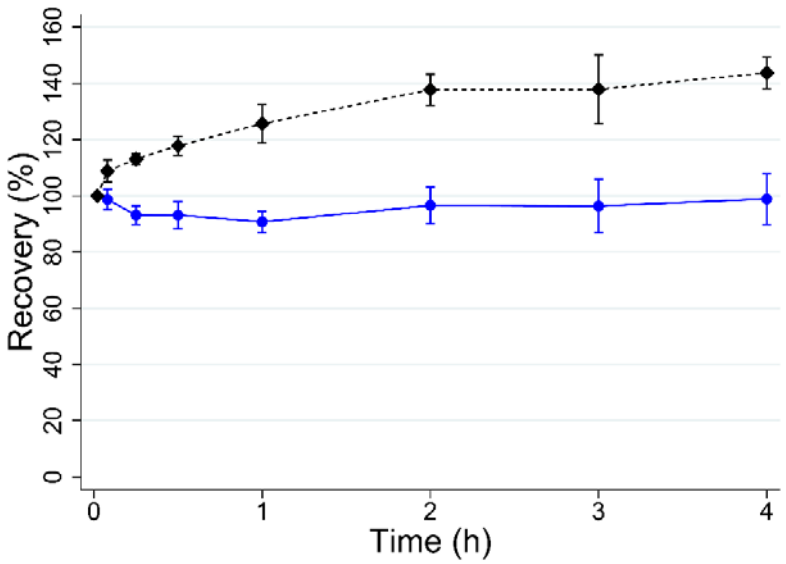

Amphotericin B deoxycholate – 12h

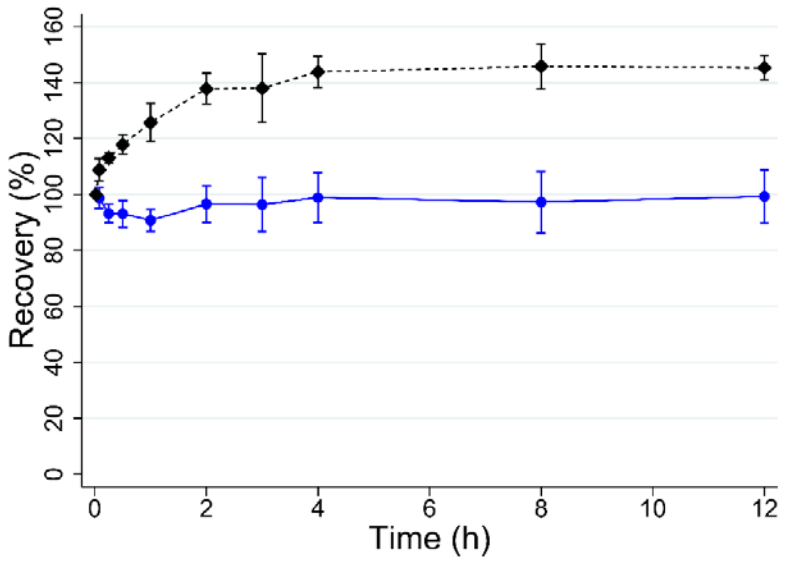

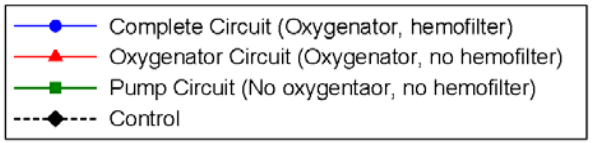

Figure 2.4. Micafungin recovery stratified by albumin concentration. Values are mean (95% confidence interval).

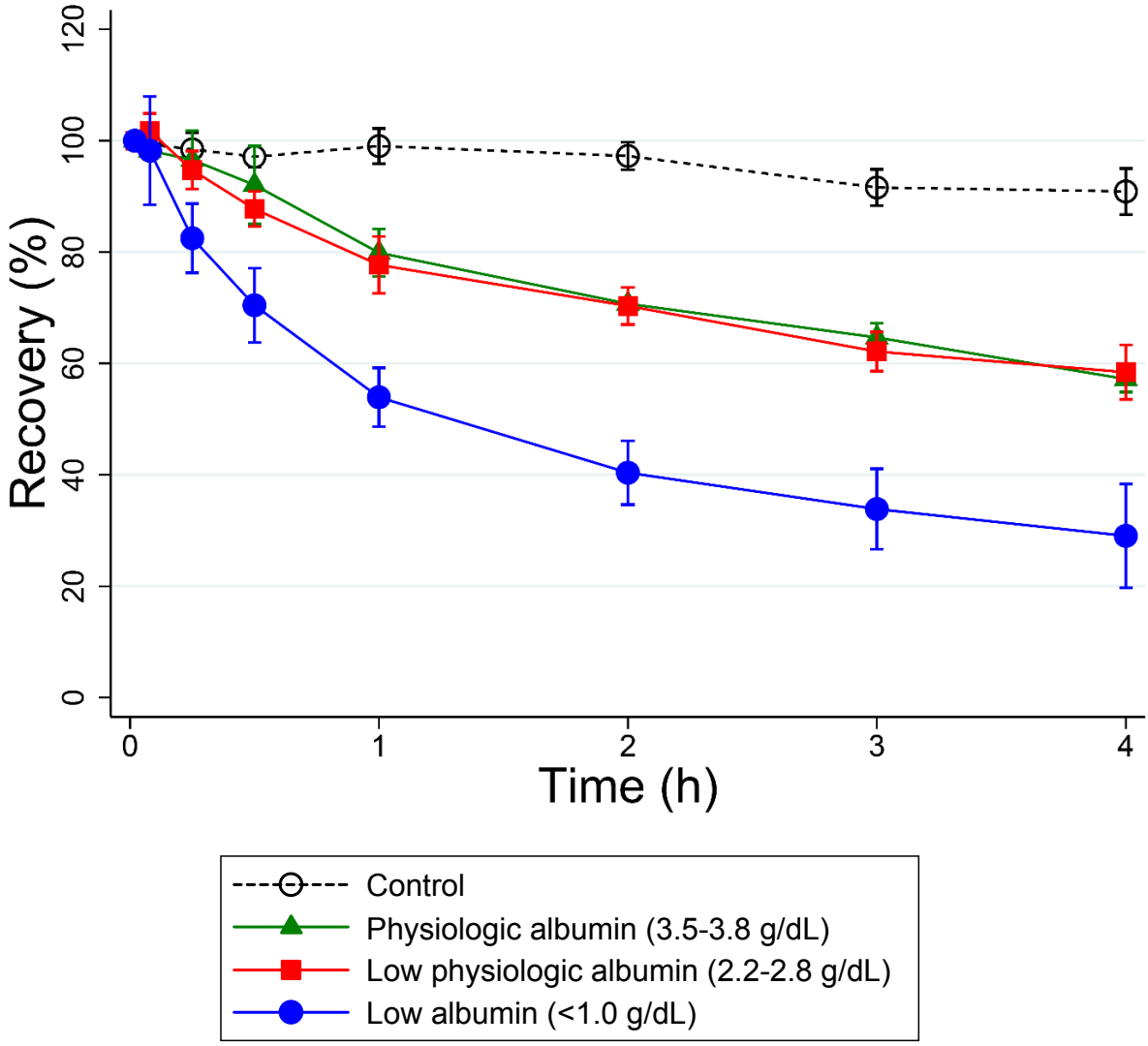

REFERENCES

1. Amaker RD, DiPiro JT, Bhatia J. Pharmacokinetics of vancomycin in critically ill infants undergoing extracorporeal membrane oxygenation. Antimicrob Agents Chemother 1996;40:1139-42.

2. Buck ML. Vancomycin pharmacokinetics in neonates receiving extracorporeal membrane oxygenation. Pharmacotherapy 1998;18:1082-6.

3. Donadello K, Roberts JA, Cristallini S, et al. Vancomycin population pharmacokinetics during extracorporeal membrane oxygenation therapy: a matched cohort study. Crit Care 2014;18:632.

4. Mulla H, Pooboni S. Population pharmacokinetics of vancomycin in patients receiving extracorporeal membrane oxygenation. Br J Clin Pharmacol 2005;60:265-75.

5. Bhatt-Mehta V, Johnson CE, Schumacher RE. Gentamicin pharmacokinetics in term neonates receiving extracorporeal membrane oxygenation. Pharmacotherapy 1992;12:28-32.

6. Cohen P, Collart L, Prober CG, Fischer AF, Blaschke TF. Gentamicin pharmacokinetics in neonates undergoing extracorporal membrane oxygenation. Pediatr Infect Dis J 1990;9:562-6.

7. Munzenberger PJ, Massoud N. Pharmacokinetics of gentamicin in neonatal patients supported with extracorporeal membrane oxygenation. ASAIO Trans 1991;37:16-8.

8. Southgate WM, DiPiro JT, Robertson AF. Pharmacokinetics of gentamicin in neonates on extracorporeal membrane oxygenation. Antimicrob Agents Chemother 1989;33:817-9.

9. Leuschen MP, Willett LD, Hoie EB, et al. Plasma fentanyl levels in infants undergoing extracorporeal membrane oxygenation. J Thorac Cardiovasc Surg 1993;105:885-91.

10. Dagan O, Klein J, Bohn D, Koren G. Effects of extracorporeal membrane oxygenation on morphine pharmacokinetics in infants. Crit Care Med 1994;22:1099-101.

11. Peters JW, Anderson BJ, Simons SH, Uges DR, Tibboel D. Morphine metabolite pharmacokinetics during venoarterial extra corporeal membrane oxygenation in neonates. Clin Pharmacokinet 2006;45:705-14.

12. Peters JW, Anderson BJ, Simons SH, Uges DR, Tibboel D. Morphine pharmacokinetics during venoarterial extracorporeal membrane oxygenation in neonates. Intensive Care Med 2005;31:257-63.

13. Ahsman MJ, Hanekamp M, Wildschut ED, Tibboel D, Mathot RA. Population pharmacokinetics of midazolam and its metabolites during venoarterial extracorporeal membrane oxygenation in neonates. Clin Pharmacokinet 2010;49:407-19.

14. Mulla H, McCormack P, Lawson G, Firmin RK, Upton DR. Pharmacokinetics of midazolam in neonates undergoing extracorporeal membrane oxygenation. Anesthesiology 2003;99:275-82.

15. Harthan AA, Buckley KW, Heger ML, Fortuna RS, Mays K. Medication adsorption into contemporary extracorporeal membrane oxygenator circuits. The journal of pediatric pharmacology and therapeutics : JPPT : the official journal of PPAG 2014;19:288-95.

16. Preston TJ, Hodge AB, Riley JB, Leib-Sargel C, Nicol KK. In vitro drug adsorption and plasma free hemoglobin levels associated with hollow fiber oxygenators in the extracorporeal life support (ECLS) circuit. The journal of extra-corporeal technology 2007;39:234-7.

17. Preston TJ, Ratliff TM, Gomez D, et al. Modified surface coatings and their effect on drug adsorption within the extracorporeal life support circuit. The journal of extra-corporeal technology 2010;42:199-202.

18. Palmgren JJ, Monkkonen J, Korjamo T, Hassinen A, Auriola S. Drug adsorption to plastic containers and retention of drugs in cultured cells under in vitro conditions. European journal of pharmaceutics and biopharmaceutics : official journal of Arbeitsgemeinschaft fur Pharmazeutische Verfahrenstechnik eV 2006;64:369-78.

19. Unger JK, Kuehlein G, Schroers A, Gerlach JC, Rossaint R. Adsorption of xenobiotics to plastic tubing incorporated into dynamic in vitro systems used in pharmacological research--limits and progress. Biomaterials 2001;22:2031-7.

20. Marchal-Heussler L, Barra J. Adsorption of Drugs. In: Hubbard AT, ed. Encyclopedia of Surface and Colloid Science. New York: Marcel Dekker, Inc.; 2002:294-306.

21. Shekar K, Fraser JF, Taccone FS, et al. The combined effects of extracorporeal membrane oxygenation and renal replacement therapy on meropenem pharmacokinetics: a matched cohort study. Crit Care 2014;18:565.

22. Shekar K, Roberts JA, McDonald CI, et al. Sequestration of drugs in the circuit may lead to therapeutic failure during extracorporeal membrane oxygenation. Crit Care 2012;16:R194.

23. Shekar K, Roberts JA, McDonald CI, et al. Protein-bound drugs are prone to sequestration in the extracorporeal membrane oxygenation circuit: results from an ex vivo study. Crit Care 2015;19:164.

24. Lemaitre F, Hasni N, Leprince P, et al. Propofol, midazolam, vancomycin and cyclosporine therapeutic drug monitoring in extracorporeal membrane oxygenation circuits primed with whole human blood. Crit Care 2015;19:40.

25. Ahsman MJ, Wildschut ED, Tibboel D, Mathot RA. Pharmacokinetics of cefotaxime and desacetylcefotaxime in infants during extracorporeal membrane oxygenation. Antimicrob Agents Chemother 2010;54:1734-41.

26. van der Vorst MM, Wildschut E, Houmes RJ, et al. Evaluation of furosemide regimens in neonates treated with extracorporeal membrane oxygenation. Crit Care 2006;10:R168.

27. Wildschut ED, de Hoog M, Ahsman MJ, Tibboel D, Osterhaus AD, Fraaij PL. Plasma concentrations of oseltamivir and oseltamivir carboxylate in critically ill children on extracorporeal membrane oxygenation support. PLoS One 2010;5:e10938.

28. Mehta NM, Halwick DR, Dodson BL, Thompson JE, Arnold JH. Potential drug sequestration during extracorporeal membrane oxygenation: results from an ex vivo experiment. Intensive Care Med 2007;33:1018-24.

29. Mulla H, Lawson G, von Anrep C, et al. In vitro evaluation of sedative drug losses during extracorporeal membrane oxygenation. Perfusion 2000;15:21-6.

30. Wildschut ED, Ahsman MJ, Allegaert K, Mathot RA, Tibboel D. Determinants of drug absorption in different ECMO circuits. Intensive Care Med 2010;36:2109-16.

31. Bizzarro MJ, Conrad SA, Kaufman DA, Rycus P. Infections acquired during extracorporeal membrane oxygenation in neonates, children, and adults. Pediatr Crit Care Med 2010.

32. FDA U. Guidance for industry bioanalytical method validation. In: Center for Drug Evaluation and Research (U.S.), Center for Veterinary Medicine (U.S.), eds. Rockville, MD: U.S. Dept. of Health and Human Services, Food and Drug Administration, Center for Drug Evaluation and Research : Center for Veterinary Medicine,; 2001:1 online resource (22 p.).

33. Dagan O, Klein J, Gruenwald C, Bohn D, Barker G, Koren G. Preliminary studies of the effects of extracorporeal membrane oxygenator on the disposition of common pediatric drugs. Ther Drug Monit 1993;15:263-6.

34. Hirata K, Aoyama T, Matsumoto Y, et al. Pharmacokinetics of antifungal agent micafungin in critically ill patients receiving continuous hemodialysis filtration. Yakugaku zasshi : Journal of the Pharmaceutical Society of Japan 2007;127:897-901.

35. Maseda E, Grau S, Villagran MJ, et al. Micafungin pharmacokinetic/pharmacodynamic adequacy for the treatment of invasive candidiasis in critically ill patients on continuous venovenous haemofiltration. J Antimicrob Chemother 2014;69:1624-32.

36. EMA. Mycamine : EPAR - Product Information In: Agency EM, ed. Leiderdorp, The Netherlands: Astellas Pharma Europe B.V.; 2010.

37. Ye SH, Arazawa DT, Zhu Y, et al. Hollow fiber membrane modification with functional zwitterionic macromolecules for improved thromboresistance in artificial lungs. Langmuir 2015;31:2463-71.

38. Ramaswamy M, Wasan KM. Differences in the method by which plasma is separated from whole blood influences amphotericin B plasma recovery and distribution following amphotericin B lipid complex incubation within whole blood. Drug development and industrial pharmacy 2001;27:871-5.

39. Edmonds LC, Davidson L, Bertino JS, Jr. Solubility and stability of amphotericin B in human serum. Ther Drug Monit 1989;11:323-6.

40. Brajtburg J, Elberg S, Bolard J, et al. Interaction of plasma proteins and lipoproteins with amphotericin B. J Infect Dis 1984;149:986-97.

41. Bekersky I, Fielding RM, Dressler DE, Lee JW, Buell DN, Walsh TJ. Plasma protein binding of amphotericin B and pharmacokinetics of bound versus unbound amphotericin B after administration of intravenous liposomal amphotericin B (AmBisome) and amphotericin B deoxycholate. Antimicrob Agents Chemother 2002;46:834-40.

42. Arredondo G, Calvo R, Marcos F, Martinez-Jorda R, Suarez E. Protein binding of itraconazole and fluconazole in patients with cancer. International journal of clinical pharmacology and therapeutics 1995;33:449-52.

43. Arredondo G, Martinez-Jorda R, Calvo R, Aguirre C, Suarez E. Protein binding of itraconazole and fluconazole in patients with chronic renal failure. International journal of clinical pharmacology and therapeutics 1994;32:361-4.

44. EMA. Assessment Report for Mycamine. In: European Medicines Agency CfMPfHU, ed. London; 2008.

45. FDA. Fluconazole Injection, USP Product Label. In: U.S. Dept. of Health and Human Services FaDA, ed.: Roerig, a division of Pfizer, Inc.; 2015.

46. FDA. MYCAMINE (micafungin sodium) For Injection Product Label. In: U.S. Dept. of Health and Human Services FaDA, ed.: Astellas Pharma US, Inc.; 2013.

47. FDA. Amphotericin B for Injection USP Product Label. In: U.S. Dept. of Health and Human Services FaDA, ed.: X-GEN Pharmaceuticals, Inc.; 2011.

CHAPTER 3: PHARMACOKINETICS OF FLUCONAZOLE IN CHILDREN SUPPORTED WITH EXTRACORPOREAL MEMBRANE OXYGENATION

PART1: Pharmacokinetics and Safety of Fluconazole in Young Infants Supported with Extracorporeal Membrane Oxygenation[1]

INTRODUCTION

Extracorporeal membrane oxygenation (ECMO) is a cardiopulmonary bypass device used in the pediatric critical care setting that is life-saving for infants with refractory cardiorespiratory failure. Blood is drained from the central venous system via a surgically placed cannula, pumped through an artificial lung (oxygenator) where oxygen is added and carbon dioxide is removed, and then oxygenated blood is returned to either the venous or arterial circulation. ECMO has been used successfully in multiple disease states including meconium aspiration syndrome, persistent pulmonary hypertension of the newborn, fulminant myocarditis, and sepsis.[2] Despite these successes, infants supported with ECMO are at high risk for ECMO-related complications, including nosocomial infections.[3]

Invasive candidiasis is the second most common nosocomial infection in infants on ECMO and is often fatal.[3,4] The incidence of fungal infections in patients on ECMO varies by center, with reports ranging from 0.7-10%.[3,4] Standard treatment for invasive

[1]This chapter previously appeared in an article in the *Pediatr Infect Dis J.* 2012 Oct;31(10):1042-7. Pharmacokinetics and safety of fluconazole in young infants supported with extracorporeal membrane oxygenation. Watt KM, Benjamin DK Jr, Cheifetz IM, Moorthy G, Wade KC, Smith PB, Brouwer KL, Capparelli EV, Cohen-Wolkowiez M

candidiasis in many patient populations consists of antifungal agents (e.g., fluconazole) and removal or replacement of intravascular catheters due to the organism's ability to adhere to indwelling catheters.[5] Catheter removal for infants on EMO is impossible if the infant cannot be disconnected from the ECMO circuit; therefore, successful treatment of invasive candidiasis in infants on ECMO relies upon optimal antifungal drug therapy.

Optimal antifungal management for patients on ECMO depends on dosing that has not been previously described and can differ greatly from other populations due to the pharmacokinetic (PK) changes induced by the ECMO circuit. PK changes attributed to the ECMO circuit include increased volume of distribution and decreased clearance, but these vary by drug.[6-9] This study describes the ECMO-related PK changes of fluconazole and their impact on pharmacodynamic (PD) targets for fungal prophylaxis and treatment of invasive candidiasis.

MATERIALS AND METHODS

This was a prospective, single-center, open-label PK and safety trial of fluconazole in infants supported with ECMO at Duke University Medical Center. Infants <120 postnatal days and supported with ECMO were enrolled. Infants were excluded if they had a history of hypersensitivity or severe vasomotor reaction to any triazole or had previously participated in the study. Infants received either prophylactic fluconazole per study protocol (25 mg/kg administered intravenously over 2 hours) or fluconazole per standard of care (12 mg/kg administered intravenously over 1 hour) if the child had a known or suspected fungal infection. Infants on prophylactic fluconazole continued to receive fluconazole 25 mg/kg once weekly for the duration of their ECMO course.

Duration of treatment for infants with suspected or culture-proven fungal infection was at the discretion of the treating physician. This trial was approved by the institutional review board of Duke University Medical Center, registered with clinicaltrials.gov (NCT01169402), and conducted under a Food and Drug Administration investigational new drug application (#108314). Written informed consent was obtained from the legal guardian of each infant.

Sample Collection and Preparation

Up to 12 paired samples (200 µL whole blood per sample) were collected from the infant via an arterial catheter (C_{out}) and the ECMO circuit just before the oxygenator (C_{in}) for each infant at dose 1 and dose 2. Sampling times for all enrolled infants included a trough level 0–4 hours prior to the start of infusion and serial samples after the end of the infusion: 15 minutes (+/– 15 minutes), 3 hours (+/– 1 hour), 9 hours (+/– 3 hours), 23 hours (+/– 1 hour), and 47 hours (+/– 1 hour). Samples were collected in ethylenediaminetetraacetic acid (EDTA) microcontainers and taken from a different site than the site used for fluconazole administration. Samples were processed immediately or placed on ice until processing. Plasma was separated via centrifugation (3000 g for 10 minutes at 4^{o} C), manually aspirated, and transferred to polypropylene tubes. Plasma samples were frozen at –80^{o} C until analysis.

Fluconazole extraction by the ECMO oxygenator was calculated using the paired samples collected from the ECMO circuit just prior to the oxygenator (C_{in}) and from the patient (C_{out}) using the equation: $[(C_{in} – C_{out}) / C_{in}] * 100$. Any extraction levels greater than 3 standard deviations above or below the mean extraction were considered outliers

and were excluded from the analysis. Venous (C_{in}) samples were used for all PK analyses.

ECMO Circuit Configuration

The ECMO circuit configuration was consistent across all infants and included tubing (Sorin Smart®, Sorin Group, Denver, CO), a centrifugal pump (Sorin Revolution®, Sorin Group, Denver, CO), and a hollow fiber membrane oxygenator (Quadrox-iD Adult® or Quadrox-iD Pediatric®, MAQUET Cardiovascular, Wayne, NJ). A hemofilter (Sorin DHFO.2®, Sorin Group, Denver, CO) was used if the infant required hemofiltration or hemodialysis. The circuit prime volume was 450 mL for the Quadrox-iD Adult® oxygenator (infants 2, 3, 5, 7, 9, 10) and 250 mL for the Quadrox-iD Pediatric® oxygenator (infants 1, 4, 6, 8).

Analytic Procedures and Analyses

Plasma fluconazole concentrations were determined using a validated liquid chromatography-tandem mass spectrometry assay.[10] The lower limit of quantification was 0.01 mg/L; intraday and interday precision ranged from 2.84% to 10.8% and 5.27% to 11.5%, respectively, within the concentration range of the standard curve (0.01 to 10 mg/L).

The primary outcomes were the fluconazole PK indices in infants on ECMO (clearance, volume of distribution) and the number of infants achieving the proposed PD target for fungal prophylaxis (fluconazole time above the minimum inhibitory concentration [t_{MIC}; 4 mg/L] for >50% of the dosing interval).[11] In addition, the proportion

of infants achieving the surrogate PD target for treatment (area under the curve from 0–24 hours [$AUC_{0–24}$] > 400 mg*h/L)[12] of invasive candidiasis was calculated. This was performed because the dose evaluated in this study has previously been evaluated for treatment of candidiasis.[13] The secondary outcome was fluconazole extraction by the ECMO circuit. The PK indices of fluconazole were examined with descriptive statistics.

PK data were analyzed by nonlinear regression with the most appropriate model using WinNonlin v. 6.2 (Pharsight Co., St. Louis, MO). The model fit was evaluated using successful minimization, diagnostic plots, goodness of fit as assessed by the Akaike Information Criterion, and precision of the parameter estimates. $AUC_{0–24}$ was computed by the linear trapezoidal method using simulated data predicted from the 1-compartment model. The t_{MIC} was estimated and expressed as a percentage of the dose interval using the following equation:

$$C_{last} = MIC * e^{-k(t_{last}-t_{MIC})}$$

where C_{last} is last simulated fluconazole concentration from the terminal elimination phase using the predicted data from the 1-compartment model; MIC is the minimum inhibitory concentration (4 mg/L); k is the elimination rate constant derived from the 1-compartment model; t_{last} is time of last fluconazole concentration using the predicted data from the 1-compartment model; and t_{MIC} is estimated time above the MIC. For an infant on standard-of-care fluconazole (12 mg/kg daily), $AUC_{0–24}$ and t_{MIC} were calculated using the simulated data after administration of a 25 mg/kg dose using the clearance and volume of distribution estimates from the 1-compartment model.

The relationships between fluconazole clearance and serum creatinine on the day of dose, as well as the fluconazole volume of distribution and the ECMO prime

volume were explored with scatter plots. Differences in PK indices between doses were evaluated using Wilcoxon signed-rank test. Correlation between ECMO circuit extraction and time was measured with Spearman's rank correlation coefficient. The sample size was based on the ability to provide reasonable estimates for safety. It was determined a priori that, with a sample size of 8, the 95% confidence interval (CI) for an adverse event (AE) in 1 infant within the patient population was 0–53%. STATA 11 (College Station, TX) was used to perform the statistical analyses. In all cases, a *P* value of <0.05 was considered statistically significant.

Safety

The safety of fluconazole was assessed by monitoring the frequency, intensity, and relationship to study drug of AEs while on study drug and for 7 days after the last dose. The results of clinical laboratory tests performed within 72 hours of study drug administration and weekly throughout the monitoring period were recorded. The primary AE of interest was liver toxicity assessed by the evaluation of aspartate aminotransferase (AST) and alanine aminotransferase (ALT) values measured at least weekly during study drug administration. AEs were graded according to the National Cancer Institute's Common Terminology Criteria and reported as mild (grade 1), moderate (grade 2), severe (grade 3), life-threatening (grade 4), or fatal (grade 5). Causality (unrelated and possibly, probably and definitely related) of AEs and study drug was determined by the principal investigator and the treating physician. AEs determined to be probably or definitely related to study drug were followed until resolution. The safety data were summarized descriptively.

RESULTS

Between August 2010 and July 2011, 10 infants with a median age of 19 days (range 1–113 days) supported with ECMO were enrolled in the study, received at least 1 dose of fluconazole, and were included in the safety analysis (Table 3.1.1). Nine infants received prophylactic intravenous fluconazole (25 mg/kg weekly infused over 2 hours), and 1 infant (#7) was treated for presumed fungal infection with standard-of-care fluconazole (12 mg/kg intravenously daily infused over 1 hour). PK samples were collected from the 9 infants on prophylaxis around the first dose, and the 6 infants who remained on ECMO for more than 1 week were also sampled around the second dose. Infant #7, who received fluconazole 12 mg/kg/day, had PK samples collected around the final seventh dose. Thirty percent of infants were female, 60% were white, and 10% were Hispanic. Three infants were born pre-term. At time of cannulation, median corrected age was 41 weeks (range 36–53 weeks). Hemofiltration and/or continuous veno-venous hemodialysis (CVVHD) was used in 3 infants. Overall serum creatinine was similar between first dose and multiple dose evaluations, although 2 infants receiving hemofiltration or CVVHD had a 3-fold increase in their serum creatinine between dose 1 and 2. The renal dysfunction in infant #3 was multifactorial, while that in infant #6 was due to intrinsic renal dysfunction following cardiac arrest. In both cases, renal dysfunction occurred prior to initiation of hemofiltration.

Pharmacokinetics

PK data were evaluated from 62 plasma samples around the first dose and 47 samples after multiple doses. The plasma concentrations after the first dose and after

multiple doses are shown in Figure 3.1.1. The PK indices after first and multiple doses are presented in Table 3.1.2. A 1-compartment model with zero-order infusion appropriately described the data, and PK indices were estimated with high precision as evidenced by median clearance coefficient of variation of 10.2% (range 2.0–25.8%) and median volume of distribution coefficient of variation of 5.7% (range 1.4–16.1%). After the first dose, the median (interquartile range [IQR]) clearance was 17 mL/kg/h (14, 22), the median volume of distribution was 1.5 L/kg (1.3, 1.7), and the median $AUC_{0–24}$ was 322 mg*h/L (307, 343). After multiple doses, the median (IQR) clearance was 22 mL/kg/h (11, 33), the median volume of distribution was 1.9 L/kg (1.4, 2.2), and the $AUC_{0–24}$ was 352 mg*h/L (344, 399). Fluconazole clearance was inversely related to serum creatinine (Figure 3.1.2). Neither fluconazole clearance (*P*=0.92) nor serum creatinine (*P*=0.67) was significantly different between the first and multiple doses. There was no relationship between the fluconazole volume of distribution and amount of the volume of exogenous blood needed to prime the ECMO circuit (data not shown). A relationship between postnatal age and clearance and gestational age and clearance was not observed during visual inspection of scatter plots (data not shown). The volume of distribution of fluconazole did not differ significantly between dose 1 and multiple doses (*P*=0.14). The median fluconazole trough concentration before dose 2 was 1.8 mg/L (range 0.2–5.4).

Pharmacodynamic Targets

After the first dose, 7 out of 9 infants (78%) achieved the prophylaxis target of t_{MIC} (4 mg/L) for >84 hours, which was 50% of the dosing interval.[10] Only 1 infant (11%)

achieved the therapeutic target for treatment of invasive candidiasis of AUC_{0-24} > 400 h*mg/L (Figure 3.1.3).[11] After multiple doses of fluconazole, 5 out of 7 infants (71%) achieved the prophylaxis target, and none achieved the therapeutic target. None of the infants developed a fungal infection while enrolled in the study.

ECMO Circuit Extraction

A total of 210 samples were included in the extraction analysis after 2 paired samples (1.9%) were identified as outliers and excluded from the analysis. Mean fluconazole extraction across the oxygenator was –2.0% (standard deviation 15.0), but there was wide dispersion around the mean. Extraction by the oxygenator did not correlate with the age of the ECMO circuit (rho= –0.05).

Safety

There were 11 AEs in 6 infants, including 3 deaths. None of the AEs were probably or definitely related to study drug (Table 3.1.3). Three infants had elevated AST or ALT levels. In all 3 cases, the transaminase levels were elevated prior to initiation of study fluconazole and declined to normal levels while on study drug. Of the 3 infants who died, 2 of the deaths were attributed to severe congenital heart disease, and 1 death was attributed to intracranial hemorrhage.

DISCUSSION

Invasive candidiasis can be a devastating complication of ECMO. Invasive candidiasis is difficult to treat in this setting and is associated with higher mortality

compared with infants on ECMO without invasive candidiasis.[3,4] Infants on ECMO with invasive disease require optimal dosing of antifungal drugs and may benefit from fungal prophylaxis. To prevent or treat invasive infection, the first step is to determine exposure of a candidate drug. This requires at least 1 PK and safety study in infants supported by ECMO because the ECMO circuit can substantially alter the PK of drugs through the addition of large volumes of exogenous blood to prime the ECMO circuit, adhesion of drug to components of the ECMO circuit, and renal insufficiency common in infants on ECMO.[14]

The complexity of the ECMO circuit and its impact on dosing have been observed for drugs that require therapeutic drug monitoring such as gentamicin[7,15–17] and vancomycin.[9,18,19] PK data of antifungals in ECMO, however, are extremely scarce. Two case reports suggested that voriconazole and caspofungin may be extracted by the ECMO circuit, resulting initially in subtherapeutic exposure with standard dosing, although voriconazole concentrations became supra-therapeutic over time, consistent with decreased clearance.[20,21] The voriconazole data were supported by an *ex vivo* ECMO model indicating that 71% of a voriconazole dose was adsorbed by the ECMO circuit within 3 hours of administration.[22]

In this PK trial of fluconazole in infants on ECMO, volume of distribution was 50–90% higher and clearance was similar in infants on ECMO compared with a similar cohort of critically ill infants not on ECMO,[13] resulting in lower fluconazole exposure ($AUC_{0–24}$) (Table 3.1.4). The increased volume of distribution in infants on ECMO is consistent with physiology: infants have a total blood volume of ~80 mL/kg (estimated range for our cohort 160–500 mL), and 250–450 mL of blood are required to prime the

ECMO circuit. Thus, the circuit effectively doubles the native blood volume of these infants. Clearance was inversely related to serum creatinine. This relationship was also expected as the kidneys constitute the primary fluconazole elimination pathway. Therefore, renal function should be considered when dosing fluconazole in this population. However, fluconazole clearance can be affected by the concurrent use of hemofiltration or CVVHD. In adults supported with CVVHD, higher doses of fluconazole were required to maintain adequate exposure due to effective drug removal by the CVVHD system.[23] Three of the infants enrolled in the present study received hemofiltration, and 1 received CVVHD. While the small sample size limits generalization of results (these 3 infants had the lowest, median, and highest fluconazole clearances, respectively), infant #3 who was supported with both hemofiltration and CVVHD had a threefold rise in serum creatinine between the start of dose 1 and start of dose 2, the lowest clearance, and the highest volume of distribution. This pattern of renal insufficiency is common in children on ECMO and supports the hypothesis that, for renally cleared drugs, a larger dose administered less frequently is appropriate.

Fluconazole undergoes minimal extraction by the ECMO circuit, and that extraction is not influenced by the age of the ECMO circuit. This finding is consistent with the low lipophilicity of fluconazole. Prior studies of drugs administered during ECMO have shown that increased lipophilicity is associated with increased adsorption by the circuit.[24] Therefore, the findings from this study should not be extrapolated to other antifungal agents within and outside of class. Echinocandins have excellent activity against *Candida* species and penetrate biofilms, an appealing quality in a population for whom catheter removal is impossible. However, as a class, they are

nearly 100% protein-bound and highly lipophilic, which may predispose them to high adhesion to the ECMO circuit.

PK/PD indices for fluconazole prophylaxis are not well defined. Dosing for fluconazole prophylaxis in immuno-compromised adults ranges from 50–200 mg/day, targeting an AUC_{0-24} of 50–200 mg*h/L, though with these strategies some resistance to fluconazole has developed. In premature infants, doses of 3–6 mg/kg given twice per week have been shown to decrease the incidence of invasive candidiasis without concurrent development of resistance, though the power to detect differences in resistance in these studies was low.[25–27] A murine model of invasive candidiasis showed that resistance could be prevented if fluconazole serum concentrations were kept above the MIC for >50% of the dosing interval.[11] The typical MIC of *Candida* species in children ranges from 0.25 to 4 mg/L.[25–28]

In this trial of fluconazole prophylaxis of infants on ECMO, fluconazole 25 mg/kg weekly resulted in exposures comparable to those seen in prophylaxis trials in adults and children with malignancy[29] and premature infants.[25–27] Further, at this dose, fluconazole serum concentrations were kept above the MIC of 4 mg/L for 50% of the dosing interval in over 70% of infants on ECMO. Fluconazole 25 mg/kg weekly should be adequate to prevent invasive candidiasis in infants supported with ECMO and prevent development of resistance.

However, a fluconazole dose of 25 mg/kg did not achieve the necessary exposure to treat invasive candidiasis (AUC_{0-24} >400 mg*h/L) in this population on ECMO. This is in contrast to a cohort of critically ill children not on ECMO, in whom this therapeutic target was achieved in 70% of infants who received a fluconazole loading

dose of 25 mg/kg.[13] Fluconazole PK is linear up to 40 mg/kg;[30,31] thus, a fluconazole loading dose of 30–40 mg/kg would be needed to achieve an $AUC_{0–24}$ effective to treat *Candida* infection in infants on ECMO. Only 1 infant in this study received daily fluconazole treatment doses (12 mg/kg/day), which limits the assessment of exposures achieved after repeat daily dosing. A fluconazole therapeutic regimen should be prospectively evaluated.

The decision to use fluconazole prophylaxis in children on ECMO should be based on individual risk factors and center-specific incidence of fungal infection. The overall rate of fungal infection for all ECMO centers is relatively low at 2 per 1000 ECMO days.[3] Prophylaxis for a low-prevalence infection must be weighed against the devastating consequences of and difficulty treating a fungal infection in this population.[4] A multi-center trial evaluating the epidemiology of fungal infection and efficacy of antifungal prophylaxis in children on ECMO is urgently needed.

Table 3.1.1. Demographics

Infant	Weight (kg)	Gestational Age (weeks)	Postnatal Age (days)	Diagnosis	Serum Creatinine (mg/dL) Dose 1	Serum Creatinine (mg/dL) Dose 2	Hemofiltration/ CVVHD
1	2.7	36	1	CHD	1	0.9	N/N
2	3.2	37	7	PPHN	0.5	0.5	N/N
3	3.9	41	7	MecAsp	0.6	1.8	Y/Y
4	2.0	38	18	CHD	1.6	-	N/N
5	3.3	40	18	CDH	0.1	0.1	N/N
6	3.4	39	20	Sepsis	0.4	1.5	Y/N
7	3.2	38	24	PPHN	-	0.6	N/N
8	2.4	34	32	CHD	0.7	-	N/N
9	2.5	30	96	CHD	0.3	0.2	Y/N
10	6.2	37	113	CHD	0.6	-	N/N
Median	**3.2**	**37**	**19**		**0.6**	**0.7**	
IQR	**2.6, 3.4**	**36, 39**	**9, 30**		**0.4, 0.7**	**0.3, 1.4**	

Gestational age refers to time elapsed between conception and delivery. Weight and postnatal age were calculated at time of enrollment, which was within 24 hours of first dose of study fluconazole for all infants except #7. Infant #7 was on standard-of-care fluconazole, and enrollment occurred between doses 6 and 7.

Serum creatinine refers to the concentration measured closest to the dose.

CHD indicates congenital heart disease; PPHN, persistent pulmonary hypertension; MecAsp, meconium aspiration; CVVHD, continuous veno-venous hemodialysis; IQR, interquartile range.

Table 3.1.2. Pharmacokinetic Indices

	First Dose						Multiple Doses					
ID	Dose (mg/kg)	CL (mL/h/kg)	V (L/kg)	$t_{1/2}$ (h)	t_{MIC} (%)	AUC_{0-24} (h*mg/L)	Dose (mg/kg)	CL (mL/h/kg)	V (L/kg)	$t_{1/2}$ (h)	t_{MIC} (%)	AUC_{0-24} (h*mg/L)
1	25	19	1.3	47	63	367	25	22	1.5	46	61	385
2	25	22	1.7	55	61	288	25	19	1.9	68	83	352
3	25	10	1.7	116	132	324	25	9	2.3	189	233	399
4	25	17	1.5	60	75	343	-	-	-	-	-	-
5	25	33	1.4	29	39	322	25	33	1.4	29	38	347
6	25	16	1.7	75	85	307	25	11	1.9	115	152	424
7*	-	-	-	-	-	-	12	22	2.2	56	438	299†
8	25	14	1.7	79	91	316	-	-	-	-	-	-
9	25	44	1.3	21	28	303	25	35	1.4	27	39	344
10	25	11	1.2	76	106	423	-	-	-	-	-	-
Median		**17**	**1.5**	**60**	**75**	**322**		**22**	**1.9**	**56**	**83**	**352**
IQR		**14, 22**	**1.3, 1.7**	**47, 76**	**61, 91**	**307, 343**		**11, 33**	**1.4, 2.2**	**37, 92**	**39, 233**	**344, 399**

*Infant 7 was on fluconazole per standard of care (12 mg/kg IV daily), and PK sampling occurred after the final (seventh) dose. All other multiple-dose data were obtained during the infants' second dose.

†t_{MIC} and AUC_{0-24} for infant 7 were obtained by simulating exposure after a dose of 25 mg/kg using clearance and volume of distribution derived from the 1-compartment model.

CL indicates clearance; V, volume of distribution; $t_{1/2}$, half-life; t_{MIC}, percentage of the dosing interval that fluconazole concentration was above the minimum inhibitory concentration of 4 mg/L (PD target was 50% of dosing interval); AUC_{0-24}, area under the curve from 0–24 hours (PD target 400 h*mg/L); IQR, interquartile range.

Table 3.1.3. Adverse Events

Infant	Adverse Event	Intensity	Causality
1	Cardiac arrest due to cardiac anatomy	Death	Unrelated
	Renal hemorrhage	Severe	Unrelated
	Conjugated hyperbilirubinemia	Moderate	Unlikely
3	Transaminitis	Mild	Unrelated
5	Supraventricular tachycardia	Moderate	Unrelated
6	Adenovirus sepsis	Life-threatening	Unrelated
	Cardiac arrest due to myocarditis	Life-threatening	Unrelated
	Cerebral hemorrhage	Death	Unrelated
	Transaminitis	Mild	Unrelated
7	Transaminitis	Mild	Unrelated
8	Cardiac arrest due to cardiac anatomy	Death	Unrelated

Table 3.1.4. Pharmacokinetic Indices in Infants on ECMO after the First Dose of Intravenous Fluconazole 25 mg/kg Compared with Historical Controls not on ECMO who Received 1 Dose of Intravenous Fluconazole 25 mg/kg[13]

	ECMO	Non-ECMO	*P*
V (L/kg)	1.5 (1.3, 1.7)	1.0 (0.8, 1.4)	0.02
CL (ml/h/kg)	17 (14, 22)	18 (14, 22)	0.57
$t_{1/2}$ (h)	60 (47, 76)	39 (24, 79)	0.49
AUC_{0-24} (h*mg/L)	322 (307, 343)	476 (366, 492)	0.01

Data for historical controls were extracted from Piper et al.[13] minus their infant on ECMO and compared using Wilcoxon signed-rank test.

ECMO indicates extracorporeal membrane oxygenation; V, volume of distribution; CL, clearance; $t_{1/2,}$ half-life; AUC_{0-24}, area under the curve from 0–24 hours. All values are median (interquartile range).

FIGURE 3.1.1. Fluconazole concentration time profiles. **A.** Dose 1: Plasma concentration-time profiles in young infants (n=9) after receiving first dose of intravenous fluconazole 25 mg/kg. Concentrations at time=0 hours are concentrations prior to first dose. Pharmacodynamic (PD) target for prevention of fungal infection is serum concentration > minimum inhibitory concentration (MIC) (4 mg/L) for 84 hours (50% of the dosing interval). **B.** Dose 2: Plasma concentration-time profiles in young infants after receiving second dose of intravenous fluconazole 25 mg/kg (n=6). Infant #7 who received treatment fluconazole (12 mg/kg daily) is not represented in this figure. Concentrations at time=0 hours are trough concentrations prior to the second dose. PD target for prevention of fungal infection is serum concentration >MIC (4 mg/L) for 50% of the dosing interval, which was 84 hours for the once-weekly 25 mg/kg dose.

A.

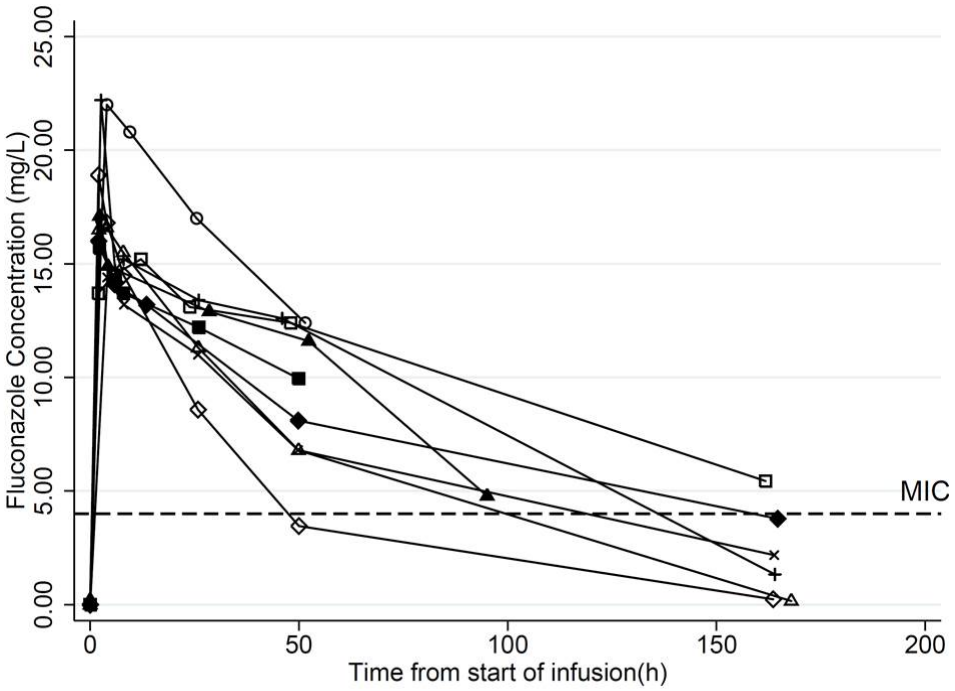

B.

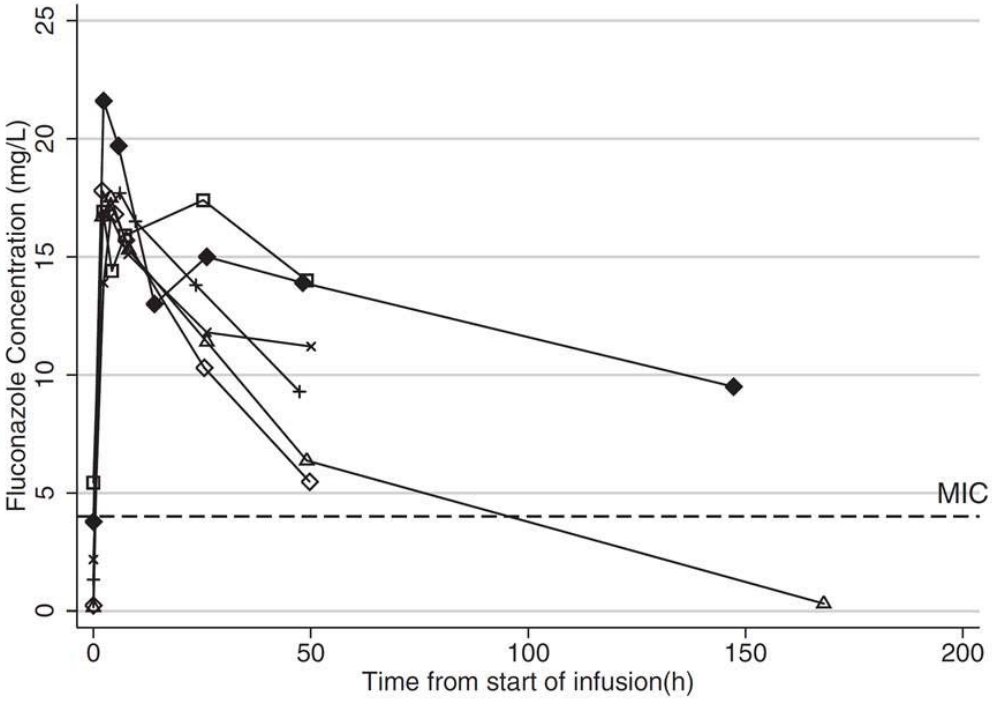
Fluconazole Concentration (mg/L)
0
5
10
15
20
25
MIC
0
50
100
150
200
Time from start of infusion(h)

Figure 3.1.2. Serum creatinine versus clearance

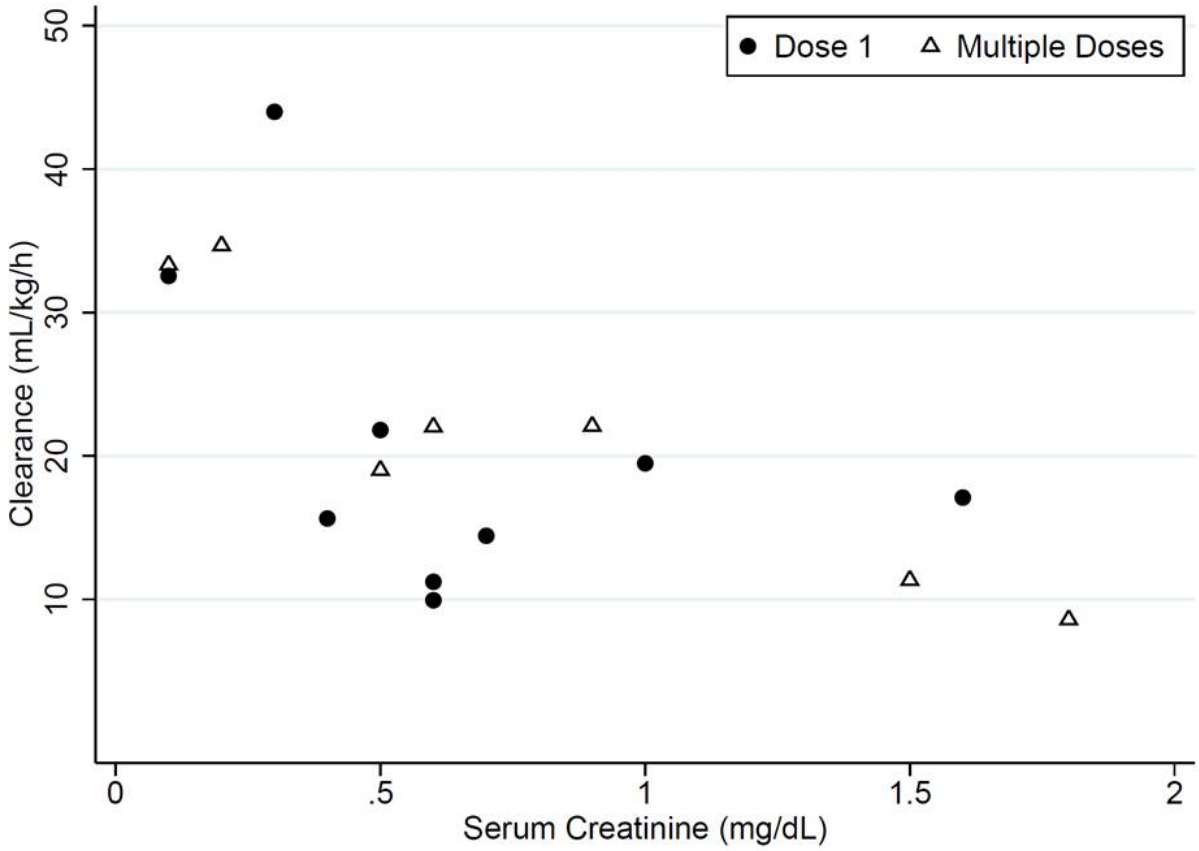

Figure 3.1.3. Median (interquartile range) fluconazole exposure in the first 24 hours ($AUC_{0–24}$) after dose 1 and multiple doses. Pharmacodynamic target for therapy is $AUC_{0–24}$ >400 h*mg/L. $AUC_{0–24}$ indicates area under the curve from 0–24 hours.

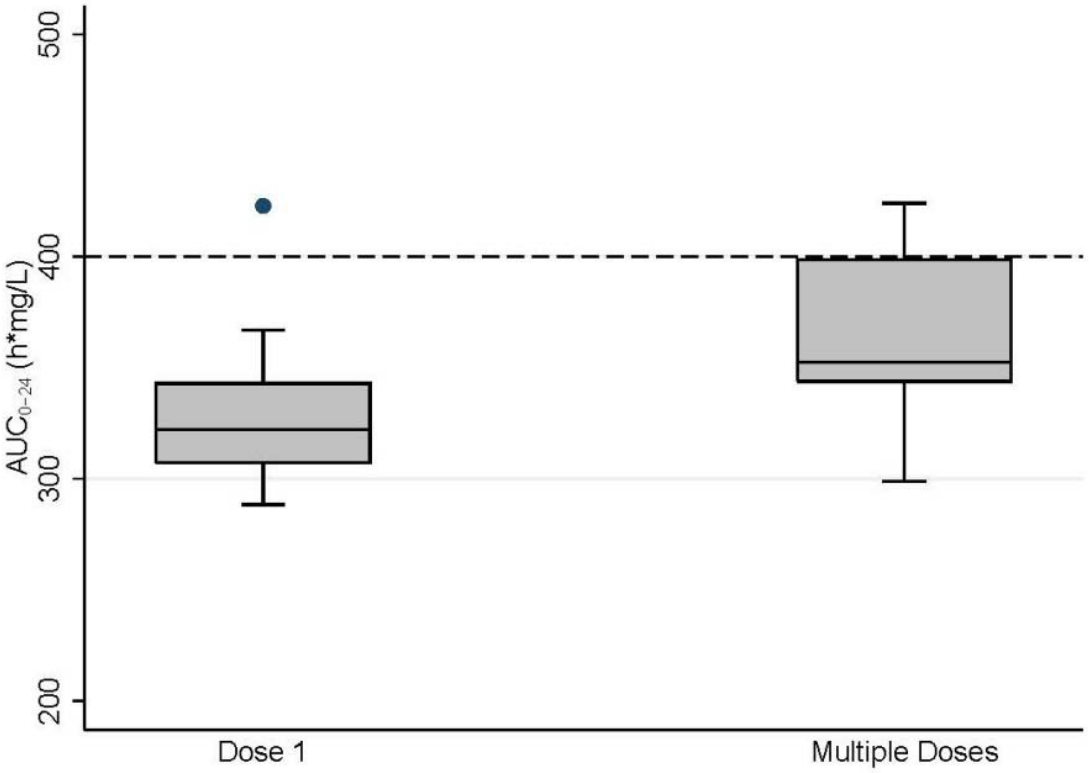

REFERENCES

1. Watt KM, Benjamin DK, Jr., Cheifetz IM, Moorthy G, Wade KC, Smith PB, Brouwer KL, Capparelli EV, Cohen-Wolkowiez M. 2012. Pharmacokinetics and safety of fluconazole in young infants supported with extracorporeal membrane oxygenation. Pediatr Infect Dis J 31:1042-1047.

2. Extracorporeal Life Support Organization (ELSO). Extracorporeal Life Support Registry Report: International Summary. Ann Arbor, MI: ELSO; 2010.

3. Bizzarro MJ, Conrad SA, Kaufman DA, Rycus P; Extracorporeal Life Support Organization Task Force on Infections, Extracorporeal Membrane Oxygenation. Infections acquired during extracorporeal membrane oxygenation in neonates, children, and adults. Pediatr Crit Care Med. 2011;12:277–281.

4. Gardner AH, Prodhan P, Stovall SH, et al. Fungal infections and antifungal prophylaxis in pediatric cardiac extracorporeal life support. J Thorac Cardiovasc Surg. 2011 Dec 15. [Epub ahead of print]

5. Eppes SC, Troutman JL, Gutman LT. Outcome of treatment of candidemia in children whose central catheters were removed or retained. Pediatr Infect Dis J. 1989;8:99–104.

6. Veinstein A, Debouverie O, Grégoire N, et al. Lack of effect of extracorporeal membrane oxygenation on tigecycline pharmacokinetics. J Antimicrob Chemother. 2011 Dec 29. [Epub ahead of print]

7. Wildschut ED, de Hoog M, Ahsman MJ, Tibboel D, Osterhaus AD, Fraaij PL. Plasma concentrations of oseltamivir and oseltamivir carboxylate in critically ill children on extracorporeal membrane oxygenation support. PLoS One. 2010;5:e10938.

8. Bhatt-Mehta V, Johnson CE, Schumacher RE. Gentamicin pharmacokinetics in term neonates receiving extracorporeal membrane oxygenation. Pharmacotherapy. 1992;12:28–32.

9. Mulla H, Pooboni S. Population pharmacokinetics of vancomycin in patients receiving extracorporeal membrane oxygenation. Br J Clin Pharmacol. 2005;60:265–275.

10. Wu D, Wade KC, Paul DJ, Barrett JS. A rapid and sensitive LC-MS/MS method for determination of fluconazole in human plasma and its application in infants with Candida infections. Ther Drug Monit. 2009;31:703–709.

11. Andes D, Forrest A, Lepak A, Nett J, Marchillo K, Lincoln L. Impact of antimicrobial dosing regimen on evolution of drug resistance in vivo: fluconazole and Candida albicans. Antimicrob Agents Chemother. 2006;50:2374–2383.

12. Wade KC, Benjamin DK Jr, Kaufman DA, et al. Fluconazole dosing for the prevention or treatment of invasive candidiasis in young infants. Pediatr Infect Dis J. 2009;28:717–723.

13. Piper L, Smith PB, Hornik CP, et al. Fluconazole loading dose pharmacokinetics and safety in infants. Pediatr Infect Dis J. 2011;30: 375–378.

14. Dagan O, Klein J, Gruenwald C, Bohn D, Barker G, Koren G. Preliminary studies of the effects of extracorporeal membrane oxygenator on the disposition of common pediatric drugs. Ther Drug Monit. 1993;15:263–266.

15. Cohen P, Collart L, Prober CG, Fischer AF, Blaschke TF. Gentamicin pharmacokinetics in neonates undergoing extracorporal membrane oxygenation. Pediatr Infect Dis J. 1990;9:562–566.

16. Munzenberger PJ, Massoud N. Pharmacokinetics of gentamicin in neonatal patients supported with extracorporeal membrane oxygenation. ASAIO Trans. 1991;37:16–18.

17. Southgate WM, DiPiro JT, Robertson AF. Pharmacokinetics of gentamicin in neonates on extracorporeal membrane oxygenation. Antimicrob Agents Chemother. 1989;33:817–819.

18. Buck ML. Vancomycin pharmacokinetics in neonates receiving extracorporeal membrane oxygenation. Pharmacotherapy. 1998;18:1082–1086.

19. Hoie EB, Swigart SA, Leuschen MP, et al. Vancomycin pharmacokinetics in infants undergoing extracorporeal membrane oxygenation. Clin Pharm. 1990;9:711–715.

20. Ruiz S, Papy E, Da Silva D, et al. Potential voriconazole and caspofungin sequestration during extracorporeal membrane oxygenation. Intensive Care Med. 2009;35:183–184.

21. Spriet I, Annaert P, Meersseman P, et al. Pharmacokinetics of caspofungin and voriconazole in critically ill patients during extracorporeal membrane oxygenation. J Antimicrob Chemother. 2009;63:767–770.

22. Mehta NM, Halwick DR, Dodson BL, Thompson JE, Arnold JH. Potential drug sequestration during extracorporeal membrane oxygenation: results from an ex vivo experiment. Intensive Care Med. 2007;33:1018–1024.

23. Yagasaki K, Gando S, Matsuda N, et al. Pharmacokinetics and the most suitable dosing regimen of fluconazole in critically ill patients receiving continuous hemodiafiltration. Intensive Care Med. 2003;29:1844–1848.

24. Wildschut ED, Ahsman MJ, Allegaert K, Mathot RA, Tibboel D. Determinants of drug absorption in different ECMO circuits. Intensive Care Med. 2010;36:2109–2116.

25. Kaufman D, Boyle R, Hazen KC, Patrie JT, Robinson M, Donowitz LG. Fluconazole prophylaxis against fungal colonization and infection in preterm infants. N Engl J Med. 2001;345:1660–1666.

26. Kaufman D, Boyle R, Hazen KC, Patrie JT, Robinson M, Grossman LB. Twice weekly fluconazole prophylaxis for prevention of invasive Candida infection in high-risk infants of <1000 grams birth weight. J Pediatr. 2005;147:172–179.

27. Manzoni P, Stolfi I, Pugni L, et al. A multicenter, randomized trial of prophylactic fluconazole in preterm neonates. N Engl J Med. 2007;356:2483–2495.

28. Kicklighter SD, Springer SC, Cox T, Hulsey TC, Turner RB. Fluconazole for prophylaxis against candidal rectal colonization in the very low birth weight infant. Pediatrics. 2001;107:293–298.

29. van Burik JA, Ratanatharathorn V, Stepan DE, et al. Micafungin versus fluconazole for prophylaxis against invasive fungal infections during neutropenia in patients undergoing hematopoietic stem cell transplantation. Clin Infect Dis. 2004;39:1407–1416.

30. Anaissie EJ, Kontoyiannis DP, Huls C, et al. Safety, plasma concentrations, and efficacy of high-dose fluconazole in invasive mold infections. J Infect Dis. 1995;172:599–602.

31. Humphrey MJ, Jevons S, Tarbit MH. Pharmacokinetic evaluation of uk-49,858, a metabolically stable triazole antifungal drug, in animals and humans. Antimicrob Agents Chemother. 1985;28:648–653.

PART 2: Fluconzole Population Pharmacokinetics and Dosing for the Prevention and Treatment of Invasive Candidiasis in Children Supported with Extracorporeal Membrane Oxygenation[1]

INTRODUCTION

Extracorporeal membrane oxygenation (ECMO) is life-saving in children with cardiorespiratory failure. ECMO is a cardiopulmonary bypass device that provides complete respiratory and cardiac support. Mechanically, blood is drained from the venous system, pumped through an artificial lung membrane where oxygen is added and carbon dioxide removed, and then returned to either the venous or arterial circulation. ECMO has been used successfully to support children with multiple disease processes including meconium aspiration syndrome, fulminant myocarditis, and sepsis.[2] Despite these successes, children supported with ECMO are at high risk for ECMO-related complications, especially nosocomial infections.[3]

Invasive candidiasis is common and fatal in children on ECMO. In this population, Candida species are the most common infectious organism.[3] Incidence varies by center and rates as high as 10% have been reported.[3,4] Candida infections cause substantial morbidity and mortality[4] and are difficult to eradicate due to the organism's ability to adhere to indwelling catheters. For this reason, routine management for candidiasis consists not only of antifungal agents but also removal of

[1]This chapter previously appeared in an article in *Antimicrobial agents and chemotherapy. 2015; 59(7):3935-43.* Fluconazole population pharmacokinetics and dosing for prevention and treatment of invasive Candidiasis in children supported with extracorporeal membrane oxygenation. Watt KM, Gonzalez D, Benjamin DK Jr, Brouwer LR, Wade KC, Capparelli E, Barrett J, and Cohen-Wolkowiez M.

catheters.[5] Catheter removal for children on ECMO is often impossible, because the ECMO cannulas connect the child to the ECMO circuit. Therefore, therapy on ECMO relies on either prevention of invasive candidiasis or optimal therapeutic dosing in children with infection. Optimal dosing for prevention or treatment of candidiasis in children on ECMO can differ greatly from other populations due to the pharmacokinetic (PK) changes induced by the ECMO circuit. PK changes attributed to ECMO support include increased volume of distribution and decreased clearance, but these vary by drug and are not consistently predicted using drug physicochemical properties.[6-9] This study describes the population PK of fluconazole in children supported with ECMO and provides rational dosing recommendations for the prevention and treatment of invasive candidiasis in this vulnerable population.

METHODS

Study Design

Fluconazole samples were obtained from three prospective trials: Study 1 was a single-center, open-label PK study of fluconazole in children on ECMO (n=20);[10] Study 2 was a single center PK study of a fluconazole loading dose in critically ill children (n=12);[11] and Study 3 was a multi-center PK study of fluconazole in infants (n=8).[12] The study designs are described in detail elsewhere.[10-12] In brief, Study 1 included critically ill children <18 years of age supported with ECMO who received intravenous (IV) fluconazole (25 mg/kg once weekly for prophylaxis or standard of care dosing for presumed fungal infection) for prevention or treatment of fungal infection. Study 2

included critically ill infants <1 year of age, one of whom was supported by ECMO, who received a fluconazole loading dose (25 mg/kg IV once) followed by daily maintenance therapy (12 mg/kg IV). Study 3 enrolled infants 23- to 42-week gestational age at birth, who were <120 days of age and were receiving IV fluconazole for prevention or treatment of candidiasis. We only included children from Study 3 who were > 36 weeks gestation to limit the PK variability introduced by prematurity. These trials were approved by the respective institutional review boards and written informed consent was obtained from the legal guardian of each child.

The following clinical variables were collected for all studies: postnatal age (PNA), weight, race, sex, presence of ECMO support, use of hemofiltration or dialysis, and serum creatinine (SCR). Serum albumin, aspartate aminotransferase (AST), and serum alanine aminotransferase (ALT) were collected for Study 1 and Study 2. PNA and weight were calculated on the day of first dose of study drug and those values imputed forward. For children with multiple measurements of SCR, albumin, AST, or ALT, values were allowed to change with time. For children without albumin, AST, or ALT measurements during the study period, values were set to the population medians (2.7 g/dL, 35 U/L, and 19 U/L, respectively). Comparison of covariate values between children on ECMO and those not on ECMO was done using Wilcoxon rank sum test in STATA 12 (College Station, TX).

PK Sample Collection

Children in Study 1 had up to 12 plasma samples (200 µL) collected around dose 1 and 2. Sampling windows at each dose included: 0–4 hours prior to the start of infusion and serial samples after the end of the infusion: 15 minutes (+/– 15 minutes), 3 hours (+/– 1 hour), 9 hours (+/– 3 hours), 23 hours (+/– 1 hour), and 47 hours (+/– 1 hour). Children in Study 2 had 6 to 8 plasma samples (200 µL) after the loading dose at the following time points after the end of the infusion: 15 minutes (+/– 15 minutes), 3 hours (+/– 1 hour), 9 hours (+/– 3 hours), 21 hours (+/– 3 hours); and multi-dose sampling after doses 3 and 5 (0 to 4 hours before dose and 2 to 6 hours after dose). Infants enrolled in Study 3 were sampled pre-infusion, at the end of infusion, and 1, 7 (+/- 1) or 11 (+/- 1), 24, and 48 h post-infusion. Samples were collected in ethylenediaminetetraacetic acid (EDTA) microcontainers and taken from a different site than the site used for fluconazole administration. Samples were processed immediately or placed on ice until processing. Plasma was separated via centrifugation (3000 g for 10 minutes at 4^{o} C), manually aspirated, and transferred to polypropylene tubes. Plasma samples were frozen at –80^{o}C until analysis. To supplement these PK samples, plasma from leftover clinical samples collected per standard of care (EDTA Microtainers) was collected up to 72 h after sample collection. Fluconazole scavenge samples have been shown previously to be stable for up to 72 hours.[12]

Analytic Procedures

Plasma fluconazole concentrations were determined using a validated liquid chromatography-tandem mass spectrometry assay.[13] The lower limit of quantification was 0.01 mg/L; intraday and interday precision ranged from 2.84% to 10.8% and 5.27% to 11.5%, respectively, within the concentration range of the standard curve (0.01 to 10 mg/L).

Population PK Analysis

PK data were analyzed with a nonlinear mixed effect modeling approach using NONMEM v7.2 (Icon Development Solutions, Ellicott City, MD) in conjunction with Perl speaks NONMEM v3.6.2.[14] Run management was performed using Pirana v2.8.0.[15] Model analysis was summarized with STATA 12 (College Station, TX). A first order conditional estimation with interaction was used for all models. One and two-compartment PK structural models were evaluated. Inter-individual random effects were evaluated on CL and V, and both diagonal and block Omega matrices for covariance were explored. An exponential model for inter-individual variance was used. ETA shrinkage was assessed to determine if the PK dataset was informative to adequately estimate inter-individual variability in PK parameter estimates. Proportional and additive plus proportional error models of residual variability were assessed. Body weight was incorporated into the base model before evaluation of other covariates due to multi-collinearity with other clinical covariates. Both linear and allometric scaling of weight was assessed for clearance. For volume and intercompartmental clearance parameters,

size-based scaling was incorporated using a linear relationship with body weight. The impact of physiologically plausible covariates was evaluated if a relationship was suggested by visual inspection of scatter and box plots (continuous and categorical variables, respectively) of individual Bayesian estimates of CL and V obtained from the base model against covariates. The following covariates were evaluated: ECMO support; volume of blood required to prime the ECMO circuit; ratio of blood prime volume to a child's estimated native blood volume; hemofiltration; use of continuous venovenous hemodialysis (CVVHD); SCR; albumin; AST; and ALT; PNA; sex; and race. All continuous variables were centered using the median value. Covariate testing was performed via standard stepwise forward addition backward elimination methods. Covariates were included in the multivariable analysis if the decrease in the objective function value relative to the base model was at least 3.84 ($p<0.05$). Covariates were retained in the final model if their removal from the multivariable model caused an increase in the objective function value of at least 6.635 ($p<0.01$). Empirical Bayesian estimates of individual PK parameters were generated from the final model using the post hoc subroutine.

Model Evaluation

Models were evaluated based on the successful minimization, goodness of fit plots, objective function values, plausibility of parameter estimates, and precision of parameter estimates. The precision of the final model was evaluated through bootstrapping with 1000 replicate datasets to generate median and 95% confidence

intervals for the PK parameter estimates. In addition, visual predictive check was used to evaluate model predictability by simulating 1000 datasets based on the final parameter estimates and their associated variance. The dosing and covariate values used to generate the predictions in the standardized visual predictive check were the same as those used in the study population. Simulated results were compared with results observed in the study and the number of observed concentrations outside of the 90% prediction interval was quantified.

Assessment of Dose-Exposure Relationship

Fluconazole exhibits time-dependent fungistatic activity with a prolonged post-antibiotic effect and efficacy is most closely associated with an area under the concentration time curve: minimum inhibitory concentration (AUC/MIC) ratio > 50.[16-18] For treatment, we chose to target a minimum AUC_{0-24} of 400 mg*h/L in 90% of children. The AUC_{0-24} of 400 mg*h/L achieves the target AUC/MIC ratio assuming a MIC of 8 mg/L, the clinical laboratory standards institute (CLSI) sensitivity breakpoint for all Candida species.[19] There are no established pharmacodynamic targets for prophylaxis; so we chose an AUC_{0-24} of 200 mg*h/L in 90% of simulated children to match the exposure seen in adults on 200-400 mg daily for prophylaxis.[20-22] For prophylaxis it is important to minimize development of Candida resistance. The risk of developing resistance increases when fluconazole concentrations are below MIC for <50% of the dosing interval.[23] Therefore, for prophylaxis, we also evaluated as a secondary endpoint the percentage of the dosing interval that concentrations were above MIC ($\%t_{MIC}$).

Monte Carlo simulations using parameter estimates from the final model were used to explore dose-exposure relationships using these targets. We explored a variety of dosing regimens based on current IDSA guidelines[20] and our previous work describing fluconazole exposure in children on ECMO.[10] We simulated 100 PK profiles for each child in the dataset based on the parameter estimates and variability derived from the final model to measure target attainment rates in the first 24 hours and at steady state. We stratified children by presence or absence of ECMO support. Using parameter estimates from the final model, we calculated the maximum (C_{max}) and minimum (C_{min}) fluconazole concentrations for each of 14 simulated dosing intervals using the equation for an intermittent infusion. We then used the C_{max} and C_{min} values to calculate AUC_{0-24} for each dosing interval using the linear-up log-down trapezoidal approach.

RESULTS

Study infants and PK specimens

PK samples were collected from 40 children who received intravenous (IV) fluconazole. The median (range) age of the children was 22 days (1 day, 17 years; Table 3.2.1). While some children were born prematurely, the median postmenstrual age for children less than 1 year of age was 41 weeks (35, 76). Data from 360 plasma PK samples with a median of 8 samples per child (1, 22) were included in the population PK analysis. Fifty-five (15%) of the PK samples were scavenge samples (Study 1 n=32; Study 2 n=6; Study 3 n=17). Twenty-one (53%) children were supported

by ECMO. Five of the children on ECMO had concomitant hemofiltration during PK sample collection and two of those children subsequently required CVVHD. The median number of SCR samples collected during the study period per child was 10 (1, 23). All children had a SCR sample at time of first dose. The median SCR value at the time of first dose was 0.4 mg/dL (0.1, 1.3) and the maximum SCR during the PK sampling period was 0.6 mg/dL (0.1, 3.2). The initial SCR was not significantly different between children on ECMO and those not on ECMO (0.5 vs 0.3 mg/dL, p=0.13). However, children on ECMO had a higher maximum SCR than children not on ECMO (0.7 vs 0.5 mg/dL, p=0.03). Albumin and AST/ALT lab values were available for all children on ECMO but only half of those not on ECMO. Median albumin levels were low at 2.7 whereas AST/ALT were within normal limits (Table 3.2.1). No children developed culture-confirmed invasive candidiasis while on study.

Population PK model development

A summary of the model building process is shown in Table 3.2.2. Based on goodness of fit criteria, a one compartment model best described the data. Weight was included in the base model for CL and V. CL and V were not correlated and use of a covariance term between CL and V did not improve model fit. ETA shrinkage of the base model was low for both CL (4.6%) and V (7.0%), allowing us to reliably estimate inter-individual variability for both parameters. Similarly the EPS shrinkage was low at 9.6% suggesting that our model was not over-parameterized. Residual variability was best described by a proportional error model. While a proportional plus additive error

model resulted in a significant drop in the objective function, we were unable to precisely estimate the additive error component. Because goodness of fit plots and estimates were virtually identical between the two error models, we used the proportional error model in the final model. Allometric scaling of weight (3/4 power) on CL did not improve model fit and increased the objective function value by 9.7 points. Similarly, use of a sigmoidal Emax maturation relationship between postmenstrual age and CL resulted in an increase in the objective function value by 4.8 points. Consequently weight was scaled to the power of 1 for both CL and V. The residual unexplained inter-individual variability in CL was visually associated with SCR, hemofiltration, CVVHD, and albumin; while ECMO support, hemofiltration, and CVVHD were associated with inter-individual variability in V. During the univariable analysis, SCR and hemofiltration on CL, and ECMO and hemofiltration on V, resulted in a significant drop in the objective function and were included in the multivariable analysis. Neither ECMO prime volume nor the ratio of prime volume to native blood volume improved the model fit on V better than presence of ECMO support. Because these covariates are collinear with ECMO, we only included the effect of ECMO on V in the multivariable analysis. In the multivariable analysis, during the forward addition step, the addition of SCR and hemofiltration to CL, and ECMO support and hemofiltration to V, resulted in a significant drop in the objective function. However, during backward elimination, hemofiltration on CL and V did not improve the model goodness of fit nor did it significantly decrease the objective function value. The final model included the effect of SCR on CL, and ECMO on V.

$$CL\ (L/h) = 0.019 * Weight * (SCR/0.5)^{-0.29} * \exp(\eta CL)$$

$$V\ (L) = 0.93 * Weight * 1.4^{ECMO} * \exp(\eta V)$$

Where ηCL and ηV refer to the interindividual variability on CL and V, respectively. ECMO=1 if ECMO is present and 0 if ECMO is not present.

Model Evaluation and Validation

The final model had good precision as evidenced by relative standard errors around the parameter point estimates for fixed effects (5.6-9.9%) and random effects (13.1-28.6%) and by 95% confidence intervals generated by bootstrapping (N = 1000 simulated trials, 999 successful runs) (Table 3.2.3). Goodness-of-fit diagnostic plots for the final model are shown in Figure 3.2.1. The visual predictive check demonstrated a good fit between observed and predicted fluconazole concentrations (Figure 3.2.2). Only 4% (13/360) of observed concentrations were outside the 90% prediction interval, with 10 observations greater than the prediction interval and 3 observations below. Of the 3 subjects with observed data greater than the prediction interval, one had the highest dose in the cohort (27 mg/kg load followed by 12 mg/kg daily) and the other two received a high loading dose (25 mg/kg and 23 mg/kg, respectively, followed by 12 mg/kg daily) in the context of mild to moderate renal dysfunction. The subject with 3 observations below the prediction interval received the lowest dose of the cohort. None of these children were on ECMO and all were less than 2 years of age.

Empirical Bayesian Estimates of CL and V

The median (range) empirical Bayesian estimates for CL and V in children not on ECMO were 0.018 L/h/kg (0.008, 0.042) and 0.93 L/kg (0.55, 1.37), respectively (Table 3.2.4). Children on ECMO had ~45% higher V (median 1.35 L/kg, range 0.81, 1.81) but similar CL (median 0.018 L/h/kg, range 0.011, 0.043) compared to children not on ECMO. We saw a trend toward decreased impact of ECMO support on V with increased age, likely reflecting the changing relationship of ECMO prime volume (250-400mL) to a child's native blood volume (~250-5000mL depending on age).

Dose-Exposure Relationship

Monte Carlo simulations showed that children, both supported and not supported by ECMO, who received the Infectious Disease Society of America (IDSA) recommended treatment dose of 12 mg/kg daily[20] achieved the therapeutic target of an AUC_{0-24} of 400 mg*h/L in 90% of simulated children (Table 3.2.5). However, the time to reach therapeutic concentrations varied markedly based on the loading dose. No children on ECMO receiving 12 mg/kg as the initial dose achieved the target of AUC_{0-24} > 400 mg*h/L in the first 24 hours, and it took 10 days before 90% of simulated children had AUC_{0-24} of at least 400 mg*h/L. A loading dose of 25 mg/kg achieved the therapeutic target within 24 hours in 77.1% of simulated children not on ECMO; but only 34.0% of children on ECMO reached the therapeutic target in the first 24 hours with this loading dose. A loading dose of 35 mg/kg was required to achieve AUC_{0-24} > 400 mg*h/L in 87.7% of children on ECMO in the first 24 hours and 90% of children

achieved the target by day 2. Providing either a 40 mg/kg loading dose or 25 mg/kg every 12 hours in the first day of therapy achieved an AUC_{0-24} > 400 mg*h/L in 95.4% and 90.8% of children, respectively, in the first 24 hours. However, the maximum simulated concentrations after the 40 mg/kg loading dose and the second 25 mg/kg dose were considerably higher (62.1 and 68.0 mg/L, respectively) than after a single loading dose of 35 mg/kg (54.6 mg/L) raising concerns for toxicity (Table 3.2.5, Figure 3.2.3).

For prophylaxis children on ECMO who received 6 mg/kg daily per current IDSA guidelines did not achieve therapeutic exposure (AUC_{0-24} > 200 mg*h/L in 90% of children) until day 7 of therapy (Table 3.2.5). If children on ECMO receive a prophylactic loading dose of 12 mg/kg followed by 6 mg/kg daily, most (68.9%) children will reach an AUC_{0-24} >200 mg*h/L by day 2, and 90.0% of children will achieve the therapeutic AUC_{0-24} by day 5 of therapy. We also simulated exposure using the prophylactic dose evaluated in the ECMO Fluconazole Study (25 mg/kg once weekly) and found that this dosing regimen achieved the target exposure during the first two days of the dosing interval, but on days 3-7, only 65.9%, 33.8%, 14.5%, 5.8%, and 2.2% of children, respectively, achieved an AUC_{0-24} > 200 mg*h/L. We simulated 12 mg/kg every 72 hours and found that even after 4 doses (12 days), there were zero days when 90% of children on ECMO had an AUC_{0-24} > 200 mg*h/L.

Because of the wide range of age and weight among study subjects, the same treatment and prophylaxis simulations were performed in children <2 years of age (data not shown). Results from these simulations were within 5% of the results above.

DISCUSSION

Current treatment recommendations for invasive candidiasis are inadequate for treatment in children supported with ECMO. For the treatment of invasive candidiasis, we chose to target exposures observed in critically ill adults taking fluconazole 800 mg per day. A dose of 12 mg/kg per day achieved therapeutic exposure in children on ECMO but it took 10 days to reach those concentrations. In a critically ill child, this delay is unacceptable. Loading doses are routinely used in adults and in a prior analysis of one of the trials included in the current study, a fluconazole loading dose of 25 mg/kg appeared safe and achieved pharmacodynamic targets in 90% of a small cohort of children.[11] Because of the increased V observed in children on ECMO, a higher loading dose (35 mg/kg) was required to achieve comparable exposure. Clinicians must balance the risk of subtherapeutic exposure against the risk of toxicity. In adults, a dose of 1600 mg per day and serum concentrations less than 80 mg/L were well tolerated.[24] The simulated 90th percentile concentration following a loading dose of 35 mg/kg was 34.2 mg/L, and after 12 mg/kg maintenance therapy was 51.8 mg/L at steady state. While loading doses of 40 mg/kg and 25 mg/kg q12 in the first 24 hours also achieved therapeutic exposure in children on ECMO, the simulated 90th percentile concentration was closer to 80 mg/L leading us to choose 35 mg/kg as the optimum loading dose. The safety of this loading dose should be prospectively evaluated in children.

Because invasive candidiasis is so difficult to treat in children on ECMO, this population might benefit from antifungal prophylaxis. Pharmacodynamic targets are not well defined for prophylaxis but IDSA guidelines recommend 200-400 mg per day in immunocompromised and critically ill adults, equating to an $AUC_{0\text{-}24}$ of 200-400 mg*h/L.

In addition to achieving appropriate prophylactic exposure, consideration must be given to limiting development of resistance to fluconazole. In vitro studies suggest that maintaining plasma concentrations above the MIC for 50% of the dosing interval limits resistance, but it is unclear if the length of the dosing interval impacts this assumption. The ECMO fluconazole prophylaxis study included in this population analysis evaluated a dose of 25 mg/kg given once weekly. While almost all of these children maintained a fluconazole concentration above an MIC of 4 mg/L for 50% of the dosing interval, many were below the MIC for the remainder of the dosing interval (3.5 days). Considering the uncertainty regarding how long fluconazole concentrations can remain below the MIC before the risk of resistance increases, we also simulated multiple daily regimens. Given the devastating results of invasive candidiasis in children on ECMO and the safety profile of fluconazole, we recommend routine fluconazole prophylaxis of 12 mg/kg on day 1, and 6 mg/kg/d while on ECMO in centers with a high incidence of Candida infection. SCR should be monitored closely during fluconazole administration given the propensity of children on ECMO to develop renal dysfunction.

The difference in fluconazole exposure in children on ECMO compared to those not on ECMO is related to the increased V seen in children on ECMO. Increased V is expected due to the large volume of exogenous blood required to prime the circuit and the physiology associated with critical illness (e.g., inflammation). Our data suggest that as children age, the impact of ECMO support on V decreases, likely reflecting the volume of the ECMO prime in relation to the child's native blood volume. For a 3kg infant, the circuit prime volume (250-400mL) might exceed the infant's native blood volume (~250mL), while in a 70kg adolescent, the prime volume is ~8% of the child's

blood volume (~5L). Our data are limited by the fact that only five of the 40 children were over the age of 2 years and all of these were on ECMO. Empirical Bayesian estimates of V in these five children (median 1.1 L/kg [range 0.8, 1.5]) were slightly higher compared to estimates of V reported in children ages 2-12 years (0.95 L/kg)[25] and critically ill adults (0.6-0.7 L/kg).[22] Given the severity of illness seen in our children and the contribution of the ECMO prime, our estimates are reasonable. However, because very few children in this study were over the age of 2 years, we recommend caution in extrapolating our results to this older population. Further study of the impact of ECMO on fluconazole V is warranted in children over 2 years of age. ECMO also can increase V through adsorption of drug by the ECMO circuit; this is well described for other drugs.[9, 26] However, a previous analysis evaluating fluconazole extraction by the ECMO circuit showed that fluconazole undergoes minimal adsorption by the circuit and is unlikely to contribute to increased V.[10]

In our model, CL decreased with increasing SCR. This relationship also was expected as fluconazole is primarily excreted by the kidneys. Renal insufficiency is common in children supported with ECMO;[2] but ECMO support itself was not significantly associated with changes in CL. When combined with the observation that neither CL nor SCR were significantly different between children on ECMO and those not on ECMO, these results suggest that dosing modification in children with renal insufficiency should adhere to label guidelines regardless of ECMO support. The possible exception to this conclusion is when ECMO is combined with hemofiltration or CVVHD. Studies in adults show that fluconazole CL increases in the presence of hemofiltration and CVVHD.[27-30] Only 5 children received hemofiltration and two received

CVVHD, limiting our ability to draw conclusions about their impact on CL. We recommend caution in extrapolating our results to children on concomitant ECMO and hemofiltration or CVVHD.

CONCLUSIONS

Fluconazole V is increased in children supported with ECMO. As a result, children on ECMO who develop invasive candidiasis require a fluconazole loading dose of 35 mg/kg followed by a daily maintenance dose of 12 mg/kg to achieve exposures similar to children not on ECMO who are loaded with 25 mg/kg and maintained on 12 mg/kg daily. Children on ECMO may benefit from antifungal prophylaxis and in this population a loading dose of 12 mg/kg followed by 6 mg/kg daily is reasonable based on adult exposures after 200-400 mg per day. Children over two years of age are underrepresented in this study and results of the present study should be extrapolated to this population with caution. In addition, these results are based on simulated clinical trials. Confirmatory, prospective trials of fluconazole exposure, safety, and efficacy in this population are needed.

Table 3.2.1. Clinical Data

	Total	ECMO Support	Non-ECMO
n	40 (100)	21 (53)	19 (47)
Body weight (kg)	3.4 (1.9, 77)	4.2 (2.0, 77)	3.2 (1.9, 8.0)
Postnatal age (days)	22 (1, 6498)	113 (1, 6498)	13 (1, 262)
Gestational age (weeks)*	38 (24, 41)	38 (30, 41)	37 (24, 40)
Postmenstrual Age (weeks)	41 (35, 76)	42 (36, 63)	39 (35, 76)
Female	14 (35)	7 (33)	7 (37)
Race			
White	17 (43)	9 (43)	8 (42)
African American	18 (45)	10 (48)	8 (42)
Other	5 (12)	2 (9)	3 (16)
Indication			
Prophylaxis	23 (57)	17 (81)	6 (32)
Treatment	17 (43)	4 (19)	13 (68)
First dose (mg/kg)	25 (2.7, 26.5)	25.0 (10.4, 25.7)	17.4 (2.7, 26.5)
PK sample collection period (days)‡	5.5 (2.0, 34.0)	8.8 (2.1, 21.3)	4.2 (2.0, 34.0)
PK samples per child	8 (1, 22)	11 (5, 22)	8 (1,14)
Serum creatinine (mg/dL)			
Initial§	0.4 (0.1, 1.3)	0.5 (0.1, 1.2)	0.3 (0.1, 1.3)
Maximum	0.6 (0.1, 3.2)	0.7 (0.3, 3.2)	0.5 (0.1, 1.3)
Albumin (g/dL)	2.7 (1.1, 4.0)	2.8 (2.0, 4.0)	2.7 (1.1, 3.1)
Aspartate Aminotransferase (U/L)	35 (15, 673)	39 (23, 673)	35 (15, 159)
Alanine Aminotransferase (U/L)	19 (8, 127)	16 (8, 127)	19 (8, 126)

Values are medians (range) for continuous variables and counts (%) for categorical variables.

*Gestational age is only reported for infants < 1 year of age (n=33)

‡ Sample collection period is the time between first dose of study drug and collection of last PK sample

§ Initial serum creatinine collected +/- 24 hours of first dose

Table 3.2.2. Population PK model development

Model description	Population model	OFV	ΔOFV
Base model and univariable analysis*			
Volume of distribution (L)	$V = \theta_V * WT$	1022.74	
ECMO	$V = \theta_V * WT * 1.41^{ECMO\ (=1\ or\ 0)}$	1008.22	-14.52
Hemofiltration	$V = \theta_V * WT * 1.54^{HMFLTR\ (=1\ or\ 0)}$	1012.13	-10.61
Clearance (L /h)	$CL = \theta_{CL} * WT$	1022.74	
Creatinine	$CL = \theta_{CL} * WT * (creatinine/0.4)^{-0.29}$	950.84	-71.91
Hemofiltration	$CL = \theta_{CL} * WT * 0.66^{HMFLTR}$	1019.18	-3.56
Multivariable analysis			
CL= f(SCR), V=f(ECMO)	$V = \theta_V * WT * 1.39^{ECMO}$ $CL = \theta_{CL} * WT * (creatinine/0.4)^{-0.29}$	936.95	-13.89†
CL = f(SCR), V = f(ECMO,HMFLTR)	$V = \theta_V * WT * 1.30^{ECMO} * 1.34^{HMFLTR}$ $CL = \theta_{CL} * WT * (creatinine/0.4)^{-0.29}$	930.70	-6.25‡
CL= f(SCR, HMFLTR), V = f(ECMO, HMFLTR)	$V = \theta_V * WT * 1.30^{ECMO} * 1.34^{HMFLTR}$ $CL = \theta_{CL} * WT * (creatinine/0.4)^{-0.29} * 0.90^{HMFLTR}$	930.33	-0.37‡
Final model			
V = f(ECMO)	$V = \theta_V * WT * 1.39^{ECMO}$		
CL= f(SCR)	$CL = \theta_{CL} * WT * (creatinine/0.4)^{-0.29}$	936.95	-13.89†

OFV – objective function value; V – volume of distribution; CL – Clearance; WT – weight; SCR – serum creatinine, HMFLTR – hemofiltration; All coefficients in the models above are estimated parameters from the respective model

* Only models of covariates that significantly improved OFV are shown in the unvariable analysis. For full list of covariates tested see Methods.

† ΔOFV calculated relative to CL~Creatinine model (950.84)

‡ ΔOFV calculated relative to preceding model

Table 3.2.3. Final population PK model parameter estimates

Parameter	Point estimate	% RSE	Bootstrap CI		
			2.5%	Median	97.5%
Fixed Effects					
V (L/kg)	0.93	5.8	0.83	0.93	1.06
CL (L/h/kg)	0.019	5.6	0.017	0.019	0.021
Coefficient for ECMO on V	1.39	7.8	1.17	1.39	1.63
Exponent for creatinine on CL	-0.29	9.9	-0.41	-0.29	-0.24
Random Effects					
V interindividual variability (CV%)	22.2	28.6	14.7	21.5	27.7
CL interindividual variability (CV%)	33.2	21.3	25.0	32.6	39.2
Residual proportional error (CV%)	15.3	13.1	13.0	15.2	16.9

Table 3.2.4. Bayesian estimates of V and CL based on ECMO support

	ECMO	**no ECMO**
V (L/kg)		
0-30d	1.5 (1.3, 1.8)	0.96 (0.55, 1.4)
31d-2y	1.2 (0.91, 1.6)	0.83 (0.72, 1.0)
>2y-17y	1.1 (0.81, 1.5)	-
All	1.3 (0.81, 1.8)	0.93 (0.55, 1.4)
CL (L/h/kg)		
0-30d	0.018 (0.013, 0.043)	0.018 (0.008, 0.042)
31d-2y	0.022 (0.011, 0.039)	0.017 (0.008, 0.029)
>2y-17y	0.014 (0.013, 0.029)	-
All	0.018 (0.011, 0.043)	0.018 (0.008, 0.042)

Values are median (range)

Table 3.2.5. Exposure in children on ECMO after different simulated dosing regimens

Indication	Loading Dose	Maintenance Dose	Dosing Interval	PD Target† achieved in first 24h	Time to therapeutic exposure†
	(mg/kg)	(mg/kg)	(h)	(% of children)	(days)
Treatment	-	12	q24	0	10
	25	12	q24	34.0	8
	35	12	q24	87.7	2
	40	12	q24	95.4	1
	25 q12h	12	q24	90.8	1
Prophylaxis	-	6	q24	0	7
	12	6	q24	27.8	5
	-	12	q72	27.8	*
	-	25	q168	99.9	*

PD – pharmacodynamics

† PD target for treatment/therapeutic exposure is AUC_{0-24} > 400 mg*h/L in 90% of simulated children; PD target for prophylaxis is AUC_{0-24} > 200 mg*h/L in 90% of simulated children.

* For q72h and q168h dosing we set the target as AUC_{0-24} > 200 mg*h/L in 90% of simulated children for each 24h period during the dosing interval. Using this approach, 90% of simulated children never maintained an AUC_{0-24} > 200 mg*h/L for each 24h period.

Figure 3.2.1. Final population PK model diagnostic plots: observed versus population prediction (A) and individual prediction (B), weighted residuals versus population predictions (C), and time (D). A, B, The line of identity is included as a reference. For conditional weighted residuals (CWRES), a solid line at y = 0 is included as a reference

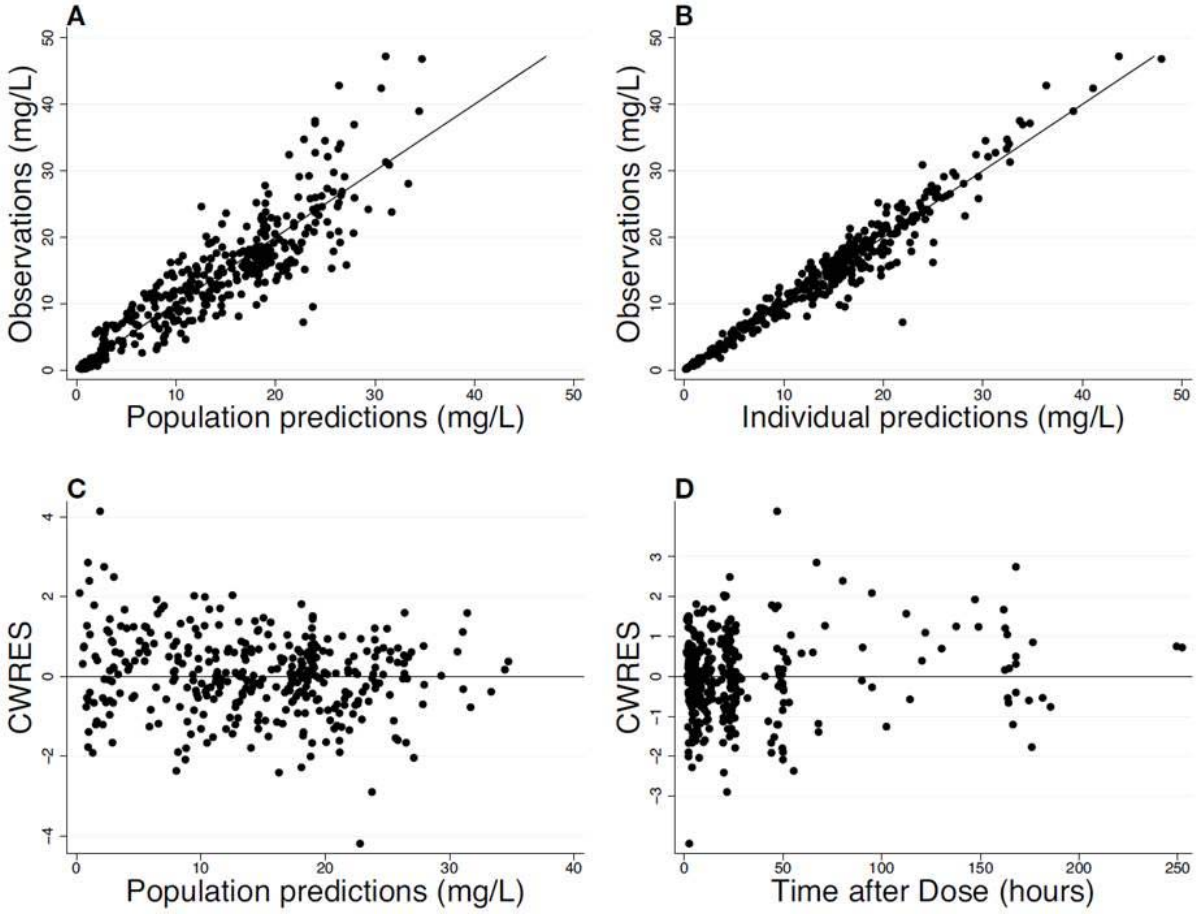

Figure 3.2.2. Visual predictive check. Shaded area represents the 95% prediction interval. Circles are observed data. Solid line represents the median of the observed data and dashed line the median of the predicted data.

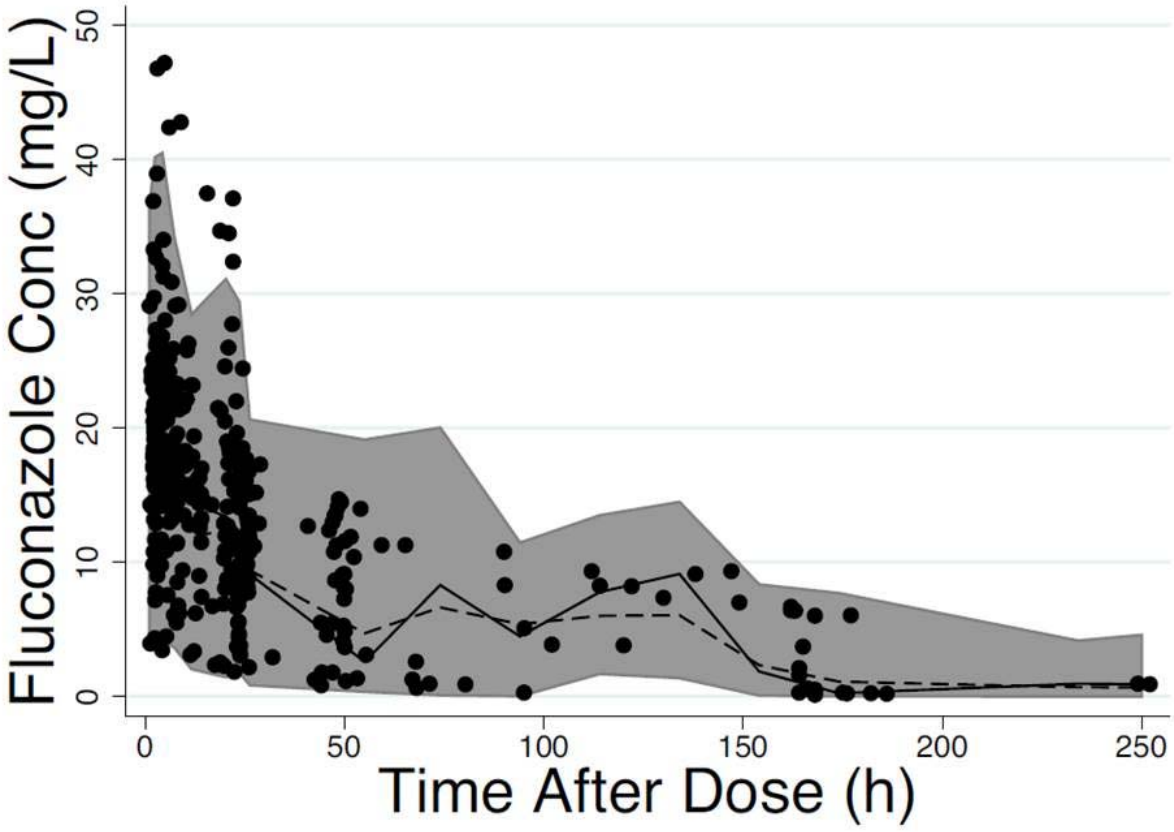

Figure 3.2.3. Simulated fluconazole plasma concentrations and exposure.

Figures A and B depict treatment doses and C-F depict prophylactic doses. A. Simulated fluconazole plasma concentrations in children on ECMO (35 mg/kg load) compared to children not on ECMO (25 mg/kg load). Both cohorts received 12 mg/kg daily as maintenance. B. Simulated fluconazole exposure in children on ECMO after different loading doses. Lines for individual dosing regimens represent 10th percentile of exposure (i.e., 90% of simulated children above the line). Horizontal dashed line represents target AUC for therapy. Simulated fluconazole plasma concentrations (C) and exposure (D) in children on ECMO receiving 12 mg/kg load then 6 mg/kg daily. Simulated fluconazole plasma concentrations (E) and exposure (F) in children on ECMO receiving 25 mg/kg once weekly. Solid line is the median and shaded regions represent the 90% prediction interval. Dashed lines in C and E represent MIC 4 mg/L. Dashed lines in D and F represent target AUC for prophylaxis. AUC is calculated for a 24 hour period for all figures.

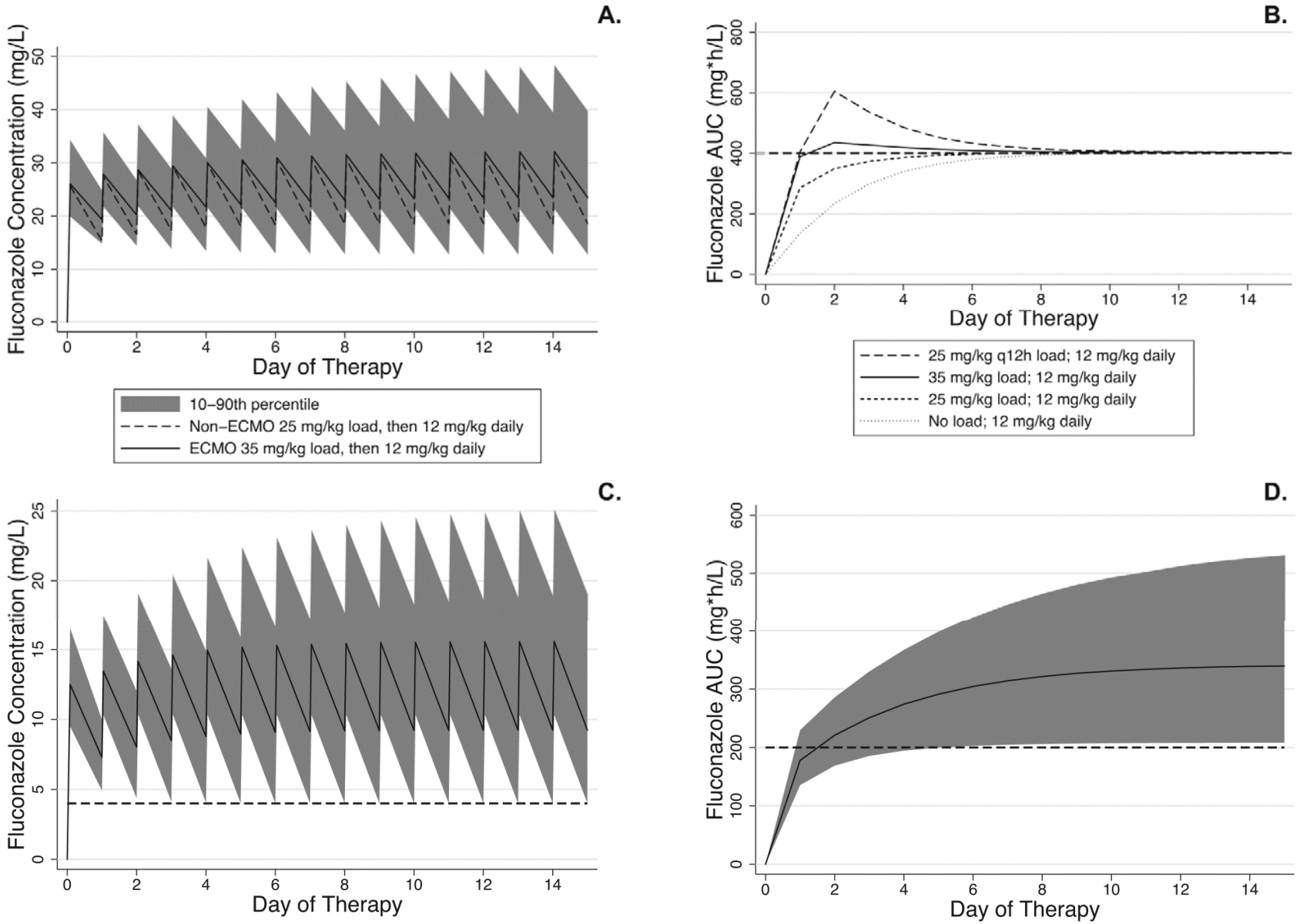
A.
Fluconazole Concentration (mg/L)
0
10
20
30
40
50
0
2
4
6
8
10
12
14
Day of Therapy
10–90th percentile
Non–ECMO 25 mg/kg load, then 12 mg/kg daily
ECMO 35 mg/kg load, then 12 mg/kg daily
B.
Fluconazole AUC (mg*h/L)
0
200
400
600
800
0
2
4
6
8
10
12
14
Day of Therapy
25 mg/kg q12h load; 12 mg/kg daily
35 mg/kg load; 12 mg/kg daily
25 mg/kg load; 12 mg/kg daily
No load; 12 mg/kg daily
C.
Fluconazole Concentration (mg/L)
0
5
10
15
20
25
0
2
4
6
8
10
12
14
Day of Therapy
D.
Fluconazole AUC (mg*h/L)
0
100
200
300
400
500
600
0
2
4
6
8
10
12
14
Day of Therapy

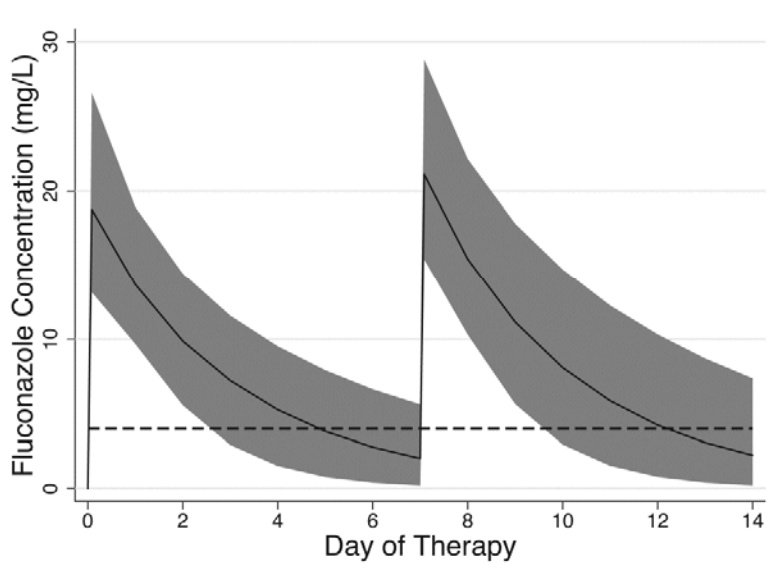
E.
Fluconazole Concentration (mg/L)
0
10
20
30
0
2
4
6
8
10
12
14
Day of Therapy

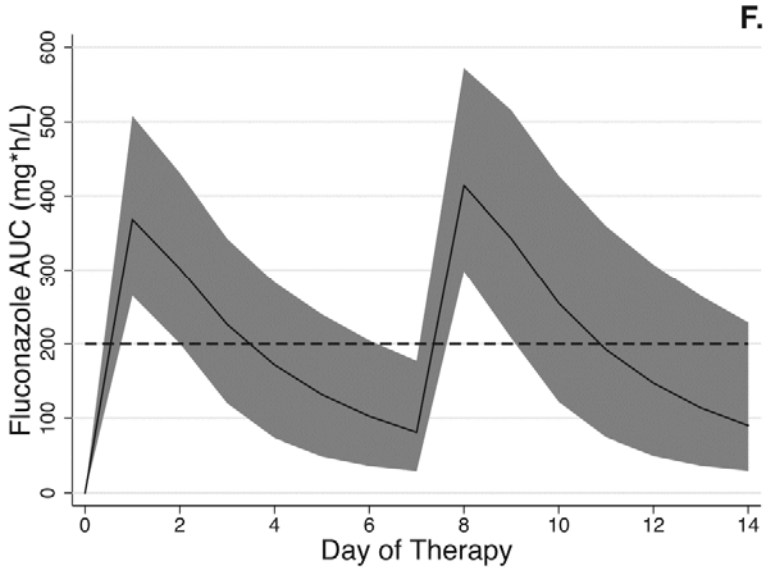
F.
Fluconazole AUC (mg*h/L)
0
100
200
300
400
500
600
0
2
4
6
8
10
12
14
Day of Therapy

REFERENCES

1. Watt KM, Gonzalez D, Benjamin DK, Jr., et al. Fluconazole population pharmacokinetics and dosing for prevention and treatment of invasive Candidiasis in children supported with extracorporeal membrane oxygenation. Antimicrob Agents Chemother 2015;59:3935-43.

2. ELSO. 2013. ECLS Registry Report: International Summary.

3. Bizzarro MJ, Conrad SA, Kaufman DA, Rycus P. 2010. Infections acquired during extracorporeal membrane oxygenation in neonates, children, and adults. Pediatr Crit Care Med 12: 277-81.

4. Gardner AH, Prodhan P, Stovall SH, Gossett JM, Stern JE, Wilson CD, Fiser RT. 2011. Fungal infections and antifungal prophylaxis in pediatric cardiac extracorporeal life support. J Thorac Cardiovasc Surg 143: 689-695

5. Eppes SC, Troutman JL, Gutman LT. 1989. Outcome of treatment of candidemia in children whose central catheters were removed or retained. Pediatr Infect Dis J 8:99-104.

6. Bhatt-Mehta V, Johnson CE, Schumacher RE. 1992. Gentamicin pharmacokinetics in term neonates receiving extracorporeal membrane oxygenation. Pharmacotherapy 12:28-32.

7. Mulla H, McCormack P, Lawson G, Firmin RK, Upton DR. 2003. Pharmacokinetics of midazolam in neonates undergoing extracorporeal membrane oxygenation. Anesthesiology 99:275-282.

8. Veinstein A, Debouverie O, Gregoire N, Goudet V, Adier C, Robert R, Couet W. 2011. Lack of effect of extracorporeal membrane oxygenation on tigecycline pharmacokinetics. J Antimicrob Chemother 67: 1047-1048.

9. Wildschut ED, Ahsman MJ, Allegaert K, Mathot RA, Tibboel D. 2010. Determinants of drug absorption in different ECMO circuits. Intensive Care Med 36:2109-2116.

10. Watt KM, Benjamin DK, Jr., Cheifetz IM, Moorthy G, Wade KC, Smith PB, Brouwer KL, Capparelli EV, Cohen-Wolkowiez M. 2012. Pharmacokinetics and safety of fluconazole in young infants supported with extracorporeal membrane oxygenation. Pediatr Infect Dis J 31:1042-1047.

11. Piper L, Smith PB, Hornik CP, Cheifetz IM, Barrett JS, Moorthy G, Hope WW, Wade KC, Cohen-Wolkowiez M, Benjamin DK, Jr. 2011. Fluconazole loading dose pharmacokinetics and safety in infants. Pediatr Infect Dis J 30:375-378.

12. Wade KC, Wu D, Kaufman DA, Ward RM, Benjamin DK, Jr., Sullivan JE, Ramey N, Jayaraman B, Hoppu K, Adamson PC, Gastonguay MR, Barrett JS. 2008. Population pharmacokinetics of fluconazole in young infants. Antimicrob Agents Chemother 52:4043-4049.

13. Wu D, Wade KC, Paul DJ, Barrett JS. 2009. A rapid and sensitive LC-MS/MS method for determination of fluconazole in human plasma and its application in infants with Candida infections. Ther Drug Monit 31:703-709.

14. Lindbom L, Pihlgren P, Jonsson EN. 2005. PsN-Toolkit--a collection of computer intensive statistical methods for non-linear mixed effect modeling using NONMEM. Computer methods and programs in biomedicine 79:241-257.

15. Keizer RJ, van Benten M, Beijnen JH, Schellens JH, Huitema AD. 2011. Pirana and PCluster: a modeling environment and cluster infrastructure for NONMEM. Computer methods and programs in biomedicine 101:72-79.

16. Andes D, van Ogtrop M. 1999. Characterization and quantitation of the pharmacodynamics of fluconazole in a neutropenic murine disseminated candidiasis infection model. Antimicrob Agents Chemother 43:2116-2120.

17. Clancy CJ, Staley B, Nguyen MH. 2006. In vitro susceptibility of breakthrough Candida bloodstream isolates correlates with daily and cumulative doses of fluconazole. Antimicrob Agents Chemother 50:3496-3498.

18. Clancy CJ, Yu VL, Morris AJ, Snydman DR, Nguyen MH. 2005. Fluconazole MIC and the fluconazole dose/MIC ratio correlate with therapeutic response among patients with candidemia. Antimicrob Agents Chemother 49:3171-3177.

19. Pai MP, Turpin RS, Garey KW. 2007. Association of fluconazole area under the concentration-time curve/MIC and dose/MIC ratios with mortality in nonneutropenic patients with candidemia. Antimicrob Agents Chemother 51:35-39.

20. Pappas PG, Kauffman CA, Andes D, Benjamin DK, Jr., Calandra TF, Edwards JE, Jr., Filler SG, Fisher JF, Kullberg BJ, Ostrosky-Zeichner L, Reboli AC, Rex JH, Walsh TJ, Sobel JD. 2009. Clinical practice guidelines for the management of candidiasis: 2009 update by the Infectious Diseases Society of America. Clin Infect Dis 48:503-535.

21. Hiemenz J, Cagnoni P, Simpson D, Devine S, Chao N, Keirns J, Lau W, Facklam D, Buell D. 2005. Pharmacokinetic and maximum tolerated dose study of micafungin in combination with fluconazole versus fluconazole alone for prophylaxis of fungal infections in adult patients undergoing a bone marrow or peripheral stem cell transplant. Antimicrob Agents Chemother 49:1331-1336.

22. Buijk SL, Gyssens IC, Mouton JW, Verbrugh HA, Touw DJ, Bruining HA. 2001. Pharmacokinetics of sequential intravenous and enteral fluconazole in critically ill surgical patients with invasive mycoses and compromised gastro-intestinal function. Intensive Care Med 27:115-121.

23. Andes D, Forrest A, Lepak A, Nett J, Marchillo K, Lincoln L. 2006. Impact of antimicrobial dosing regimen on evolution of drug resistance in vivo: fluconazole and Candida albicans. Antimicrob Agents Chemother 50:2374-2383.

24. Anaissie EJ, Kontoyiannis DP, Huls C, Vartivarian SE, Karl C, Prince RA, Bosso J, Bodey GP. 1995. Safety, plasma concentrations, and efficacy of high-dose fluconazole in invasive mold infections. Journal of Infectious Diseases 172:599-602.

25. Brammer KW, Coates PE. 1994. Pharmacokinetics of fluconazole in pediatric patients. Eur J Clin Microbiol Infect Dis 13:325-329.

26. Dagan O, Klein J, Gruenwald C, Bohn D, Barker G, Koren G. 1993. Preliminary studies of the effects of extracorporeal membrane oxygenator on the disposition of common pediatric drugs. Ther Drug Monit 15:263-266.

27. Muhl E, Martens T, Iven H, Rob P, Bruch HP. 2000. Influence of continuous veno-venous haemodiafiltration and continuous veno-venous haemofiltration on the pharmacokinetics of fluconazole. Eur J Clin Pharmacol 56:671-678.

28. Yagasaki K, Gando S, Matsuda N, Kameue T, Ishitani T, Hirano T, Iseki K. 2003. Pharmacokinetics and the most suitable dosing regimen of fluconazole in critically ill patients receiving continuous hemodiafiltration. Intensive Care Med 29:1844-1848.

29. Valtonen M, Tiula E, Neuvonen PJ. 1997. Effect of continuous venovenous haemofiltration and haemodiafiltration on the elimination of fluconazole in patients with acute renal failure. J Antimicrob Chemother 40:695-700.

30. Patel K, Roberts JA, Lipman J, Tett SE, Deldot ME, Kirkpatrick CM. 2011. Population pharmacokinetics of fluconazole in critically ill patients receiving continuous venovenous hemodiafiltration: using Monte Carlo simulations to predict doses for specified pharmacodynamic targets. Antimicrob Agents Chemother 55:5868-5873.

CHAPTER 4. PHYSIOLOGICALLY-BASED PHARMACOKINETICS OF FLUCONAZOLE IN CHILDREN ON ECMO

INTRODUCTION

Fluconazole is a triazole antifungal drug available in both intravenous (IV) and oral formulations that is rapidly absorbed from the gastrointestinal tract with high oral availability (~92% bioavailability).[1] Fluconazole is not bound extensively to plasma proteins (11%, alpha-1-acid glycoprotein [AAG][2,3]), and exhibits excellent penetration into the cerebrospinal fluid with concentrations approximating 80% of those measured in plasma.[1] Penetration into other body tissues also approximates or exceed concentrations found in the plasma; the urine:plasma concentration ratio is 10:1.[1] Mass balance studies in humans show that fluconazole is eliminated primarily by the kidneys with 80% of the dose excreted as unchanged drug, and 11% recovered as metabolites.[4,5] Fluconazole is metabolized primarily by UDP-Glucuronosyltransferase-2B7 (UGT2B7).[6] The triazoles inhibit the enzyme responsible for converting lanosterol to ergosterol, a key component of fungal cell membranes, resulting in cell lysis and death.[7-9] Fluconazole has excellent activity against *Candida*, and is labeled for treatment of invasive candidiasis in infants and children.[1] Although it is a first-line drug for treatment of invasive candidiasis in the pediatric intensive care unit, fluconazole pharmacokinetics (PK) and dosing may be affected by the altered physiology observed in critically ill children.[10-18]

Critical illness can affect PK by altering absorption, distribution, metabolism, and excretion (ADME) of drugs. Absorption can be both decreased (e.g., intestinal hypoperfusion, decreased absorptive capacity),[19-21] and increased (e.g., intestinal hypomotility).[22] Drug distribution typically is increased due to inflammation and capillary leak that results in edema and increased volume of distribution (V), and hypoalbuminemia, which commonly occurs in critical illness.[23-28] However, AAG is an acute phase reactant protein that often is elevated in critical illness. Some data suggest that the elevated AAG concentrations in critical illness increase the amount of protein available for binding and consequently increase the fraction of bound drug.[2,3] Hepatic metabolism typically is decreased due to decreased expression and function of drug metabolizing enzymes.[29-32] Renal clearance can be affected by the competing phenomena of augmented renal clearance and acute kidney injury that both occur in critical illness.[33-35] The impact of critical illness on hepatic transporter function and biliary elimination is not well described. However, inflammation, which is common in critical illness, is known to impact transporter expression and function in animal models.[36-38] The impact of critical illness on drug disposition is exacerbated in the setting of extracorporeal membrane oxygenation (ECMO). In addition to direct interaction between the drug and ECMO circuit, ECMO support results in altered blood flow and increased inflammation, edema, hemolysis, and renal dysfunction.[39-44]

Physiologically-based pharmacokinetic (PBPK) modeling is ideally suited to describe the PK in critically ill children supported with ECMO. PBPK models are structured to represent physiologically relevant spaces (Figure 4.1). Each virtual “organ” is parameterized with mass-balance differential equations describing the disposition of

drug within the compartment. Because PBPK models are mechanistic, age-related processes of drug disposition can be incorporated into the model to predict exposure across the pediatric age spectrum. Further, the model parameters can be adjusted to account for the altered physiology associated with critical illness (e.g., decreased renal blood flow). In order to model drug exposure in children on ECMO, an ECMO "organ" can be linked to the PBPK model and parameterized using data from *ex vivo* studies (Chapter 2). By defining the volume, blood flows, and drug clearance of the ECMO compartment, the impact of ECMO on drug disposition can be predicted *in vivo*, and the ECMO PBPK model can be used to determine optimal dosing in this vulnerable population.

METHODS

Model Building Workflow

The model building process followed an established workflow (Figure 4.2).[45-47] A PBPK model was developed in adults (Adult PBPK Model) to gain confidence in the model structure using robust adult data before proceeding with pediatric model development. After model validation, the Adult PBPK Model was scaled to children (Pediatric PBPK Model). Once the Pediatric PBPK Model met acceptance criteria (see PBPK Model Acceptance Criteria below), an ECMO compartment was added to the Pediatric PBPK Model to form the ECMO PBPK Model.

Adult PBPK Model

The whole-body PBPK model was structured with 15 organ compartments using mass balance differential equations describing drug entering and exiting the compartments (Figure 4.1). The link between physiologic spaces was the blood circulation. The model assumed a 30-year-old Caucasian male with a mean body weight of 73kg and height of 176cm based on population-level data from the National Health and Nutrition Examination Survey (NHANES) dataset.[48] Based on these anthropometric measurements, organ weights, volumes, and blood flows were generated using the International Commission on Radiological Protection (ICRP) database.[49]

The distribution model assumed each organ consisted of 4 sub-compartments: plasma, red blood cells (together forming the vascular space), interstitial fluid, and cellular space. A permeation barrier exists between the vascular space and the interstitial fluid, and between the interstitial fluid and the cellular space. The organ-to-plasma partition coefficients and cellular permeabilities were determined using drug physicochemical properties based on methods described by Willmann et al.[50,51] For fluconazole, a perfusion–rate-limited model was assumed where each tissue or organ represented a well-stirred compartment.[52] This implied that drug reaching the tissue or organ was distributed instantaneously in the whole volume of the physiological space. Other distribution models (e.g., permeation limited) were included if they improved model predictions.

Drug-specific information from the literature included physicochemical properties and clearance pathways of the drug (Table 4.1). Mass balance studies with radiolabeled

IV fluconazole indicated that 91% of fluconazole was eliminated in the urine, with 80% as unchanged drug, 2% was eliminated in the feces, and 7% was not recovered.[53] Because biliary elimination was a small fraction of total elimination, this process was not included in the model. As a result, the model assumed 15% of the plasma clearance of fluconazole was due to hepatic metabolism and 85% to renal elimination. Metabolism was attributed to glucuronidation via UGT2B7, and unbound intrinsic clearance (CL_I') was calculated using hepatic clearance (CL_H).[6] CL_H was assumed to be 15% of total empiric clearance. Fluconazole is highly reabsorbed in the renal tubule, so renal clearance (CL_R) was adjusted by calculating the glomerular filtration rate (GFR) fraction as follows:

$$GFR\ Fraction = \frac{Empiric\ CL_R}{Expected\ CL_R} \quad \text{(eq. 1)}$$

where Empiric CL_R equals the renal clearance reported in the literature.[54] Expected CL_R is the clearance expected due to GFR if there was no reabsorption or tubular secretion (Expected CL_R = fraction unbound*GFR = f_u *110 ml/min). A summary of the assumptions used in the model building process is included in Table 4.2 Plasma concentration vs. time profiles were generated using the initial model and compared with observed data from the literature (Table 4.3, Adult Development Datasets). Model parameters were optimized based on the observed data using the Nelder-Mead algorithm in the MoBi® Toolbox for Matlab.[55] The optimized model was used to generate population predictions of plasma concentration vs. time profiles for a virtual population of healthy adults (n=1000) created using the PK-Sim® population module.[56]

Inter-individual variability of UGT2B7 expression was assumed to have log-normal distribution with a geometric standard deviation of 1.34.[57] Fluconazole's unbound fraction (f_u) was assumed to have a normal distribution with an arithmetic standard deviation of 7%.[2,3] Optimized model predictions for the virtual population were compared first with the observed data from the Adult Development Datasets to determine if the model met acceptance criteria (see PBPK Model Acceptance Criteria below). In order to evaluate the model performance, the optimized model predictions were then compared with observed data from the literature that were not used in the model building process (Adult Validation Datasets, Table 4.3). After acceptance criteria were met, the model was scaled to children.

Pediatric PBPK Model

Age-dependencies in physiological parameters (e.g., body weight, organ weight, blood flow) were included to scale the Adult PBPK Model to children according to the methods described by Edginton et al.[45] In short, parameters were assigned for each simulated individual: age, race, gender, mean body weight and height.[49] Based on body weight and height, organ weights and volumes were obtained from the ICRP database.[49] Age-dependent blood flows for some organs were available in the literature.[58-71] For the organs in which no data were available, the same percentage of cardiac output in adults was assumed.[49,72]

The mechanistic drug clearance method was used to scale adult plasma clearance to children using 1) adult clearance, 2) the proportion of total clearance (CL_T) attributed to each clearance process (e.g., renal versus hepatic), 3) the fraction of

unbound drug and major protein responsible for binding, and 4) the age of the child.[73] CL_T was assumed to be the sum of CL_R and CL_H. CL_R was attributed to GFR and passive reabsorption. GFR was scaled to children by calculating the percentage of adult GFR expected in a child of a specific age, and adjusted for $f_{u(child)}$:

$$CL_{GFR(child)} = \frac{GFR_{(child)}}{GFR_{(adult)}} \times \frac{f_{u\,(child)}}{f_{u\,(adult)}} \times CL_{GFR\,(adult)} \quad \text{(eq. 2)}$$

Where $CL_{GFR(child)}$ is the child's clearance due to GFR, $GFR_{(child)}$ is the estimated GFR of the child, $GFR_{(adult)}$ is the GFR in adults (assumed to be 110 mL/min[73]), and $CL_{GFR(adult)}$ is the clearance due to GFR in adults. The $GFR_{(child)}$ was calculated using a postmenstrual age model,[74] and $f_{u\,(child)}$ was estimated using an age-specific model considering plasma protein concentrations in children and the affinity of drugs for binding proteins.[73,75] Reabsorption (GFR Fraction) was assumed to have no ontogeny.

To scale CL_H to children, the adult plasma clearance was converted to hepatic unbound intrinsic clearance (CL_I');

$$CL_I{}' = CL_H \times \frac{Q_H}{Q_H - CL_H} \times \frac{1}{f_u} \quad \text{(eq. 3)}$$

Where Q_H is hepatic blood flow. Adult CL_I' was then scaled to children using age- and enzyme-specific percent of adult activity (ontogeny);

$$CL_I{}'_{UGT2B7(child\ g\ liver)} = OSF_{UGT2B7} \times\ CL_I{}'_{UGT2B7(adult\ g\ liver)} \quad \text{(eq. 4)}$$

Where $CL_I'_{UGT2B7(child\ g\ liver)}$ is the scaled CL_I' due to UGT2B7 per gram of liver, OSF_{UGT2B7} is the ontogeny scaling factor for UGT2B7,[73] and $CL_I'_{UGT2B7(adult\ g\ liver)}$ is the adult CL_I' due to UGT2B7.

Finally, the child CL_I' was converted back to child plasma CL using pediatric body weight, liver weight, and blood flow.

$$CL_I'_{(child\ total\ liver)} = CL_I'_{UGT2B7(child\ g\ liver)} \times LW_{child} \quad \text{(eq. 5)}$$

$$CL_{H\ (child)} = \frac{Q_{H\ (child)} \times f_{u\ (child)\ total\ liver} \times CL_I'_{(child) total\ liver}}{Q_{H\ (child)} + (f_{u\ (child)} \times CL_I'_{(child) total\ liver}) / \frac{B}{P}_{(child)}} \quad \text{(eq. 6)}$$

Where LW_{child} is the liver weight of the child and $B/P_{(child)}$ is the blood/plasma ratio. Previously described ontogeny models were used for the hepatic enzyme of interest (UGT2B7) to calculate the percent of adult activity at specific ages.[73] The mechanistic pediatric scaling information was included in software databases. In order to evaluate the performance of the Pediatric PBPK Model, model predictions were generated using a simulated population of infants (N=1000) created with the PK-Sim® population module[56] and compared with raw data from a PK study of fluconazole in critically ill infants (Pediatric Validation Dataset, Table 4.3). The median (5^{th}, 95^{th} %ile) area under the concentration time curve for 0-24 hours (AUC_{0-24}) for these 13 children was 485 mg*h/L (350, 664) and was calculated using compartmental methods as described in Piper et. al 2011.[76]

ECMO PBPK Model

The Pediatric PBPK Model was exported into MoBi® where a new compartment reflecting the ECMO circuit was added (Figure 4.1). Flow into and out of the ECMO compartment was assigned by partitioning pulmonary blood, with 80% assigned to the ECMO compartment and 20% assigned to the lungs. The ECMO compartment was assigned a volume of 400mL to reflect the standard volume of blood required to prime the ECMO circuit. Because the *ex vivo* results from Chapter 2 showed that fluconazole was not extracted by the circuit, no additional clearance function was added to the ECMO compartment. As children on ECMO develop severe edema secondary to capillary leak syndrome, edema was added to the model by increasing the child's body weight by 50%, and assigning the resulting increase in volume to the interstitial space of all organ compartments.[44,77] The ECMO PBPK Model with edema was then exported back into PK-Sim® to perform population simulations. The population simulations were evaluated by comparing model predictions with observed data from the Fluconazole ECMO Trial described in Chapter 3. To determine the optimal loading dose that achieves target exposures for fluconazole in children on ECMO, new simulations were performed using the ECMO PBPK Model with distinct dosing regimens for different age groups. [78,79]

Assessment of Dose-Exposure Relationship

Fluconazole is fungistatic and has a prolonged post-antibiotic effect. Efficacy is associated with an AUC to minimum inhibitory concentration ratio (AUC/MIC) ≥ 50.[80-82] Assuming a MIC of 8 mg/L, based on the Clinical and Laboratory Standards Institute's

guideline sensitivity breakpoint for all *Candida* species, an $AUC_{0\text{-}24}$ of 400 mg*h/L achieves the target AUC/MIC ratio.[83] For treatment, a target minimum $AUC_{0\text{-}24}$ of 400 mg*h/L in 90% of children was chosen. The $AUC_{0\text{-}24}$ was calculated for the PBPK model simulations using the linear-up log-down trapezoidal approach. The $AUC_{0\text{-}24}$ for the observed data was calculated using the final population PK model from Chapter 3 and Monte Carlo simulations, also using the linear-up log-down trapezoidal approach (see Chapter 3 Methods). In order to balance efficacy and safety, predicted exposures also were compared with maximum tolerated $AUC_{0\text{-}24}$ (1600 mg*h/L) and concentration (C_{max} 70 mg/L).[84]

PBPK Model Acceptance Criteria

The population predictability was assessed by generating a prediction interval (5^{th} to 95^{th} percentile) of drug concentrations for the population, and quantifying the number of observed concentrations that fell outside of the prediction interval. Because the goal of this model was to determine dosing, and because dosing is based on AUC, minimal bias in AUC estimates was desired. Model precision was assessed by calculating the fold error between PBPK predicted AUC and observed AUC.

$$Fold\ Error = \frac{AUC_{0-24}PBPK}{AUC_{0-24}Observed} \quad \text{(eq. 7)}$$

Parameters with 0.7-1.3 fold error were considered as reasonable predictions.[45]

RESULTS

Adult PBPK Model

Mean GFR fraction, LogP, and adult CL_I' were optimized to 0.16, 0.2, and 0.007 L/min, respectively (Table 4.1). Optimized Adult PBPK Model predictions versus dose-normalized observed data from the two Model Development Datasets showed good agreement. Based on visual inspection of the plots, approximately 85% of the observed data fell within the 90% prediction interval of the simulated population concentrations (Figure 4.3). Observed data in the initial phase of distribution (5-15 minutes) were over predicted by the model; however, subsequent data were well described. The predicted AUC was within 16% of observed AUC (Table 4.4).

When optimized model predictions were compared with observed data from Adult Validation Datasets (i.e., data not used to build the model), over 90% of the observed data fell within the 90% prediction interval of the model and predicted AUC was within 10% of observed (Figure 4.4, Table 4.4). Based on the excellent predictive power of the optimized model, the Adult PBPK Model was scaled to children.

Scaling to Children

Pediatric simulations evaluating the recommended loading dose of 25mg/kg[76,85] showed good agreement between observed versus predicted concentrations. Based on visual inspection of the plots, 70% (30/43) of the observed data fell within the 90% prediction interval of the simulated population concentrations (Figure 4.5). If concentrations from infants with renal dysfunction or severe edema were excluded (n=10), the model captured 89% (28/32) of the observed data. The observed AUC_{0-24}

estimate using compartmental modeling was 485 mg*h/L, and 84% of the individuals were above the target AUC_{0-24} of 400 mg*h/L. The Pediatric PBPK Model predicted an AUC_{0-24} of 507 mg*h/L (Fold Error 1.05) with 95% of simulated individuals achieving the target AUC_{0-24} of 400 mg*h/L (Figure 4.6).

ECMO PBPK Model

When the observed data from the Fluconazole ECMO Trial were compared to the model predictions from the Pediatric PBPK Model, only 26% of the observed data fell within the 90% prediction interval (Figure 4.7.1). Compared to the observed AUC_{0-24} (371 mg*h/L) reported in Chapter 3, the AUC_{0-24} was over-predicted (520mg*h/L; 1.40 fold error). Adding the ECMO compartment to the Pediatric PBPK Model modestly improved predictions, although still only 26% of the observed data fell within the 90% prediction interval (Figure 4.7.2). The AUC_{0-24} was still over-predicted, but to a lesser extent (502 mg*h/L; 1.35 fold error). After adding the Edema disease state, 71% (30/42) of the observed data fell within the 90% model prediction interval (Figure 4.7.3). The PBPK predicted AUC_{0-24} for a loading dose of 25 mg/kg for the ECMO PBPK Model was 420 mg*h/L, which equated to a 1.13 fold error compared to the observed AUC_{0-24} of 371 mg*h/L that was estimated using the final population PK model described in Chapter 3 (Figure 4.8).

Based on the precision of AUC estimates, the ECMO PBPK Model was used to simulate multiple dosing regimens and identify the optimal loading dose for each age group. The following age-dependent loading doses were found to achieve the target AUC_{0-24} in ≥ 90% of simulated children on ECMO in the first 24 hours of therapy:

neonates (0-29d) 35 mg/kg, infants (30d-<2y) 30 mg/kg, children (2y-<6y) 25 mg/kg, school-age children (6y-<12y) 25 mg/kg, and adolescents 20 mg/kg (Figure 4.9).

Because complicated dosing regimens are often difficult to implement, the ECMO PBPK Model also was used to simulate exposures after a loading dose of 35 mg/kg for all age cohorts (Figure 4.10). This approach achieved the target $AUC_{0\text{-}24}$ in ≥ 90% of simulated children on ECMO in the first 24 hours of therapy and no simulated child had an $AUC_{0\text{-}24}$ (701 [307, 1036]) or C_{max} (50.5 [12.3, 65.4]) greater than the safety threshold values of 1600 mg*h/L and 70 mg/L, respectively.

DISCUSSION

The critically ill child, especially with extracorporeal support, represents an ideal population for the use of PBPK modeling. Surprisingly, this approach has never been used in this population. In the present study, an established workflow for PBPK-based scaling from adults to children was employed, and then the ECMO device and disease state effects (i.e., edema) were added to successfully predict exposure in children on ECMO. The Adult PBPK Model provided an excellent description of the data, except for the early distribution phase. Over-prediction in the early phase may be attributed to the assumption in the model that initial mixing and distribution is instantaneous. This assumption fails to account for the lag time between drug administration to a peripheral site and distribution to the systemic circulation.[86] Although drug binding to the IV catheter used to administer fluconazole also could account for model over-prediction, this is unlikely based on the *ex vivo* results detailed in Chapter 2 that demonstrate limited interaction of fluconazole with circuit materials. Given that 1) model over-

prediction was limited to the early distribution phase, 2) the AUC_{0-24} between observed and predicted data showed good agreement, and 3) external validation with other datasets showed good agreement, the model performance was deemed to be acceptable for scaling to children.

The healthy adult model was scaled to children, and then the healthy infant model was used to predict exposures in critically ill infants. In the process of scaling to children, drug-specific inputs used in the optimized Adult PBPK Model were held constant, and system-specific inputs were scaled to the population of interest. The Pediatric PBPK Model only captured 70% of the observed data for critically ill infants, but this was expected because the model was based on healthy infants. PBPK model-predicted exposures were compared with exposures from critically ill children. Critically ill children have more variability in exposure due to disease. An examination of the data that fell below the 90% prediction interval revealed that 8 of the 10 observations (80%) were from children who had just undergone cardiac surgery and had substantial edema and inflammation, which would result in a higher V and lower initial fluconazole exposure.[44,87,88] Similarly, of the 3 concentrations that were greater than the 90% prediction interval, one (33%) came from an infant with decreased GFR. Decreased GFR for fluconazole, which undergoes renal clearance, resulted in decreased CL and higher than expected exposures. Adjustments in the model depend on the purpose of the model. For example, if the purpose is to predict dosing in children after cardiac surgery, then an edema disease state should be added to better describe the altered physiology in that population. The purpose of the Pediatric PBPK Model was to build the ECMO PBPK Model and predict dosing in children on ECMO. Before adding an ECMO

compartment, confidence in the scaling process from adults to children needed to be established. The Pediatric PBPK Model was deemed acceptable for developing the ECMO PBPK Model as it explained the majority of concentrations that fell outside the 90% prediction interval, and because observed AUC_{0-24} and PBPK-predicted AUC_{0-24} showed close agreement.

Observed data from the Fluconazole ECMO Trial showed that exposures were substantially lower in infants on ECMO compared to critically ill infants not on ECMO. As a result, the Pediatric PBPK Model over-predicted exposure in children on ECMO. Adding the ECMO compartment only lowered exposure by ~5%. This is not surprising as the only direct impact of ECMO was the addition of 400mL of blood required to prime the ECMO circuit. The impact of the ECMO prime volume was decreased because of fluconazole distribution from the plasma into other body tissues. The ECMO PBPK Model suggests that the bigger impact on fluconazole exposure may be attributed to edema common in infants on ECMO. ECMO support results in inflammation and subsequent capillary leak and edema.[44,87,88] In addition, ongoing fluid resuscitation can result in a substantial increase in interstitial fluid volume.[44] When the interstitial fluid volume in the ECMO PBPK Model was increased, predicted exposure showed good agreement with the observed data. The remaining over-prediction based on the model was likely due to other factors that increase V but were not captured in the model (e.g., ongoing fluid resuscitation, repeated blood product transfusions).

The edema disease state was based on the assumption that edema caused a 50% increase in body weight, and that the increase in volume was added to the interstitial compartment of each organ. A 50% increase in body weight is on the upper

end of what would be expected.[44,87,88] The model predictions were sensitive to the extent of edema. If a 10% increase in body weight was assumed, the model-predicted AUC increased by 14%. In order to improve accuracy of this parameter, future studies should capture both the extent of edema in each individual and the other factors such as ongoing fluid resuscitation that can lead to altered PK.

Overall the ECMO PBPK Model showed good agreement with observed data, and was used to predict the loading dose for different age groups. Based on simulations, the loading dose required for >90% of children to achieve the therapeutic target (AUC_{0-24} >400 mg*h/L), decreased with age. This is in part a function of the decreasing impact of ECMO on fluconazole exposure in older children with increased body size. Because the direct impact of ECMO on fluconazole exposure is due to the prime volume of the circuit (400mL), that impact is decreased as the ratio of prime volume to native blood volume decreases from neonates (400mL:250mL) to adolescents (400mL:5L).

One of the advantages of PBPK modeling is the ability to predict dosing across the pediatric age spectrum. However, this must be balanced with clinical feasibility. The age-specific dosing regimen predicted with the ECMO PBPK model is optimized for each age group but is likely too complicated for clinical implementation. Choosing a single weight-based dose for all children involves balancing the consequences of underexposure with the risk of toxicity due to overexposure. Fluconazole is safe up to a C_{max} of 70 mg/L and a maximum AUC_{0-24} of 1600 mg*h/L.[84] Based on the wide therapeutic index and because the consequences of an inadequately treated fungal infection in a child on ECMO are devastating, dosing should target a higher exposure to

ensure all children are adequately treated. A dosing regimen of 35 mg/kg for all children achieves the therapeutic exposure in over 99% of simulated children while no simulated children exceed the known safety thresholds. Based on this, a fluconazole loading dose of 35 mg/kg is recommended for all children with suspected or confirmed fungal infection who are supported with ECMO.

In conclusion, an Adult PBPK Model of fluconazole was developed, and scaled to children. By adding an ECMO compartment and the impact of ECMO-related changes in physiology, the modified model successfully predicted exposure (PBPK AUC within 0.7-1.3 fold error of observed AUC) in infants on ECMO. The dosing recommendations derived for neonates and infants are comparable to the dosing recommendations developed from the population PK model in Chapter 3. More importantly, because the PBPK model is mechanistic in nature, and able to take into account developmental changes in size and ADME processes, dosing was predicted in pediatric populations that have not been studied previously. In addition, when new ECMO technology is introduced, *ex vivo* ECMO experiments could be performed to determine the interaction of fluconazole with the new circuit. Information generated based on the fluconazole-circuit interactions could then be incorporated into the ECMO compartment of the ECMO PBPK Model and new dosing recommendations developed, thereby circumventing the need to repeat a large PK trial. While these recommendations will still need to be prospectively validated, the validation trial should be smaller and more efficient.

Table 4.1. Fluconazole physicochemical properties and elimination pathways

Parameter	Reported value	Optimized value
Physicochemical properties		
Lipophilicity (LogP)	0.4[89]	0.2
Protein binding partner	Alpha-1 acid glycoprotein[2,3]	
Fraction unbound (%)	89[90]	
Molecular weight (g/mol)	306.27[89]	
Compound type/pKa	Weak base/2.56[89]	
Charge	Neutral[89]	
Blood/Plasma ratio	1.0[53]	
Metabolism and elimination		
GFR fraction	0.16 (0.15-0.18)[53,54]	0.16
UGT2B7 CL_i' (L/min)	0.0052 (0.0031-0.0073)[53,54]	0.007

Table 4.2. Assumptions used in the model building process

Factor	Assumption	Reference
Mass balance	Because biliary clearance plays only a minor role (2.3%), total clearance was partitioned between CL_R (85%) and CL_H (15%; UGT2B7).	Brammer et al. 1991[53]
Renal clearance via GFR	Fluconazole is highly reabsorbed. 84% reabsorption was assumed based on eq. 1 using a CL_R of 17.6 ml/min from the literature.	Brammer et al. 1991[53] Debruyne 1993[54]
Metabolism via UGT2B7	Fluconazole has at least two metabolites, but only UGT2B7 has been identified as a metabolizing enzyme.	Bourcier et al. 2010[6]
UGT2B7 interindividual variability	Interindividual variability of UGT2B7 was assumed to have log-normal distribution with a geometric SD of 1.34.	Sim et al. 1991[57]
UGT2B7 ontogeny	UGT2B7 reaches adult concentrations and function by 1 year of age.	Edginton et al. 2006 [45]
Edema	Body weight in children on ECMO can be increased by >50% due to edema.	Anderson et. al 1992[91]
Protein binding	Protein binding is variable in critical illness; f_u = 89% with standard deviation = 7% was assumed.	Arredondo et al. 1994[3] Arredondo et al. 1995[2]

Table 4.3. Studies used in model development and evaluation

Population	N	Age	Dosing interval	Dose	Reference
Adult Development Datasets					
Healthy volunteers	10	27y (SD 4)	Single dose	100mg	Yeates et al. 1994[92]
Healthy volunteers	8	21.1y (range 21, 22)	Single dose	50mg	Shiba et al. 1990[93]
	8	21.1y (range 21, 22)	Single dose	25mg	Shiba et al. 1990[93]
Adult Validation Datasets					
Healthy volunteers	10	NR	Single dose	50mg	Brammer et al. 1990[94]
Healthy volunteers	10	NR	q24 hours	50mg	Brammer et al. 1987[95]
Healthy volunteers	10	NR	q24 hours	100mg	Foulds et al. 1988[96]
Pediatric Validation Dataset					
Critically ill infants	13	36d (range 6-262d)	q24 hours	25mg/kg	Piper et al. 2015[76]
ECMO Validation Dataset					
Critically ill infants on ECMO	11	24d (range 1-165d)	q24-168 hours[a]	25mg/kg	Watt et al. 2015[97]

[a]The dosing interval for the Fluconazole ECMO Trial was variable based on indication, so only data from the first 24 hours was used.

NR – not reported

Table 4.4. Observed versus PBPK Predicted AUCs for adult studies used in model development and validation.

Population	N	Dose	Observed AUC (mg*h/L)	PBPK Predicted AUC (mg*h/L)	Fold Error
Adult Development Datasets					
Healthy volunteers[92]	10	100mg	73[a]	85	1.16
Healthy volunteers[93]	8	50mg	34[b]	36	1.06
		25mg	17[b]	19	1.12
Adult Validation Datasets					
Healthy volunteers[95]	10	50mg	39[c]	41	1.05
Healthy volunteers[96]	10	100mg	32[d]	34	1.06

AUC time intervals reported in the Adult Development and Validation Datasets varied by study, so PBPK model generated a corresponding AUC for each study: [a] $AUC_{0-\infty}$ after a single dose; [b] AUC_{0-72} after a single dose; [c] $AUC_{0-\infty}$ after a single dose; [d] AUC_{0-24} after a single dose. One of the adult validation datasets[94] did not report AUC and was not included in this table..

Figure 4.1. PBPK model structure.

Standard model structure

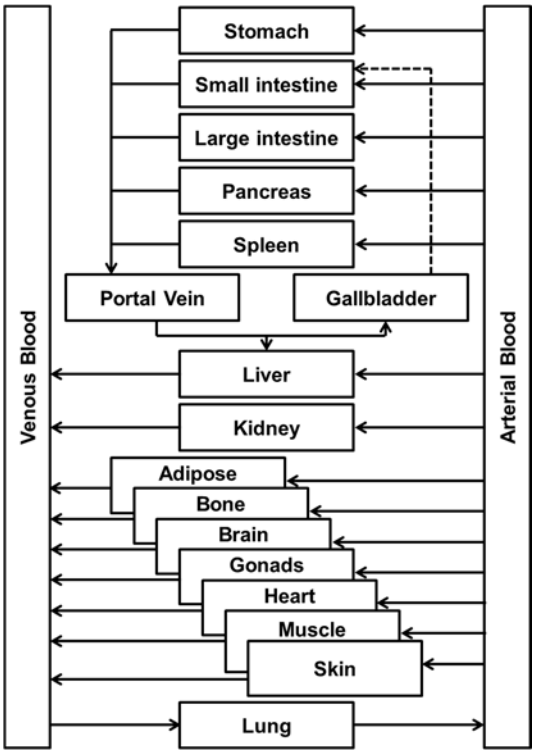

Model structure with ECMO compartment

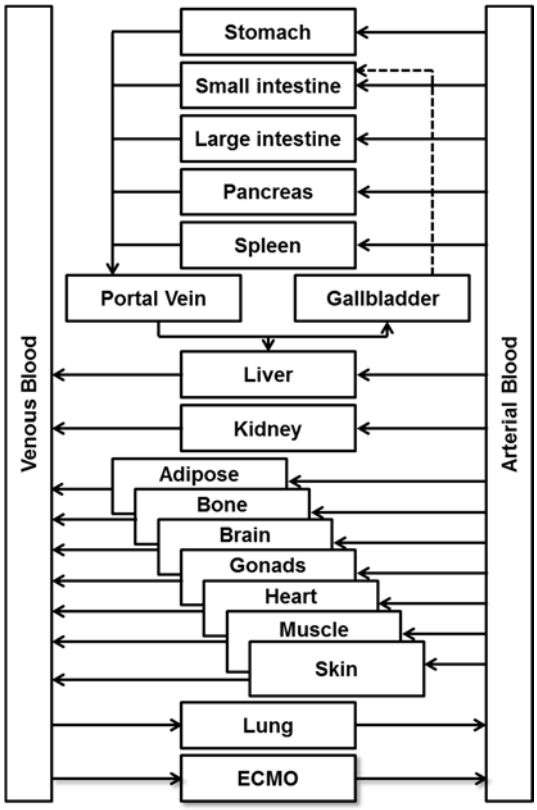

Figure 4.2. PBPK workflow

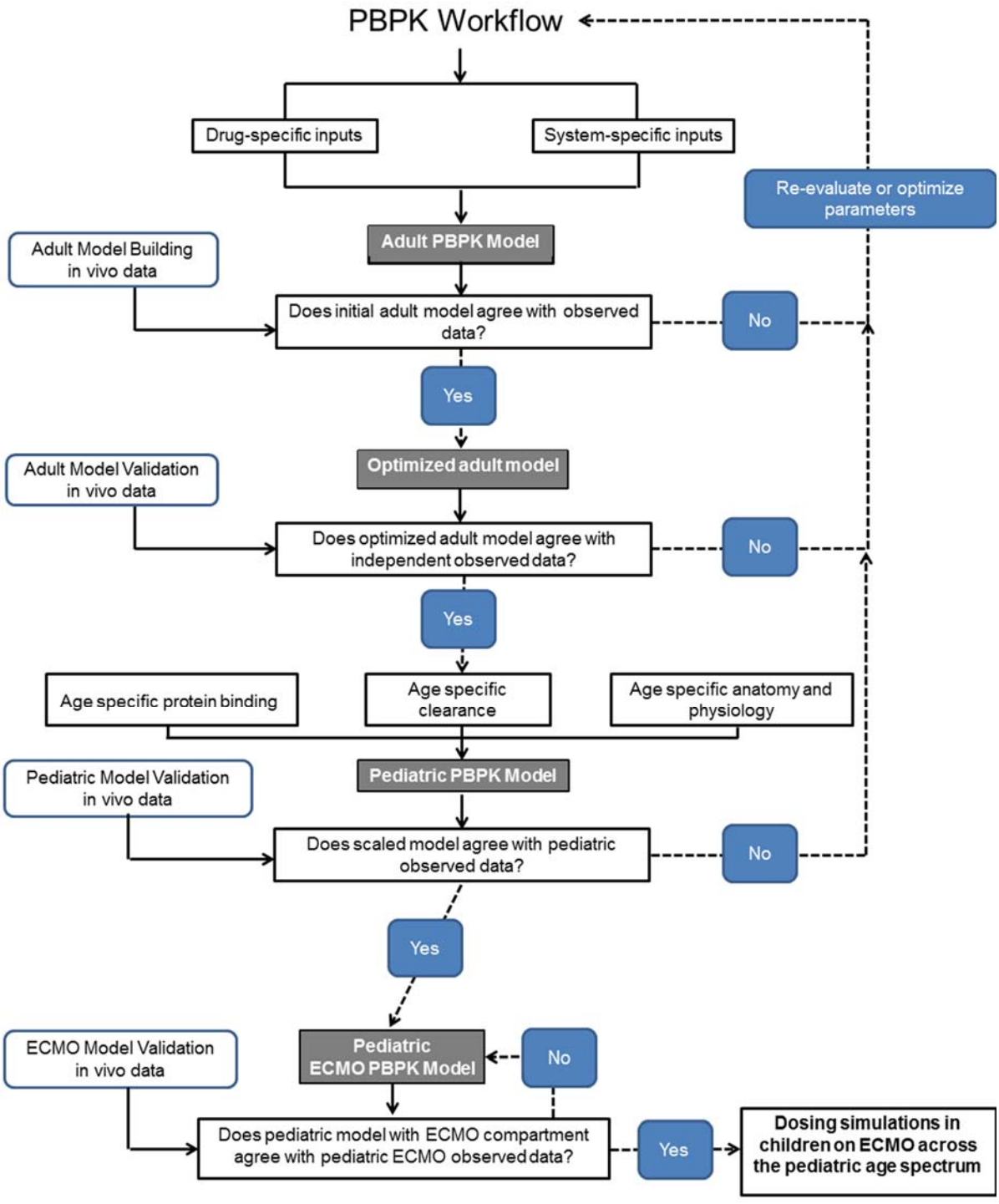

Figure 4.3. Adult optimized model. PBPK model predictions for a dose of 1mg versus dose-normalized observed concentrations from the Adult Development Datasets. Solid black line represents the median predicted concentration; grey shaded area represents the 90% prediction interval; observed data (mean +/- 90% confidence interval) are represented by symbols.

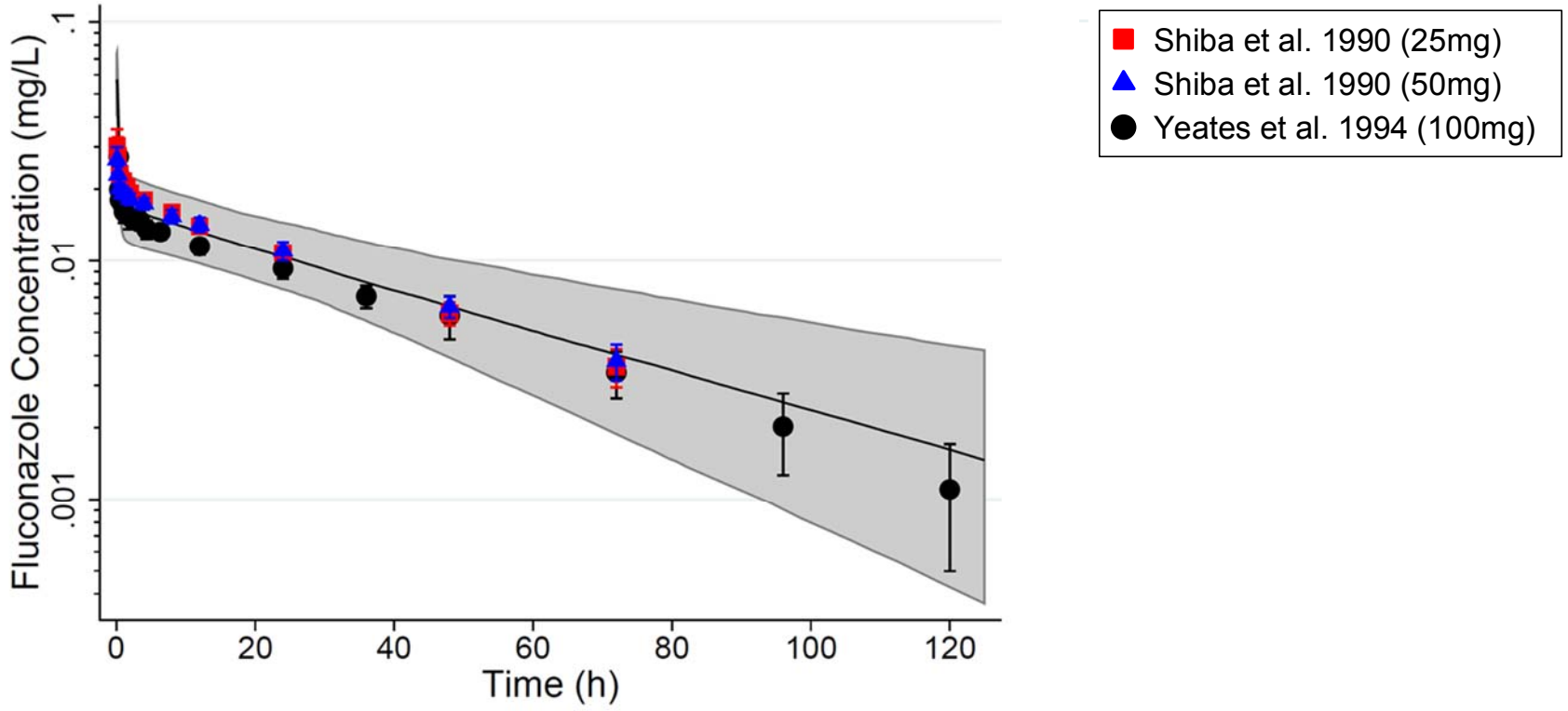

Figure 4.4. Adult model validation. PBPK predicted exposures versus observed data from Adult Validation Datasets. Solid black line is median predicted concentration; grey shaded area represents the 90% prediction interval; observed data (mean +/- 90% confidence interval when reported) are represented by symbols.

Brammer et al. 1990[94]; 50mg single dose

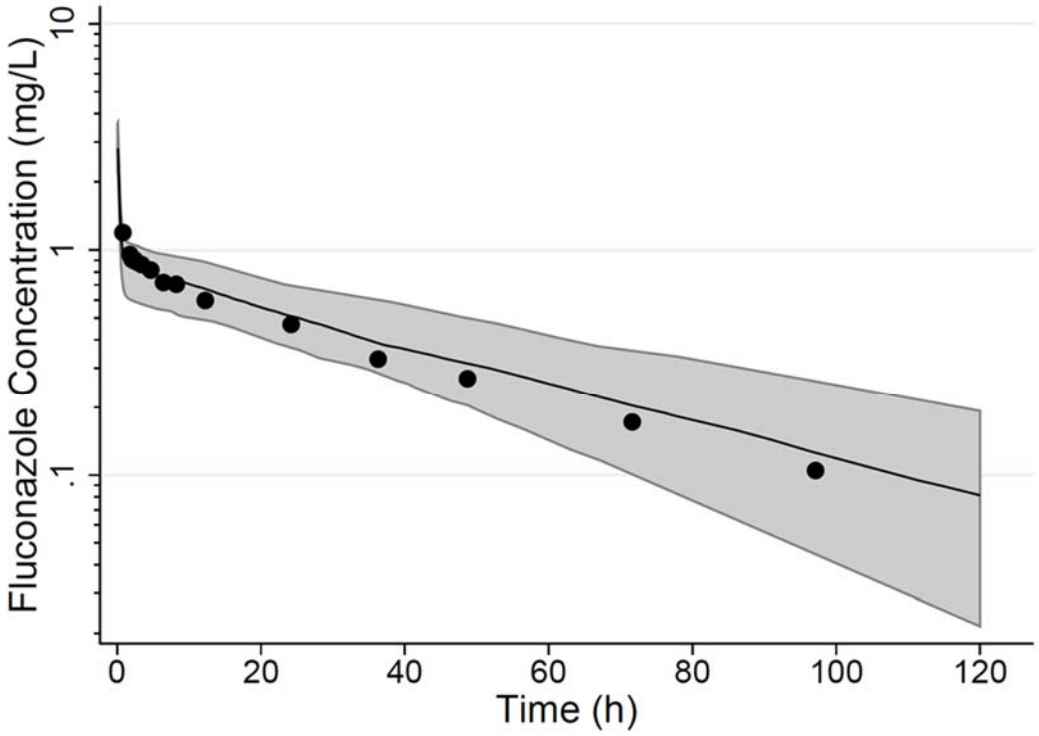

Brammer et al.1987[95]; 50mg q24 hours

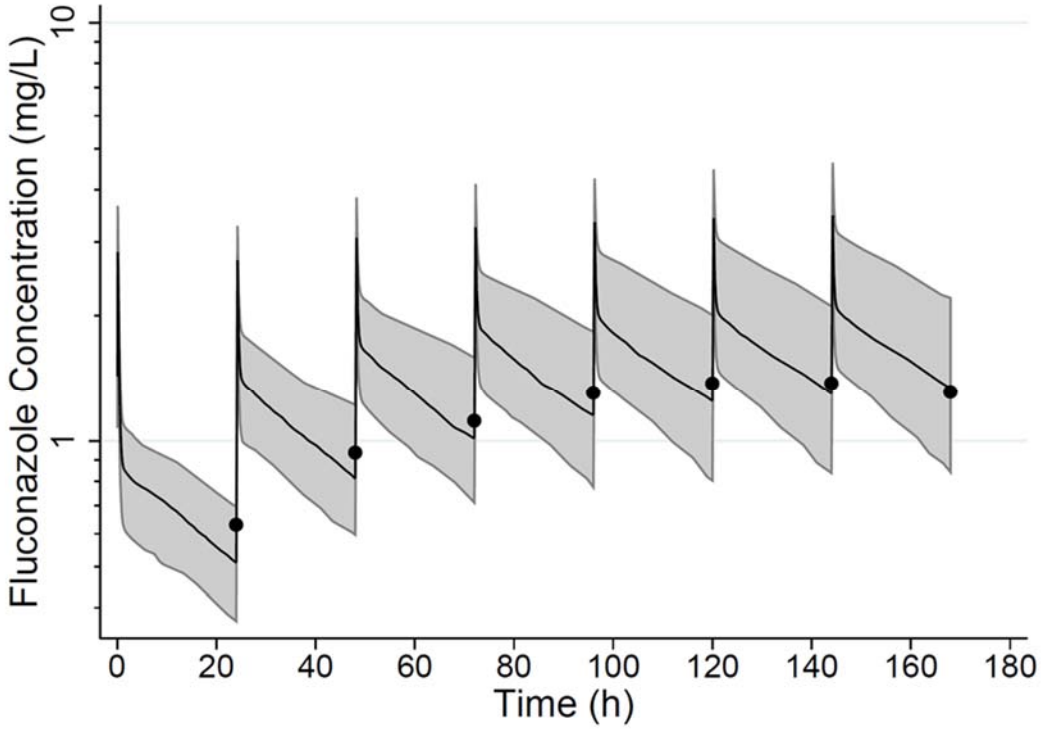

Foulds et al. 1988[96]; 100mg q24 hours

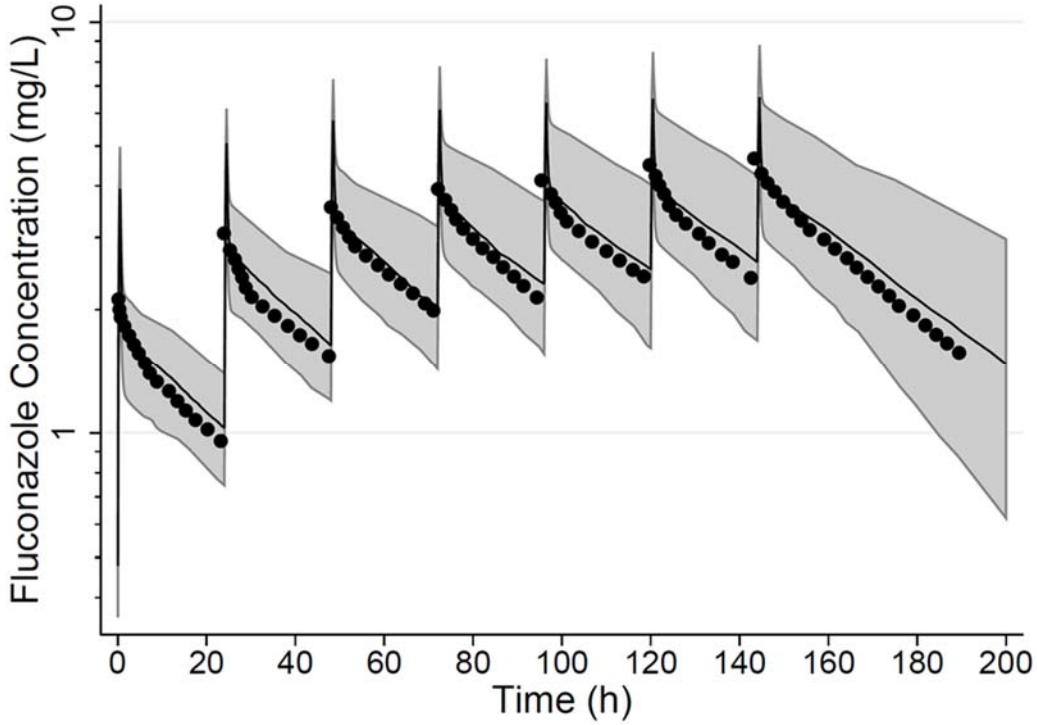

Figure 4.5. Pediatric PBPK Model predictions versus observed data from critically ill infants. All infants received a single 25 mg/kg loading dose. Solid black line is median predicted concentration; grey shaded area represents the 90% prediction interval; observed data are represented by symbols.

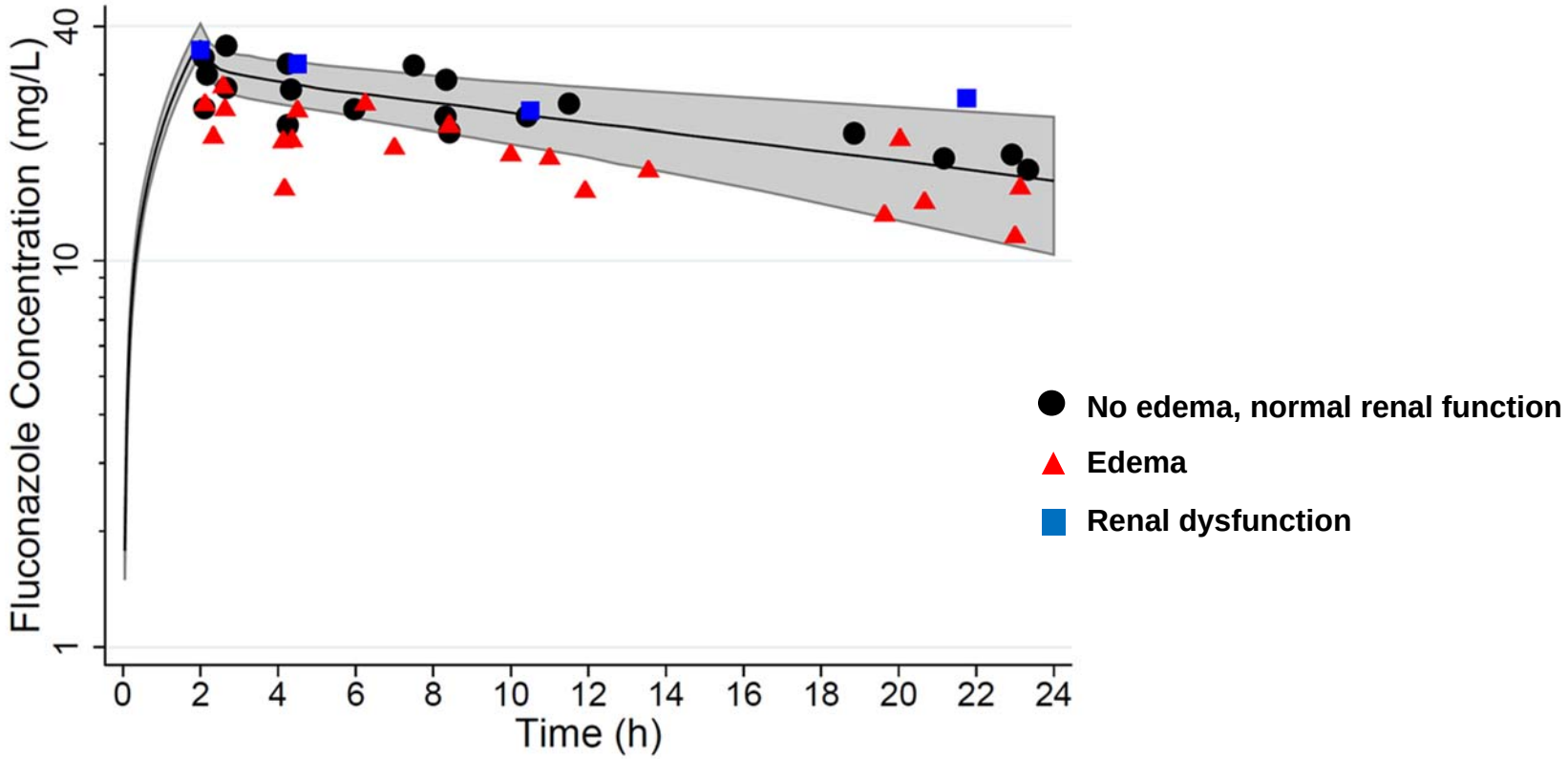

Figure 4.6. Pediatric PBPK Model $AUC_{0\text{-}24}$ predicted versus observed[a] following a 25 mg/kg loading dose. Solid black horizontal line is median, box represents interquartile range and whiskers are 90% confidence interval. Dashed blue horizontal line represents target $AUC_{0\text{-}24}$. Median $AUC_{0\text{-}24}$ and percentage of children achieving target $AUC_{0\text{-}24}$ shown below each plot.

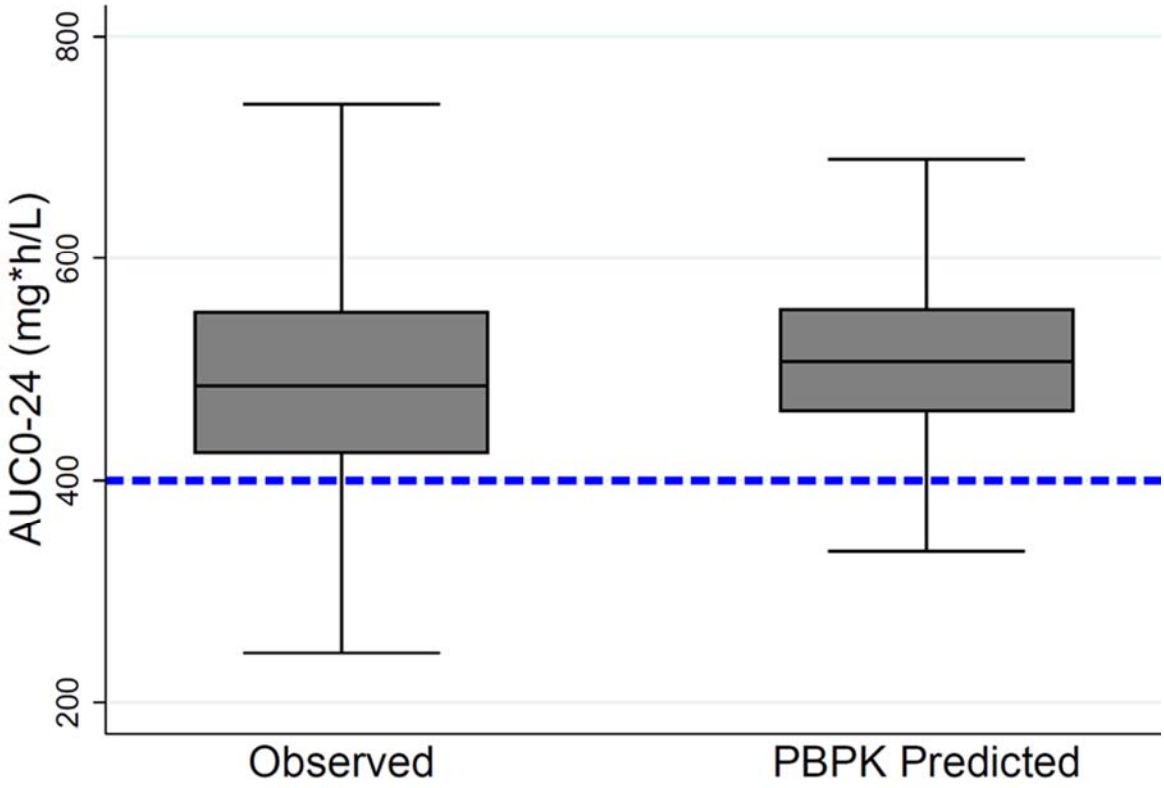

$AUC_{0\text{-}24}$ 485 mg*h/L
84% ≥ 400 mg*h/L

$AUC_{0\text{-}24}$ 507 mg*h/L
95% ≥ 400 mg*h/L

[a]Observed $AUC_{0\text{-}24}$ was calculated using compartmental modeling described in Chapter 3.

Figure 4.7. ECMO PBPK Model development. Model predictions and observed data were based on a loading dose of 25 mg/kg in infants.

1. Base PBPK model: Pediatric PBPK Model predictions versus observed concentrations in infants on ECMO

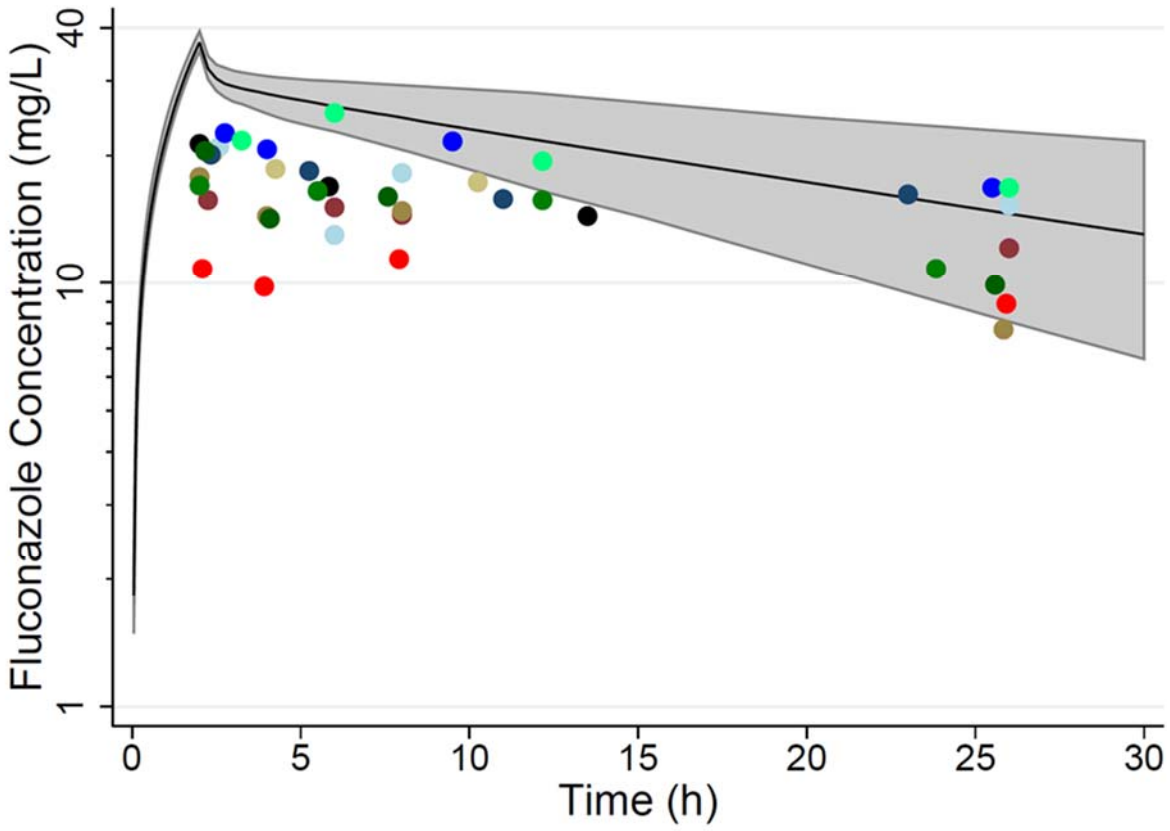

$AUC_{0\text{-}24}$ 520 mg*h/L

2. Addition of ECMO compartment to the Pediatric PBPK Model

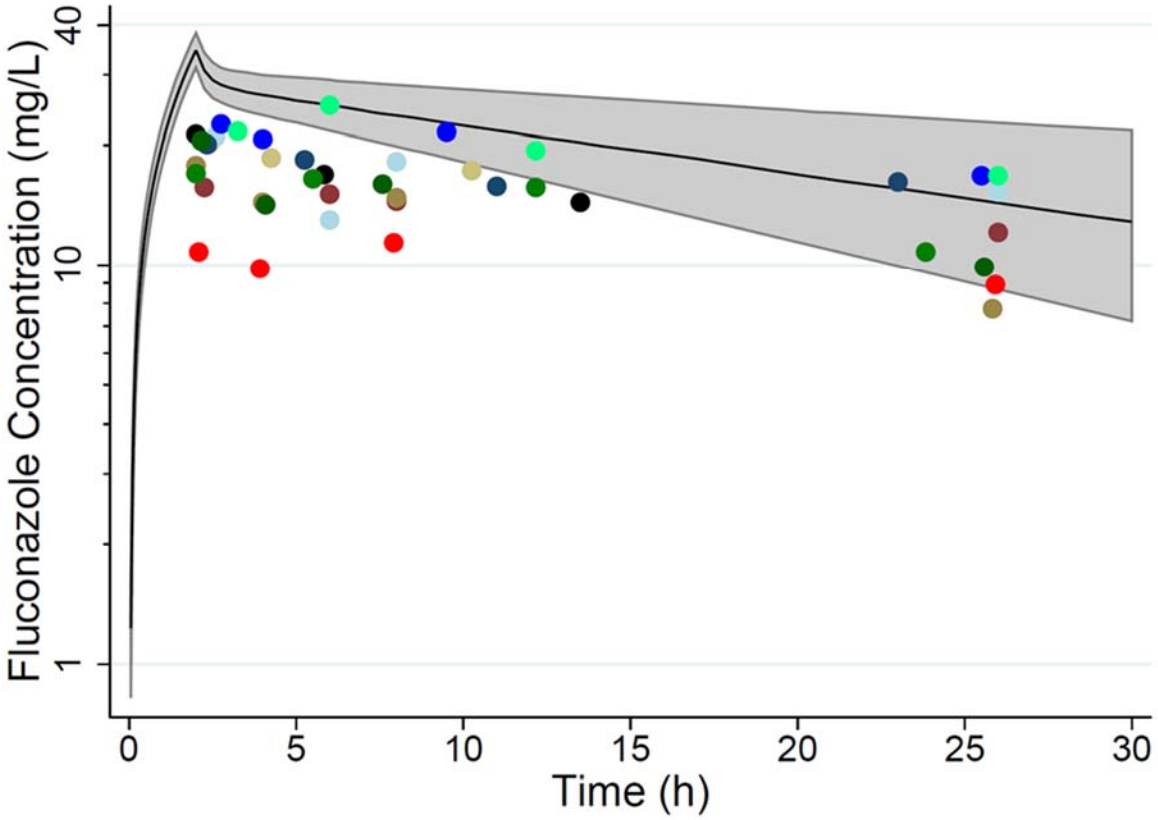

$AUC_{0\text{-}24}$ 502 mg*h/L

3. Addition of the ECMO compartment and incorporation of Edema to the Pediatric PBPK Model

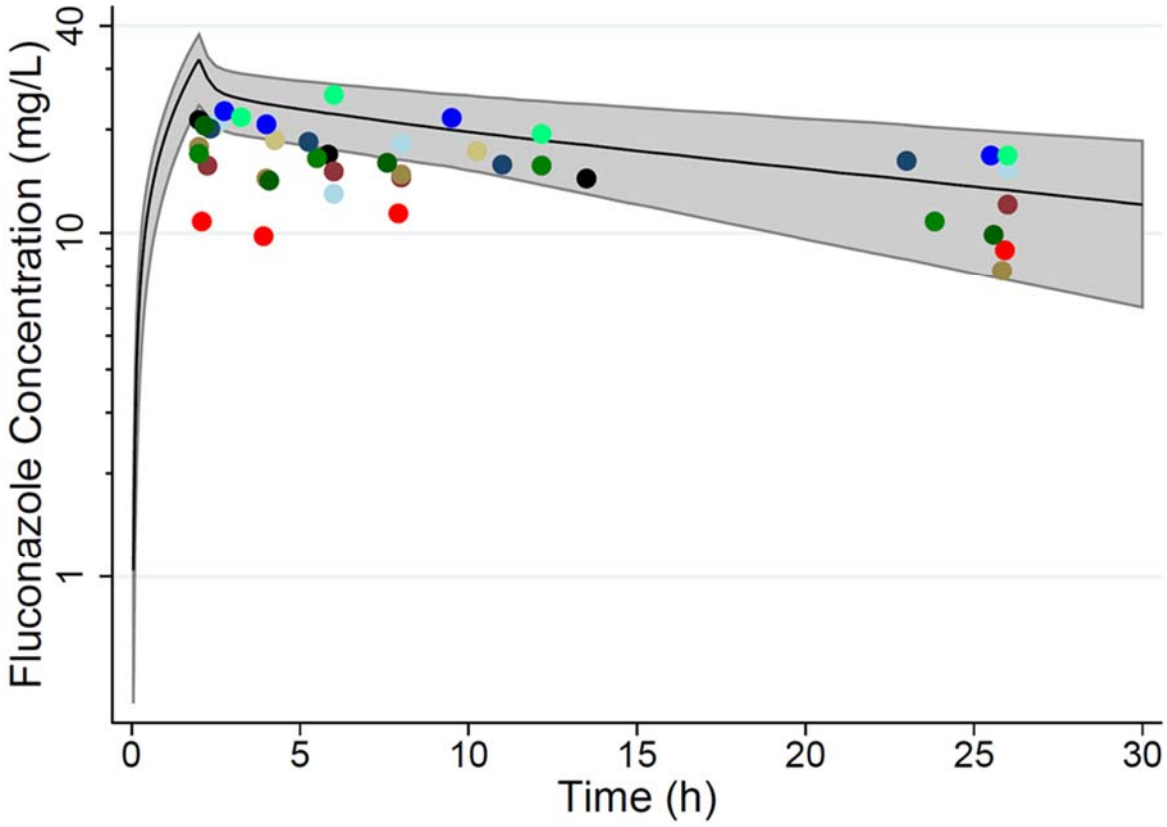

$AUC_{0\text{-}24}$ 420 mg*h/L

Figure 4.8. ECMO PBPK Model $AUC_{0\text{-}24}$ predicted versus observed[a] following a 25 mg/kg loading dose. Solid black horizontal line is median, box represents interquartile range, and whiskers are 90% confidence interval. Dashed blue horizontal line represents target $AUC_{0\text{-}24}$. Median $AUC_{0\text{-}24}$ and percentage of children achieving target AUC shown below each plot.

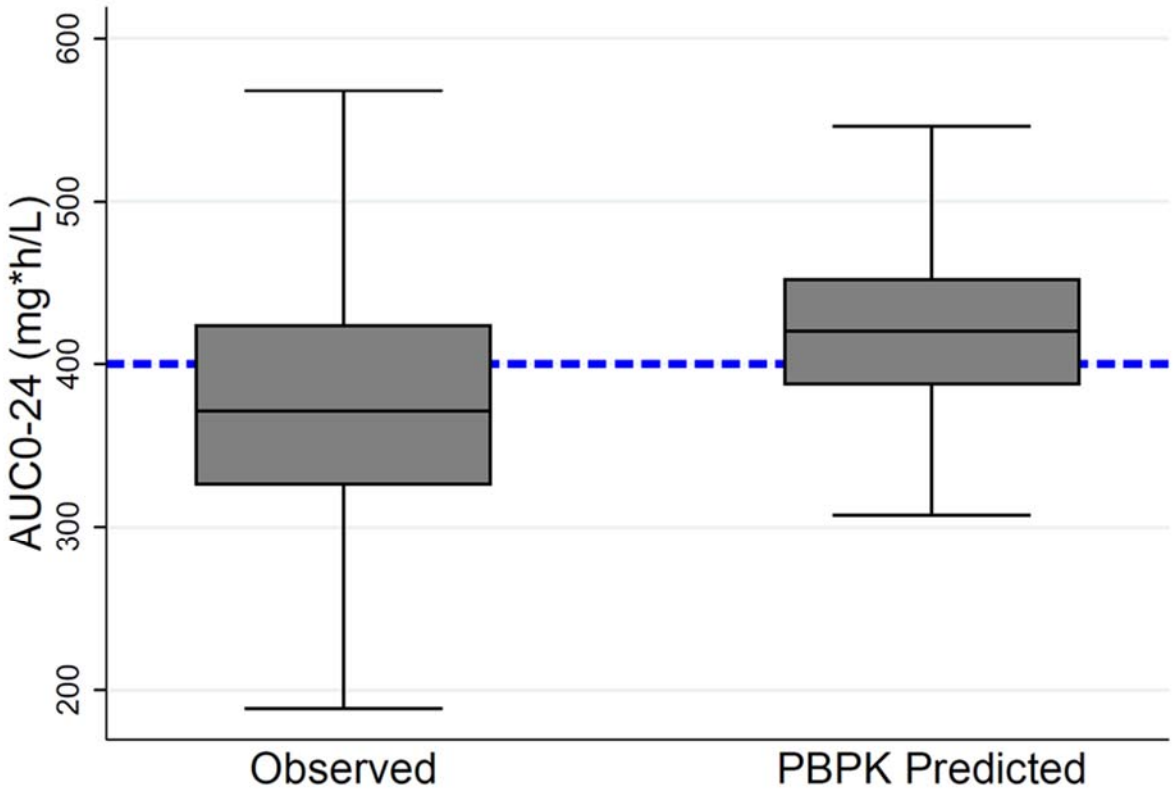

$AUC_{0\text{-}24}$ 371 mg*h/L
35% ≥ 400

$AUC_{0\text{-}24}$ 420 mg*h/L
67% ≥ 400

[a]Observed $AUC_{0\text{-}24}$ was calculated using the final population PK model and Monte Carlo simulations described in Chapter 3.

Figure 4.9. ECMO PBPK Model-predicted optimized fluconazole dosing and exposure in children on ECMO across the pediatric age spectrum. Solid line represents the median, box represents interquartile range, and whiskers represent 90% prediction interval. Dosing achieved the target $AUC_{0\text{-}24}$ (>400 mg*h/L, blue dashed line) in ≥ 90% of simulated children on ECMO in the first 24 hours of therapy.

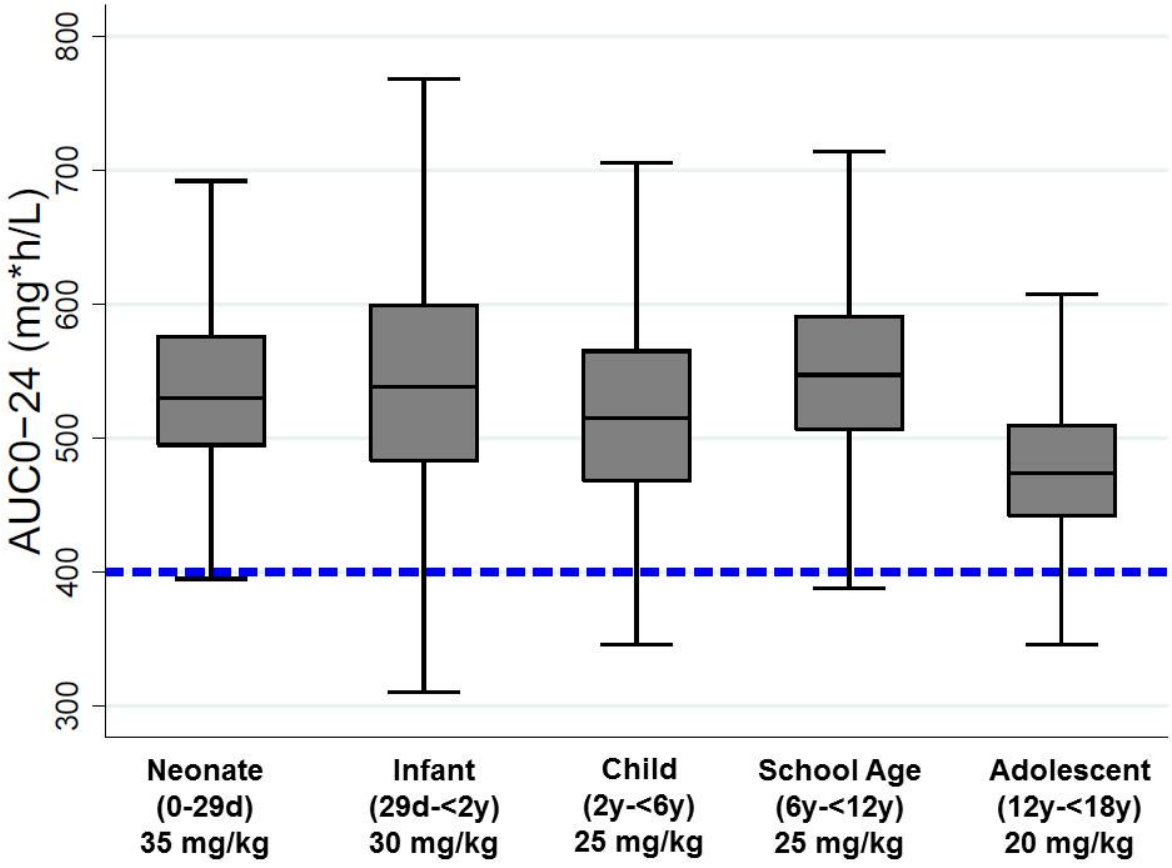

Figure 4.10. ECMO PBPK Model-predicted fluconazole exposure after a loading dose of 35 mg/kg in children on ECMO across the pediatric age spectrum. Solid line represents the median, box represents interquartile range, and whiskers represent 90% prediction interval. Dosing achieved the target $AUC_{0\text{-}24}$ (>400 mg*h/L, blue dashed line) in ≥ 99% of simulated children on ECMO in the first 24 hours of therapy.

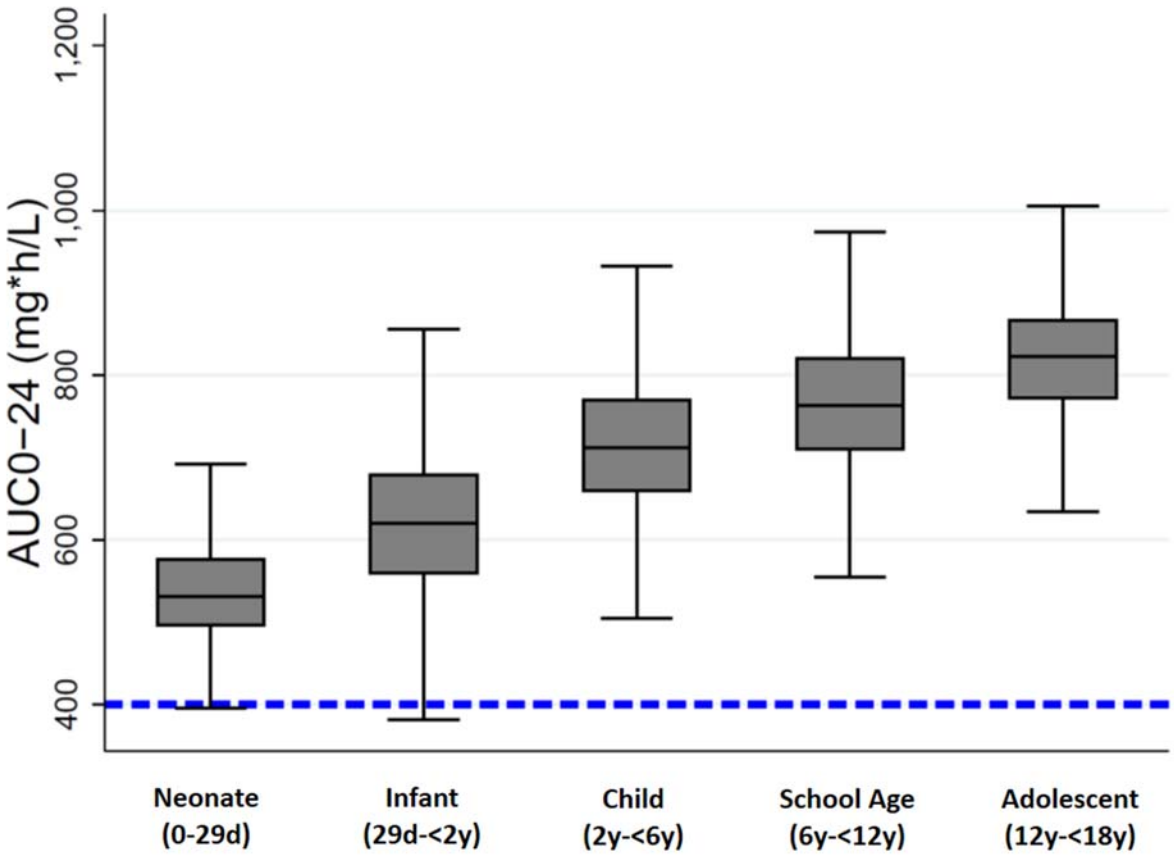

REFERENCES

1. FDA. Fluconazole Injection, USP Product Label. In: U.S. Dept. of Health and Human Services FaDA, ed.: Roerig, a division of Pfizer, Inc.; 2015.

2. Arredondo G, Calvo R, Marcos F, Martinez-Jorda R, Suarez E. Protein binding of itraconazole and fluconazole in patients with cancer. International journal of clinical pharmacology and therapeutics 1995;33:449-52.

3. Arredondo G, Martinez-Jorda R, Calvo R, Aguirre C, Suarez E. Protein binding of itraconazole and fluconazole in patients with chronic renal failure. International journal of clinical pharmacology and therapeutics 1994;32:361-4.

4. Debruyne D. Clinical pharmacokinetics of fluconazole in superficial and systemic mycoses. Clin Pharmacokinet 1997;33:52-77.

5. Wildfeuer A, Laufen H, Schmalreck AF, Yeates RA, Zimmermann T. Fluconazole: comparison of pharmacokinetics, therapy and in vitro susceptibility. Mycoses 1997;40:259-65.

6. Bourcier K, Hyland R, Kempshall S, et al. Investigation into UDP-glucuronosyltransferase (UGT) enzyme kinetics of imidazole- and triazole-containing antifungal drugs in human liver microsomes and recombinant UGT enzymes. Drug metabolism and disposition: the biological fate of chemicals 2010;38:923-9.

7. Anaissie EJ, Darouiche RO, Abi-Said D, et al. Management of invasive candidal infections: results of a prospective, randomized, multicenter study of fluconazole versus amphotericin B and review of the literature. Clin Infect Dis 1996;23:964-72.

8. Rex JH, Bennett JE, Sugar AM, et al. A randomized trial comparing fluconazole with amphotericin B for the treatment of candidemia in patients without neutropenia. Candidemia Study Group and the National Institute. N Engl J Med 1994;331:1325-30.

9. Phillips JR, Karlowicz MG. Prevalence of Candida species in hospital-acquired urinary tract infections in a neonatal intensive care unit. Pediatric Infectious Disease Journal 1997;16:190-4.

10. Marr KA, Seidel K, White TC, Bowden RA. Candidemia in allogeneic blood and marrow transplant recipients: evolution of risk factors after the adoption of prophylactic fluconazole. J Infect Dis 2000;181:309-16.

11. Pappas PG, Kauffman CA, Andes D, et al. Clinical practice guidelines for the management of candidiasis: 2009 update by the Infectious Diseases Society of America. Clin Infect Dis 2009;48:503-35.

12. Perlroth J, Choi B, Spellberg B. Nosocomial fungal infections: epidemiology, diagnosis, and treatment. Medical mycology : official publication of the International Society for Human and Animal Mycology 2007;45:321-46.

13. Pfaller MA, Diekema DJ. Epidemiology of invasive candidiasis: a persistent public health problem. Clin Microbiol Rev 2007;20:133-63.

14. Riddell Jt, Kauffman CA. The evolution of resistant Candida species in cancer centers: implications for treatment and prophylaxis. Cancer 2008;112:2334-7.

15. Spellberg BJ, Filler SG, Edwards JE, Jr. Current treatment strategies for disseminated candidiasis. Clin Infect Dis 2006;42:244-51.

16. Wilson AG, Micek ST, Ritchie DJ. A retrospective Evaluation of fluconazole for the treatment of Candida glabrata fungemia. Clin Ther 2005;27:1228-37.

17. Baddley JW, Patel M, Bhavnani SM, Moser SA, Andes DR. Association of fluconazole pharmacodynamics with mortality in patients with candidemia. Antimicrob Agents Chemother 2008;52:3022-8.

18. Bilgen H, Ozek E, Korten V, Ener B, Molbay D. Treatment of systemic neonatal candidiasis with fluconazole. Infection 1995;23:394.

19. Johnston JD, Harvey CJ, Menzies IS, Treacher DF. Gastrointestinal permeability and absorptive capacity in sepsis. Crit Care Med 1996;24:1144-9.

20. Singh G, Chaudry KI, Chudler LC, Chaudry IH. Sepsis produces early depression of gut absorptive capacity: restoration with diltiazem treatment. The American journal of physiology 1992;263:R19-23.

21. Tarling MM, Toner CC, Withington PS, Baxter MK, Whelpton R, Goldhill DR. A model of gastric emptying using paracetamol absorption in intensive care patients. Intensive Care Med 1997;23:256-60.

22. Heyland DK, Tougas G, King D, Cook DJ. Impaired gastric emptying in mechanically ventilated, critically ill patients. Intensive Care Med 1996;22:1339-44.

23. Etzel JV, Nafziger AN, Bertino JS, Jr. Variation in the pharmacokinetics of gentamicin and tobramycin in patients with pleural effusions and hypoalbuminemia. Antimicrob Agents Chemother 1992;36:679-81.

24. Beckhouse MJ, Whyte IM, Byth PL, Napier JC, Smith AJ. Altered aminoglycoside pharmacokinetics in the critically ill. Anaesthesia and intensive care 1988;16:418-22.

25. Dasta JF, Armstrong DK. Variability in aminoglycoside pharmacokinetics in critically ill surgical patients. Crit Care Med 1988;16:327-30.

26. Gous AG, Dance MD, Lipman J, Luyt DK, Mathivha R, Scribante J. Changes in vancomycin pharmacokinetics in critically ill infants. Anaesthesia and intensive care 1995;23:678-82.

27. Hanes SD, Wood GC, Herring V, et al. Intermittent and continuous ceftazidime infusion for critically ill trauma patients. Am J Surg 2000;179:436-40.

28. Ronchera-Oms CL, Tormo C, Ordovas JP, Abad J, Jimenez NV. Expanded gentamicin volume of distribution in critically ill adult patients receiving total parenteral nutrition. Journal of clinical pharmacy and therapeutics 1995;20:253-8.

29. Abdel-Razzak Z, Loyer P, Fautrel A, et al. Cytokines down-regulate expression of major cytochrome P-450 enzymes in adult human hepatocytes in primary culture. Mol Pharmacol 1993;44:707-15.

30. Rivory LP, Slaviero KA, Clarke SJ. Hepatic cytochrome P450 3A drug metabolism is reduced in cancer patients who have an acute-phase response. British journal of cancer 2002;87:277-80.

31. Siewert E, Bort R, Kluge R, Heinrich PC, Castell J, Jover R. Hepatic cytochrome P450 down-regulation during aseptic inflammation in the mouse is interleukin 6 dependent. Hepatology 2000;32:49-55.

32. Richardson TA, Sherman M, Kalman D, Morgan ET. Expression of UDP-glucuronosyltransferase isoform mRNAs during inflammation and infection in mouse liver and kidney. Drug metabolism and disposition: the biological fate of chemicals 2006;34:351-3.

33. Claus BO, Hoste EA, Colpaert K, Robays H, Decruyenaere J, De Waele JJ. Augmented renal clearance is a common finding with worse clinical outcome in critically ill patients receiving antimicrobial therapy. J Crit Care 2013;28:695-700.

34. Fuster-Lluch O, Geronimo-Pardo M, Peyro-Garcia R, Lizan-Garcia M. Glomerular hyperfiltration and albuminuria in critically ill patients. Anaesthesia and intensive care 2008;36:674-80.

35. Zappitelli M, Parikh CR, Akcan-Arikan A, Washburn KK, Moffett BS, Goldstein SL. Ascertainment and epidemiology of acute kidney injury varies with definition interpretation. Clinical journal of the American Society of Nephrology : CJASN 2008;3:948-54.

36. Piquette-Miller M, Pak A, Kim H, Anari R, Shahzamani A. Decreased expression and activity of P-glycoprotein in rat liver during acute inflammation. Pharm Res 1998;15:706-11.

37. Trauner M, Nathanson MH, Rydberg SA, et al. Endotoxin impairs biliary glutathione and HCO3- excretion and blocks the choleretic effect of nitric oxide in rat liver. Hepatology 1997;25:1184-91.

38. Hartmann G, Cheung AK, Piquette-Miller M. Inflammatory cytokines, but not bile acids, regulate expression of murine hepatic anion transporters in endotoxemia. J Pharmacol Exp Ther 2002;303:273-81.

39. B. MR, Timpa JG, Kurundkar AR, et al. Plasma concentrations of inflammatory cytokines rise rapidly during ECMO-related SIRS due to the release of preformed stores in the intestine. Lab Invest 2010;90:128-39.

40. Paden ML, Warshaw BL, Heard ML, Fortenberry JD. Recovery of renal function and survival after continuous renal replacement therapy during extracorporeal membrane oxygenation. Pediatr Crit Care Med 2011;12:153-8.

41. Askenazi DJ, Ambalavanan N, Hamilton K, et al. Acute kidney injury and renal replacement therapy independently predict mortality in neonatal and pediatric noncardiac patients on extracorporeal membrane oxygenation. Pediatr Crit Care Med 2011;12:e1-6.

42. Roy BJ, Cornish JD, Clark RH. Venovenous extracorporeal membrane oxygenation affects renal function. Pediatrics 1995;95:573-8.

43. Williams DC, Turi JL, Hornik CP, et al. Circuit oxygenator contributes to extracorporeal membrane oxygenation-induced hemolysis. ASAIO J 2015;61:190-5.

44. Anderson HL, 3rd, Coran AG, Drongowski RA, Ha HJ, Bartlett RH. Extracellular fluid and total body water changes in neonates undergoing extracorporeal membrane oxygenation. J Pediatr Surg 1992;27:1003-7; discussion 7-8.

45. Edginton AN, Schmitt W, Willmann S. Development and evaluation of a generic physiologically based pharmacokinetic model for children. Clin Pharmacokinet 2006;45:1013-34.

46. Leong R, Vieira ML, Zhao P, et al. Regulatory Experience With Physiologically Based Pharmacokinetic Modeling for Pediatric Drug Trials. Clin Pharmacol Ther 2012.

47. Johnson TN, Rostami-Hodjegan A, Tucker GT. Prediction of the clearance of eleven drugs and associated variability in neonates, infants and children. Clin Pharmacokinet 2006;45:931-56.

48. Statistics NCfH. Third National Health and Nutrition Examination Survey (NHANES III). In. Hyattsville, MD; 1997.

49. ICRP. Basic Anatomical and Physiological Data for Use in Radiological Protection Reference Values. Annals of the International Commission on Radiological Protection 2002;32.

50. Willmann S, Lippert J, Schmitt W. From physicochemistry to absorption and distribution: predictive mechanistic modelling and computational tools. Expert Opin Drug Metab Toxicol 2005;1:159-68.

51. Kawai R, Lemaire M, Steimer JL, Bruelisauer A, Niederberger W, Rowland M. Physiologically based pharmacokinetic study on a cyclosporin derivative, SDZ IMM 125. J Pharmacokinet Biopharm 1994;22:327-65.

52. Nestorov IA, Aarons LJ, Arundel PA, Rowland M. Lumping of whole-body physiologically based pharmacokinetic models. J Pharmacokinet Biopharm 1998;26:21-46.

53. Brammer KW, Coakley AJ, Jezequel SG, Tarbit MH. The disposition and metabolism of [14C]fluconazole in humans. Drug metabolism and disposition: the biological fate of chemicals 1991;19:764-7.

54. Debruyne D, Ryckelynck JP. Clinical pharmacokinetics of fluconazole. Clin Pharmacokinet 1993;24:10-27.

55. Lagarias JC, Reeds JA, Wright MH, Wright PE. Convergence Properties of the Nelder-Mead Simplex Method in Low Dimensions. SIAM Journal of Optimization 1998;9:112-47.

56. Willmann S, Hohn K, Edginton A, et al. Development of a physiology-based whole-body population model for assessing the influence of individual variability on the pharmacokinetics of drugs. J Pharmacokinet Pharmacodyn 2007;34:401-31.

57. Sim SM, Back DJ, Breckenridge AM. The effect of various drugs on the glucuronidation of zidovudine (azidothymidine; AZT) by human liver microsomes. Br J Clin Pharmacol 1991;32:17-21.

58. Segel SA, Fanelli CG, Dence CS, et al. Blood-to-brain glucose transport, cerebral glucose metabolism, and cerebral blood flow are not increased after hypoglycemia. Diabetes 2001;50:1911-7.

59. Epstein HT. Stages of increased cerebral blood flow accompany stages of rapid brain growth. Brain & development 1999;21:535-9.

60. Wintermark M, Lepori D, Cotting J, et al. Brain perfusion in children: evolution with age assessed by quantitative perfusion computed tomography. Pediatrics 2004;113:1642-52.

61. Visser MO, Leighton JO, van de Bor M, Walther FJ. Renal blood flow in neonates: quantification with color flow and pulsed Doppler US. Radiology 1992;183:441-4.

62. Scholbach T. Color Doppler sonographic determination of renal blood flow in healthy children. Journal of ultrasound in medicine : official journal of the American Institute of Ultrasound in Medicine 1999;18:559-64.

63. Scholbach TM. Changes of renal flow volume in the hemolytic-uremic syndrome--color Doppler sonographic investigations. Pediatr Nephrol 2001;16:644-7.

64. Raitakari M, Nuutila P, Ruotsalainen U, et al. Evidence for dissociation of insulin stimulation of blood flow and glucose uptake in human skeletal muscle: studies using [15O]H2O, [18F]fluoro-2-deoxy-D-glucose, and positron emission tomography. Diabetes 1996;45:1471-7.

65. Goetzova J, Skovranek J, Samanek M. Muscle blood flow in children, measured by 133Xe clearance method. Cor et vasa 1977;19:161-4.

66. Skovranek J, Samenek M. Chronic impairment of leg muscle blood flow following cardiac catheterization in childhood. AJR American journal of roentgenology 1979;132:71-5.

67. Wu PY, Wong WH, Guerra G, et al. Peripheral blood flow in the neonate; 1. Changes in total, skin, and muscle blood flow with gestational and postnatal age. Pediatric research 1980;14:1374-8.

68. Mikasa H, Sakuragi T, Higa K, Yasumoto M. Skin blood flow and plasma catecholamine concentrations during removal of a phaeochromocytoma in a child. Br J Anaesth 2004;92:757-60.

69. Chimoskey JE. Skin blood flow by 133 Xe disappearance validated by venous occlusion plethysmography. J Appl Physiol 1972;32:432-5.

70. Irazuzta JE, Berde CB, Sethna NF. Laser Doppler measurements of skin blood flow before, during, and after lumbar sympathetic blockade in children and young adults with reflex sympathetic dystrophy syndrome. Journal of clinical monitoring 1992;8:16-9.

71. Moustogiannis AN, Raju TN, Roohey T, McCulloch KM. Intravenous morphine attenuates pain induced changes in skin blood flow in newborn infants. Neurological research 1996;18:440-4.

72. Leggett RW, Williams LR. A proposed blood circulation model for Reference Man. Health physics 1995;69:187-201.

73. Edginton AN, Schmitt W, Voith B, Willmann S. A mechanistic approach for the scaling of clearance in children. Clin Pharmacokinet 2006;45:683-704.

74. Rhodin MM, Anderson BJ, Peters AM, et al. Human renal function maturation: a quantitative description using weight and postmenstrual age. Pediatr Nephrol 2009;24:67-76.

75. McNamara PJ, Alcorn J. Protein binding predictions in infants. AAPS pharmSci 2002;4:E4.

76. Piper L, Smith PB, Hornik CP, et al. Fluconazole loading dose pharmacokinetics and safety in infants. Pediatr Infect Dis J 2011;30:375-8.

77. Vrancken SL, Heijst AF, Zegers M, et al. Influence of volume replacement with colloids versus crystalloids in neonates on venoarterial extracorporeal membrane oxygenation on fluid retention, fluid balance, and ECMO runtime. ASAIO J 2005;51:808-12.

78. Andes D, Forrest A, Lepak A, Nett J, Marchillo K, Lincoln L. Impact of antimicrobial dosing regimen on evolution of drug resistance in vivo: fluconazole and Candida albicans. Antimicrob Agents Chemother 2006;50:2374-83.

79. Wade KC, Benjamin DK, Jr., Kaufman DA, et al. Fluconazole dosing for the prevention or treatment of invasive candidiasis in young infants. Pediatr Infect Dis J 2009;28:717-23.

80. Andes D, van Ogtrop M. Characterization and quantitation of the pharmacodynamics of fluconazole in a neutropenic murine disseminated candidiasis infection model. Antimicrob Agents Chemother 1999;43:2116-20.

81. Clancy CJ, Staley B, Nguyen MH. In vitro susceptibility of breakthrough Candida bloodstream isolates correlates with daily and cumulative doses of fluconazole. Antimicrob Agents Chemother 2006;50:3496-8.

82. Clancy CJ, Yu VL, Morris AJ, Snydman DR, Nguyen MH. Fluconazole MIC and the fluconazole dose/MIC ratio correlate with therapeutic response among patients with candidemia. Antimicrob Agents Chemother 2005;49:3171-7.

83. Pai MP, Turpin RS, Garey KW. Association of fluconazole area under the concentration-time curve/MIC and dose/MIC ratios with mortality in nonneutropenic patients with candidemia. Antimicrob Agents Chemother 2007;51:35-9.

84. Anaissie EJ, Kontoyiannis DP, Huls C, et al. Safety, plasma concentrations, and efficacy of high-dose fluconazole in invasive mold infections. Journal of Infectious Diseases 1995;172:599-602.

85. Bradley JS, Nelson JD, eds. Nelson's Pediatric Antimicrobial Therapy. 22nd Edition ed: American Academy of Pediatrics; 2016.

86. Chiou WL. Potential pitfalls in the conventional pharmacokinetic studies: effects of the initial mixing of drug in blood and the pulmonary first-pass elimination. J Pharmacokinet Biopharm 1979;7:527-36.

87. Butler J, Pathi VL, Paton RD, et al. Acute-phase responses to cardiopulmonary bypass in children weighing less than 10 kilograms. Ann Thorac Surg 1996;62:538-42.

88. Seghaye MC, Grabitz RG, Duchateau J, et al. Inflammatory reaction and capillary leak syndrome related to cardiopulmonary bypass in neonates undergoing cardiac operations. J Thorac Cardiovasc Surg 1996;112:687-97.

89. Wishart DS, Knox C, Guo AC, et al. DrugBank: a comprehensive resource for in silico drug discovery and exploration. Nucleic Acids Res 2006;34:D668-72.

90. Humphrey MJ, Jevons S, Tarbit MH. Pharmacokinetic evaluation of UK-49,858, a metabolically stable triazole antifungal drug, in animals and humans. Antimicrob Agents Chemother 1985;28:648-53.

91. Abi-Said D, Anaissie E, Uzun O, Raad I, Pinzcowski H, Vartivarian S. The epidemiology of hematogenous candidiasis caused by different Candida species. Clin Infect Dis 1997;24:1122-8.

92. Yeates RA, Ruhnke M, Pfaff G, Hartmann A, Trautmann M, Sarnow E. The pharmacokinetics of fluconazole after a single intravenous dose in AIDS patients. Br J Clin Pharmacol 1994;38:77-9.

93. Shiba K, Saito A, Miyahara T. Safety and pharmacokinetics of single oral and intravenous doses of fluconazole in healthy subjects. Clin Ther 1990;12:206-15.

94. Brammer KW, Farrow PR, Faulkner JK. Pharmacokinetics and tissue penetration of fluconazole in humans. Reviews of infectious diseases 1990;12 Suppl 3:S318-26.

95. Brammer KW, Tarbit MH, eds. A review of the pharmacokinetics of fluconazole (UK-49,858) in laboratory animals and man. Barcelona: J.R. Prous Science Publishers; 1987.

96. Foulds G, Wajszczuk C, Weidler DJ, Garg DJ, Gibson P. Steady state parenteral kinetics of fluconazole in man. Annals of the New York Academy of Sciences 1988;544:427-30.

97. Watt KM, Gonzalez D, Benjamin DK, Jr., et al. Fluconazole population pharmacokinetics and dosing for prevention and treatment of invasive Candidiasis in children supported with extracorporeal membrane oxygenation. Antimicrob Agents Chemother 2015;59:3935-43.

CHAPTER 5: PHARMACOKINETICS AND SAFETY OF MICAFUNGIN IN INFANTS SUPPORTED WITH EXTRACORPOREAL MEMBRANE OXYGENATION[1]

INTRODUCTION

Extracorporeal membrane oxygenation (ECMO) provides respiratory and cardiac support in critically ill infants when conventional modes of life-support fail.[2] Although potentially life-saving, ECMO support is associated with a high risk of nosocomial infections in children (8-16%).[3] The most common cause of ECMO-related nosocomial infection in infants and children and the second most common cause in neonates is invasive candidiasis.[3] Invasive candidiasis causes high rates of morbidity and mortality and is difficult to treat because of the organism's ability to form biofilms on indwelling catheters.[4] For this reason, recommended treatment of invasive candidiasis consists of both antifungal therapy and removal of indwelling catheters.[5,6] However, catheter removal for children on ECMO is impossible; therefore, therapy relies upon optimal dosing of antifungal agents.

Micafungin is an attractive antifungal drug in infants on ECMO because it is fungicidal against a broad spectrum of *Candida* spp, and can penetrate biofilms.[7-9] However, the optimal dosing of micafungin remains to be established in the setting of

[1]This chapter was accepted for publication in *Pediatric Infectious Disease Journal. 2016.* Pharmacokinetics and Safety of Micafungin in Infants Supported with Extracorporeal Membrane Oxygenation (ECMO). Autmizguine, J; Hornik, CP; Benjamin, DK, Jr; Brouwer, KLR; Hupp, S; Cohen-Wolkowiez, M; and Watt, KM

ECMO because ECMO support can alter drug pharmacokinetics (PK).[10,11] In infants on ECMO, the volume of distribution (V) of drugs typically increases due to the large volume of blood required to prime the ECMO circuit, disease state (e.g., inflammation, anasarca), and drug adsorption by the ECMO circuit itself.[10-14] Clearance (CL) of drugs can be affected by the organ dysfunction commonly observed in infants on ECMO, as well as non-specific drug extraction by the circuit itself. Micafungin may be more vulnerable to adsorption by the circuit because it is highly protein bound (>99%).[15] Therefore, it is likely that current micafungin dosing recommendations for treatment (2-3 mg/kg every 24h) are inadequate for infants on ECMO.[16] In this open-label PK trial, we determined micafungin PK in infants on ECMO and compared the resulting micafungin exposure to adult exposures known to be effective against invasive candidiasis.

MATERIALS AND METHODS

Design and study population

This was a prospective, open-label, PK and safety study of micafungin conducted at Duke University Medical Center. We enrolled infants (0-2y) supported with ECMO, excluding those with a history of echinocandin allergy. Infants without fungal infection were enrolled in the prophylaxis arm and received intravenous (IV) micafungin per study protocol (4 mg/kg every 24h, infused over 1h). Infants with suspected or confirmed fungal infections who were prescribed micafungin per standard of care, were enrolled in the treatment arm and dosing was adjusted per study protocol to 8 mg/kg every 24h, infused over 1h. Duration of micafungin prophylaxis was up to 8 days, whereas duration of therapy in the treatment arm was determined by the treating physician. Because

micafungin is light-sensitive, drug vials and infusion bags were protected from light.[17] However, the ECMO circuit is not protected from light, so it is possible that micafungin in the blood was exposed to light while transiting the ECMO circuit. This trial was approved by the institutional review board of Duke University Medical Center, registered with clinicaltrials.gov (NCT01666769), and conducted under a Food and Drug Administration investigational new drug application (No.115255). Written informed consent was obtained from the legal guardian of each infant.

PK sampling

We collected up to 14 plasma PK samples (200 μL of whole blood per sample) around dose 1 and 4 via a peripheral arterial catheter. The protocol did not allow drawing PK samples from site of administration. Sampling intervals were as follows (1 sample per interval): 0-4h before the start of infusion, and 0-30 min, 60-90 min, 2-4h, 8-10h, 12-16h, and 22-24h after the end of micafungin infusion. Samples were collected in ethylenediaminetetraacetic acid microcontainers and processed immediately or placed on ice (<30 minutes) until processing. Plasma was separated via centrifugation (3000g for 10 minutes at 4°C), manually aspirated and transferred to polypropylene tubes. Plasma samples were frozen at –20°C for a maximum of 24h, and stored at -80°C until analysis. PK samples were protected from light when stored in the freezer. No special precautions were undertaken during processing of samples because reconstituted micafungin was shown to be stable up to 24 hours at room temperature when exposed to light, as suggested in the drug label.[17]

ECMO Circuit Configuration

Two types of ECMO circuits were used; S3 and CardioHelp (Figure 5.1). A hemofilter (Sorin DHFO.2, Sorin Group, Milan, Italy) was used in infants requiring hemofiltration. The prime volume for each circuit was 450mL and included packed red blood cells (350mL), fresh frozen plasma (50mL), Plasmalyte® crystalloid (50mL), sodium bicarbonate (25mEq), and heparin (100units).

PK analysis

Plasma micafungin concentrations were determined using a validated high performance liquid chromatography assay with fluorescent detection.[18] The lower limit of quantification was 0.05 mg/L. Intraday precision ranged from 1.28% for the highest concentration of the standard curve (25.00 mg/L) to 17.90% for the lowest concentration (0.05 mg/L). Interday precision ranged from 3.27% to 14.41% within the concentration range of the standard curve (0.05–25.00 mg/L).

Primary outcomes were micafungin CL and V. PK data were analyzed by nonlinear regression with the most appropriate model using Winonlin v6.3 (Pharsight Co., St. Louis, MO). The model fit was evaluated using successful minimization, diagnostic plots, goodness of fit as assessed by the Akaike Information Criterion and precision of the parameter estimates. We assessed systemic exposure by estimating area under the concentration-time curve from 0 to 24h ($AUC_{0–24}$) after the 1st and the 4th

dose. $AUC_{0–24}$ was computed by the linear up log down trapezoidal method using observed data. We assessed the relationship between PK parameters and covariates potentially affecting micafungin disposition (age, serum albumin, aspartate aminotransferase, total bilirubin, and duration of ECMO support) by visual inspection of scatter plots.[19-21] Finally, we explored the relationship between PK parameters and the number of doses (single vs multiple doses), and the presence of the hemofilter in the ECMO circuit, using a Wilcoxon rank-sum test.

Assessment of dose-exposure relationship

For a target efficacy exposure, we used an AUC_{0-24} range of 75-139 mg*h/L as a surrogate pharmacodynamic (PD) endpoint.[20,22] This endpoint matches the micafungin exposure achieved by adult participants who cleared their fungal infection in the large, phase III efficacy trial.[23] There is no established target exposure for *Candida* prophylaxis, however, IV micafungin 50 mg (1 mg/kg in children) daily was proven effective in preventing fungal infections in 882 adults and children undergoing hematopoietic stem cell transplantation.[24] Because micafungin PK is linear in this dosing range, the prophylactic exposure target was set to 50% of the therapeutic target (37.5-69.5 mg*h/L).[20,22,25]

In order to characterize micafungin exposure, we simulated a variety of dosing regimens and measured the proportion of infants in our population who achieved the therapy and prophylaxis exposure targets after the 1st and 4th micafungin dose. Simulations were performed by estimating the maximum (C_{max}) and minimum (C_{min})

micafungin concentrations for each individual for the first dosing interval and at steady state using the equation for an intermittent infusion with the individual parameter estimates from the final model. We then used the predicted C_{max} and C_{min} values to calculate the AUC for the dosing interval from 0 to 24h and at steady state using the equations for the linear-up log-down trapezoidal approach.

Safety

The secondary outcome was the proportion of infants experiencing adverse events (AEs). AEs were defined as any untoward medical occurrence whether or not considered drug-related during the conduct of the clinical trial. AEs were recorded while on study drug and for 7 days after the last study dose of micafungin. Liver toxicity and hypokalemia were the AEs of special interest because they were described previously in 3% and 2% of infants and children, respectively, receiving micafungin.[22] Levels of serum aspartate aminotransferase, alanine aminotransferase and potassium were therefore measured at baseline (within 72h prior to the first study dose), and at the end of the study (within 72h after the last study dose). Other laboratory determinations were recorded from consent through 72h after the last study dose, if performed per standard of care. Other laboratory determinations included albumin, blood urea nitrogen, serum creatinine, sodium, complete blood count and microbiology culture results. The safety data were summarized descriptively. We used STATA 13 (College Station, TX) to perform the statistical analyses.

RESULTS

We enrolled 12 infants on ECMO support with a median (range) postnatal age of 59 days (0, 574) (Table 5.1). Two infants were born preterm (27 and 34 weeks of gestational age [GA]) and were 122 and 187 days postnatal age at time of enrollment, respectively. Infants were supported by ECMO for a median time of 4 days (2, 10) before the first micafungin dose. Of the 12 infants, 11 (92%) received prophylactic intravenous (IV) micafungin (4 mg/kg every 24h) for 4 (2, 8) days. One infant (ID # 2) was treated for presumed fungal infection with IV micafungin (8 mg/kg every 24h) for 6 days. Site of drug administration included central venous catheter (n=7) and ECMO circuit, post-oxygenator (n=1). Site of drug administration was not listed for 4 infants. All 11 infants from the prophylactic group had PK samples collected around dose 1, and 5/11 (45%) of these infants remained on micafungin long enough to complete sampling around dose 4. The one infant in the therapeutic group had PK samples collected around doses 2 and 5. PK samples were collected from a peripheral arterial line in all infants but one for whom site of PK sampling was not listed. Hemofiltration was used in 4/12 (33%) infants (Table 5.2).

Pharmacokinetics

We collected a total of 124 plasma samples, with a median of 11 (6, 14) samples per infant. Plasma concentration-time profiles are shown in Figure 5.2. A 1-compartment model with zero-order infusion appropriately fit the data (Table 5.2). PK parameters were estimated with high precision as evidenced by median CL and V

coefficient of variation of 6% (5, 14) and 11% (8, 14), respectively. Three/124 (2%) PK samples were excluded from the analysis; one concentration was below the lower limit of quantification (subject ID#5), and 2 plasma samples lacked confirmation of sampling time (Subject ID#12). PK parameter estimates did not change when these 3 concentrations were removed from the analysis. Median [95% confidence interval] CL decreased over the study period from 0.04 L/kg/h [0.03, 0.05], to 0.02 L/kg/h [0.02, 0.03] after single and multiple doses, respectively. Median [95% CI] V was 0.62 L/kg [0.53, 0.73) and 0.52 L/kg [0.31, 0.67] after a single and multiple doses, respectively.

We did not observe a significant difference in CL between infants with and without a hemofilter in the circuit (median [range] CL of 0.04 L/kg/h [0.03, 0.04] vs 0.04 L/kg/h [0.03, 0.06], respectively, p=0.50) nor did we observe a significant relationship between V and the presence of a hemofilter (0.54 L/kg [0.46, 0.75] and 0.67 L/kg [0.44, 0.98] in infants with and without a hemofilter, respectively; p=0.17). In evaluating other covariates of interest, we observed an inverse correlation between CL and age, with older infants demonstrating lower CL per kg of bodyweight (Figure 5.3A). The same relationship also was observed for V and age where older infants had lower V per kg of bodyweight (Figure 5.3B). An inverse relationship also was observed between CL and serum albumin; subjects with low serum albumin had higher CL (Figure 5.3C). However, no relationship was observed between V and serum albumin (Figure 5.3D), or between CL and the following covariates: AST, serum creatinine, or total bilirubin (data not shown). Finally, no relationship was observed between duration of ECMO support and CL or V (data not shown).

Dose-exposure relationship

Prophylactic arm (4 mg/kg IV every 24h)

Median AUC_{0-24} were 74 mg*h/L (53, 106) and 117 mg*h/L (84, 187) after dose 1 and 4, respectively (Figure 5.4). After a single dose, all infants were at or higher than the prophylaxis range (Figure 5.4). After dose 4, all infants sampled (5/5) exceeded the prophylactic range. Although infants in the prophylactic arm were not treated for active fungal infection, 5/11 (45%) achieved the therapeutic exposure target (75-139 mg*h/L) after a single dose, while the remaining infants were below the lower limit of the therapeutic exposure target (Figure 5.4). Among the 5 infants who were sampled around dose 4, 3/5 (60%) were within the therapeutic range, and 2 were supratherapeutic. Four infants had a hemofilter in line (Table 5.2). When a hemofilter was in line, all infants (4/4) achieved AUC_{0-24} within or above the prophylactic target range after dose 1 and 4. Two/4 (50%) infants with a hemofilter achieved AUC_{0-24} within or above the therapeutic target range after dose 1 and 4.

Treatment arm (8 mg/kg IV every 24h)

The one infant (ID#2) who received micafungin for suspected *Candida* infection had AUC_{0-24} of 213 and 178 mg*h/L after doses 2 and 5, respectively. This infant achieved an AUC_{0-24} that exceeded both prophylactic and therapeutic target ranges after doses 2 and 5 (Figure 5.4).

Dose-exposure simulations

A daily dose of 2.5 mg/kg infused over 1 h achieved the prophylactic target (AUC_{0-24} of 37.5 - 69.5 mg*h/L) within 24 h in 100% of the cohort. At steady state all

children achieved an AUC_{0-24} of at least 37.5 mg*h/L, with 3 (25%) above the target range (AUC_{0-24} of 84, 88, 94 mg*h/L).

A daily dose of 5 mg/kg infused over 1 h achieved the therapeutic target range (AUC_{0-24} of 75 - 139 mg*h/L) within 24 h in 100% of the cohort. At steady state all children achieved an AUC_{0-24} of at least 75 mg*h/L, with 3 (25%) above the target range (AUC_{0-24} of 169, 177, 189 mg*h/L).

Safety

Five infants died during the study period. None of the deaths were considered related to micafungin. Two infants died following severe intracranial hemorrhage in the setting of systemic anticoagulation with heparin while on ECMO, and 1 died of refractory pulmonary hypertension after ECMO decannulation. Three additional AEs, unrelated to micafungin, were observed in 2 infants; 1 infant had severe intracranial hemorrhage but survived, and another had necrotizing enterocolitis likely related to prematurity and anticoagulation resulting in mild gastrointestinal bleeding.

DISCUSSION

This is the first PK trial of micafungin in infants supported with ECMO. Infants on ECMO had altered PK requiring higher doses to achieve the same exposure as historical controls not on ECMO.[16,20,25-27] We suggest an alternate dosing regimen of 2.5 and 5 mg/kg/day for prophylaxis and treatment of invasive candidiasis, respectively.

However, preterm neonates at high risk for hematogenous Candida meningoencephalitis should be excluded from this recommendation because we did not evaluate the higher dosages (e.g., 10mg/kg) usually recommended in this populations.[28,29]

The V of micafungin in our cohort was 20-90% higher than that reported in infants not on ECMO (0.34 – 0.54 L/kg).[16,26] There are three probable explanations for the increased V: 1) the large volume of blood required to prime the ECMO circuit (~450mL) relative to an infant's native blood volume (80 mL/kg); 2) direct adsorption of micafungin by components of the ECMO circuit,[13-15] and 3) altered physiology (e.g., anasarca, inflammation) commonly seen in critically ill infants. The impact of the ECMO prime volume is most pronounced in smaller infants where an infant's circulating blood volume may be doubled or even tripled. Because the impact of prime volume is directly related to the ratio between prime volume and native blood volume, our results should not be extrapolated to older children where the ratio of exogenous (450 mL) to native blood volume (~2000-5000 mL) is much lower. Our findings are consistent with previous literature reporting increased V due to the ECMO prime volume in infants on fluconazole, vancomycin and gentamicin.[11,19,21,30-33]

Drug adsorption to the ECMO circuit itself, which is well described in *ex vivo* studies, is also likely to contribute to the increase in V. Drug characteristics including lipophilicity and high protein binding are key factors driving adsorption.[14,15] While micafungin is not lipophilic (logP -1.5), it is >99% protein bound.[34] Other drugs with comparable protein binding and logP such as caspofungin were substantially adsorbed (56%) in an isolated *ex vivo* ECMO circuit.[15] Preliminary results from a micafungin

ECMO *ex vivo* study conducted by our group showed that micafungin concentrations dropped by 58% over 24h (Watt unpublished data). In summary, our study was not designed to isolate the source of altered V, but the increase in V was probably due to a combination of circuit prime volume, circuit adsorption of drug, and patient disease state.

In the current study, total CL after the first dose (0.041 L/kg/h [0.026, 0.062]) was in the upper range of previously reported values for infants not supported by ECMO (0.020-0.039 L/kg/h).[20,25-27] The increase in CL may be explained by altered drug metabolism. Micafungin is excreted primarily unchanged into bile and feces (71%) via hepatic transporter proteins.[35] Limited metabolism also occurs in the liver by arylsulfatase and catechol-O-methyltransferase into metabolites with little or no antifungal activity.[16] While the impact of ECMO on renal dysfunction is well described,[36] the effect of ECMO on hepatic transporters and metabolic capacity is unknown. Micafungin PK studies in adults with severe hepatic dysfunction, revealed lower micafungin exposure and higher CL compared with healthy controls.[37,38] This phenomenon was attributed to lower albumin concentrations in adults with hepatic dysfunction, resulting in higher availability of the unbound fraction to be cleared. In our cohort, no subjects had hepatic dysfunction, but critically ill infants on ECMO typically have serum albumin concentrations in the lower range of normal. In our study, we did observe an inverse relationship between clearance and serum albumin (Figure 5.3C), with a higher micafungin CL in infants who had low serum albumin. Finally, we did not find a relationship between PK parameters and serum creatinine. This is consistent with

previous literature and the product label that states no adjustment is necessary for renal dysfunction.[16,37]

Higher apparent micafungin elimination with ECMO may also be due to non-specific and irreversible drug adsorption by the circuit if adsorption is an ongoing process.[13-15] As described above, substantial extraction was observed over 24h in *ex vivo* circuits (58%).[13]. The origin of this loss is still under investigation but could be due to circuit adsorption. It could also be explained by micafungin degradation due to light exposure, because the ECMO circuit is not protected from light, as opposed to drug vials and infusion bags.

The type of ECMO support could also impact micafungin disposition. Veno-venous ECMO, in which blood is drained and returned to the venous system via a single, double lumen cannula, is subject to a recirculation phenomenon. In recirculation, a portion of the oxygenated blood returned to the venous system is immediately taken back into the ECMO circuit via the drainage lumen of the cannula.[39] The impact of recirculation on drug PK is unknown. However, this phenomenon increases the time drug spends in the circuit; and for drugs that are adsorbed by the circuit, this could decrease exposure (AUC). In our cohort, only 1 infant (ID #6) was on VV ECMO and had a high CL and a low $AUC_{0\text{-}24h}$ compared to the rest of the cohort. In veno-arterial (VA) ECMO deoxygenated blood is drained from the venous system and pumped directly to the arterial circulation, completely bypassing the heart and lungs. The return flow is non-pulsatile. Non-pulsatile blood flow may be associated with reduced renal function, but its impact on a drug cleared by transporters in the liver such as micafungin is unknown.[40]

PK changes described above translated into micafungin exposure within or above the prophylaxis target range for infants who received 4 mg/kg/day. Thus, a dose 4 mg/kg/day may be too high for prophylaxis. However, assuming linear micafungin PK, standard prophylaxis dosing (1 mg/kg/day) recommended for older children would likely result in underexposure in infants on ECMO.[16,22,24,25] Based on the dose-exposure simulations in our cohort, a dose of 2.5 mg/kg/day appears to be the most appropriate dose for *Candida* prophylaxis. Although simulations showed that some children will likely become supratherapeutic on 2.5 mg/kg/day, we believe that it is better to err on the higher side of exposure for two reasons: 1) invasive candidiasis is exceedingly difficult to treat in this population and 2) the highest simulated exposure on 2.5 mg/kg/day (94 mg*h/L) was well below the mean (standard deviation) exposure of 438 mg*h/L (99) that was deemed safe in a neonatal trial of 15 mg/kg/day.[27] This dosing regimen needs to be prospectively evaluated.

The one infant who received micafungin 8 mg/kg/day for suspected *Candida* infection achieved $AUC_{0\text{-}24}$ above the therapeutic target range, and survived until hospital discharge Based on these findings, and on dose-exposure simulations performed in all infants of the cohort, we recommend a dose of 5 mg/kg/day for invasive candidiasis therapy. Dose-exposure simulations were performed in all infants because PK is linear in this dosing range.[22,41] On 5 mg/kg/day some children may achieve exposures exceeding the target range. Similar to the prophylactic regimen, we feel it is better to target higher exposure because these exposures are still in a “safe” range; and higher exposures may be needed to treat through potential fungal biofilms. Moreover, target exposure used in this study, was derived from a phase III efficacy study in which

>85% of adults had their central catheter removed during candidemia treatment.[23] In the setting of ECMO, removal of catheter is impossible and therefore, micafungin exposure required to clear the infection may be higher. This dosing regimen also needs prospective validation.

Although dosing in the current study was higher than recommended in term infants not on ECMO, micafungin had a favorable safety profile without any observed drug-related AEs. This is consistent with previous literature describing the safe use of micafungin up to 15 mg/kg/day in young preterm infants.[27] Safety assessment is however limited by our small sample size.

Our study is the first PK trial of micafungin in infants supported by ECMO. Because our study population includes vulnerable infants, enrollment was challenging and resulted in a limited sample size. In spite of the small sample size and critical illness of our population, interindividual variability in PK parameters was as expected. Other factors may affect micafungin PK in this population, including transfusion of blood products which we did not collect. Our data were also limited by the lack of documentation of site of drug administration in 4 infants. However, the effect of site of drug administration on PK is unknown, and PK parameters of those 4 infants (ID #5; 8-10) were similar to those with complete documentation. Site of PK sampling was also lacking in 1 infant (ID #5), but our protocol did not allow drawing PK samples from site of drug administration. Therefore we do not expect any significant impact on PK results. Finally, our assessment of the ECMO impact on micafungin PK was limited by the lack of controls.

CONCLUSION

In this cohort of infants supported by ECMO, micafungin was well tolerated and the PK model indicated that V was higher and CL was in the upper range of what had been described previously in infants not on ECMO. In order to match exposure observed in adults, we recommend dosing of 2.5 and 5 mg/kg/day for prophylaxis and treatment of invasive candidiasis, respectively. These dosing regimens need prospective validation.

Table 5.1. Clinical Characteristics*

	N=12
Age (days)	59 (0.0, 574)
Gestational age (weeks)	39 (27, 39)
Weight (kg)	3.7 (2.9, 9.6)
Birth weight (kg)	3 (2.4, 4.3)
Male, n (%)	5 (42)
Race, n (%)	
White	6 (50)
African American	6 (50)
Diagnosis, n (%)	
Cardiomyopathy	4 (34)
Pulmonary hypertension	3 (25)
Congenital heart disease	3 (25)
Congenital diaphragmatic hernia	1 (8)
Respiratory failure	1 (8)
Serum creatinine (mg/dL)†	0.5 (0.2, 1.6)
ECMO support, n (%)	
Veno-arterial	11 (92)
Veno-venous	1 (8)
ECMO circuit configuration, n (%)	
S3	8 (67)

Cardiohelp	4 (33)
Micafungin indication n (%)	
Prophylaxis	11 (92)
Therapy	1 (8)
Micafungin dosing (mg/kg/day)	4 (4, 8)
Duration of therapy (days)	4 (2, 8)
Duration of ECMO support at time of first micafungin dosing (days)	4 (2, 10)
Number of PK samples per infant	11 (6, 14)
PK samples obtained around, n (%)	
Dose 1-2	12 (100)
Dose 4-5	6 (50)

*Results are expressed as median (range) unless otherwise specified

† Median serum creatinine for each subject over the study period.

Table 5.2. Pharmacokinetic Parameters

ID	Age (days)	Clearance (L/kg/h)	Volume of distribution (L/kg)	Half-life (h)	Dose (mg/kg/day)	AUC (mg*h/L)		Albumin* (g/dL)
						0-24h	72-96h	
1	0	0.036	0.98	19	4	69	117	3.1
2	1	0.040	0.76	13	8	213§	178†	3.6
3	1	0.046	0.64	10	4	72	-	2.5
4†	4	0.042	0.75	12	4	68	-	2.8
5	16	0.062	0.91	10	4	53	-	2.5
6	44	0.058	0.65	8	4	59	-	2.1
7†	74	0.026	0.56	15	4	93	163	4.2
8†	108	0.043	0.53	9	4	74	109	2.5
9	122	0.044	0.69	11	4	77	84	2.7
10	135	0.030	0.44	10	4	105	-	3.1
11†	187	0.040	0.46	8	4	84	-	3.8
12	574	0.028	0.61	15	4	89	187**	3.7
Median	**59**	**0.041**	**0.64**	**11**	**4**	**74‡**	**117‡**	**3.0**

Clearance and volume of distribution estimates were determined using a one-compartmental model fitting micafungin concentrations after both dose 1 and 4; AUC: area under the concentration-time curve; † Hemofilter in line; *Median serum albumin value over the study period (from 72h prior to first study dose through 72h after last study dose); §AUC 24-48h; †AUC 96-120h; **AUC 79-103h

‡Summary statistics do not include AUC values from subject #2

Figure 5.1. Extracorporeal membrane oxygenation (ECMO) circuit configuration

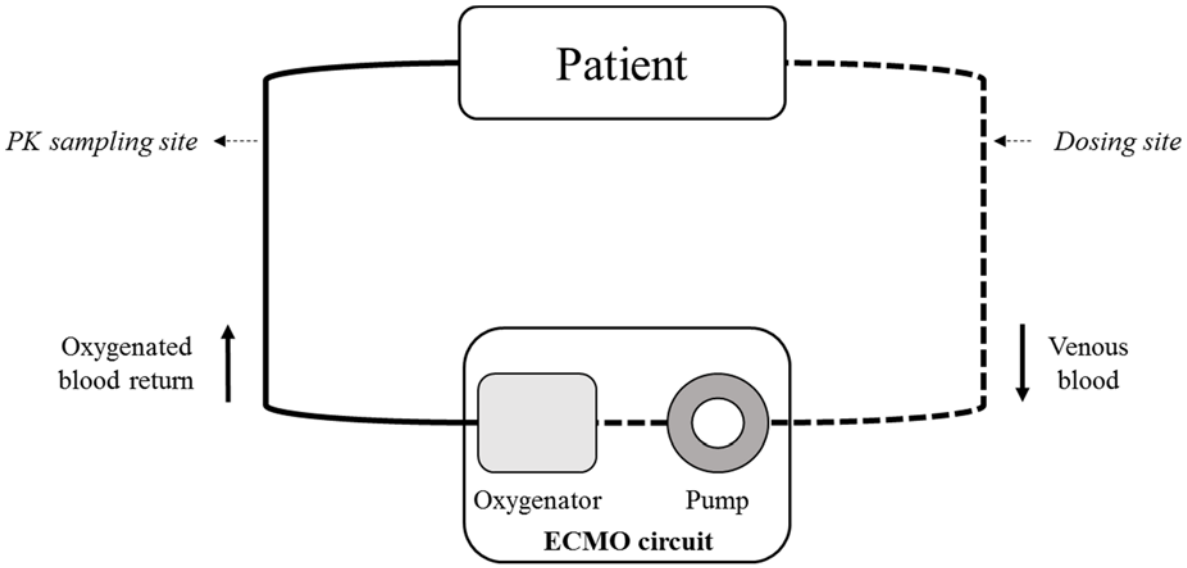

	Model	Manufacturer
S3		
Pump	Revolution Centrifugal	Sorin®
Oxygenator	Quadrox iD (polymethylpentene diffusion oxygenator) [1 or 2]	Maquet®
Tubing	Smart [3]	Sorin®
Cardiohelp		
Pump	Integrated Centrifugal [1 or 2]	Maquet®
Oxygenator	Integrated [1 or 2]	Maquet®
Tubing	Softline/Bioline [1 or 2]	Maquet®

[1]Softline coating: biopassive polymer

[2]Bioline coating: heparin + recombinant human albumin

[3]Smart coating: Silicone/caprolactam copolymer

Figure 5.2. Micafungin Concentration-Time Profiles. All subjects received IV micafungin 4 mg/kg every 24h, except for subject ID #2 who received 8 mg/kg every 24h**.** Subject ID # 2 PK samples were collected around dose 2 and 5. Subject ID # 12 the fourth dose was given 79h after the first dose, instead of 72h.

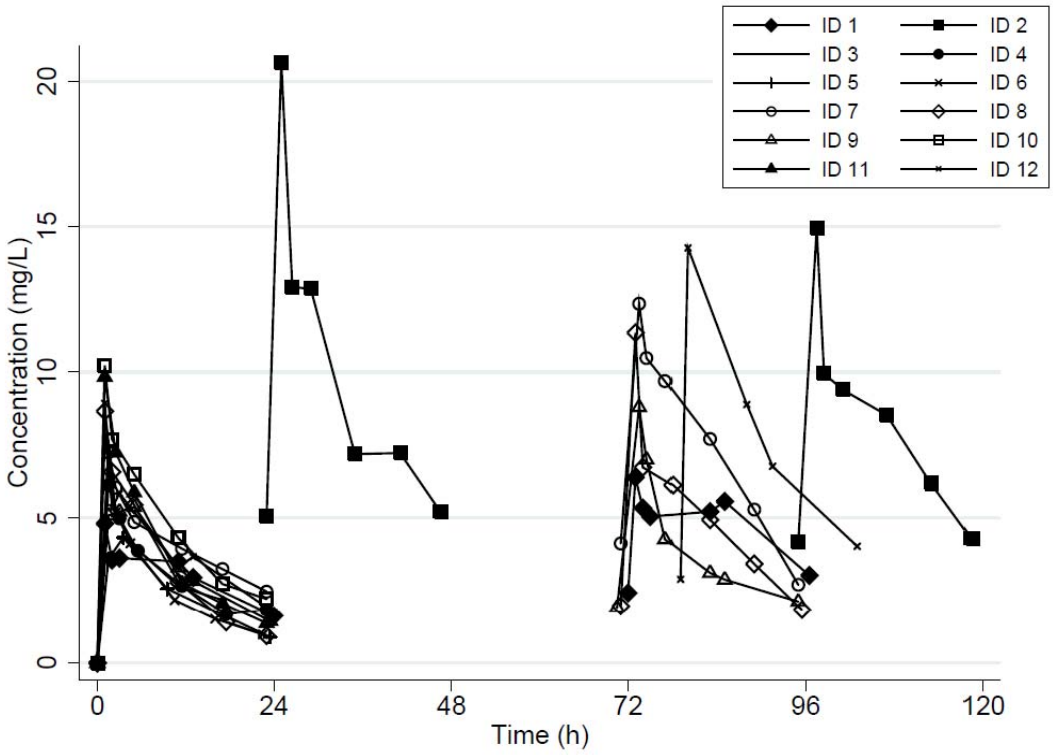

Figure 5.3. Micafungin Exposure

AUC: Area under the concentration-time curve 0-24h

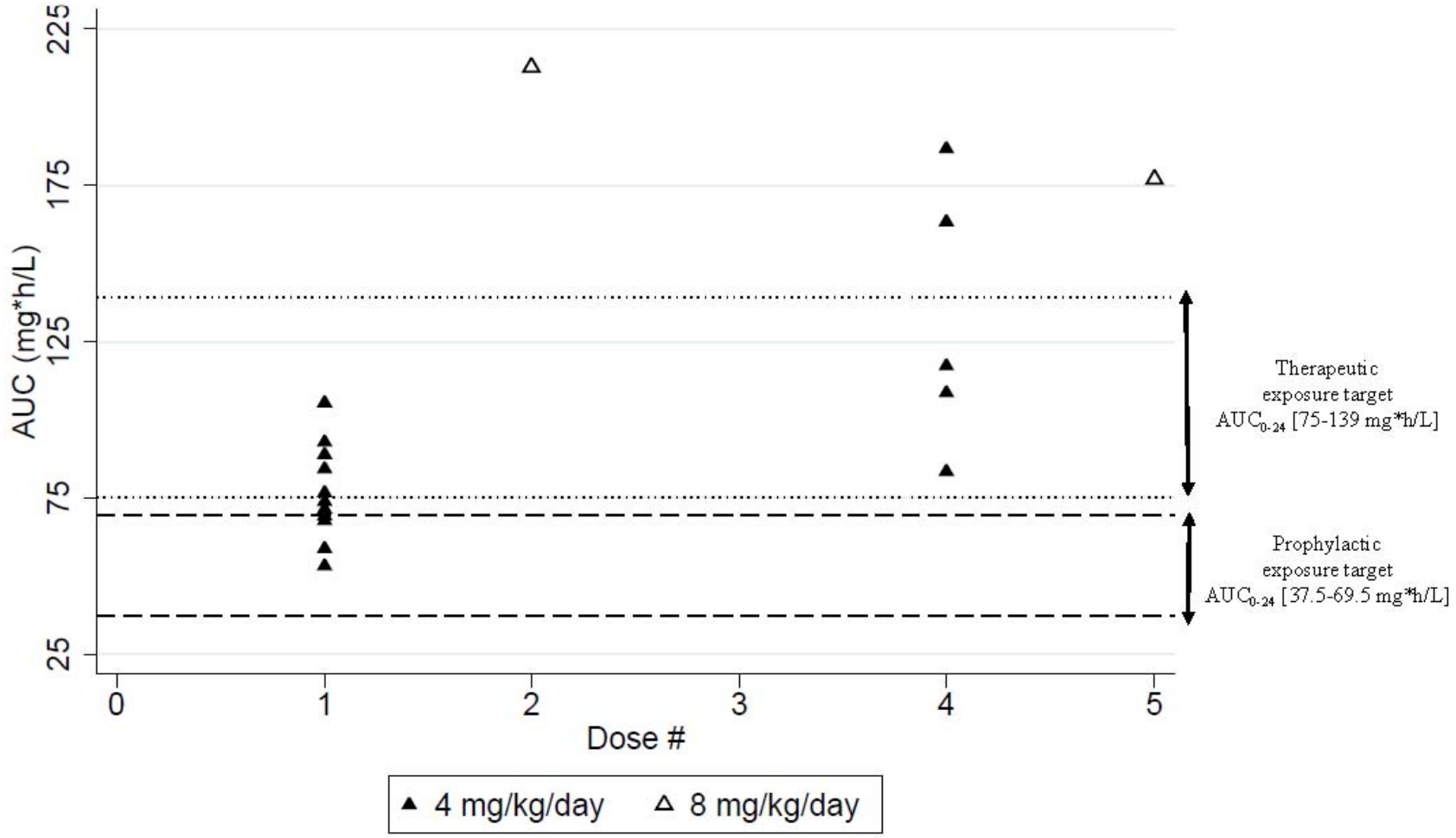

Figure 5.4. Pharmacokinetic parameters vs covariates

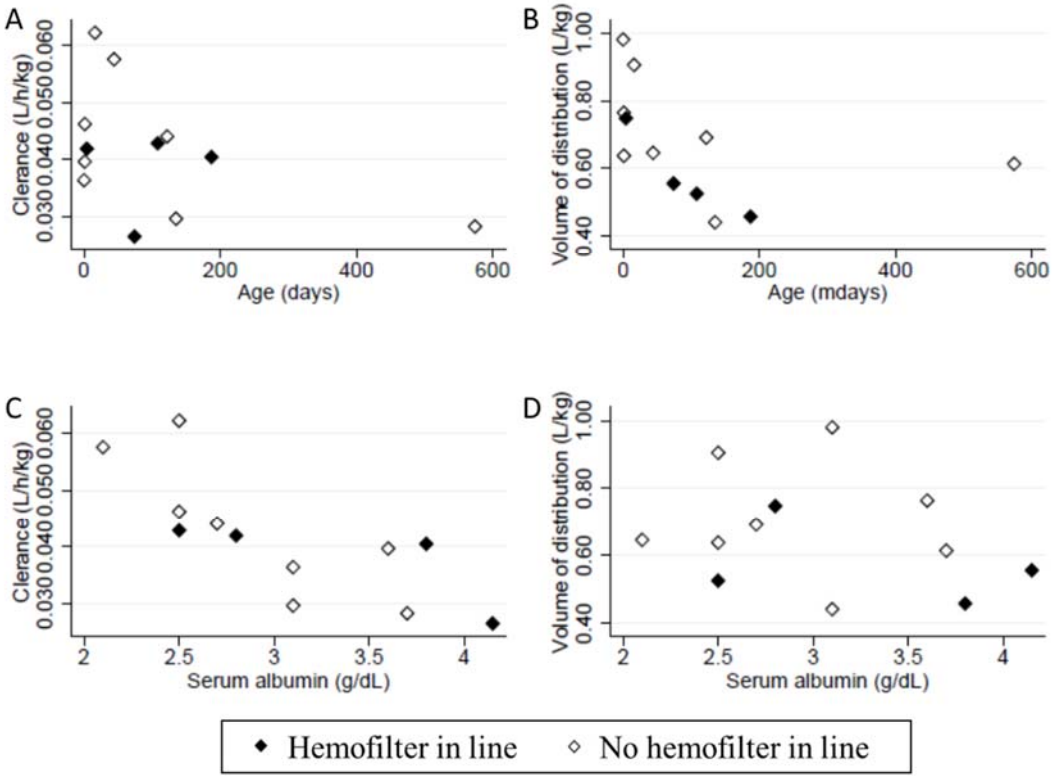

A: Clearance vs age; B: Volume of distribution vs age; C: Clearance vs serum albumin; D: Volume of distribution vs serum albumin

REFERENCES

1. Autmizguine, J; Hornik, CP; Benjamin, DK, Jr; Brouwer, KLR; Hupp, S; Cohen-Wolkowiez, M; and Watt, KM. . Pharmacokinetics and Safety of Micafungin in Infants Supported with Extracorporeal Membrane Oxygenation (ECMO). Ped Infect Dis Journal. 2016. Accepted for publication.

2. Bartlett RH, Gattinoni L. Current status of extracorporeal life support (ECMO) for cardiopulmonary failure. Minerva anestesiologica 2010;76:534-40.

3. Bizzarro MJ, Conrad SA, Kaufman DA, Rycus P. Infections acquired during extracorporeal membrane oxygenation in neonates, children, and adults. Pediatr Crit Care Med 2010;12:277-81.

4. Andes D, Nett J, Oschel P, Albrecht R, Marchillo K, Pitula A. Development and characterization of an in vivo central venous catheter Candida albicans biofilm model. Infection and immunity 2004;72:6023-31.

5. Eppes SC, Troutman JL, Gutman LT. Outcome of treatment of candidemia in children whose central catheters were removed or retained. Pediatr Infect Dis J 1989;8:99-104.

6. Pappas PG, Kauffman CA, Andes D, et al. Clinical practice guidelines for the management of candidiasis: 2009 update by the Infectious Diseases Society of America. Clin Infect Dis 2009;48:503-35.

7. Ikeda F, Wakai Y, Matsumoto S, et al. Efficacy of FK463, a new lipopeptide antifungal agent, in mouse models of disseminated candidiasis and aspergillosis. Antimicrob Agents Chemother 2000;44:614-8.

8. Kaneko Y, Ohno H, Fukazawa H, et al. Anti-Candida-biofilm activity of micafungin is attenuated by voriconazole but restored by pharmacological inhibition of Hsp90-related stress responses. Medical mycology : official publication of the International Society for Human and Animal Mycology 2010;48:606-12.

9. Tawara S, Ikeda F, Maki K, et al. In vitro activities of a new lipopeptide antifungal agent, FK463, against a variety of clinically important fungi. Antimicrob Agents Chemother 2000;44:57-62.

10. Amaker RD, DiPiro JT, Bhatia J. Pharmacokinetics of vancomycin in critically ill infants undergoing extracorporeal membrane oxygenation. Antimicrob Agents Chemother 1996;40:1139-42.

11. Watt KM, Benjamin DK, Jr., Cheifetz IM, et al. Pharmacokinetics and safety of fluconazole in young infants supported with extracorporeal membrane oxygenation. Pediatr Infect Dis J 2012;31:1042-7.

12. Mehta NM, Halwick DR, Dodson BL, Thompson JE, Arnold JH. Potential drug sequestration during extracorporeal membrane oxygenation: results from an ex vivo experiment. Intensive Care Med 2007;33:1018-24.

13. Watt K M C-WM, Williams D, Bonadonna D, Cheifetz I, Benjamin Jr DK, Brouwer K L. Antifungal extraction by the extracorporeal membrane oxygenation (ECMO) circuit ex vivo

In: American Society for Clinical Pharmacology and Therapeutics Annual meeting; 2015 March 3-7, 2015; New Orleans, LA; 2015.

14. Wildschut ED, Ahsman MJ, Allegaert K, Mathot RA, Tibboel D. Determinants of drug absorption in different ECMO circuits. Intensive Care Med 2010;36:2109-16.

15. Shekar K, Roberts JA, McDonald CI, et al. Protein-bound drugs are prone to sequestration in the extracorporeal membrane oxygenation circuit: results from an ex vivo study. Crit Care 2015;19:164.

16. Mycamine (micafungin) [package insert]. 2013. (Accessed 03-04-2015, 2015, at http://www.astellas.us/docs/mycamine.pdf.)

17. Use EMAEoMfH. ASSESSMENT REPORT FOR Mycamine In; 2008.

18. Lat A, Thompson GR, 3rd, Rinaldi MG, Dorsey SA, Pennick G, Lewis JS, 2nd. Micafungin concentrations from brain tissue and pancreatic pseudocyst fluid. Antimicrob Agents Chemother 2010;54:943-4.

19. Bhatt-Mehta V, Johnson CE, Schumacher RE. Gentamicin pharmacokinetics in term neonates receiving extracorporeal membrane oxygenation. Pharmacotherapy 1992;12:28-32.

20. Hope WW, Kaibara A, Roy M, et al. Population pharmacokinetics of micafungin and its metabolites M1 and M5 in children and adolescents. Antimicrob Agents Chemother 2015;59:905-13.

21. Southgate WM, DiPiro JT, Robertson AF. Pharmacokinetics of gentamicin in neonates on extracorporeal membrane oxygenation. Antimicrob Agents Chemother 1989;33:817-9.

22. Seibel NL, Schwartz C, Arrieta A, et al. Safety, tolerability, and pharmacokinetics of Micafungin (FK463) in febrile neutropenic pediatric patients. Antimicrob Agents Chemother 2005;49:3317-24.

23. Kuse ER, Chetchotisakd P, da Cunha CA, et al. Micafungin versus liposomal amphotericin B for candidaemia and invasive candidosis: a phase III randomised double-blind trial. Lancet 2007;369:1519-27.

24. van Burik JA, Ratanatharathorn V, Stepan DE, et al. Micafungin versus fluconazole for prophylaxis against invasive fungal infections during neutropenia in patients undergoing hematopoietic stem cell transplantation. Clin Infect Dis 2004;39:1407-16.

25. Heresi GP, Gerstmann DR, Reed MD, et al. The pharmacokinetics and safety of micafungin, a novel echinocandin, in premature infants. Pediatr Infect Dis J 2006;25:1110-5.

26. Benjamin DK, Jr., Smith PB, Arrieta A, et al. Safety and pharmacokinetics of repeat-dose micafungin in young infants. Clin Pharmacol Ther 2010;87:93-9.

27. Smith PB, Walsh TJ, Hope W, et al. Pharmacokinetics of an elevated dosage of micafungin in premature neonates. Pediatr Infect Dis J 2009;28:412-5.

28. Fernandez M, Moylett EH, Noyola DE, Baker CJ. Candidal meningitis in neonates: a 10-year review. Clin Infect Dis 2000;31:458-63.

29. Hope WW, Seibel NL, Schwartz CL, et al. Population pharmacokinetics of micafungin in pediatric patients and implications for antifungal dosing. Antimicrob Agents Chemother 2007;51:3714-9.

30. Buck ML. Vancomycin pharmacokinetics in neonates receiving extracorporeal membrane oxygenation. Pharmacotherapy 1998;18:1082-6.

31. Cohen P, Collart L, Prober CG, Fischer AF, Blaschke TF. Gentamicin pharmacokinetics in neonates undergoing extracorporal membrane oxygenation. Pediatr Infect Dis J 1990;9:562-6.

32. Hoie EB, Swigart SA, Leuschen MP, et al. Vancomycin pharmacokinetics in infants undergoing extracorporeal membrane oxygenation. Clin Pharm 1990;9:711-5.

33. Munzenberger PJ, Massoud N. Pharmacokinetics of gentamicin in neonatal patients supported with extracorporeal membrane oxygenation. ASAIO Trans 1991;37:16-8.

34. Wishart DS, Knox C, Guo AC, et al. DrugBank: a knowledgebase for drugs, drug actions and drug targets. Nucleic acids research 2008;36:D901-6.

35. Yanni SB, Augustijns PF, Benjamin DK, Jr., Brouwer KL, Thakker DR, Annaert PP. In vitro investigation of the hepatobiliary disposition mechanisms of the antifungal agent micafungin in humans and rats. Drug metabolism and disposition: the biological fate of chemicals 2010;38:1848-56.

36. Gupta P, Carlson J, Wells D, et al. Relationship between renal function and extracorporeal membrane oxygenation use: a single-center experience. Artificial organs 2015;39:369-74.

37. Hebert MF, Smith HE, Marbury TC, et al. Pharmacokinetics of micafungin in healthy volunteers, volunteers with moderate liver disease, and volunteers with renal dysfunction. J Clin Pharmacol 2005;45:1145-52.

38. Undre N, Pretorius B, Stevenson P. Pharmacokinetics of micafungin in subjects with severe hepatic dysfunction. European journal of drug metabolism and pharmacokinetics 2015;40:285-93.

39. Abrams D, Bacchetta M, Brodie D. Recirculation in venovenous extracorporeal membrane oxygenation. ASAIO journal (American Society for Artificial Internal Organs : 1992) 2015;61:115-21.

40. Nam MJ, Lim CH, Kim HJ, et al. A Meta-Analysis of Renal Function After Adult Cardiac Surgery With Pulsatile Perfusion. Artificial organs 2015;39:788-94.

41. Tabata K, Katashima M, Kawamura A, Tanigawara Y, Sunagawa K. Linear pharmacokinetics of micafungin and its active metabolites in Japanese pediatric patients with fungal infections. Biol Pharm Bull 2006;29:1706-11.

CHAPTER 6. PHYSIOLOGICALLY-BASED PHARMACOKINETICS OF MICAFUNGIN IN CHILDREN ON ECMO

INTRODUCTION

Micafungin is an echinocandin antifungal drug with a broad spectrum of activity against *Candida* and *Aspergillus* species.[1,2] Micafungin inhibits the synthesis of 1,3-beta-D-glucan, an essential component of the fungal cell wall. In children older than 4 months, micafungin is labeled by the FDA for the prophylaxis and treatment of invasive candidiasis. *Candida* is a common pathogen in children supported with ECMO. In this population, *Candida* is difficult to treat due to the organism's ability to adhere to vascular catheters and form biofilms. Micafungin can penetrate biofilms, making it an attractive drug for use in children on ECMO.[3-5] Unfortunately, ECMO can alter drug pharmacokinetics (PK), thus requiring important dosing modifications. Optimal dosing on ECMO can be affected by 1) multi-organ dysfunction; 2) the large volume of exogenous blood required to prime the ECMO circuit; and 3) drug extraction by the circuit. The extent of interaction with the ECMO circuit depends, in part, on the physicochemical properties of the drug, circuit components (e.g., oxygenator, hemofilter), and drug clearance mechanisms.

The oral bioavailability of micafungin is extremely low due to its physicochemical properties (high molecular weight, hydrophilicity); thus, micafungin is only administered intravenously. Following intravenous administration of radiolabeled ^{14}C-micafungin in humans, approximately 90% of the dose was recovered in feces with <10% in urine.[6]

The membrane transport protein organic anion-transporting polypeptide (OATP) OATP1B1 is primarily responsible for hepatic uptake of micafungin.[7] Within the hepatocyte, micafungin is metabolized to M-1 (catechol form) by arylsulfatase, with subsequent metabolism to M-2 (methoxy form) by catechol-O-methyltransferase.[8] M-5 formation is catalyzed by cytochrome P450 (CYP) isozymes and occurs by hydroxylation at the omega-1 position.[6] Although M-1 and M-2 have some *in vitro* antifungal activity, they are unlikely to play a role in the *in vivo* antifungal activity of micafungin given their low plasma concentrations (~1/20th of parent).[8] Micafungin undergoes biliary elimination via efflux transporters on the cannalicular membrane.[7] However, recovery in feces of parent drug and metabolites is low in the first 6 hours relative to the rapid decline in plasma concentrations during that time period.[8,9] This suggests that initial plasma clearance is due primarily to distribution rather than elimination. Insight into the mechanism of this process can be found with caspofungin, an echinocandin with a very similar structure, physicochemical properties, and elimination pathways. In human and animal studies, caspofungin rapidly distributed into extracellular space before slower uptake into the liver via OATP1B1.[10,11] Studies of caspofungin in *in situ* rat livers suggests that the two-step uptake process involves an initial adsorption to the cell surface followed by slower transport across the cell membrane.[12]

Knowledge of micafungin physicochemical properties and clearance pathways can be combined with system specific inputs (e.g., organ weights and blood flows) for the population of interest to build a physiologically-based pharmacokinetic (PBPK) model of micafungin. PBPK models differ from traditional compartmental models in that

they are structured in a physiologically relevant manner with multiple compartments reflecting the various organs in the body (Figure 6.1). Because PBPK models are mechanistic in nature, model parameters can be modified based on age (i.e., adding ontogeny to system specific inputs) and disease state (e.g., adjusting renal function) to predict dosing in special populations. Importantly for children on ECMO, an ECMO compartment can be added to the model to adjust for the factors that alter micafungin PK during ECMO support. The objective of this study was to develop a PBPK model of micafungin in adults, scale it to children, and add an ECMO compartment in order to predict optimal dosing in children supported with ECMO.

METHODS

Model Building Workflow

The model building workflow is described in Figure 6.2. The model was first constructed in adults (Adult PBPK Model) and then scaled to children (Pediatric PBPK Model). An ECMO compartment was then added to the Pediatric PBPK Model to form the ECMO PBPK Model.

Adult PBPK Model

The whole-body PBPK model was structured with 15 compartments representing physiologic organ spaces linked by blood flow. The blood flow into and out of the compartments and disposition within the compartments was parameterized using differential equations. Each organ consisted of 4 sub-compartments: plasma and red blood cells making up the vascular space, interstitial fluid, and cellular space. The

organ-to-plasma unbound partition coefficients (*K*pu) were estimated using drug physicochemical properties based on the method described by Rogers and Rowland.[13,14] All PBPK simulations were performed using PK Sim® and MoBi® (v6.03, Bayer Technology Services, Leverkusen, Germany).

A PBPK model was first developed in adults in order determine the most appropriate model structure using robust adult data (Figure 6.2).[15-17] Drug physicochemical properties and clearance pathways for micafungin were extracted from the literature in order to inform the drug-specific model inputs (Table 6.1). The system-specific inputs were based on the average 30 year-old, healthy, Caucasian male using population datasets.[18] Based on a weight of 74kg and a height of 173cm, organ weights, volumes, and blood flows were assigned based on mean values reported in the International Commission on Radiological Protection (ICRP) database.[19]

Because micafungin disposition is mediated by both passive and active processes and data are lacking for some of these processes, the following assumptions were made when parameterizing the model. 1) Micafungin was assumed to distribute rapidly from plasma based on the fact that micafungin is cleared rapidly from the plasma (pronounced α–distribution)[20-22] and is not quickly eliminated in feces or urine suggesting that the rapid plasma clearance is due to distribution rather than elimination processes.[8,9] 2) Micafungin was assumed to reside preferentially in the interstitial space and not readily cross back into the vascular space because of binding to the cellular membrane. Relatively slow uptake into tissues suggests that micafungin first undergoes rapid distribution into interstitial space.[9] Micafungin is highly protein bound, and binds to multiple proteins, presumably including those in the interstitial space.[23] *In vitro* studies of

caspofungin showed distribution into interstitial space and reversible adsorption to the cell wall prior to uptake by OATP1B1.[11,12] 3) Micafungin is actively transported from the interstitial space into the hepatocyte via OATP1B1 where it undergoes metabolism via arylsulfatase, catechol-O-methyltransferase, and CYP3A4.[7,8] 4) The majority of micafungin is excreted into bile via an efflux transporter on the canalicular membrane.[6,7] A summary of model assumptions is listed in Table 6.3.

With these assumptions, the model was anchored in the following known parameters: 1) the mass balance data (fraction eliminated in feces and urine),[6] 2) the hepatic uptake by OATP1B1,[7] and 3) empiric liver tissue concentrations that showed concentrations in the liver exceeded those in plasma by 6h.[8,9] Renal clearance (CL_R) represents a minor route of micafungin elimination (<10%), and CL_R was included in the base model with an assumed glomerular filtration rate (GFR) of 110 ml/min. CL_R was based on the following equation because there was no evidence of tubular secretion or reabsorption:[6]

$$CL_R = f_u x\ GFR \qquad \text{(eq. 1)}$$

where f_u is the fraction of unbound drug. Adult model development then proceeded according to the following steps:

Step 1. Rapid Equilibrium Compartment – rapid distribution into the interstitial space was adjusted to describe the observed data (Adult Development Dataset) by increasing the Interstitial:Plasma K_{pu} and decreasing endothelial permeability to account for distribution out of the vascular space and binding to the cellular membrane, respectively.[24,25]

Step 2. OATP1B1 uptake was added to the basolateral membrane of the hepatocyte. Uptake V_{max} from the literature was scaled from milligrams of protein to grams of liver in order to generate a liver V_{max} via the following equation;

$$V_{max}\ (liver\ tissue) = V_{max}(microsome)xMPPGL \quad \text{(eq. 2)}$$

Where MPPGL represents the microsomal protein per gram of liver and was assumed to be 45 mg protein/g of liver.[26] A specific V_{max} was calculated from intrinsic liver V_{max} normalized to the organ weight based on the following;

$$V_{max} = V_{max}(liver\ tissue) * \frac{f_{int} + f_{cell}}{f_{cell}} \quad \text{(eq. 3)}$$

where f_{int} and f_{cell} are the fraction of the liver that make up the interstitial and cellular sub-compartments, respectively. K_m was obtained from the literature.[7]

Step 3. A canalicular transporter was added to account for secretion of micafungin from the hepatocyte into bile. The known fraction excreted in bile was used to optimize a V_{max} and K_m for this transporter. Because no metabolism was included in the model at this point, the apparent fraction excreted in the bile was the total fraction including parent and metabolites, assumed to be ~50-60% of the dose at 168h.[8]

Step 4. Metabolism was added to the model by assigning an unbound intrinsic clearance (CL_I') to the three primary metabolizing enzymes. The CL_I' was optimized so that fraction excreted in the bile now represented only the parent (~44% at 168h). The CL_I' was partitioned between the three enzymes, assuming a ratio of 5:1:6 for arylsulfatase, catechol-O-methyltransferase, and CYP3A4, respectively, based on mass balance data.[8]

Based on these data, the model was used to generate plasma and liver concentration versus time curves and fraction excreted in the bile and urine for the standard healthy adult described above. Model parameters were optimized based on the observed data (Adult Development Dataset) using the Nelder-Mead algorithm in the MoBi® Toolbox for Matlab and methods described by Stader.[25,27] The optimized model was used to generate drug concentration versus time profiles for a virtual population of healthy adults (n=1000) created using the PK Sim® population module.[28] Drug concentration versus time profiles for the virtual population were compared with observed data obtained from studies that were not used in model development (Adult Validation Dataset, Table 6.2). The optimized model was considered acceptable if it met the PBPK Model Acceptance Criteria detailed below.

Pediatric PBPK Model

In order to scale from adults to children, drug-specific inputs were held constant and system-specific inputs were scaled by including age-dependencies in physiological parameters (e.g., body weight, organ weight, blood flow).[16] The PK Sim® population module was used to generate populations (n=1000) of neonates (0d-<29d), infants (30d-<2y), children (2y-<6y), school age children (6y-<12y), and adolescents (12y-<18y).[28] Based on age and gender, each individual was assigned a weight and height according to the distribution in population datasets.[18] The weight and height of each simulated individual was used to assign organ weights, volumes, and blood flows based on mean values reported in the ICRP database.[19]

In the Adult PBPK Model, the equilibrium compartment (Step 1) and the biliary efflux clearance (Step 3) parameters were optimized using *in vivo* adult data; it was assumed for the Pediatric PBPK Model that there was no ontogeny to these processes. In addition, because limited data exist describing ontogeny of OATP1B1 activity, the OATP1B1 uptake used in the Adult PBPK Model was held constant in the Pediatric PBPK Model (Step 2).

Other clearance processes were scaled using the mechanistic drug clearance method described by Edginton et al.[29] GFR was scaled by calculating the ratio of expected GFR for unbound drug in a child to that in an adult;

$$CL_{GFR(child)} = \frac{GFR_{(child)}}{GFR_{(adult)}} \times \frac{f_{u\,(child)}}{f_{u\,(adult)}} \times CL_{GFR\,(adult)} \quad \text{(eq. 4)}$$

Where $CL_{GFR(child)}$ is the child's clearance due to GFR, $GFR_{(child)}$ is the estimated GFR of the child, $GFR_{(adult)}$ is the GFR in adults (assumed to be 110 mL/min[29]), and $CL_{GFR(adult)}$ is the clearance due to GFR in adults. $GFR_{(child)}$ was calculated using a postmenstrual age model[30] and the $f_{u\,(child)}$ was estimated using methods described by McNamara and Alcorn.[29,31]

To scale hepatic clearance (CL_H) to children, CL_I' was calculated using adult plasma CL;

$$CL_I{}' = CL_H \times \frac{Q_H}{Q_H - CL_H} \times \frac{1}{f_u} \quad \text{(eq. 5)}$$

Adult CL_I' was then scaled to children using an ontogeny factor;

$$CL_I{}'_{CYP3A4(child\ g\ liver)} = OSF_{CYP3A4} \times CL_I{}'_{CYP3A4(adult\ g\ liver)} \quad \text{(eq. 6)}$$

Where $CL_I{}'_{CYP3A4(child\ g\ liver)}$ is the scaled CL_I' due to CYP3A4 per gram of liver, OSF_{CYP3A4} is the ontogeny scaling factor for CYP3A4,[29] and $CL_I{}'_{CYP3A4(adult\ g\ liver)}$ is the adult CL_I' due to CYP3A4. No ontogeny data were available for arylsulfatase and catechol-O-

methyltransferase, so the $OSF_{arylsulfatase}$ and $OSF_{catechol\text{-}O\text{-}methyltransferase}$ were assumed to equal one.

Finally, child CL_H was estimated using the equation for the well-stirred model after adjusting for liver weight (LW_{child}) and the blood/plasma (B/P) concentration ratio;

$$CL_I{}'_{(child\ total\ liver)} = CL_I{}'_{CYP3A4(child\ g\ liver)} \times LW_{child} \quad \text{(eq. 7)}$$

$$CL_{H\ (child)} = \frac{Q_{H\ (child)} \times f_{u\ (child)\ total\ liver} \times CL_I{}'_{(child) total\ liver}}{Q_{H\ (child)} + (f_{u\ (child)} \times CL_I{}'_{(child) total\ liver}) / \frac{B}{P}_{(child)}} \quad \text{(eq. 8)}$$

In order to evaluate the Pediatric PBPK Model, model predictions were compared with observed data. Multiple pediatric datasets encompassing a range of ages and doses were available for model evaluation (Pediatric Validation Datasets, Table 6.2). Once acceptance criteria were met, an ECMO compartment was linked to the Pediatric PBPK Model.

ECMO PBPK Model

The Pediatric PBPK Model was exported into MoBi® where an ECMO compartment was added (Figure 6.1). The ECMO compartment was set in parallel with the Lung compartment and pulmonary blood flow was partitioned, with 80% assigned to the ECMO compartment and 20% assigned to the lungs.

$$\frac{dX_{ECMO}}{dt}(plasma) = Q_{Lung} * Fraction2ECMO * C_{pls} * (1 - Hct) \quad \text{(eq. 9)}$$

$$\frac{dX_{ECMO}}{dt}(blood\ cells) = Q_{Lung} * Fraction2ECMO * C_{bc} * Hct \quad \text{(eq. 10)}$$

Where dX_{ECMO} represents the change in the amount of drug in the ECMO compartment; Q_{Lung} is the lung blood flow, Fraction2ECMO is the fraction of the lung blood flow that is

partitioned to the ECMO circuit (0.80); C_{pls} is the plasma concentration; Hct is the hematocrit, and C_{bc} is the concentration in red blood cells.

The volume of the ECMO compartment was 400mL based on the standard volume of blood used to prime the ECMO circuit.

Because the *ex vivo* results from Chapter 2 showed that micafungin was extracted extensively by the circuit, a first-order elimination rate constant (k_{ECMO}, min^{-1}) was added to the ECMO compartment to describe the extraction determined in the *ex vivo* experiments;

$$\frac{dX_{ECMO}}{dt}(plasma) = -k_{ECMO} * f_u * (Q_{Lung} * Fraction2ECMO * C_{pls} * (1 - Hct)) \quad \text{(eq. 11)}$$

$$\frac{dX_{ECMO}}{dt}(blood\ cells) = -k_{ECMO} * f_u * (Q_{Lung} * Fraction2ECMO * C_{bc} * Hct) \quad \text{(eq. 12)}$$

The *ex vivo* experiments showed that circuit extraction resulted in a median decrease in $AUC_{0\text{-}24}$ of 29%. The median decrease in AUC was determined by subtracting the actual AUC for each circuit from the AUC assuming no adsorption (Figure 6.3, Appendix 4). This calculation also was performed for the control samples and the circuit adsorption was corrected for loss in the control samples. Because 80% of the blood flow was exposed to the ECMO circuit, the k_{ECMO} term was optimized so that the PBPK-predicted $AUC_{0\text{-}24}$ prior to adding the ECMO compartment decreased by 23% (29% x 0.8) after adding the ECMO compartment.

An Edema disease state was added to the model to reflect the anasarca observed in children on ECMO. The Edema disease state assumed a 50% increase in body weight; that increase was assigned to the interstitial space of all organ compartments.[32,33] The ECMO PBPK Model with Edema was considered the final ECMO PBPK Model and was used for all subsequent ECMO PBPK simulations.

The PK Sim® population module was used to generate an infant population (n=1000) based on the demographics of infants in the Micafungin ECMO Trial. The ECMO PBPK Model was used to predict concentration versus time curves for this population of infants. Model predicted concentrations were compared with observed data from the Micafungin ECMO Trial described in Chapter 5.

Assessment of Dose-Exposure Relationship

After meeting acceptance criteria, the ECMO PBPK Model was used to determine the micafungin dose needed to achieve target exposures in 90% of children on ECMO.[34,35] Simulations of 1000 individuals were performed for neonates, infants, children, school age children, and adolescents. Efficacy was assessed based on the number of individuals who attained a target AUC from 0-24 hours (AUC_{0-24}) of at least 75 mg*h/L.[34,35] This surrogate endpoint matches the minimum micafungin exposure achieved by adult participants who cleared their fungal infection in the primary efficacy trial.[36] Safety of the proposed dosing regimens was assessed by comparing predicted maximum AUC_{0-24} for each individual with maximum tolerated AUC_{0-24} (600 mg*h/L).[20,37]

PBPK Model Acceptance Criteria

Population predictability was evaluated by visual inspection of the observed data captured within the model's 90% prediction interval. Because dosing is based on AUC, the primary method of assessing model precision was to evaluate the fold error between the PBPK-predicted AUC and observed AUC

$$Fold\ Error = \frac{AUC_{0-24}PBPK}{AUC_{0-24}Observed} \quad \text{(eq. 13)}$$

A fold error between 0.7–1.3 was considered acceptable. For Adult and Pediatric Development and Validation Datasets, each reported AUC was compared with a PBPK-predicted AUC for the same dosing interval. For the Micafungin ECMO Trial, the observed $AUC_{0\text{-}24}$ was compared with PBPK-predicted $AUC_{0\text{-}24}$.

RESULTS

Adult model

Figure 6.4 shows the results of each step of the adult model building process. The model was optimized by assigning f_u 0.006 (Table 6.1). The base model shows that with only GFR as a clearance process, there was virtually no clearance of micafungin, and predicted concentrations in liver tissue were low (less than plasma concentrations) relative to reported concentrations (greater than plasma concentration) at 6 hours (Figure 6.4).[9] In Step 1, the interstitial:plasma partition coefficient for all organs was increased by a factor of 4, and the endothelial permeability was decreased to 0.03 cm/min except for the brain compartment, which was kept at $1.26x10^{-09}$ cm/min. These adjustments provided a better description of the α-distribution phase, but concentrations in liver tissue remained low, plasma clearance was not accurately characterized, and all elimination occurred via the kidneys. In Step 2, OATP1B1 uptake was added to the model, which improved the description of the terminal elimination of micafungin from the plasma based on the observed data. However, all elimination was still via kidneys and liver tissue concentrations showed continued accumulation. In Step 3, a biliary efflux process was added, dividing elimination between bile and urine. At 168h the predicted

micafungin fraction eliminated via bile was 61% and urine was 5% compared with the observed fraction eliminated of 44% and 7% in feces and urine, respectively.[8] Finally, in Step 4, metabolism was incorporated into the micafungin ECMO PBPK Model by adding CL_I', which was partitioned between arylsulfatase, catechol-O-methyltransferase, and CYP3A4 metabolic pathways. After addition of metabolism into the model, the predicted fraction of micafungin excreted via bile decreased to 45% and the fraction excreted in urine remained at 5%. These fractions were in close agreement with mass balance data. Concentrations in the liver exceeded those in plasma after 4 hours, consistent with observed animal data.[9]

The final model showed excellent agreement between observed versus predicted data from the Adult Development Dataset (Figure 6.4, Step 4). The predicted AUC_{0-24} after dose 1 was 108 mg*h/L compared to the observed AUC_{0-24} of 104 mg*h/L for the same dosing interval (1.04 fold error, Table 6.4). When optimized model predictions were compared with observed data from Model Validation Datasets (i.e., data not used to build the model), over 90% of the mean observed data fell within the 90% prediction interval of the model (Figure 6.5). The PBPK-predicted AUC_{0-24} values were within 3% of observed AUC_{0-24} values after multiple doses (Table 6.4). Based on this excellent predictive performance, this optimized Adult PBPK Model was scaled to children.

Scaling to Children

Pediatric simulations were performed for multiple dosing regimens and showed good agreement with corresponding observed exposures from the Pediatric Validation Datasets. For children ≥ 2 years of age, 97% (29/30) of the observed mean

concentrations from the Benjamin et al. study[38], and 96% (52/54) from the Seibel et al. study[35], were within the 90% prediction interval of the Pediatric PBPK Model (Figure 6.6). Additionally, median fold errors between observed versus predicted AUC values were 1.04 and 1.05 for Benjamin et al. and Seibel et al., respectively (Table 6.5). In infants < 2 years of age, observed data from Undre et al.[39] were over-predicted in the initial phase of distribution (5-15 minutes), but subsequent data were well described (Figure 6.7). In contrast, observed data from Benjamin et al. were under-predicted. Nonetheless, PBPK-predicted AUC values had acceptable fold errors of 1.11 for Undre et al. and 0.72 for Benjamin et al (Table 6.5). Based on these results, the model was exported into MoBi® where the ECMO compartment was added.

ECMO model

Results of the ECMO PBPK Model building process are shown in Figure 6.8. Prior to adding the ECMO compartment, the Pediatric PBPK Model predictions were compared with observed data from the Micafungin ECMO trial, and only 55% (33/60) of the observed data fell within the 90% prediction interval (Figure 6.8.1) The model over-predicted AUC (117 mg*h/L) compared to the observed AUC reported in Chapter 5 (74 mg*h/L; 1.58 fold error). Addition of the ECMO compartment to the Pediatric PBPK Model improved model predictions; 70% (42/60) of the observed data fell within the 90% prediction interval (Figure 6.8.2). However, $AUC_{0\text{-}24}$ was still over-predicted (97 mg*h/L; 1.31 fold error). After incorporating edema into the Pediatric PBPK model, 95% (57/60) of the observed data fell within the 90% model prediction interval (Figure 6.8.3), and the

median PBPK predicted AUC_{0-24} was 86 mg*h/L compared to the observed AUC of 74 mg*h/L (1.16 fold error, Figure 6.9).

Based on the precision of AUC estimates, the ECMO PBPK Model was used to simulate exposures for different dosing regimens for each pediatric age cohort. The following age-dependent dosing regimens were found to achieve the target AUC_{0-24} in ≥ 90% of simulated children on ECMO in the first 24 hours of therapy: neonates (0-29d) 10 mg/kg, infants (30d-<2y) 6 mg/kg, children (2y-<6y) 4 mg/kg, school-age children (6y-<12y) 3 mg/kg, and adolescents 2 mg/kg (Figure 6.10).

Complicated dosing regimens such as the age-based regimen above are often difficult to implement. In order to simplify the dosing regimen, maximize efficacy, and minimize toxicity, the ECMO PBPK Model also was used to simulate exposures after a dose of 10 mg/kg for neonates and infants <2 years of age and 6 mg/kg for children 2 years-<18 years of age (Figure 6.11). This approach achieved the target AUC_{0-24} in 100% of simulated children on ECMO in the first 24 hours of therapy and 99.5% had an AUC_{0-24} (233 [76, 867]) below the safety threshold value of 600 mg*h/L.

DISCUSSION

This study used an established workflow to successfully develop a PBPK model in adults and scale it to children. By adding a novel ECMO compartment and accounting for disease state effects (i.e., edema), the model was able to generate dosing predictions in children on ECMO across the pediatric age spectrum. The adult model was successfully parameterized using drug specific and system specific data from the

literature. Because of the inherent complexity of PBPK models, it is challenging to know all parameters with certainty and invariably, assumptions must be made. In order to minimize bias introduced by these assumptions, the model was first parameterized according to the following known processes: 1) mass balance data,[8] 2) transporter-mediated hepatic uptake,[7] and 3) liver concentrations in excess of plasma concentrations.[8,9] Anchored in these known processes, the model was parameterized assuming rapid distribution from the vascular space into the interstitial space and that unbound concentrations in the interstitial fluid exceeded those in plasma. This approach was justified based on the fact that micafungin binds to multiple proteins in addition to albumin, and could preferentially bind to proteins in the interstitial space.[23] In addition, data for caspofungin showed that it distributed into interstitial space and reversibly adsorbed to the cellular membrane.[10,11] This rapid equilibrium process has been used in PBPK models for other organic anions such as caspofungin[25] and pravastatin.[24] Similarly, the micafungin CL_I' for the metabolizing enzymes of interest, and the rate of efflux, were optimized to achieve the appropriate fraction excreted in bile from mass balance data. The use of observed in vivo concentration versus time data to optimize PBPK model parameters is well described, the so-called "middle-out approach."[40] However, this approach can limit generalizability. This was not the case for the micafungin model, where model predictions were in close agreement with both the Adult Development and Validation Datasets.

After development of the adult model, the PBPK model was scaled to children based on known anatomic and physiologic data. Some of the processes had well-described ontogeny data (e.g., maturation of GFR),[41,42] but for many of the processes,

ontogeny data were lacking. For processes where ontogeny data were lacking (e.g., rapid equilibrium, transporter expression), the initial assumption was that there was no ontogeny, and this assumption held for the micafungin model. For children greater than two years of age, the model predictions were in close agreement with observed data. Both over- and under-predictions were observed, which makes population variability, rather than ontogeny, the more likely explanation. Variability would be expected as these children were all critically ill (e.g., cancer, invasive fungal infection). Model predictions for infants were less accurate, but again over- and under-predictions were observed. Failure to incorporate ontogeny data could play a role in model mis-specification, especially considering that many maturation processes occur before two years of age.[43] However, these processes were not explored because the small sample sizes in the infant studies would make evaluation impossible.

The observed data from the Micafungin ECMO Trial showed that micafungin exposure was lower in children on ECMO. Based on the *ex vivo* experiments in Chapter 2, this was due, in part, to the impact of the ECMO circuit, specifically hemodilution from the exogenous blood required to prime the circuit and extraction by the circuit. The impact of ECMO on micafungin PK was incorporated into the Pediatric PBPK Model by linking an ECMO compartment to the model with assigned flows, a volume reflecting the exogenous blood, and an elimination rate constant accounting for extraction by the circuit that was measured in the *ex vivo* experiments described in Chapter 2. The total extraction by the *ex vivo* ECMO circuits was corrected for extraction observed in the control samples. This assumed that the extraction observed in the control samples was not occurring *in vivo*, which was a reasonable assumption if extraction in the control

samples was due to adsorption by the control tubes. However, if extraction in the control samples was due to light degradation or plasma metabolism, it is possible that these processes also could be observed *in vivo*. However, if total circuit extraction was not corrected for the extraction in the controls, then the AUC would be expected to decrease by ~40% after adding the ECMO compartment. A 40% decrease would result in substantial under-prediction of exposure compared to observed exposures. The excellent agreement between the ECMO PBPK Model-predicted and observed concentrations in children on ECMO supports the assumptions used in model development, and the use of circuit extraction corrected for extraction in controls. However, additional *ex vivo* experiments are planned to determine the mechanism(s) of extraction in the control tubes, and this model could be modified based on those results.

Two important assumptions in the ECMO PBPK Model were the partitioning of pulmonary blood flow and the extent of edema. The pulmonary blood flow was partitioned such that 80% flowed through the ECMO circuit and 20% returned to the lungs. A sensitivity analysis was performed to evaluate the physiologically plausible range of blood flowing through the ECMO circuit (70-95%) and found a minimal effect on AUC (+/- 5%). The model was more sensitive to changes in the extent of edema. The Edema disease state in the final ECMO PBPK Model assumed a 50% increase in body weight due to edema with the resulting volume assigned to the interstitial compartment of each virtual organ. When a 10% increase in body weight was assumed, the resulting AUC was 20% higher. Future studies should quantify the extent of edema (e.g., daily weights) in order to more accurately estimate this parameter. Capturing other

treatments such as blood transfusions and crystalloid administration could provide additional detail about alterations in PK.

The ECMO PBPK Model-predicted dosing was consistent with dosing trends observed in children not on ECMO. In general, neonates require higher doses to achieve comparable micafungin exposure to that observed in infants and older children.[44] Work by Yanni et al. suggests that higher micafungin clearance in neonates and infants is due to age-dependent serum protein binding.[45] For a low extraction drug like micafungin, clearance is directly proportional to f_u. Micafungin is highly protein bound in adults (>99%), and small changes in f_u can markedly change clearance. Yanni et al. measured the f_u of micafungin in 6 neonates and reported a mean f_u of 0.033 compared to 0.004 measured in adults. The ECMO PBPK Model used the method developed by McNamara to scale f_u from adults to children.[31] Based on this model, the mean f_u in neonates was 0.003 compared to the optimized f_u in adults of 0.006, and this was likely responsible for the higher clearance and higher dose requirements in this population. Because the model accuracy was excellent using the scaling method reported by McNamara et al., a distinct ontogeny function was not developed to describe the Yanni data.

Optimized dosing based on the ECMO PBPK Model in all age cohorts except adolescents exceeded the recommended dose of 2 mg/kg.[46] Although age-based predictions optimized dosing to achieve the minimum necessary exposure, a simplified dosing regimen of 10 mg/kg in neonates and infants < 2 years of age and 6 mg/kg in children 2 years-<18 years of age is more appropriate for several reasons: 1) clinical feasibility; 2) higher exposures may be needed to clear biofilms; and 3) micafungin is

safe even at high exposures. Micafungin is known to be safe at doses up to 15 mg/kg and AUC_{0-24} exposures exceeding 600 mg*h/L.[37,47] The adult efficacy trial that linked an exposure of AUC_{0-24} 75-139 mg*h/L to eradication of candidemia also included a recommendation that intravascular catheters be removed. Because catheter removal on ECMO is difficult, if not impossible, micafungin exposures need to be adequate to clear biofilms. *In vitro* work suggests that maintaining micafungin concentrations ≥ 2 mg/L may be sufficient to eradicate biofilms, but these results have not been confirmed *in vivo*.[48] The simplified dosing recommendations in Figure 6.11 achieve a trough concentration of ≥ 2 mg/L in 96% of simulated children (data not shown). Based on these results, micafungin 10 mg/kg is recommended for neonates and infants <2 years of age and 6 mg/kg is recommended for children 2 years-<18 years of age.

For neonates who are at risk for hematogenous candida meningoencephalitis, 10 mg/kg is the recommended micafungin dose to achieve appropriate penetration of the cerebrospinal fluid, resulting in a plasma AUC_{0-24} of ~300 mg*h/L.[47] Based on this information, assuming linear kinetics, a dose of > 20 mg/kg would be necessary to achieve appropriate CSF penetration in neonates on ECMO. Until a dose this high can be evaluated prospectively, fluconazole, with its better CSF penetration and limited interaction with the ECMO circuit should be considered in neonates on ECMO where candida meningoencephalitis is suspected.

In conclusion, the ECMO PBPK Model developed in this study demonstrates proof of concept for translation of *ex vivo* ECMO results into dosing recommendations for children on ECMO. The Adult PBPK Model of micafungin was developed using data from the literature and physiologically justified assumptions. Although some parameters

were optimized using observed adult data, the model accurately predicted observed data in independent adult populations and after scaling to children. The addition of an ECMO compartment and incorporation of edema, consistent with that observed in children on ECMO, resulted in excellent agreement between PBPK predicted and observed data (ECMO PBPK Model-predicted AUC within 0.7-1.3 fold error of observed AUC). Consequently, the ECMO PBPK Model was used to determine the optimal dose of micafungin needed to treat invasive candidiasis in children supported with ECMO.

Table 6.1. Micafungin physicochemical properties and elimination pathways

Parameter	Reported value	Optimized value
Physicochemical properties		
Lipophilicity (LogP)	-0.39[6]	
Protein binding partner	Albumin[6]	
Fraction unbound (%)	<1%[6]	0.6%
Molecular weight (g/mol)	1292.26[49]	
Compound type/pKa	Weak acid/9.15[6]	
Charge	Negative	
B/P Ratio	0.9[8]	
Metabolism and elimination		
Hepatic Uptake		
V_{max} liver tissue (pmol/min/g tissue)	36630[7]	
V_{max} (µmol/L/min)	45.58	
K_m (µmol/L)	40[7]	
Hepatic Efflux		
V_{max} liver tissue (pmol/min/g tissue)	NR	300
V_{max} (µmol/L/min)	NR	0.37
K_m (µmol/L)	NR	10
Fraction excreted via bile (168h)	44%[6]	45%
Fraction excreted via urine (168h)	7%[6]	5%
Ayrlsulfatase CL_I' (L/min)	NR	0.003
Catechol-O-methyltrasnsferase CL_I' (L/min)	NR	0.0007
CYP3A4 CL_I' (L/min)	NR	0.004
K_{ECMO} (1/min)	NR	0.45

NR – not reported

Table 6.2. Studies used in model development and evaluation

Population	N	Age	Dosing interval	Dose	Reference
Adult Development Dataset					
Healthy volunteers	12	44 (4)	Single dose	150 mg	Hiemenz et al. 2005[20]
Adult Validation Datasets					
Healthy volunteers	23	NR	q24 hours	150 mg	Keirns et al. 2007[21]
Healthy volunteers	34	23 (3)	q24 hours	200 mg	Undre et. al 2014[22]
Pediatric Validation Datasets					
Immunocompromised children	84	4mo-<18y	q24 hours	3-4.5 mg/kg	Benjamin et al. 2013[38]
Immunocompromised children	77	2y-<18y	q24 hours	0.5-4 mg/kg	Seibel et al. 2005[35]
Children with fungal infection	7	0-2y	q24 hours	2 mg/kg	Undre et al. 2012[39]
ECMO Validation Dataset					
Critically ill infants on ECMO	11	59d (0-574d)	q24 hours	4 mg/kg	Autmizguine et al. 2016[50]

Age is reported as mean (standard deviation) or range except for the ECMO Validation Dataset where age is median (range); NR – not reported

Table 6.3. Assumptions used in the model building process

Factor	Assumption	Reference
Mass balance	90% eliminated in feces via bile and 10% in urine Fraction of the dose excreted at 168 hours: 44% in bile and 7% in urine	EMA Summary[6]
f_u	0.006 with a normal distribution and SD of 0.002	Yanni et al. 2011[45]
OATP1B1 V_{max}	Vmax [pmol/(min*mg protein)] 814 with a normal distribution and SD of 248 and no ontogeny	Yanni et al. 2010[7]
OATP1B1 K_m	Km (μM) 40 with a normal distribution and SD of 5 and no ontogeny	Yanni et al. 2010[7]
Edema	Body weight in children on ECMO can be increased by over 50% due to edema	Anderson et al 1992[32]

SD – standard deviation

Table 6.4. Observed versus predicted area under the concentration time curve for a 24 hour dosing interval (AUC_{0-24}) for adult studies used in model development and evaluation

Study	Population	N	Dose	AUC_{OBS} (mg*h/L)	AUC_{PBPK} (mg*h/L)	Fold Error
Adult Development Datasets						
Hiemenz et al.[20]	Healthy Adult	12	150 mg	104[a]	108	1.04
Adult Validation Datasets						
Keirns et al.[21]	Healthy Adult	23	150 mg	181[b]	178	0.98
Undre et al.[22]	Healthy Adult	34	200 mg	236[c]	233	0.99

AUC_{OBS} observed AUC_{0-24}
AUC_{PBPK} predicted AUC_{0-24}
[a] AUC_{0-24} measured after dose 1
[b] AUC_{0-24} measured after dose 20
[c] AUC_{0-24} measured after dose 5

Table 6.5. Observed versus predicted area under the concentration time curve for a 24 hour dosing interval (AUC_{0-24}) for pediatric studies used in model evaluation

Study	Population	N	Dose	AUC_{OBS} (mg*h/L)	AUC_{PBPK} (mg*h/L)	Fold Error
Benjamin et al.[38]	12-<18y	1	4.5 mg/kg	339[a]	351	1.04
	12-<18y	12	3 mg/kg	184	185	1.01
	6-<12y	20	4.5 mg/kg	264	340	1.29
	6-<12y	13	3 mg/kg	249	227	0.91
	2-<6y	31	4.5 mg/kg	248	292	1.18
	0-<2y	9	4.5 mg/kg	264	189	0.72
	median					1.04[d]
Seibel et al.[35]	2-<18y	15	0.5 mg/kg	28[b]	31	1.11
	2-<18y	16	1 mg/kg	52	63	1.21
	2-<18y	16	1 mg/kg	52	63	1.21
	2-<18y	13	1.5 mg/kg	101	94	0.93
	2-<18y	11	2 mg/kg	94	126	1.34
	2-<18y	9	3 mg/kg	191	189	0.99
	2-<18y	9	3 mg/kg	191	189	0.99
	median					1.05
Undre et al.[39]	0-2y	7	2 mg/kg	53[c]	59	1.11

AUC_{OBS} observed AUC
AUC_{PBPK} predicted AUC
[a] Benjamin et al. measured AUC_{0-24} after dose 8
[b] Seibel et al. measured AUC_{0-24} after dose 5
[c] Undre et al. measured AUC_{0-24} after dose 1
[d] Median for Benjamin et al. excludes the results from Infants (0-<2y) as they are considered separately

Figure 6.1. PBPK model structure.

Standard model structure

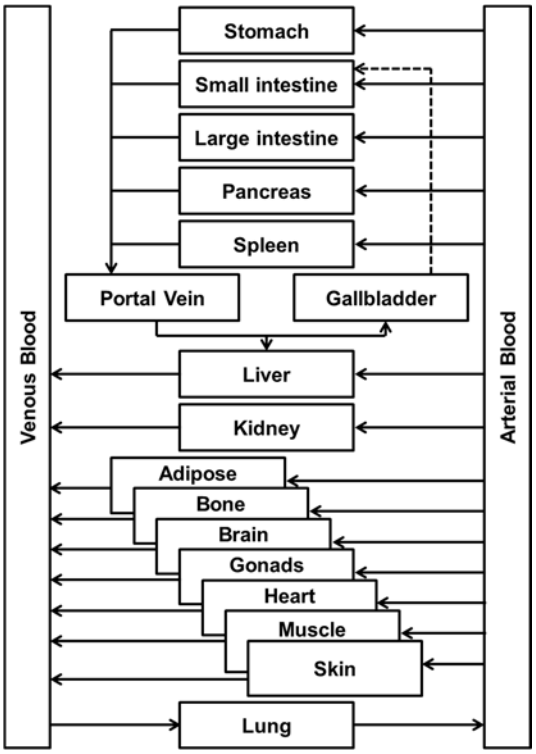

Model structure with ECMO compartment

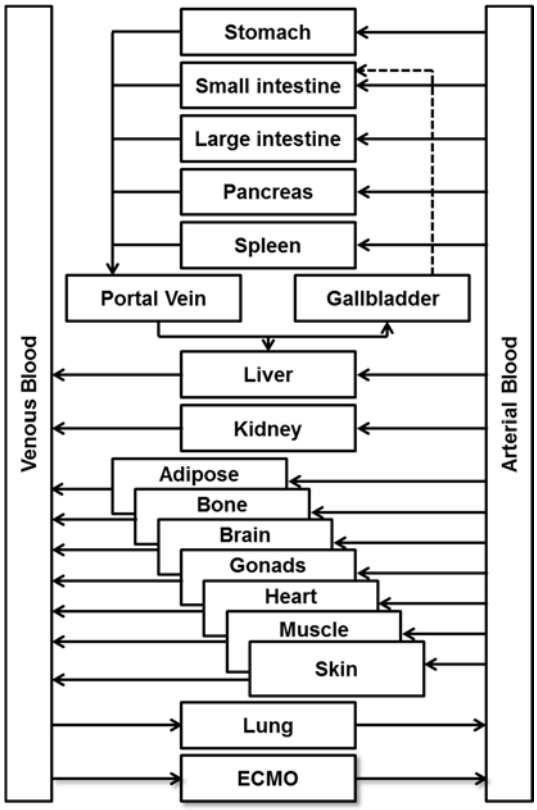

Figure 6.2. PBPK workflow

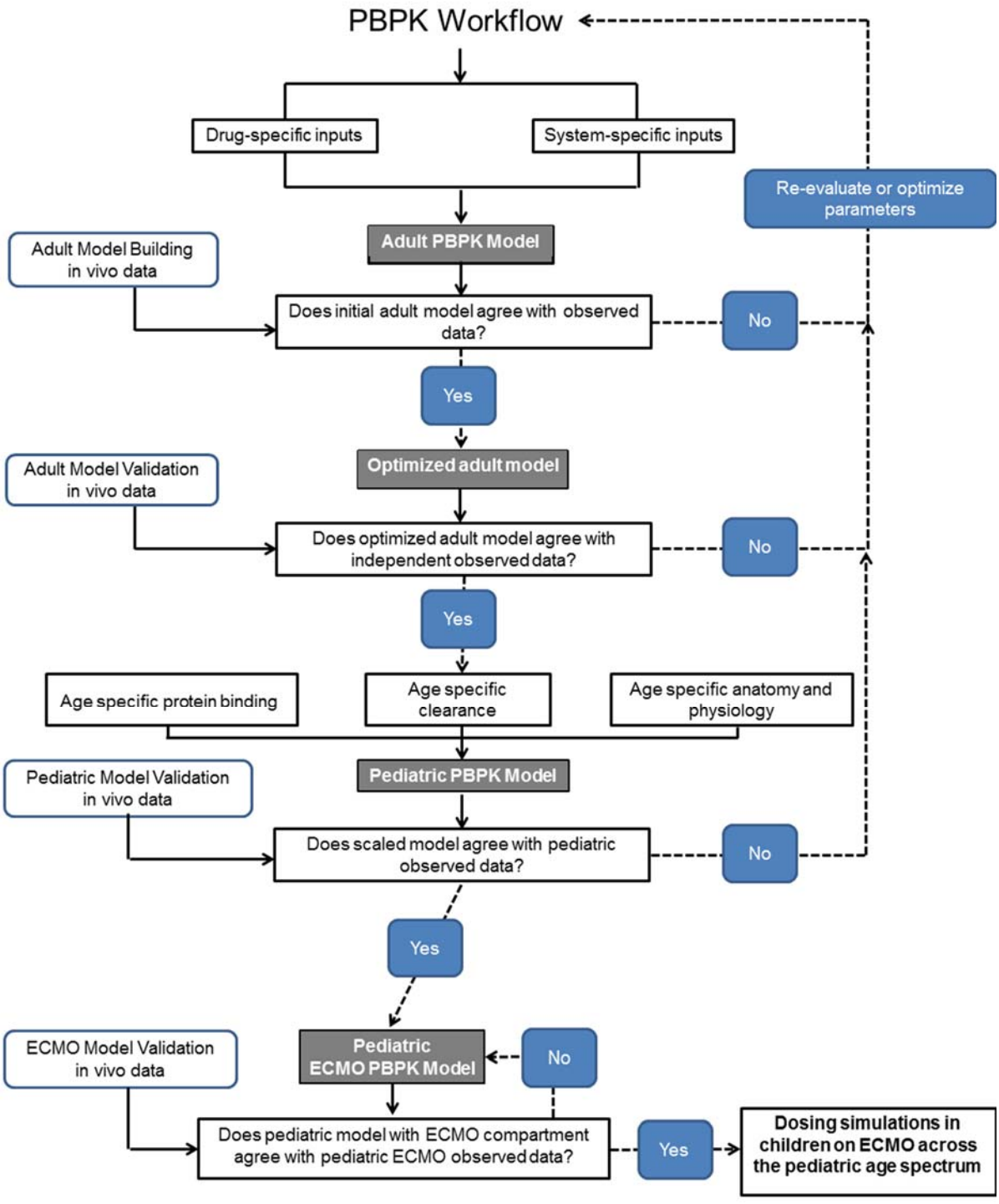

Figure 6.3. Steps to calculate a change in AUC due to extraction by the ECMO circuit. Median change in AUC for circuits corrected for change in AUC in controls is used to parameterize micafungin extraction in the ECMO compartment of the ECMO PBPK Modelhe Adult Development Dataset.

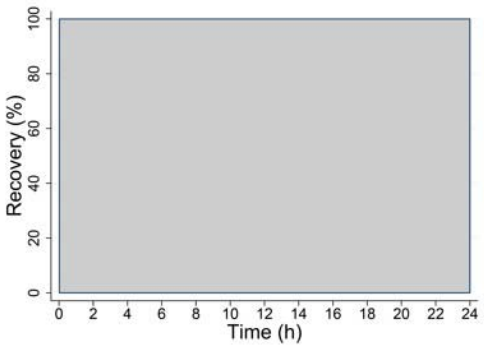

Step 1: AUC_{0-24} Base
AUC_{0-24} calculated assuming no extraction (grey)

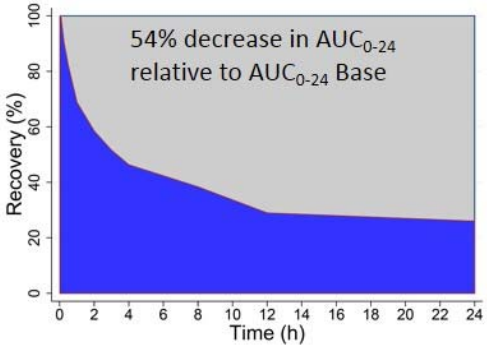

Step 2: AUC_{0-24} Circuit
AUC_{0-24} calculated for circuits (blue)

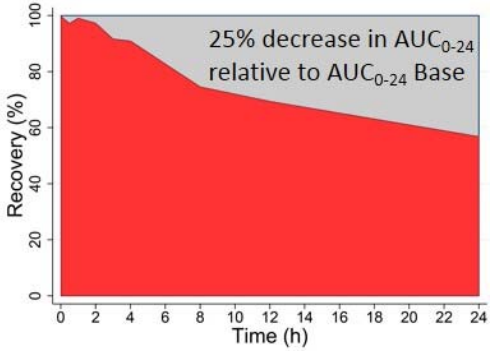

Step 3: AUC_{0-24} Control
AUC_{0-24} calculated for control samples (red)

Step 4: Calculate median decrease in AUC_{0-24} due to circuit and degradation in control
(AUC_{0-24} Base - AUC_{0-24} Circuit) / AUC_{0-24} Base = 0.54
(AUC_{0-24} Base - AUC_{0-24} Control) / AUC_{0-24} Base = 0.25

Step 5: Correct for loss in the control
AUC_{0-24} Circuit - AUC_{0-24} Control = 0.54 – 0.25 = 0.29

Step 6: Adjust based on relative fraction of blood going through ECMO circuit (0.80)
Corrected AUC_{0-24} Circuit x 0.80 = 0.29 * 0.90 = 0.23

Figure 6.4. Adult PBPK Model Development. PBPK model predictions for a dose of 50 mg compared with observed concentrations from the Adult Development Dataset.

Base Adult PBPK Model assuming only passive distribution based on Rodgers and Rowland generated partition coefficients and elimination via GFR.

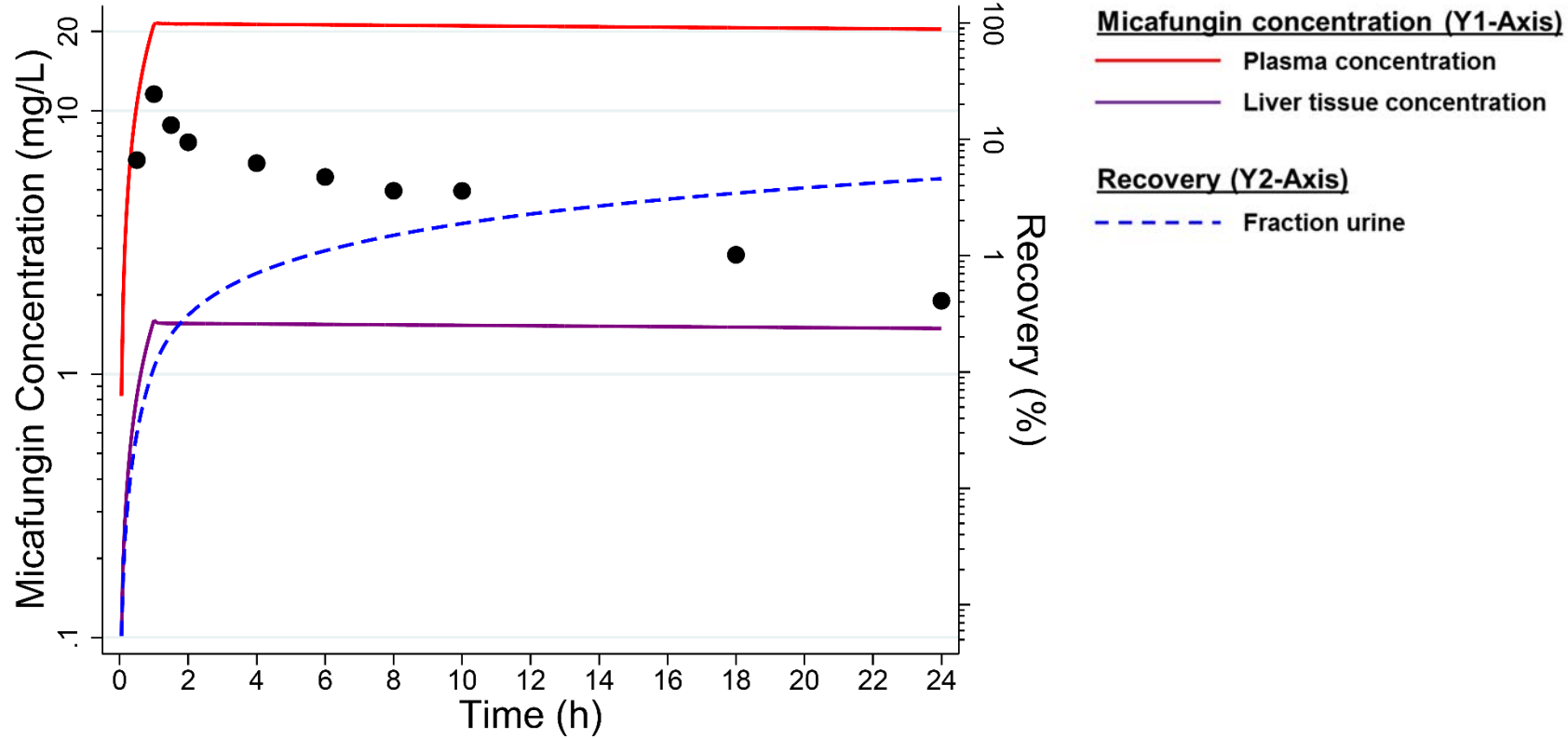

Step 1. Rapid equilibrium process compared to observed data in early distribution phase.

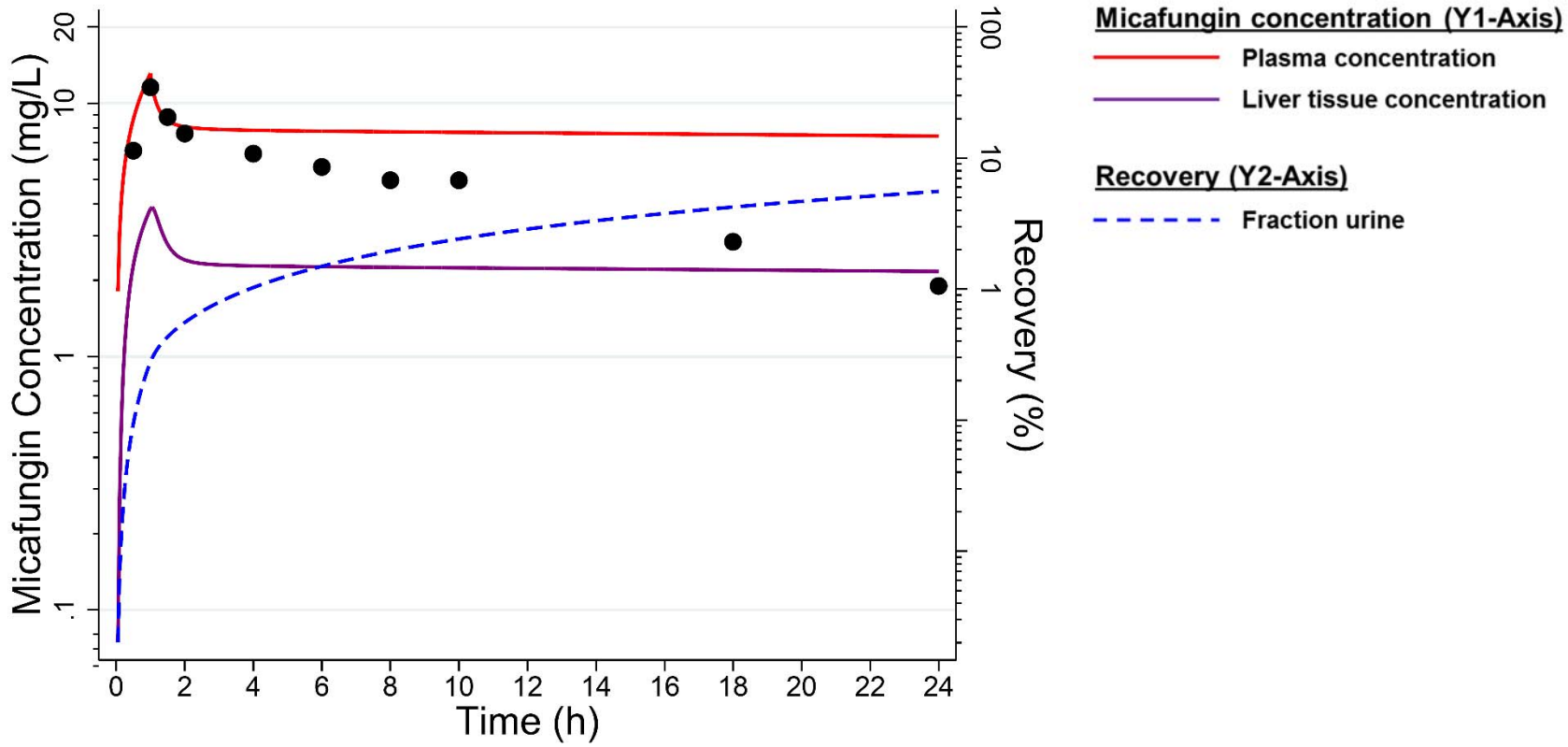

Step 2. Addition of hepatic uptake by OATP1B1.

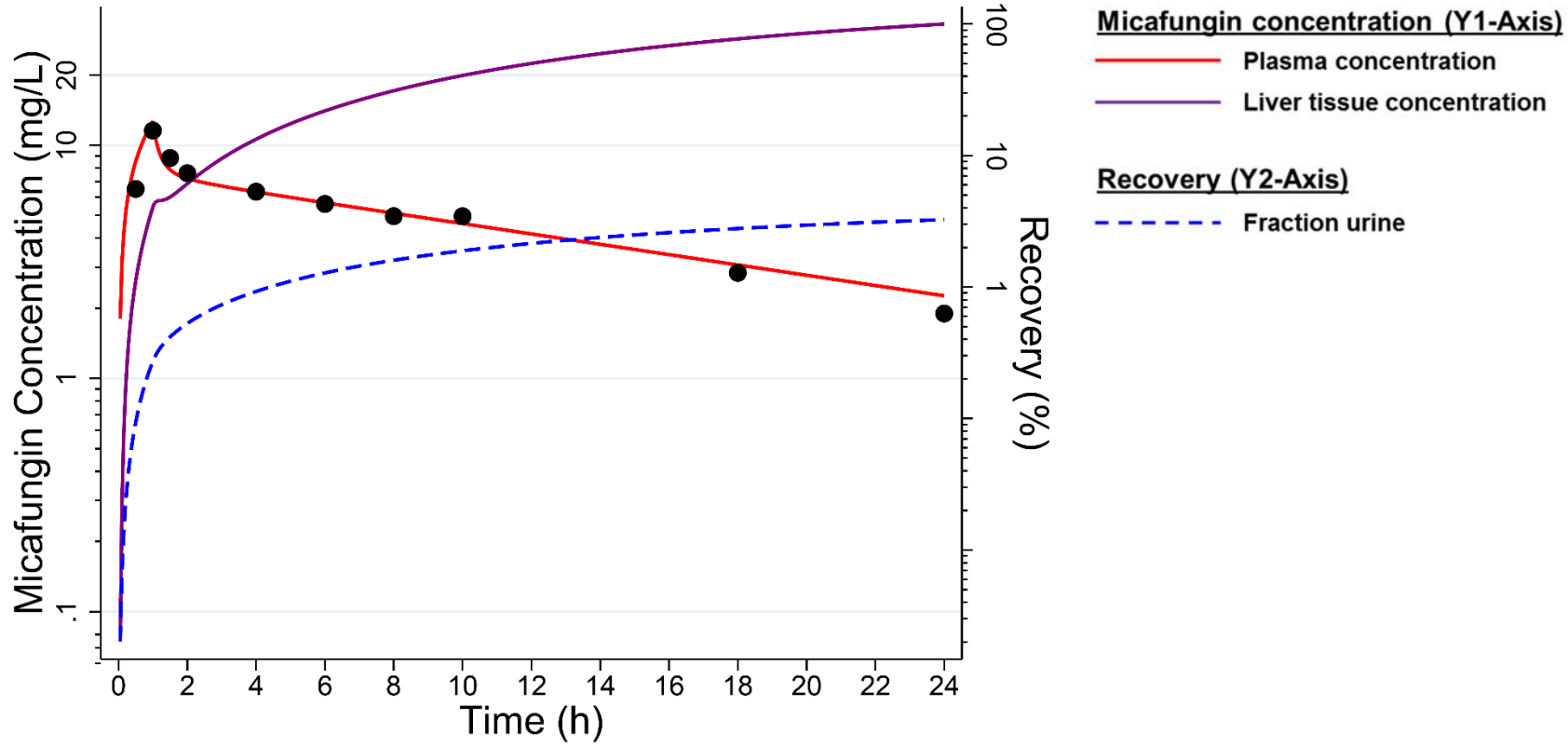

Step 3. Addition of hepatic efflux into bile optimized to fraction excreted in bile equal to fraction excreted for parent and metabolite. Predicted fraction excreted in bile of micafungin at 168h (61%) exceeded observed fraction (44%) from mass balance study.

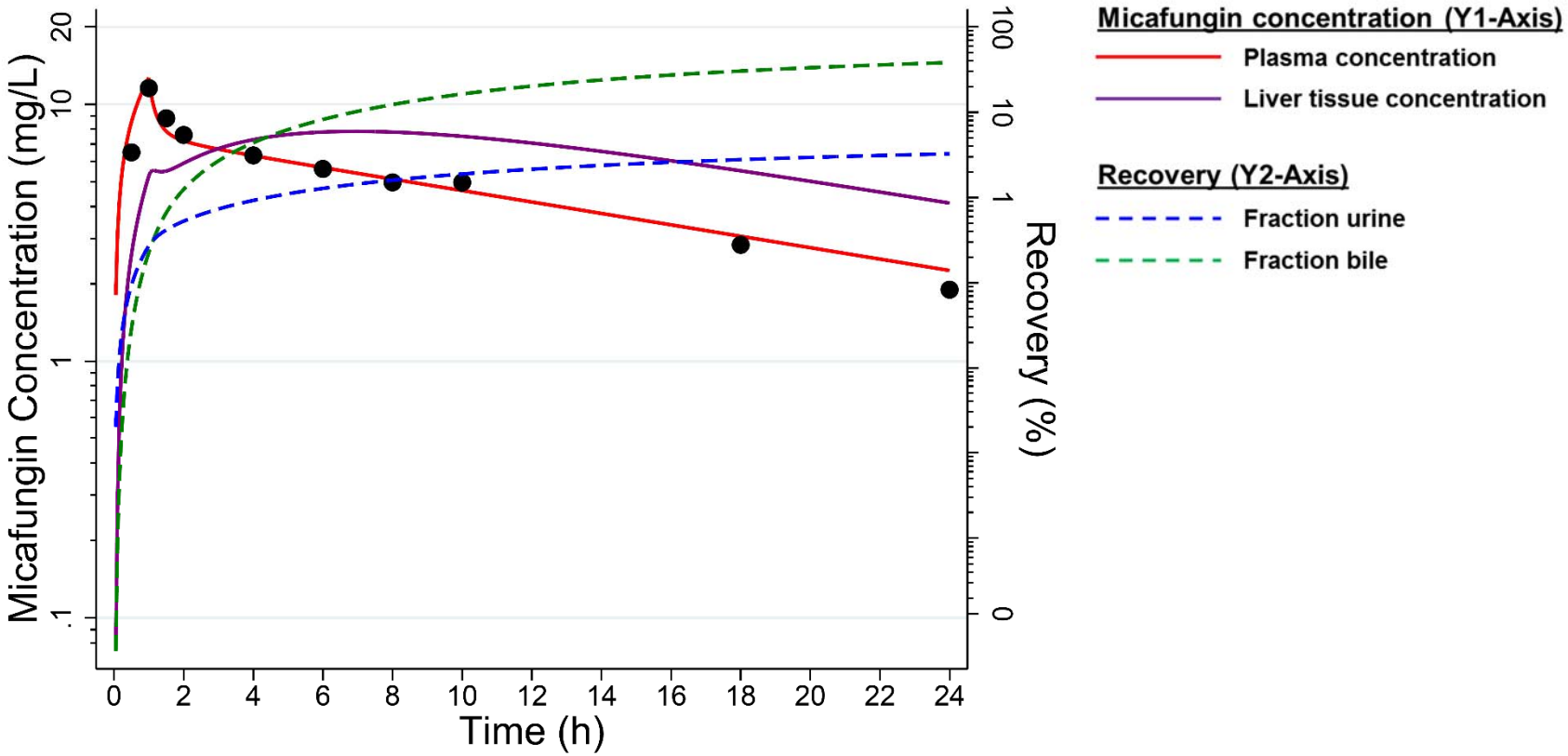

Step 4. Addition of metabolism via arylsulfatase, catechol-O-methyltransferase, and CYP3A4. The predicted fraction excreted in bile (45%) approximated the observed fraction excreted in feces (44%) at 168h. The predicted fraction excreted in urine (5%) approximated the observed fraction excreted in urine (7%) at 168h. The predicted and observed $AUC_{0\text{-}24}$ (mg*h/L) were 104 and 108, respectively (1.04 fold error).

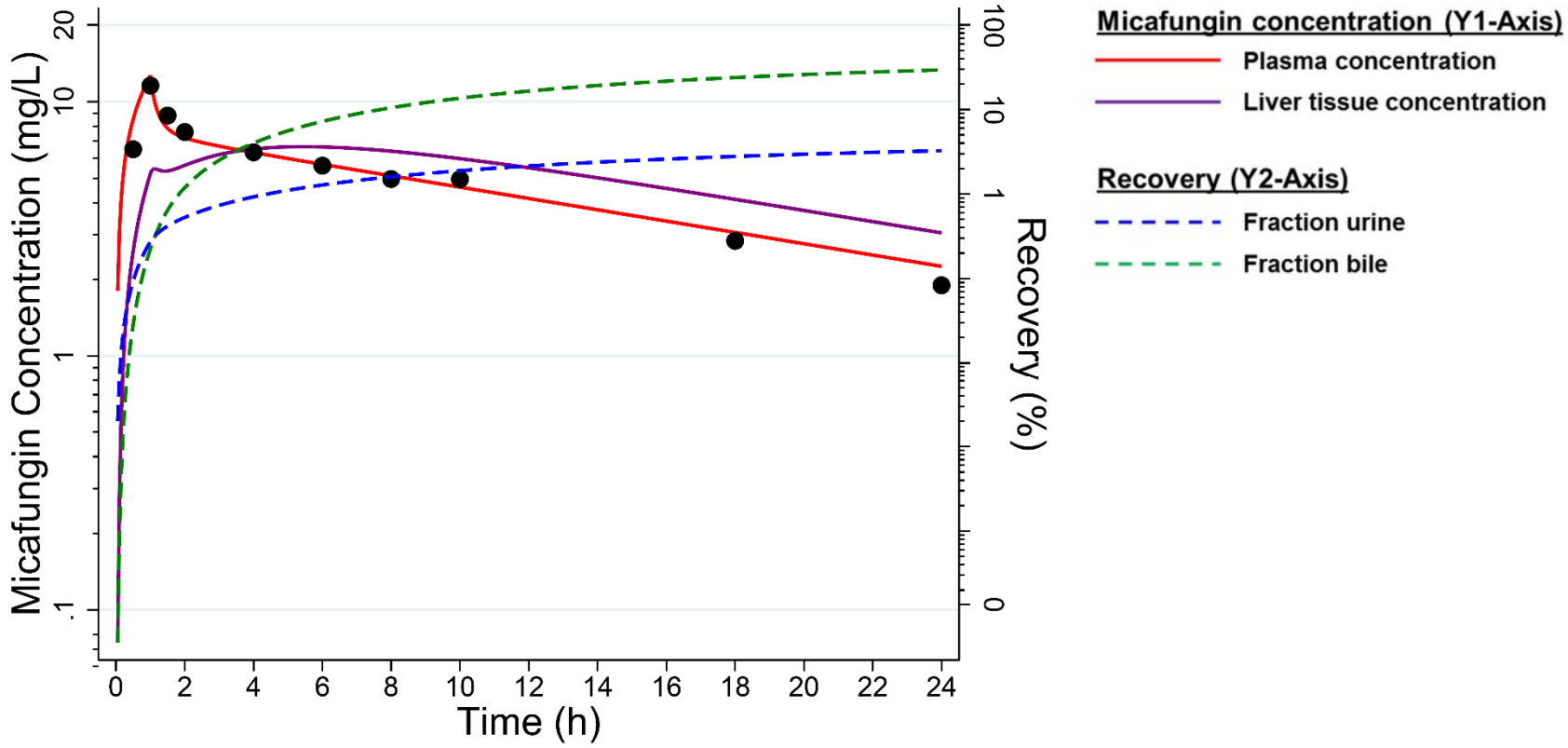

Figure 6.5. Adult model validation. PBPK predicted exposures versus observed data from Adult Validation Datasets. Solid black line represents median predicted concentration; grey shaded area represents the 90% prediction interval; observed data (mean +/- 90% confidence interval) are represented by symbols.

A. Keirns et al. 2007[21] Observed vs predicted exposure after 20 doses of 150 mg every 24 hours

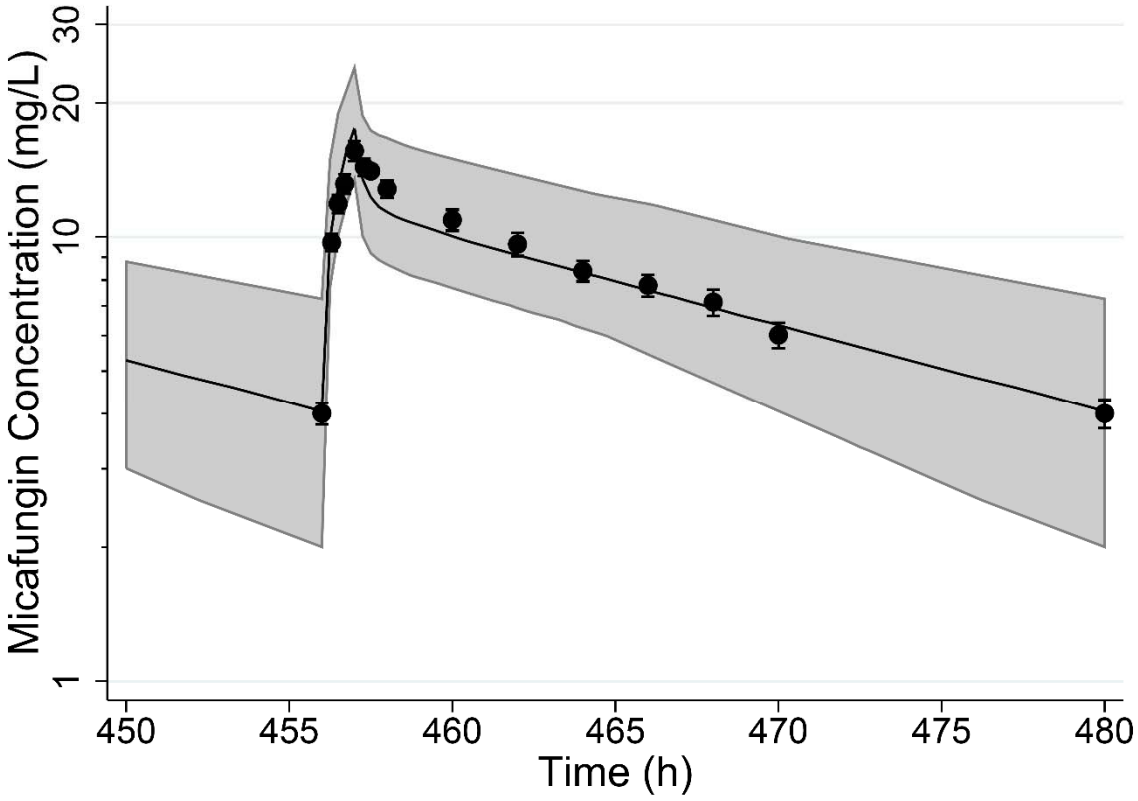

AUC_{0-24} Observed
181 mg*h/L

AUC_{0-24} Predicted
178 mg*h/L

B. Undre et al. 2014[22] Observed vs predicted exposure after 5 doses of 200 mg every 24 hours

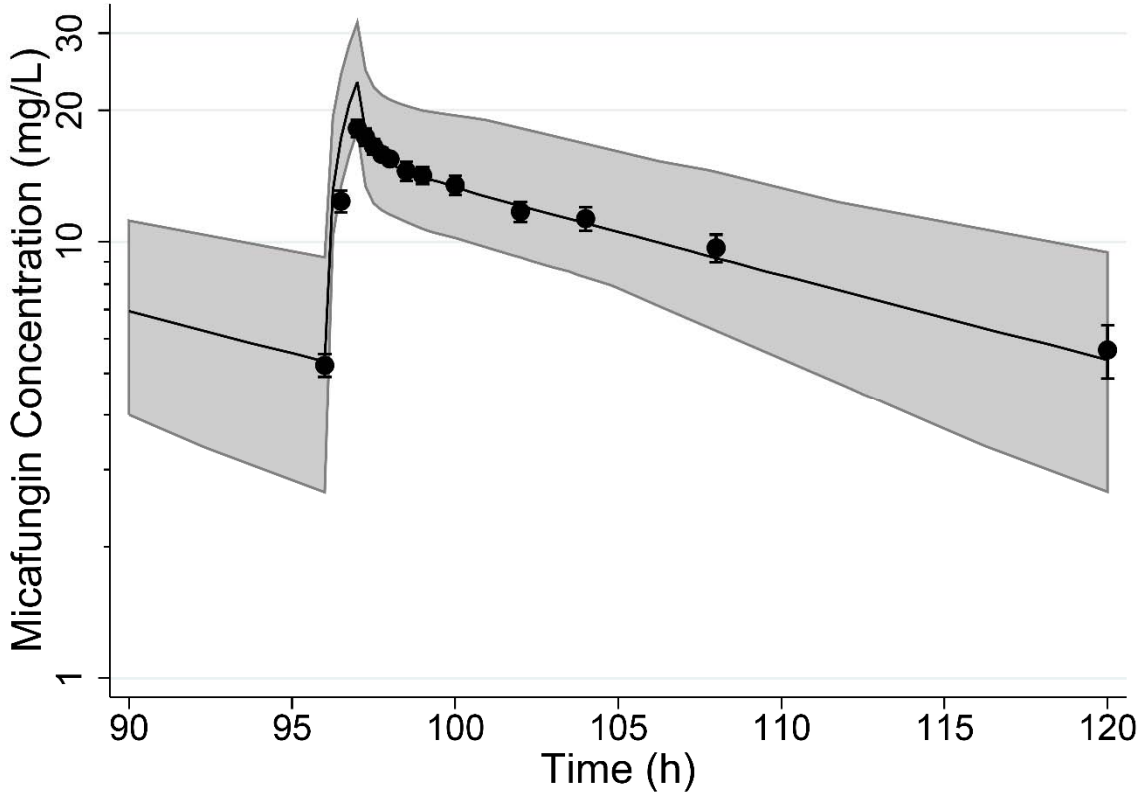

$AUC_{0\text{-}24}$ Observed
236 mg*h/L

$AUC_{0\text{-}24}$ Predicted
233 mg*h/L

Figure 6.6. Pediatric PBPK Model predictions versus observed data for children (2-<18y). PBPK model predictions for a dose of 1 mg/kg versus dose-normalized observed mean concentrations from children 2-<18y included in the Pediatric Validation Datasets. Solid black line represents the median predicted concentration; grey shaded area represents the 90% prediction interval; symbols represent observed mean data for Benjamin et al.[38] (●) and for Seibel et al.[35] (●).

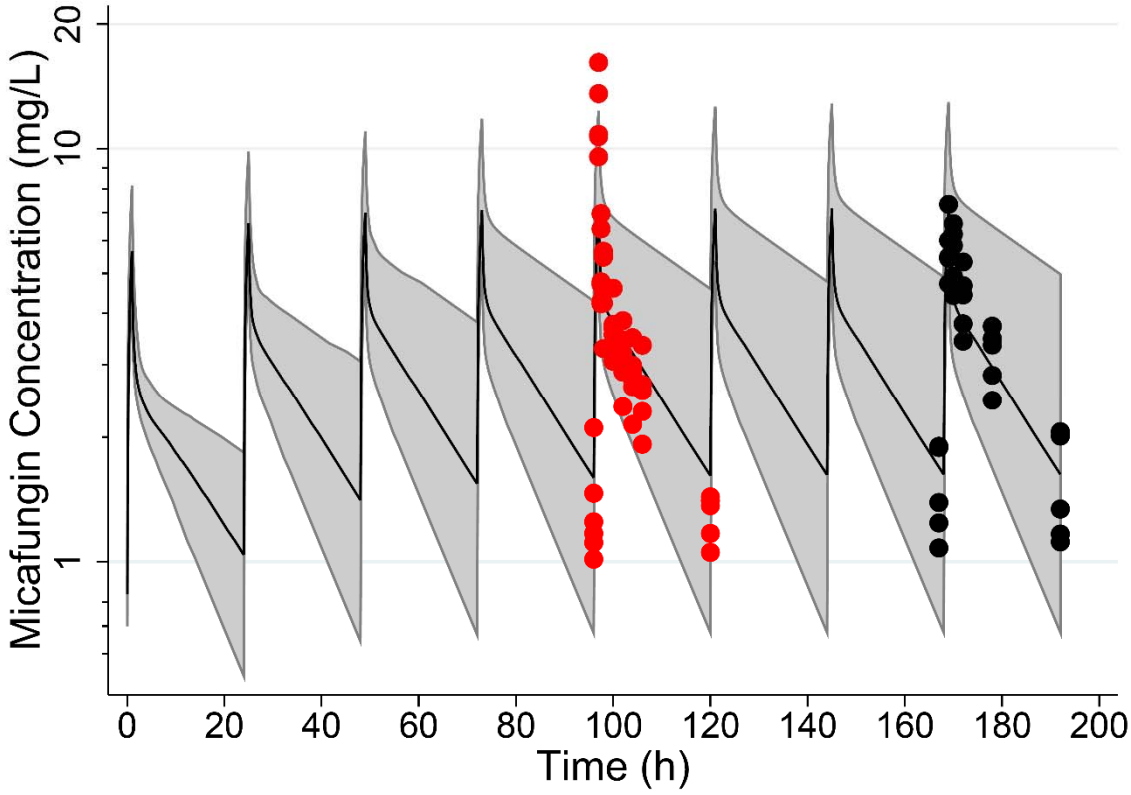

Figure 6.7. Pediatric PBPK Model predictions versus observed data for infants (0-2y). PBPK model predictions for a dose of 1 mg/kg versus dose-normalized observed mean concentrations from infants 0-2y included in the Pediatric Validation Datasets. Solid black line represents the median predicted concentration; grey shaded area represents the 90% prediction interval; symbols represent observed data for Benjamin et al.[38] (•; mean +/- 90% confidence interval) are represented by and for Undre et al.[39] (•; mean).Inset shows first 14 hours; initial concentration from Undre et al over-predicted.

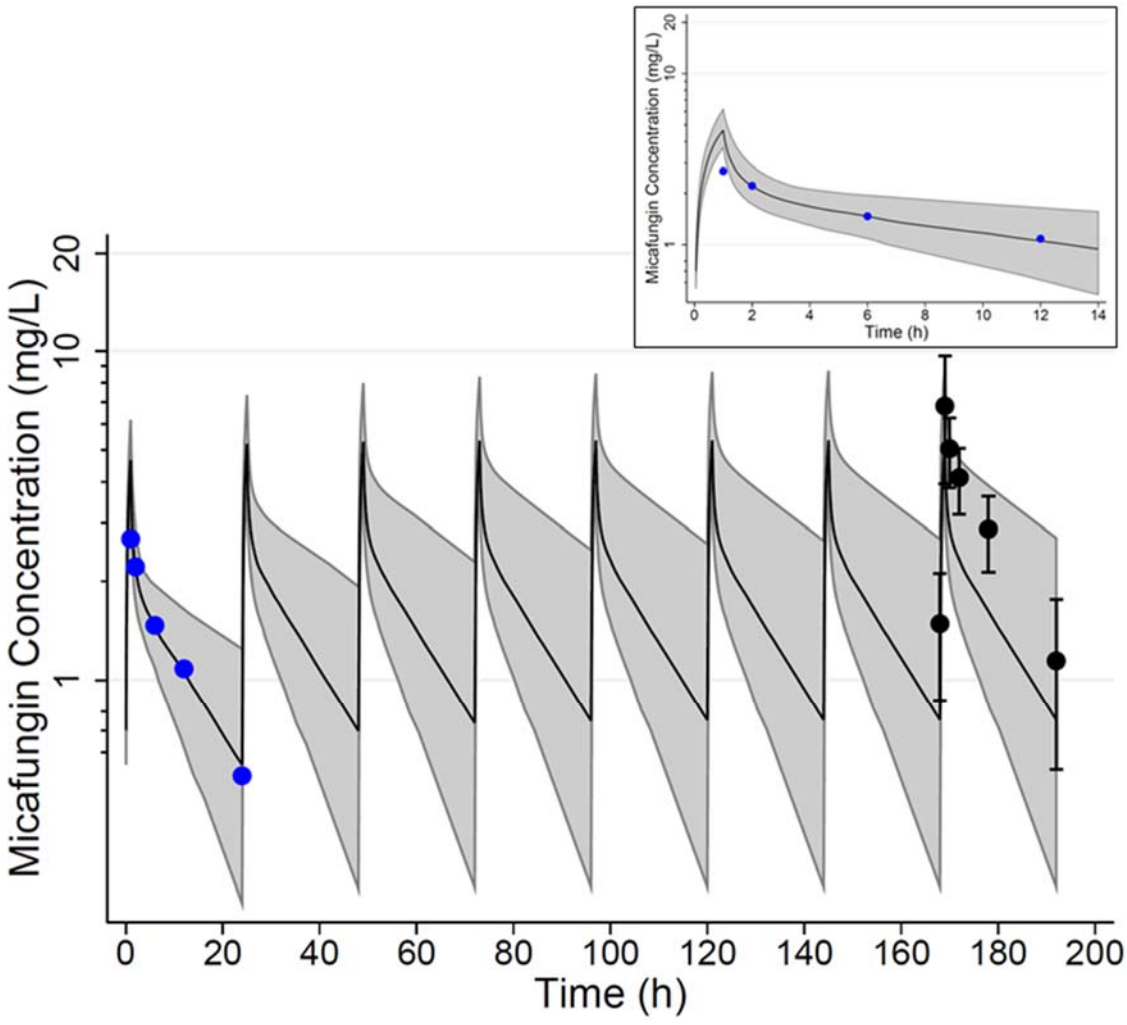

Figure 6.8. ECMO PBPK Model development. Model predictions and observed data from infants on ECMO following a single dose of 4 mg/kg. Solid black line represents the median predicted concentration; grey shaded area represents the 90% prediction interval; observed data from each patient is represented by a unique color. PBPK-predicted $AUC_{0\text{-}24}$ shown below each plot.

1. Base PBPK model: Pediatric PBPK Model predictions versus observed concentrations in infants on ECMO

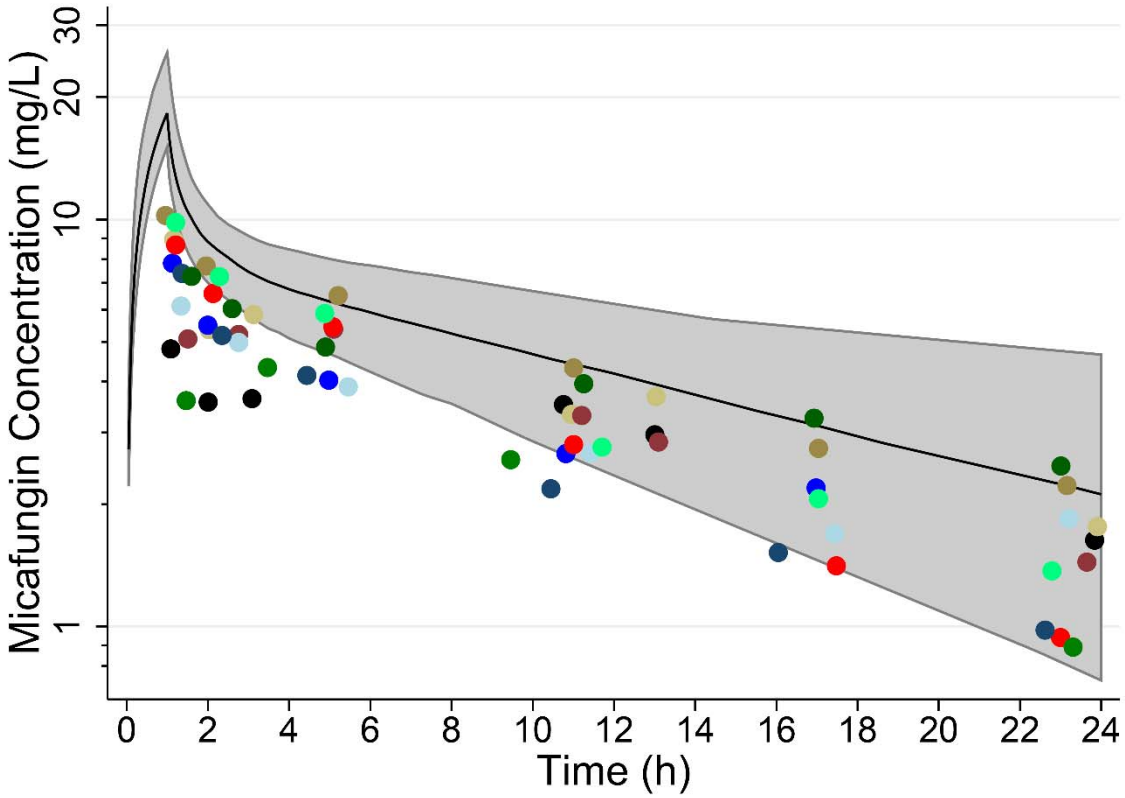

$AUC_{0\text{-}24}$ 117 mg*h/L

2. Addition of ECMO compartment to the Pediatric PBPK Model

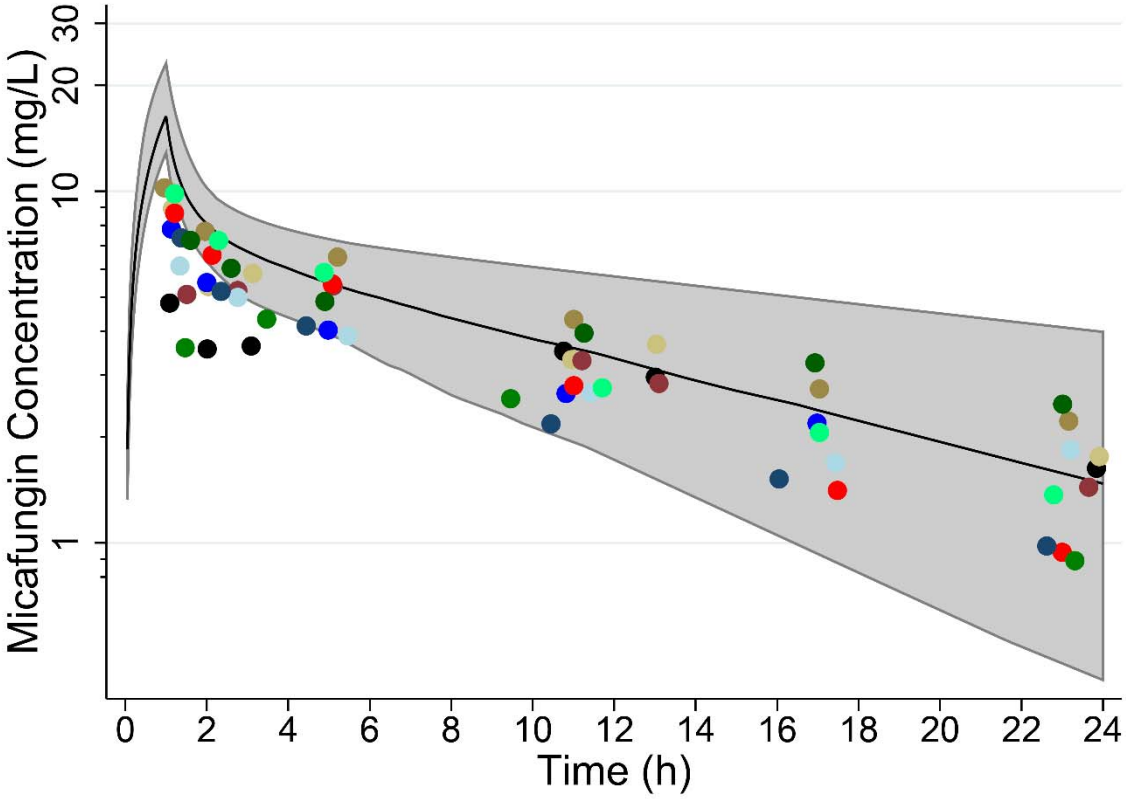

$AUC_{0\text{-}24}$ 97 mg*h/L

3. Addition of the ECMO compartment and incorporation of Edema to the Pediatric PBPK Model to form final ECMO PBPK Model

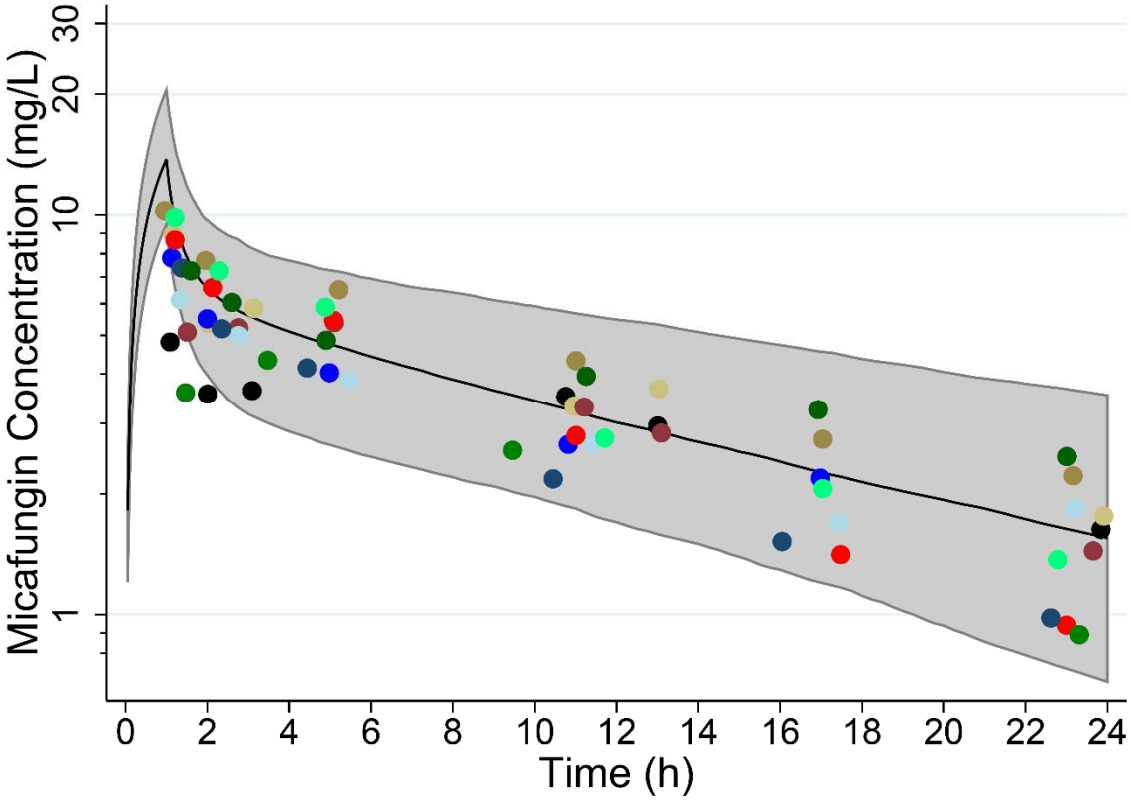

$AUC_{0\text{-}24}$ 86 mg*h/L

Figure 6.9. ECMO PBPK Model-predicted versus observed micafungin AUC_{0-24} in infants on ECMO after a dose of 4 mg/kg. Solid black horizontal line is median, box represents interquartile range and whiskers are 90% confidence interval. Dashed blue horizontal line represents target AUC_{0-24}. Median AUC_{0-24} and percentage of children achieving target AUC_{0-24} shown below each plot.

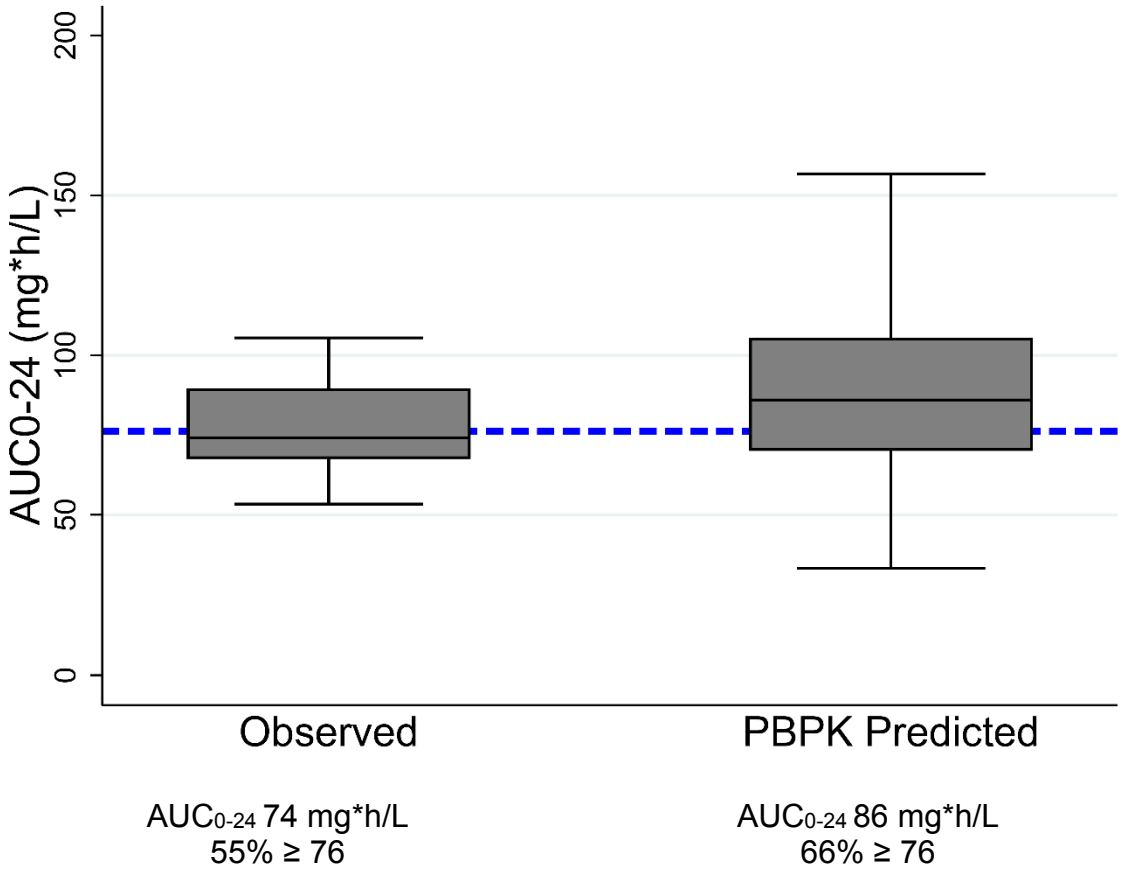

Figure 6.10. ECMO PBPK Model-predicted optimized micafungin dosing and exposure in children on ECMO across the pediatric age spectrum. Solid line represents the median, box represents interquartile range, and whiskers represent 90% prediction interval. Dosing achieved the target $AUC_{0\text{-}24}$ (>75 mg*h/L, blue dashed line) in ≥ 90% of simulated children on ECMO in the first 24 hours of therapy.

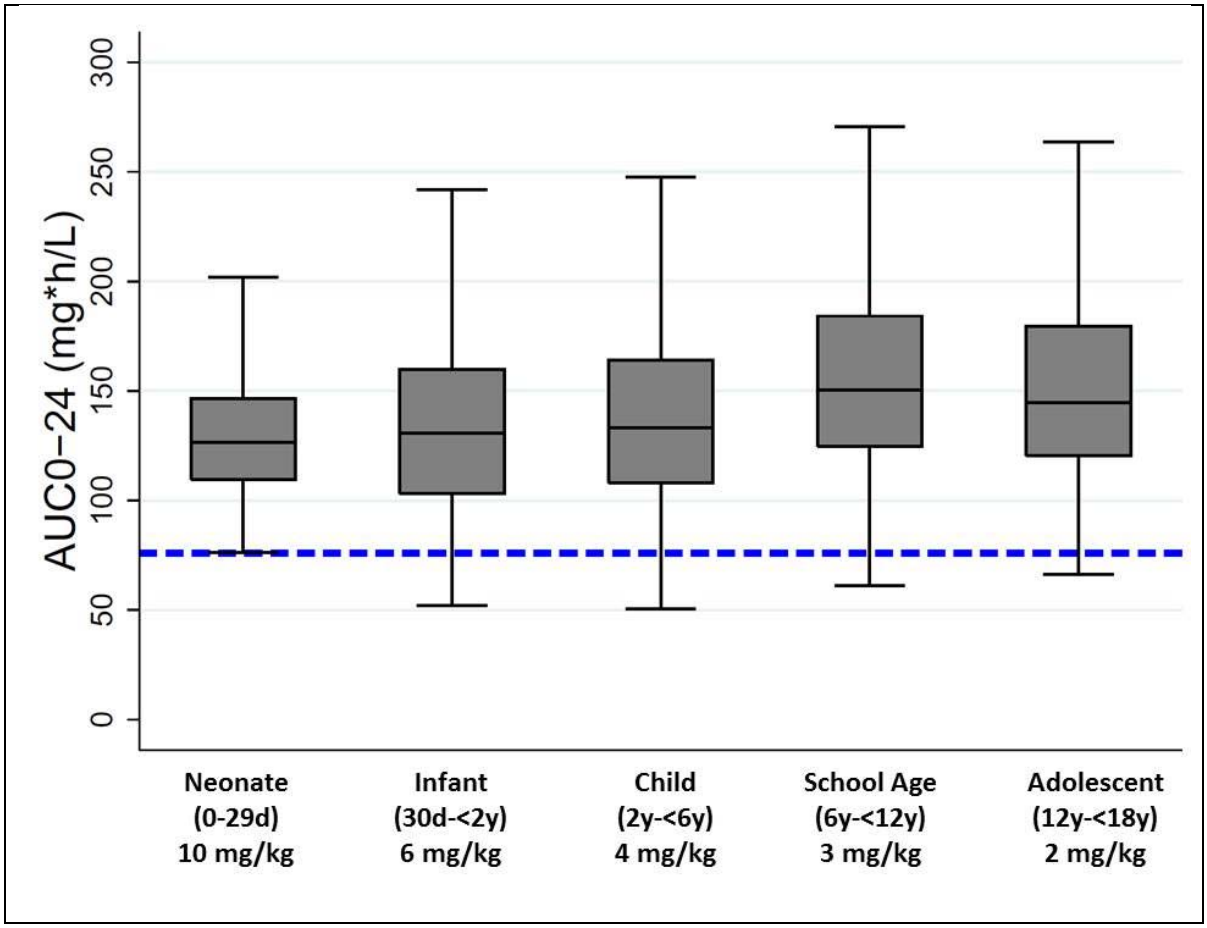

Figure 6.11. ECMO PBPK Model-predicted micafungin exposure in children on ECMO across the pediatric age spectrum. Solid line represents the median, box represents interquartile range, and whiskers represent 90% prediction interval. Dosing achieved the target $AUC_{0\text{-}24}$ (>75 mg*h/L, blue dashed line) in 100% of simulated children on ECMO in the first 24 hours of therapy.

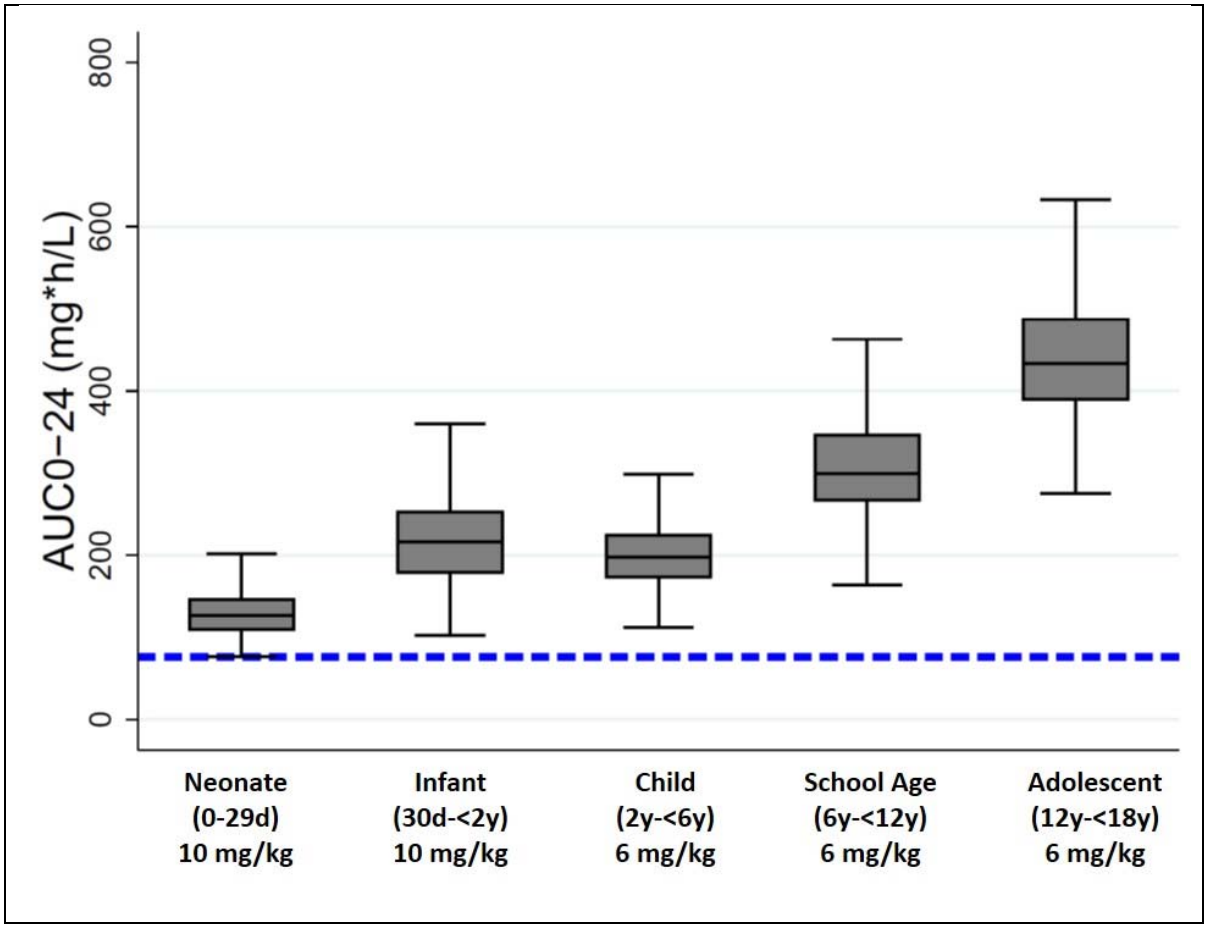

REFERENCES

1. Ernst EJ. Investigational antifungal agents. Pharmacotherapy 2001;21:165S-74S.

2. Walsh TJ, Viviani MA, Arathoon E, et al. New targets and delivery systems for antifungal therapy. Medical mycology : official publication of the International Society for Human and Animal Mycology 2000;38 Suppl 1:335-47.

3. Ikeda F, Wakai Y, Matsumoto S, et al. Efficacy of FK463, a new lipopeptide antifungal agent, in mouse models of disseminated candidiasis and aspergillosis. Antimicrob Agents Chemother 2000;44:614-8.

4. Kaneko Y, Ohno H, Fukazawa H, et al. Anti-Candida-biofilm activity of micafungin is attenuated by voriconazole but restored by pharmacological inhibition of Hsp90-related stress responses. Medical mycology : official publication of the International Society for Human and Animal Mycology 2010;48:606-12.

5. Tawara S, Ikeda F, Maki K, et al. In vitro activities of a new lipopeptide antifungal agent, FK463, against a variety of clinically important fungi. Antimicrob Agents Chemother 2000;44:57-62.

6. EMA. Assessment Report for Mycamine. In: European Medicines Agency CfMPfHU, ed. London; 2008.

7. Yanni SB, Augustijns PF, Benjamin DK, Jr., Brouwer KL, Thakker DR, Annaert PP. In vitro investigation of the hepatobiliary disposition mechanisms of the antifungal agent micafungin in humans and rats. Drug metabolism and disposition: the biological fate of chemicals 2010;38:1848-56.

8. TGA. Australian Public Assessment Report for Micafungin (as sodium). In: Department of Health and Ageing TGA, ed. Woden ACT; 2013.

9. Fujisawa. Micafungin (FK463) Investigator Brochure. In. Deerfield, IL: Fujisawa Healthcare; 2004.

10. Sandhu P, Lee W, Xu X, et al. Hepatic uptake of the novel antifungal agent caspofungin. Drug metabolism and disposition: the biological fate of chemicals 2005;33:676-82.

11. Stone JA, Xu X, Winchell GA, et al. Disposition of caspofungin: role of distribution in determining pharmacokinetics in plasma. Antimicrob Agents Chemother 2004;48:815-23.

12. Xu X, deLuna F, Cartwright M, et al. A two-step process for the hepatic uptake of L-743,872 in rats: an initial rapid adsorption on the cell surface followed by a slow transport across the cell membrane. Pharmaceutical Research 1996;13:Abstr. S454.

13. Rodgers T, Rowland M. Physiologically based pharmacokinetic modelling 2: predicting the tissue distribution of acids, very weak bases, neutrals and zwitterions. J Pharm Sci 2006;95:1238-57.

14. Rodgers T, Rowland M. Mechanistic approaches to volume of distribution predictions: understanding the processes. Pharm Res 2007;24:918-33.

15. Leong R, Vieira ML, Zhao P, et al. Regulatory experience with physiologically based pharmacokinetic modeling for pediatric drug trials. Clin Pharmacol Ther 2012;91:926-31.

16. Edginton AN, Schmitt W, Willmann S. Development and evaluation of a generic physiologically based pharmacokinetic model for children. Clin Pharmacokinet 2006;45:1013-34.

17. Johnson TN, Rostami-Hodjegan A, Tucker GT. Prediction of the clearance of eleven drugs and associated variability in neonates, infants and children. Clin Pharmacokinet 2006;45:931-56.

18. Statistics NCfH. Third National Health and Nutrition Examination Survey (NHANES III). In. Hyattsville, MD; 1997.

19. ICRP. Basic Anatomical and Physiological Data for Use in Radiological Protection Reference Values. Annals of the International Commission on Radiological Protection 2002;32.

20. Hiemenz J, Cagnoni P, Simpson D, et al. Pharmacokinetic and maximum tolerated dose study of micafungin in combination with fluconazole versus fluconazole alone for prophylaxis of fungal infections in adult patients undergoing a bone marrow or peripheral stem cell transplant. Antimicrob Agents Chemother 2005;49:1331-6.

21. Keirns J, Sawamoto T, Holum M, Buell D, Wisemandle W, Alak A. Steady-state pharmacokinetics of micafungin and voriconazole after separate and concomitant dosing in healthy adults. Antimicrob Agents Chemother 2007;51:787-90.

22. Undre NA, Stevenson P, Wilbraham D. Pharmacokinetic profile of micafungin when co-administered with amphotericin B in healthy male subjects. International journal of clinical pharmacology and therapeutics 2014;52:237-44.

23. Abe F, Ueyama J, Kawasumi N, et al. Role of plasma proteins in pharmacokinetics of micafungin, an antifungal antibiotic, in analbuminemic rats. Antimicrob Agents Chemother 2008;52:3454-6.

24. Watanabe T, Kusuhara H, Maeda K, Shitara Y, Sugiyama Y. Physiologically based pharmacokinetic modeling to predict transporter-mediated clearance and distribution of pravastatin in humans. J Pharmacol Exp Ther 2009;328:652-62.

25. Stader F, Wuerthwein G, Groll AH, Vehreschild JJ, Cornely OA, Hempel G. Physiology-based pharmacokinetics of caspofungin for adults and paediatrics. Pharm Res 2015;32:2029-37.

26. Obach RS, Baxter JG, Liston TE, et al. The prediction of human pharmacokinetic parameters from preclinical and in vitro metabolism data. J Pharmacol Exp Ther 1997;283:46-58.

27. Lagarias JC, Reeds JA, Wright MH, Wright PE. Convergence Properties of the Nelder-Mead Simplex Method in Low Dimensions. SIAM Journal of Optimization 1998;9:112-47.

28. Willmann S, Hohn K, Edginton A, et al. Development of a physiology-based whole-body population model for assessing the influence of individual variability on the pharmacokinetics of drugs. J Pharmacokinet Pharmacodyn 2007;34:401-31.

29. Edginton AN, Schmitt W, Voith B, Willmann S. A mechanistic approach for the scaling of clearance in children. Clin Pharmacokinet 2006;45:683-704.

30. Rhodin MM, Anderson BJ, Peters AM, et al. Human renal function maturation: a quantitative description using weight and postmenstrual age. Pediatr Nephrol 2009;24:67-76.

31. McNamara PJ, Alcorn J. Protein binding predictions in infants. AAPS pharmSci 2002;4:E4.

32. Anderson HL, 3rd, Coran AG, Drongowski RA, Ha HJ, Bartlett RH. Extracellular fluid and total body water changes in neonates undergoing extracorporeal membrane oxygenation. J Pediatr Surg 1992;27:1003-7; discussion 7-8.

33. Vrancken SL, Heijst AF, Zegers M, et al. Influence of volume replacement with colloids versus crystalloids in neonates on venoarterial extracorporeal membrane oxygenation on fluid retention, fluid balance, and ECMO runtime. ASAIO J 2005;51:808-12.

34. Hope WW, Kaibara A, Roy M, et al. Population pharmacokinetics of micafungin and its metabolites M1 and M5 in children and adolescents. Antimicrob Agents Chemother 2015;59:905-13.

35. Seibel NL, Schwartz C, Arrieta A, et al. Safety, tolerability, and pharmacokinetics of Micafungin (FK463) in febrile neutropenic pediatric patients. Antimicrob Agents Chemother 2005;49:3317-24.

36. Kuse ER, Chetchotisakd P, da Cunha CA, et al. Micafungin versus liposomal amphotericin B for candidaemia and invasive candidosis: a phase III randomised double-blind trial. Lancet 2007;369:1519-27.

37. Smith PB, Walsh TJ, Hope W, et al. Pharmacokinetics of an elevated dosage of micafungin in premature neonates. Pediatr Infect Dis J 2009;28:412-5.

38. Benjamin DK, Jr., Deville JG, Azie N, et al. Safety and pharmacokinetic profiles of repeated-dose micafungin in children and adolescents treated for invasive candidiasis. Pediatr Infect Dis J 2013;32:e419-25.

39. Undre NAP, P. Stevenson, PhD, A. Freire, MD, and A. Arrieta, MD. Pharmacokinetics of Micafungin in Pediatric Patients with Invasive Candidiasis and Candidemia. In. Staines, Middlesex: Astellas Pharma Europe Ltd.; 2012.

40. Tsamandouras N, Rostami-Hodjegan A, Aarons L. Combining the 'bottom up' and 'top down' approaches in pharmacokinetic modelling: fitting PBPK models to observed clinical data. Br J Clin Pharmacol 2015;79:48-55.

41. van den Anker JN, Schoemaker RC, Hop WC, et al. Ceftazidime pharmacokinetics in preterm infants: effects of renal function and gestational age. Clin Pharmacol Ther 1995;58:650-9.

42. Arant BS, Jr. Developmental patterns of renal functional maturation compared in the human neonate. J Pediatr 1978;92:705-12.

43. Kearns GL, Abdel-Rahman SM, Alander SW, Blowey DL, Leeder JS, Kauffman RE. Developmental pharmacology--drug disposition, action, and therapy in infants and children. N Engl J Med 2003;349:1157-67.

44. Hope WW, Smith PB, Arrieta A, et al. Population pharmacokinetics of micafungin in neonates and young infants. Antimicrob Agents Chemother 2010;54:2633-7.

45. Yanni SB, Smith PB, Benjamin DK, Jr., Augustijns PF, Thakker DR, Annaert PP. Higher clearance of micafungin in neonates compared with adults: role of age-dependent micafungin serum binding. Biopharmaceutics & drug disposition 2011;32:222-32.

46. Pappas PG, Kauffman CA, Andes D, et al. Clinical practice guidelines for the management of candidiasis: 2009 update by the Infectious Diseases Society of America. Clin Infect Dis 2009;48:503-35.

47. Benjamin DK, Jr., Smith PB, Arrieta A, et al. Safety and pharmacokinetics of repeat-dose micafungin in young infants. Clin Pharmacol Ther 2010;87:93-9.

48. Guembe M, Guinea J, Marcos-Zambrano LJ, et al. Micafungin at physiological serum concentrations shows antifungal activity against Candida albicans and Candida parapsilosis biofilms. Antimicrob Agents Chemother 2014;58:5581-4.

49. Wishart DS, Knox C, Guo AC, et al. DrugBank: a comprehensive resource for in silico drug discovery and exploration. Nucleic Acids Res 2006;34:D668-72.

50. Autmizguine J, Hornik CP, Jr. BD, et al. Pharmacokinetics and safety of micafungin in infants supported with extracorporeal membrane oxygenation (ECMO). Pediatric Infectious Disease Journal 2016;Accepted for publication.

CHAPTER 7. SUMMARY AND FUTURE DIRECTIONS

Extracorporeal membrane oxygenation (ECMO) is used to support cardiorespiratory failure in critically ill infants, children, and increasingly, in adults. In these vulnerable populations, the effect of ECMO on drug disposition leaves clinicians with uncertainty about dosing. Historically, drug dosing on ECMO was determined with dedicated pharmacokinetics (PK) trials in patients supported with ECMO, and based on these trials, dosing recommendations for some antibiotics and sedatives were adjusted.[1-3] However, there are three limitations to this approach. First, the effect of ECMO on exposure is drug specific, necessitating a trial for each drug of interest.[4] Second, the impact of ECMO can vary by age of the patient.[5] Most ECMO PK trials were done in infants; and it is unclear whether the results can be extrapolated to older children and adults. Third, ECMO technology changes over time, and with it, the impact on drug disposition.[6] Given the differences reported in drug extraction between older components (e.g., silicone membrane oxygenators) and newer technology (e.g., polymethylepentane hollow-fiber oxygenators), it is unknown whether dosing recommendations derived from trials using the older technology can be extrapolated to patients supported with modern ECMO circuits. In order to better understand circuit-drug interactions, multiple *ex vivo* studies of drug extraction in isolated ECMO circuits have been performed. These studies allow quantification of drug extraction, and have resulted in general recommendations.[4,7-9]

However, the ability to directly translate results from ECMO *ex vivo* experiments into dosing recommendations has been challenging. Until recently, ECMO PK studies and *ex vivo* experiments lacked a systematic approach. The ECMO PK project initiated in 2013 attempted to address this problem through an approach that combined *ex vivo* studies with PK trials and population PK analyses for commonly used drugs.[10] This approach will provide greater insight into the mechanism of drug extraction and should determine dosing for the targeted drugs. However, the number of drugs proposed for study (n=19) makes it unlikely that mechanisms causing drug interaction with the circuit will be determined. Further, the work with fluconazole in this dissertation shows the limitations of population PK analysis in the ECMO system. Based on the fluconazole population PK analysis of the Fluconazole ECMO Trial (n=40, 88% were infants) and the ECMO *ex vivo* experiments with fluconazole, the effect of ECMO on volume of distribution and clearance was quantified. There is confidence in the dosing recommendations submitted to the FDA for fluconazole in infants on ECMO. There is less confidence in how to dose in children and adults. As new ECMO circuit equipment evolves, it is unknown whether the dosing recommendations will still be valid.

The research described in this dissertation used an alternative approach that translated ECMO *ex vivo* results to bedside dosing recommendations using Physiologically Based Pharmacokinetic (PBPK) modeling. Studies focused on antifungal drugs in children on ECMO because invasive candidiasis is common, and often fatal, in this population.[11,12] *Candida* infections are difficult to treat on ECMO due to the organism's ability to form biofilms on the ECMO cannulas that connect the

child to the ECMO circuit. Thus, treatment relies on optimal antifungal dosing. To determine optimal dosing, the impact of the ECMO circuit on antifungal disposition was first assessed in isolation through *ex vivo* studies. Then, PBPK models for fluconazole and micafungin were developed in adults and scaled to children. Finally, the ECMO circuit was incorporated as a virtual organ into the PBPK models to predict dosing in this population. The PBPK models were evaluated with prospective clinical trials of fluconazole and micafungin in children on ECMO. Fluconazole and micafungin were chosen because they are used commonly to treat candidiasis in children on ECMO, and they have different physicochemical properties and clearance processes, which facilitated testing the generalizability of this approach.

This approach demonstrated proof of concept for an ECMO PBPK Model that was developed using existing data from the literature, scaled to special populations (e.g., children, disease), and modified to include the effects of extracorporeal support. The PBPK Model-predicted dosing in infants on ECMO was in close agreement with the dosing recommendations from the Fluconazole and Micafungin ECMO PK Trials that were generated using traditional compartmental modeling. However, the real utility of the ECMO PBPK Model is its flexibility. By including information about organ ontogeny, the PBPK models can predict dosing in populations across the pediatric age spectrum, including populations that were not studied in the trials. In addition, the PBPK models can be modified to account for different disease states to provide disease-specific dosing. This was demonstrated in the present studies by incorporation of edema into the Pediatric ECMO PBPK Model, which adequately described the data in infants on ECMO. Most importantly

for ECMO, as ECMO technology evolves, the PBPK models can be modified to reflect the impact of the new circuit components on drug disposition. More broadly, these methods can be applied to other forms of extracorporeal support such as dialysis.

As this work goes forward, a number of important questions remain unanswered. An overview of the key findings and future directions are discussed below.

Understanding ECMO circuit-drug interactions through *ex vivo* experiments (Chapter 2)

The *ex vivo* experiments in this dissertation were the first to focus on the ECMO circuit extraction of antifungals, and to isolate the circuit component responsible for extraction. At the time of study design, ECMO *ex vivo* studies had been performed for 27 drugs,[4,8,13-20] primarily antibiotics and sedatives, but only one antifungal—voriconazole.[19] During the course of this dissertation, ECMO *ex vivo* results were published for fluconazole using a circuit configuration similar to the Oxygenator Circuit in the present study.[4] Results were nearly identical in showing that fluconazole was not extracted by the ECMO circuit. In general, extraction by the circuit is driven by hydrophobic and ionic adsorption. Neither of these processes were likely to affect fluconazole because it has a neutral charge and low lipophilicity.

Similar to fluconazole, amphotericin B deoxycholate was not extracted by the circuit. Amphotericin B deoxycholate is slightly lipophilic but is a zwitterion, which may have limited its ionic adsorption by the circuit materials. However, the present

experiments only evaluated the extraction of the amphotericin B deoxycholate formulation. Further work is needed to understand whether amphotericin disposition in the ECMO circuit is different for other formulations. Several lipid-coated amphotericin formulations exist and are used commonly because they are associated with less renal toxicity.[21-26] Decreased toxicity is thought to occur because the lipid coating limits the drug's interaction with the renal tubular cells.[27] The lipid coatings are hydrophobic and, in some cases, charged. It is possible that these properties will lead to hydrophobic and/or ionic interactions resulting in adsorption by the ECMO circuit. If adsorption occurs, it is unknown whether the active drug will be removed from circulation, or if only the coating will be removed. If the coating is adsorbed but the active drug is released into plasma, it is possible that the renal-protective effects of lipid formulations will be negated. The current *ex vivo* experimental design can be used in future studies to determine whether overall exposure of amphotericin is decreased. However, in order to determine the differential impact on renal toxicity, ECMO animal studies would be necessary.

Micafungin interacted with the ECMO circuit in both a time- and albumin concentration-dependent manner. Micafungin extraction was substantial over the first four hours of the experiment in a Complete Circuit, but not in the Oxygenator or Pump Circuits, or the control samples. Further, micafungin was extracted to a greater extent when albumin concentrations were <1 g/dL. There are two possible explanations. First, because albumin is the primary protein binding partner for micafungin, low albumin concentrations led to a higher fraction of unbound drug and unbound drug was bound by the circuit. The alternative is that albumin binds to the

circuit and occupies binding sites, thereby preventing micafungin adsorption. This raises an interesting clinical question about strategies to limit binding – can preloading the circuit with albumin limit drug interactions with a circuit? The answer is that the interaction is likely drug and circuit specific, but should be explored in future studies.

While micafungin extraction during the first 4 hours was most likely due to adsorption by the hemofilter membrane, these results are in contrast to *in vivo* studies of micafungin in patients supported with continuous venovenous hemofiltration (CVVH). The CVVH studies used hemofilters of similar materials, but no significant difference in concentrations pre- and post-membrane was reported.[28,29] Further research is necessary to understand the mechanism(s) by which the hemofilter extracts micafungin. Future experiments should sample pre- and post- hemofilter in the ECMO *ex vivo* system under a variety of conditions including different flow and filtration rates. The most accurate measure would be to extract drug from the hemofilter itself. However, methods would need to be developed that could effectively displace micafungin from the hemofilter membrane and accurately quantify it under those conditions. Alternatively, a mass balance study using radiolabeled drug and imaging (e.g., gamma camera) could isolate the sites of extraction.

Micafungin is dosed clinically once every 24 hours. Therefore, it is important to understand disposition in the *ex vivo* system over an entire dosing interval. Unexpectedly, after 24 hours, all of the micafungin circuits and controls showed substantial extraction. The fact that extraction occurred in the controls suggested

one of three mechanisms: 1) slow adsorption by the materials of both the circuits and control tubes, 2) metabolism in the plasma (e.g., peptidases), or 3) drug degradation (e.g., micafungin is degraded by light[30]). Further studies are needed to understand the mechanism because both adsorption and light degradation could have important dosing implications. Adsorption can be quantified by measuring micafungin concentrations in sample tubes of different materials (e.g., polyvinylchloride versus silanized glass). The impact of plasma metabolism can be determined using different media such as whole blood versus crystalloid. Finally, the effect of light degradation can be assessed by measuring micafungin concentrations in tubes that were protected from light compared to those exposed to light. These experiments are planned and the methods currently are being refined.

Alternatively, mass balance studies with radiolabeled micafungin also can be used to answer this question. There are certain methods that make mass balance studies more challenging in ECMO (e.g., how to remove all of the blood in the ECMO circuit? Will flushing the ECMO circuit displace micafungin adsorbed to ECMO components? Is this impacted by the type of flush selected?). Mass balance studies will be more expensive because they require radiolabeled micafungin and construction of multiple ECMO circuits as opposed to inexpensive control tubes of various materials. The mass balance approach will be employed if the above control tube experiments do not explain why micafungin concentrations decreased in the control samples.

Future ECMO *ex vivo* studies should focus on two areas: 1) specific drug-circuit interactions and 2) understanding broadly how drugs interact with the circuit.

There will always be a need to conduct dedicated studies for clinically important drugs. *Ex vivo* experiments are a quick, relatively inexpensive method to quantify the extraction in a specific ECMO circuit configuration. For a given circuit configuration, knowing how much extraction occurs can help clinicians decide whether higher doses might be necessary. Further, as demonstrated in this dissertation, the extraction can be translated directly to dosing recommendations using the ECMO PBPK Model. These experiments can also help determine if the extraction is saturable and/or reversible for specific drugs. Multiple dose experiments, dosing over a range of concentrations, and conducting experiments for prolonged times can help determine the saturability and reversibility of extraction by the ECMO circuit. The latter have important dosing ramifications, and could be used to develop dosing algorithms based on the age of the circuit.

The ultimate goal of ECMO *ex vivo* research is to achieve an accurate *a priori* prediction of which drug(s) interact with different ECMO components, and to what extent. The traditional ECMO *ex vivo* system is ill-suited to answer this question. While inexpensive compared to clinical trials, each circuit can cost thousands of dollars. When perfusion experiments are conducted in triplicate with all of the different combinations of circuit components, the costs quickly become prohibitive. Based on the studies that have been conducted so far, even with the traditional ECMO *ex vivo* approach, the ability to broadly generalize is difficult. This is evidenced by the fact that over the past 40 years, less than 30 drugs have been studied in an *ex vivo* ECMO system, and there is no definitive understanding of what causes drugs to interact with the ECMO circuit, and certainly no quantitative

prediction of the extent of extraction. To accurately predict extraction by the ECMO circuit, data will need to be gathered for 100's of drugs. This argues for a high throughput system that draws on expertise from the fields of materials science and quantitative structure-activity relationship (QSAR) modeling.

There is extensive expertise and literature in the field of materials science with regard to drug sorption. Much of this literature describes the relationship between a drug and a storage container (e.g., vial, IV bag),[31-34] and models predicting this interaction between a drug and storage material have been developed.[35] Although, this approach has never been applied to ECMO, the principles remain the same. Similarly QSAR modeling uses computational methods to predict drug action based on physicochemical properties. QSAR modeling has been applied to predict drug-enzyme interactions and drug-protein binding.[36,37] If the mechanism of circuit-drug interactions is known for a sufficient number of drugs and circuit materials, the same QSAR methods should be applicable to ECMO. By using materials science to understand the mechanism(s) by which drugs interact with the ECMO circuit, and using QSAR modeling to predict the degree of interaction between a drug and a surface, ECMO researchers should be able to predict whether a drug will interact with an ECMO circuit based on the physicochemical properties of the drug and the materials of the circuit. It is unlikely that many ECMO scientists will have expertise in both fields, so future research will rely on collaboration.

Physiologically based pharmacokinetics in critically ill children (Chapters 4 and 6)

The PBPK models develop in this dissertation were the first PBPK models for fluconazole and micafungin, the first to include an extracorporeal compartment, and the first to predict the effect of edema on drug exposure. The models for both fluconazole and micafungin followed an established work flow whereby an adult PBPK model was developed first to determine the appropriate model structure using robust adult data.[38] Once there was confidence in the model structure, the adult model was scaled to children using known ontogeny of anatomy and physiology. Because dosing of both drugs is based on area under the concentration vs. time curve (AUC), performance of the models was evaluated by comparing both observed versus predicted concentrations and precision of the AUC estimates.

The fluconazole Adult PBPK Model was relatively straightforward. Fluconazole is a small molecule with distribution that is perfusion-rate limited, has minimal metabolism, and is eliminated almost exclusively by the kidneys. Extensive drug-specific data existed for fluconazole, and only a few assumptions were made that were critical to the model structure. Optimized adult model predictions versus observed data from the literature showed good agreement, and PBPK-predicted AUC estimates were within 10% of the observed AUC. The adult model was successfully scaled to children by including age-dependencies in physiological parameters. Because the Pediatric PBPK Model was scaled from healthy adults, it did not capture the variability seen in critically ill children. However, the median PBPK-predicted AUC was within 5% of observed. Successful scaling to children

likely reflects the fact that fluconazole clearance is driven primarily by glomerular filtration rate (GFR),[39] and GFR ontogeny is well described in children.[40] One of the advantages of PBPK modeling is the ability to predict drug concentrations at the site of action. There are extensive data describing fluconazole concentrations in multiple organs.[39] Future work should focus on refining the model to validate concentration predictions in sites other than the plasma. In this way, fluconazole dosing can be optimized for specific fungal infections.

The same process of PBPK model development was applied to micafungin. Micafungin plasma disposition exhibited a pronounced distribution phase, and clearance was influenced by transporter-mediated hepatic uptake and biliary excretion. Because of uncertainty in the multiple processes involved in micafungin disposition, the micafungin model included several assumptions. One of the goals of this dissertation was to develop PBPK models using existing data, and the micafungin model provided proof of concept for this approach. When the known PK processes were combined with physiologically reasonable assumptions, the Adult PBPK Model showed excellent agreement between model predictions and observed data. The assumption in scaling to children was that the parameters for which ontogeny data were limited (e.g., transporter function) were similar between adults and children. When the system specific inputs were adjusted with known ontogeny (e.g. organ weights, GFR), the pediatric PBPK model also showed excellent agreement with observed data. Concerns that optimizing certain parameters with *in vivo* data might limit generalizability were mitigated for this molecule as PBPK

predictions showed excellent agreement with several independent validation datasets.

The major focus and novel contribution of this dissertation research was inclusion of the ECMO compartment in the PBPK model. Extracorporeal devices such as ECMO are known to alter PK. This effect is drug dependent, and as noted above, not easily predicted based on physicochemical properties. The ECMO PBPK Models demonstrated that an ECMO compartment could be added to the Pediatric PBPK Model to accurately describe fluconazole and micafungin concentration versus time profiles. When the ECMO compartment was informed by the ECMO *ex vivo* experiments, the model was able to quantify the effect of ECMO on disposition of a particular drug. Because exposure to ECMO results in a profound inflammatory reaction, which leads to edema,[41-44] an edema physiologic state also was added to the ECMO model. After accounting for both circuit and disease, the ECMO PBPK Models successfully predicted exposure for both fluconazole and micafungin in infants on ECMO. Going forward it will be important to capture clinical factors that can explain alterations in PK (e.g., extent of edema, volume of transfusions) so that these parameters can be more accurately estimated in the models.

Validation of PBPK models remains an area of debate. The top-down approach (e.g., population PK) has well defined criteria for validation both in the literature and from a regulatory standpoint.[45,46] A recent meeting at the FDA discussed validation criteria for PBPK models but there was no consensus on criteria.[47] Because of the bottom-up approach, PBPK models are built on certain assumptions. If these assumptions are inaccurate, the models are vulnerable to

multiplicity of errors. In order to account for these errors, model bias can be assessed by calculating the average fold error (AFE) between predicted and observed concentrations: $AFE=10^{[1/N\Sigma log(predicted/observed)]}$.[38,48] The AFE indicates model under- (AFE<1) or over-prediction (AFE>1) when compared with observed values. Model precision can be assessed by calculating the absolute average fold error: $AAFE= 10^{[1/N\Sigma|log(predicted/observed)|]}$ for each individual curve.[48] The cutoff that is acceptable for AFE and AAFE depends on the molecule and purpose of the model. Population predictability can be assessed by generating a prediction interval (5^{th} to 95^{th} percentile) of drug concentrations for the population and quantifying the number of observed concentrations that fall outside of the prediction interval. In general, the model is acceptable if 90% of observed concentrations fall within the prediction interval, but, again, this depends on the molecule and purpose of the model.[38] However, in order to apply these approaches, it is necessary to have observed data at the individual level. Many of the datasets used to evaluate models in this dissertation were obtained from the literature and only included summary data (e.g., mean concentration +/- standard deviation). As a result, in this dissertation population predictability was evaluated by visual inspection of the observed data captured within the model's 90% prediction interval and comparing the fold error between the PBPK-predicted AUC and observed AUC.

Because the PBPK models are mechanistic and can predict dosing for any age, the ECMO PBPK Models were used to define optimal dosing regimens in children of all ages. In the future, this concept could be extended to adults. The majority of ECMO research has been focused on infants and *ex vivo* systems. With

adult ECMO programs expanding, this ECMO PBPK modeling approach can reverse the paradigm of scaling down to children, and scale up to predict optimal dosing in adults.

Modeling and simulation to support clinical trials (Chapters 3 and 5)

Modeling and simulation is a powerful tool in pediatric drug development. However, pediatric clinical drug trials remain the gold standard, and in the foreseeable future will continue to be necessary to evaluate model predictions. As part of this dissertation, two clinical PK trials of fluconazole and micafungin were performed in children on ECMO. Both of these trials were performed under Food and Drug Administration (FDA) Investigational New Drug applications so that data collected could be submitted to the FDA for consideration of amended product labeling. Dosing recommendations were derived for both drugs using traditional compartmental modeling. The dosing recommendations for fluconazole were submitted to the FDA in 2015 and currently are under review. The time from initial study design to FDA submission was more than 5 years, and there remains a concern that if ECMO technology changes, the submitted dosing recommendations may no longer be valid. Dosing recommendations for micafungin will be submitted to the FDA in 2016 but face the same challenges. These challenges were the impetus for the PBPK methodology developed in this dissertation.

Going forward, the ECMO PBPK modeling approach will be used to develop dosing recommendations focusing on drugs that are prioritized by the Best

Pharmaceuticals for Children Act (BPCA).[49] Dosing recommendations will need to be evaluated using PK data from children for the drugs of interest. The NIH-sponsored Pediatric Trials Network supports an opportunistic PK study in children, whereby PK samples are collected for BPCA-prioritized drugs that are prescribed per standard of care to certain target populations. One target population is children on ECMO. Currently, 279 PK samples from 148 children for 20 drugs have been collected and enrollment is ongoing. The ECMO PBPK modeling approach can be used to leverage these data to develop optimal dosing recommendations for patients on ECMO, and label changes for dosing, if needed.

PBPK modeling has tremendous potential beyond ECMO to understand drug disposition and to predict dosing in children. In children, PBPK models have been used to scale adult data to children. If scaling a validated adult model fails to accurately describe the observed pediatric data, this suggests that a mechanism regulating drug disposition is either missing or inaccurately described. Knowing where model inaccuracies affect PK (e.g., clearance) can point to future studies to elucidate the mechanism. PBPK models also hold potential to extrapolate from animals to humans. For example, most of the studies on transporter ontogeny come from developmental studies in animals. Relevant tissue samples are hard to obtain in children, and even when tissue is available, multiple confounders (e.g., disease state, tissue handling) can limit generalizability. Studies in developing animals allow for more control but it is frequently unknown whether the ontogeny determined in animals directly translates to children. PBPK provides a tool to explore those relationships.

For these reasons, PBPK models are recommended increasingly by regulators for pediatric drug development.[50] Both the European Medicines Agency and Office of Clinical Pharmacology at the FDA have seen an increase in pediatric development plans incorporating PBPK modeling.[51,52] Regulator's from the FDA's Office of Clinical Pharmacology published a summary of the regulatory experience with PBPK modeling for pediatric drug development detailing the potential advantages, but also noting the current weaknesses.[53] In general, the authors list several of the advantages noted in this dissertation. PBPK modeling can facilitate optimal trial design by determining optimal sample times and decreasing the number of children needed to have confidence in model predictions. PBPK models can be scaled from animals to humans as mentioned above, although this approach is primarily applicable in early phases of drug development when limited data exist in humans. PBPK-PD models can leverage the burgeoning field of pediatric biomarkers by linking mechanisms of drug disposition with surrogate markers of effect. In order to facilitate submission of PBPK models to support pediatric drug development, the FDA has published a pediatric decision tree that describes the required clinical studies, criteria for extrapolation, and the number of children required in clinical trials.[53-55]

However, PBPK models have important limitations, primarily the lack of data to inform PBPK models, particularly in infants and neonates.[53] In order to successfully scale to children, the PBPK models must be informed by data describing the ontogeny of relevant anatomic and physiologic processes. Anatomic data (e.g., organ weights) are available from large databases;[56,57] and ontogeny for

GFR and common metabolizing enzymes (e.g., CYP3A4) are described reasonably well in the literature.[40,58] However, huge knowledge gaps remain about the ontogeny of non-CYP enzymes and drug transporters. In the recent Pediatric Transporter White Paper, the Pediatric Transporter Working Group outlines these knowledge gaps, and proposes methods to determine transporter ontogeny.[59] As these gaps are filled, PBPK models will be better able to capture the developmental changes affecting drug absorption, distribution, metabolism, and elimination.

The pediatric intensive care unit (PICU) provides unique resources for the study of age- and disease-related changes in expression and function of drug metabolizing enzymes and membrane transporters. These children tend to have invasive lines and tubes that mitigate the sample collection challenges common in pediatric trials. In addition to easy collection of blood samples, duodenal and jejunal feeding tubes are common and allow for collection of bile. Many children in the PICU also will have urinary catheters that make collection of 24 hour urine specimens straightforward. Further many of the established probe substrates (e.g., CYP3A4-midazolam) are prescribed per standard of care. There remains a large body of foundational work that needs to be done (e.g. bile acid profiling in different disease states). However, more exciting are studies such as that by Ferslew and Brouwer of the disease effects on drug disposition.[60] They identified a disease state (non-alcoholic steatohepatitis) associated with a known alteration in transporter function and compared the PK and bile acid profiles between healthy and diseased subjects. Such studies could be easily translated to the PICU to assess the functional changes of transporters and drug metabolizing enzymes in different disease states.

In conclusion, this dissertation was the first to establish antifungal dosing recommendations for children on ECMO. The dosing recommendations from this research have been, or will be, submitted to the FDA for inclusion in the label, and were incorporated in antifungal dosing guidelines for children on ECMO.[61] Although determining optimal dosing for these two commonly used drugs in children on ECMO was important, more importantly, the PBPK modeling developed in this dissertation demonstrated the utility of this approach to understand and quantify the physiologic alterations driving drug disposition in critically ill children. The modeling will also provide the necessary construct for using data from PBPK modeling to support dosing recommendations and inform study design for future PK trials. A more precise, refined, integrated approach for drug dosing in this pediatric sub-population will improve both the safety and efficacy of drug therapy in critically ill children supported.

REFERENCES

1. Amaker RD, DiPiro JT, Bhatia J. Pharmacokinetics of vancomycin in critically ill infants undergoing extracorporeal membrane oxygenation. Antimicrob Agents Chemother 1996;40:1139-42.

2. Cohen P, Collart L, Prober CG, Fischer AF, Blaschke TF. Gentamicin pharmacokinetics in neonates undergoing extracorporal membrane oxygenation. Pediatr Infect Dis J 1990;9:562-6.

3. Dagan O, Klein J, Bohn D, Koren G. Effects of extracorporeal membrane oxygenation on morphine pharmacokinetics in infants. Crit Care Med 1994;22:1099-101.

4. Shekar K, Roberts JA, McDonald CI, et al. Protein-bound drugs are prone to sequestration in the extracorporeal membrane oxygenation circuit: results from an ex vivo study. Crit Care 2015;19:164.

5. Watt KM, Gonzalez D, Benjamin DK, Jr., et al. Fluconazole population pharmacokinetics and dosing for prevention and treatment of invasive Candidiasis in children supported with extracorporeal membrane oxygenation. Antimicrob Agents Chemother 2015;59:3935-43.

6. Wildschut ED, Ahsman MJ, Allegaert K, Mathot RA, Tibboel D. Determinants of drug absorption in different ECMO circuits. Intensive Care Med 2010;36:2109-16.

7. DeBerry BB, Lynch JE, Chernin JM, Zwischenberger JB, Chung DH. A survey for pain and sedation medications in pediatric patients during extracorporeal membrane oxygenation. Perfusion 2005;20:139-43.

8. Shekar K, Roberts JA, McDonald CI, et al. Sequestration of drugs in the circuit may lead to therapeutic failure during extracorporeal membrane oxygenation. Crit Care 2012;16:R194.

9. Shekar K, Roberts JA, Mullany DV, et al. Increased sedation requirements in patients receiving extracorporeal membrane oxygenation for respiratory and cardiorespiratory failure. Anaesthesia and intensive care 2012;40:648-55.

10. Shekar K, Roberts JA, Smith MT, Fung YL, Fraser JF. The ECMO PK Project: an incremental research approach to advance understanding of the pharmacokinetic alterations and improve patient outcomes during extracorporeal membrane oxygenation. BMC anesthesiology 2013;13:7.

11. Bizzarro MJ, Conrad SA, Kaufman DA, Rycus P. Infections acquired during extracorporeal membrane oxygenation in neonates, children, and adults. Pediatr Crit Care Med 2010.

12. Gardner AH, Prodhan P, Stovall SH, et al. Fungal infections and antifungal prophylaxis in pediatric cardiac extracorporeal life support. J Thorac Cardiovasc Surg 2011.

13. Dagan O, Klein J, Gruenwald C, Bohn D, Barker G, Koren G. Preliminary studies of the effects of extracorporeal membrane oxygenator on the disposition of common pediatric drugs. Ther Drug Monit 1993;15:263-6.

14. Rosen DA, Rosen KR, Silvasi DL. In vitro variability in fentanyl absorption by different membrane oxygenators. J Cardiothorac Anesth 1990;4:332-5.

15. Preston TJ, Hodge AB, Riley JB, Leib-Sargel C, Nicol KK. In vitro drug adsorption and plasma free hemoglobin levels associated with hollow fiber oxygenators in the extracorporeal life support (ECLS) circuit. The journal of extra-corporeal technology 2007;39:234-7.

16. Preston TJ, Ratliff TM, Gomez D, et al. Modified surface coatings and their effect on drug adsorption within the extracorporeal life support circuit. The journal of extra-corporeal technology 2010;42:199-202.

17. Mulla H, Lawson G, von Anrep C, et al. In vitro evaluation of sedative drug losses during extracorporeal membrane oxygenation. Perfusion 2000;15:21-6.

18. Harthan AA, Buckley KW, Heger ML, Fortuna RS, Mays K. Medication adsorption into contemporary extracorporeal membrane oxygenator circuits. The journal of pediatric pharmacology and therapeutics : JPPT : the official journal of PPAG 2014;19:288-95.

19. Mehta NM, Halwick DR, Dodson BL, Thompson JE, Arnold JH. Potential drug sequestration during extracorporeal membrane oxygenation: results from an ex vivo experiment. Intensive Care Med 2007;33:1018-24.

20. Lemaitre F, Hasni N, Leprince P, et al. Propofol, midazolam, vancomycin and cyclosporine therapeutic drug monitoring in extracorporeal membrane oxygenation circuits primed with whole human blood. Crit Care 2015;19:40.

21. White MH, Bowden RA, Sandler ES, et al. Randomized, double-blind clinical trial of amphotericin B colloidal dispersion vs. amphotericin B in the empirical treatment of fever and neutropenia. Clin Infect Dis 1998;27:296-302.

22. Walsh TJ, Finberg RW, Arndt C, et al. Liposomal amphotericin B for empirical therapy in patients with persistent fever and neutropenia. National Institute of Allergy and Infectious Diseases Mycoses Study Group. N Engl J Med 1999;340:764-71.

23. Prentice HG, Hann IM, Herbrecht R, et al. A randomized comparison of liposomal versus conventional amphotericin B for the treatment of pyrexia of unknown origin in neutropenic patients. British journal of haematology 1997;98:711-8.

24. Leenders AC, Daenen S, Jansen RL, et al. Liposomal amphotericin B compared with amphotericin B deoxycholate in the treatment of documented and suspected neutropenia-associated invasive fungal infections. British journal of haematology 1998;103:205-12.

25. Sharkey PK, Graybill JR, Johnson ES, et al. Amphotericin B lipid complex compared with amphotericin B in the treatment of cryptococcal meningitis in patients with AIDS. Clin Infect Dis 1996;22:315-21.

26. Sorkine P, Nagar H, Weinbroum A, et al. Administration of amphotericin B in lipid emulsion decreases nephrotoxicity: results of a prospective, randomized, controlled study in critically ill patients. Crit Care Med 1996;24:1311-5.

27. Wasan KM, Morton RE, Rosenblum MG, Lopez-Berestein G. Decreased toxicity of liposomal amphotericin B due to association of amphotericin B with high-density lipoproteins: role of lipid transfer protein. J Pharm Sci 1994;83:1006-10.

28. Hirata K, Aoyama T, Matsumoto Y, et al. Pharmacokinetics of antifungal agent micafungin in critically ill patients receiving continuous hemodialysis filtration. Yakugaku zasshi : Journal of the Pharmaceutical Society of Japan 2007;127:897-901.

29. Maseda E, Grau S, Villagran MJ, et al. Micafungin pharmacokinetic/pharmacodynamic adequacy for the treatment of invasive candidiasis in critically ill patients on continuous venovenous haemofiltration. J Antimicrob Chemother 2014;69:1624-32.

30. FDA. MYCAMINE (micafungin sodium) For Injection Product Label. In: U.S. Dept. of Health and Human Services FaDA, ed.: Astellas Pharma US, Inc.; 2013.

31. De Rudder D, Remon JP, Neyt EN. The sorption of nitroglycerin by infusion sets. The Journal of pharmacy and pharmacology 1987;39:556-8.

32. Grillo JA, Gonzalez ER, Ramaiya A, Karnes HT, Wells B. Chemical compatibility of inotropic and vasoactive agents delivered via a multiple line infusion system. Crit Care Med 1995;23:1061-6.

33. Lee MG. Sorption of four drugs to polyvinyl chloride and polybutadiene intravenous administration sets. Am J Hosp Pharm 1986;43:1945-50.

34. Martens HJ, De Goede PN, Van Loenen AC. Sorption of various drugs in polyvinyl chloride, glass, and polyethylene-lined infusion containers. Am J Hosp Pharm 1990;47:369-73.

35. Jenke DR. Modeling of solute sorption by polyvinyl chloride plastic infusion bags. J Pharm Sci 1993;82:1134-9.

36. Kirchmair J, Williamson MJ, Tyzack JD, et al. Computational prediction of metabolism: sites, products, SAR, P450 enzyme dynamics, and mechanisms. Journal of chemical information and modeling 2012;52:617-48.

37. Ghafourian T, Amin Z. QSAR models for the prediction of plasma protein binding. BioImpacts : BI 2013;3:21-7.

38. Edginton AN, Schmitt W, Willmann S. Development and evaluation of a generic physiologically based pharmacokinetic model for children. Clin Pharmacokinet 2006;45:1013-34.

39. FDA. Fluconazole Injection, USP Product Label. In: U.S. Dept. of Health and Human Services FaDA, ed.: Roerig, a division of Pfizer, Inc.; 2015.

40. McNamara PJ, Alcorn J. Protein binding predictions in infants. AAPS pharmSci 2002;4:E4.

41. Kozik DJ, Tweddell JS. Characterizing the inflammatory response to cardiopulmonary bypass in children. Ann Thorac Surg 2006;81:S2347-54.

42. Butler J, Pathi VL, Paton RD, et al. Acute-phase responses to cardiopulmonary bypass in children weighing less than 10 kilograms. Ann Thorac Surg 1996;62:538-42.

43. B. MR, Timpa JG, Kurundkar AR, et al. Plasma concentrations of inflammatory cytokines rise rapidly during ECMO-related SIRS due to the release of preformed stores in the intestine. Lab Invest 2010;90:128-39.

44. Anderson HL, 3rd, Coran AG, Drongowski RA, Ha HJ, Bartlett RH. Extracellular fluid and total body water changes in neonates undergoing extracorporeal membrane oxygenation. J Pediatr Surg 1992;27:1003-7; discussion 7-8.

45. FDA U. Guidance for industry population pharmacokinetics. In: (U.S.) CfDEaR, (U.S.) CfBEaR, eds. Rockville, MD: U.S. Department of Health and Human Services, Food and Drug Administration, Center for Drug Evaluation and Research (CDER), Center for Biologics Evaluation and Research (CBER); 1999.

46. Sherwin CM, Kiang TK, Spigarelli MG, Ensom MH. Fundamentals of population pharmacokinetic modelling: validation methods. Clin Pharmacokinet 2012;51:573-90.

47. Wagner C, Zhao P, Pan Y, et al. Application of Physiologically Based Pharmacokinetic (PBPK) Modeling to Support Dose Selection: Report of an FDA Public Workshop on PBPK. CPT Pharmacometrics Syst Pharmacol 2015;4:226-30.

48. Poulin P, Jones RD, Jones HM, et al. PHRMA CPCDC initiative on predictive models of human pharmacokinetics, part 5: Prediction of plasma concentration-time profiles in human by using the physiologically-based pharmacokinetic modeling approach. J Pharm Sci 2011.

49. NIH. Best Pharmaceuticals for Children Act (BPCA) Priority List of Needs in Pediatric Therapeutics. Federal Register 2015:51827 -8.

50. Manolis E, Pons G. Proposals for model-based paediatric medicinal development within the current European Union regulatory framework. Br J Clin Pharmacol 2009;68:493-501.

51. Manolis E, Osman TE, Herold R, et al. Role of modeling and simulation in pediatric investigation plans. Paediatr Anaesth 2011;21:214-21.

52. Zhao P, Zhang L, Grillo JA, et al. Applications of physiologically based pharmacokinetic (PBPK) modeling and simulation during regulatory review. Clin Pharmacol Ther 2011;89:259-67.

53. Leong R, Vieira ML, Zhao P, et al. Regulatory Experience With Physiologically Based Pharmacokinetic Modeling for Pediatric Drug Trials. Clin Pharmacol Ther 2012.

54. Maharaj AR, Edginton AN. Physiologically based pharmacokinetic modeling and simulation in pediatric drug development. CPT Pharmacometrics Syst Pharmacol 2014;3:e150.

55. Dunne J, Rodriguez WJ, Murphy MD, et al. Extrapolation of adult data and other data in pediatric drug-development programs. Pediatrics 2011;128:e1242-9.

56. Statistics NCfH. Third National Health and Nutrition Examination Survey (NHANES III). In. Hyattsville, MD; 1997.

57. ICRP. Basic Anatomical and Physiological Data for Use in Radiological Protection Reference Values. Annals of the International Commission on Radiological Protection 2002;32.

58. Johnson TN, Tucker GT, Rostami-Hodjegan A. Development of CYP2D6 and CYP3A4 in the first year of life. Clin Pharmacol Ther 2008;83:670-1.

59. Brouwer KL, Aleksunes LM, Brandys B, et al. Human Ontogeny of Drug Transporters: Review and Recommendations of the Pediatric Transporter Working Group. Clin Pharmacol Ther 2015;98:266-87.

60. Ferslew BC, Johnston CK, Tsakalozou E, et al. Altered morphine glucuronide and bile acid disposition in patients with nonalcoholic steatohepatitis. Clin Pharmacol Ther 2015;97:419-27.

61. Bradley JS, Nelson JD, eds. Nelson's Pediatric Antimicrobial Therapy. 22nd Edition ed: American Academy of Pediatrics; 2016.

APPENDIX 1

ECMO *ex vivo* data

circuit	drug	samp	site	date	time	nom_time	doseno	amt	flow	dv
32	B	0	A	2/23/2015	9:15	0			1.0	0
32	B			2/23/2015	9:30	0	1	3		
32	B	1	A	2/23/2015	9:31	0.02			1.0	3.01
32	B	2	A	2/23/2015	9:35	0.08			1.0	2.86
32	B	3	A	2/23/2015	9:45	0.25			1.0	2.7
32	B	4	A	2/23/2015	10:00	0.5			1.0	2.64
32	B	5	A	2/23/2015	10:30	1			1.0	2.6
32	B	6	A	2/23/2015	11:30	2			1.0	2.72
32	B	7	A	2/23/2015	12:30	3			1.0	2.57
32	B	8	A	2/23/2015	13:30	4			1.0	2.69
32	B	9	A	2/23/2015	17:30	8			1.0	2.55
32	B	10	A	2/23/2015	21:30	12			1.0	2.69
32	B	11	A	2/24/2015	9:30	24			1.0	2.71
32	B	12	A	2/25/2015	9:30	48			0.9	2.27
32	B	13	A	2/26/2015	9:30	72			0.9	1.47
33	B	0	A	2/23/2015	9:42	0			1.0	0
33	B			2/23/2015	9:50	0	1	3		
33	B	1	A	2/23/2015	9:51	0.02			1.0	2.6
33	B	2	A	2/23/2015	9:55	0.08			1.0	2.57
33	B	3	A	2/23/2015	10:05	0.25			1.0	2.43
33	B	4	A	2/23/2015	10:20	0.5			1.0	2.47
33	B	5	A	2/23/2015	10:50	1			1.0	2.44
33	B	6	A	2/23/2015	11:50	2			1.0	2.69
33	B	7	A	2/23/2015	12:50	3			1.0	2.68
33	B	8	A	2/23/2015	13:50	4			1.0	2.79

33	B	9	A	2/23/2015	17:50	8			1.0	2.74
33	B	10	A	2/23/2015	21:50	12			1.0	2.82
33	B	11	A	2/24/2015	9:50	24			1.0	0.87
33	B	12	A	2/25/2015	9:50	48			1.0	0.87
33	B	13	A	2/26/2015	9:50	72			1.0	0.95
34	B	0	A	2/23/2015	10:20	0			1.0	0
34	B			2/23/2015	10:20	0	1	3		
34	B	1	A	2/23/2015	10:21	0.02			1.0	2.99
34	B	2	A	2/23/2015	10:25	0.08			1.0	3.06
34	B	3	A	2/23/2015	10:35	0.25			1.0	2.88
34	B	4	A	2/23/2015	10:50	0.5			1.0	2.89
34	B	5	A	2/23/2015	11:20	1			1.0	2.75
34	B	6	A	2/23/2015	12:20	2			1.0	2.87
34	B	7	A	2/23/2015	13:20	3			1.0	3.01
34	B	8	A	2/23/2015	14:20	4			1.0	2.99
34	B	9	A	2/23/2015	18:20	8			1.0	3.04
34	B	10	A	2/23/2015	22:20	12			1.0	2.99
34	B	11	A	2/24/2015	10:20	24			1.0	0.73
34	B	12	A	2/25/2015	10:20	48			1.0	0.69
34	B	13	A	2/26/2015	10:20	72			1.0	0.49
301	B	1	C	2/23/2015	9:31	0.02			1.0	2.25
301	B	2	C	2/23/2015	9:35	0.08			1.0	2.55
301	B	3	C	2/23/2015	9:45	0.25			1.0	2.5
301	B	4	C	2/23/2015	10:00	0.5			1.0	2.67
301	B	5	C	2/23/2015	10:30	1			1.0	2.79
301	B	6	C	2/23/2015	11:30	2			1.0	2.96
301	B	7	C	2/23/2015	12:30	3			1.0	2.8
301	B	8	C	2/23/2015	13:30	4			1.0	3.15
301	B	9	C	2/23/2015	17:30	8			1.0	3.08
301	B	10	C	2/23/2015	21:30	12			1.0	3.19

301	B	11	C	2/24/2015	9:30	24	1.0	2.4
301	B	12	C	2/25/2015	9:30	48	0.9	2.23
301	B	13	C	2/26/2015	9:30	72	0.9	1.04
302	B	1	C	2/23/2015	9:51	0.02	1.0	2.57
302	B	2	C	2/23/2015	9:55	0.08	1.0	2.72
302	B	3	C	2/23/2015	10:05	0.25	1.0	2.91
302	B	4	C	2/23/2015	10:20	0.5	1.0	2.93
302	B	5	C	2/23/2015	10:50	1	1.0	3.08
302	B	6	C	2/23/2015	11:50	2	1.0	3.65
302	B	7	C	2/23/2015	12:50	3	1.0	3.81
302	B	8	C	2/23/2015	13:50	4	1.0	3.86
302	B	9	C	2/23/2015	17:50	8	1.0	3.92
302	B	10	C	2/23/2015	21:50	12	1.0	3.86
302	B	11	C	2/24/2015	9:50	24	1.0	3.76
302	B	12	C	2/25/2015	9:50	48	1.0	2.78
302	B	13	C	2/26/2015	9:50	72	1.0	2.8
303	B	1	C	2/23/2015	10:21	0.02	1.0	2.89
303	B	2	C	2/23/2015	10:25	0.08	1.0	3.1
303	B	3	C	2/23/2015	10:35	0.25	1.0	3.32
303	B	4	C	2/23/2015	10:50	0.5	1.0	3.49
303	B	5	C	2/23/2015	11:20	1	1.0	3.85
303	B	6	C	2/23/2015	12:20	2	1.0	4.04
303	B	7	C	2/23/2015	13:20	3	1.0	4.08
303	B	8	C	2/23/2015	14:20	4	1.0	4.08
303	B	9	C	2/23/2015	18:20	8	1.0	4.28
303	B	10	C	2/23/2015	22:20	12	1.0	4.16
303	B	11	C	2/24/2015	10:20	24	1.0	4.24
303	B	12	C	2/25/2015	10:20	48	1.0	3.48
303	B	13	C	2/26/2015	10:20	72	1.0	2.83
351	B	1	H	2/23/2015	9:31	0.02	1.0	0

351	B	5	H	2/23/2015	10:30	1			1.0	0
351	B	11	H	2/24/2015	9:30	24			1.0	0.17
351	B	12	H	2/25/2015	9:30	48			0.9	0.23
351	B	13	H	2/26/2015	9:30	72			0.9	0.15
352	B	1	H	2/23/2015	9:51	0.02			1.0	0
352	B	5	H	2/23/2015	10:50	1			1.0	0
352	B	11	H	2/24/2015	9:50	24			1.0	0.17
352	B	12	H	2/25/2015	9:50	48			1.0	0.09
352	B	13	H	2/26/2015	9:50	72			1.0	0.11
353	B	1	H	2/23/2015	10:21	0.02			1.0	0
353	B	5	H	2/23/2015	11:20	1			1.0	
353	B	11	H	2/24/2015	10:20	24			1.0	0.11
353	B	12	H	2/25/2015	10:20	48			1.0	
353	B	13	H	2/26/2015	10:20	72			1.0	0.07
1	F	0	A	4/25/2012	16:50	0			1.1	0
1	F			4/25/2012	16:52	0	1	250		
1	F	1	A	4/25/2012	16:53	0.02			1.1	296
1	F	1	V	4/25/2012	16:53	0.02			1.1	211
1	F	2	A	4/25/2012	16:57	0.08			1.1	308
1	F	2	V	4/25/2012	16:57	0.08			1.1	319
1	F	3	A	4/25/2012	17:07	0.25			1.1	329
1	F	3	V	4/25/2012	17:07	0.25			1.1	293
1	F	4	A	4/25/2012	17:22	0.5			1.1	297
1	F	4	V	4/25/2012	17:22	0.5			1.1	294
1	F	5	A	4/25/2012	17:53	1			1.1	264
1	F	5	V	4/25/2012	17:53	1			1.1	256
1	F	6	A	4/25/2012	18:52	2			1.1	283
1	F	6	V	4/25/2012	18:52	2			1.1	289
1	F	7	A	4/25/2012	19:52	3			1.1	293
1	F	7	V	4/25/2012	19:52	3			1.1	263

1	F	8	A	4/25/2012	20:52	4			1.1	262
1	F	8	V	4/25/2012	20:52	4			1.1	299
2	F	0	A	4/30/2012	16:07	0			1.0	0
2	F			4/30/2012	16:22	0	1	250		
2	F	1	A	4/30/2012	16:23	0.02			1.1	400
2	F	1	V	4/30/2012	16:23	0.02			1.1	369
2	F	2	A	4/30/2012	16:27	0.08			1.1	387
2	F	2	V	4/30/2012	16:27	0.08			1.1	338
2	F	3	A	4/30/2012	16:37	0.25			1.1	337
2	F	3	V	4/30/2012	16:37	0.25			1.1	365
2	F	4	A	4/30/2012	16:52	0.5			1.1	366
2	F	4	V	4/30/2012	16:52	0.5			1.1	353
2	F	5	A	4/30/2012	17:24	1			1.1	401
2	F	5	V	4/30/2012	17:24	1			1.1	390
2	F	6	A	4/30/2012	18:24	2			1.1	398
2	F	6	V	4/30/2012	18:24	2			1.1	419
2	F	7	A	4/30/2012	19:30	3			1.1	397
2	F	7	V	4/30/2012	19:30	3			1.1	410
2	F	8	A	4/30/2012	20:32	4			1.1	325
2	F	8	V	4/30/2012	20:32	4			1.1	401
3	F	0	A	4/30/2012	17:32	0			1.0	0
3	F			4/30/2012	17:56	0	1	250		
3	F	1	A	4/30/2012	17:57	0.02			1.0	219
3	F	1	V	4/30/2012	17:57	0.02			1.0	208
3	F	2	A	4/30/2012	18:02	0.08			1.0	203
3	F	2	V	4/30/2012	18:02	0.08			1.0	200
3	F	3	A	4/30/2012	18:10	0.25			1.0	200
3	F	3	V	4/30/2012	18:10	0.25			1.0	203
3	F	4	A	4/30/2012	18:28	0.5			1.0	194
3	F	4	V	4/30/2012	18:28	0.5			1.0	191

3	F	5	A	4/30/2012	19:00	1			1.0	195
3	F	5	V	4/30/2012	19:00	1			1.0	187
3	F	6	A	4/30/2012	20:01	2			1.0	208
3	F	6	V	4/30/2012	20:01	2			1.0	203
3	F	7	A	4/30/2012	21:11	3			1.0	205
3	F	7	V	4/30/2012	21:11	3			1.0	211
3	F	8	A	4/30/2012	22:07	4			1.0	216
3	F	8	V	4/30/2012	22:07	4			1.0	212
12	F	0	A	4/25/2012	14:40	0			1.0	0
12	F			4/25/2012	14:43	0	1	13		
12	F	1	A	4/25/2012	14:44	0.02			1.0	18.2
12	F	1	V	4/25/2012	14:44	0.02			1.0	18.8
12	F	2	A	4/25/2012	14:48	0.08			1.0	17.1
12	F	2	V	4/25/2012	14:48	0.08			1.0	17.8
12	F	3	A	4/25/2012	14:58	0.25			1.0	18.3
12	F	3	V	4/25/2012	14:58	0.25			1.0	12.5
12	F	4	A	4/25/2012	15:13	0.5			1.0	19.7
12	F	4	V	4/25/2012	15:13	0.5			1.0	18.7
12	F	5	A	4/25/2012	15:43	1			1.0	18.8
12	F	5	V	4/25/2012	15:43	1			1.0	18.7
12	F	6	A	4/25/2012	16:43	2			1.0	16.4
12	F	6	V	4/25/2012	16:43	2			1.0	16.4
12	F	7	A	4/25/2012	17:43	3			1.0	18.1
12	F	7	V	4/25/2012	17:43	3			1.0	18.1
12	F	8	A	4/25/2012	18:43	4			1.0	17.6
12	F	8	V	4/25/2012	18:43	4			1.0	18.5
16	F	0	A	4/30/2012	14:29	0			1.1	0
16	F			4/30/2012	14:30	0	1	8		
16	F	1	A	4/30/2012	14:31	0.02			1.1	15.4
16	F	1	V	4/30/2012	14:31	0.02			1.1	15.8

16	F	2	A	4/30/2012	14:35	0.08			1.1	15
16	F	2	V	4/30/2012	14:35	0.08			1.1	15.3
16	F	3	A	4/30/2012	14:45	0.25			1.1	14.9
16	F	3	V	4/30/2012	14:45	0.25			1.1	16.2
16	F	4	A	4/30/2012	15:00	0.5			1.1	16.9
16	F	4	V	4/30/2012	15:00	0.5			1.1	16.2
16	F	5	A	4/30/2012	15:30	1			1.1	16.9
16	F	5	V	4/30/2012	15:30	1			1.1	15.7
16	F	6	A	4/30/2012	16:30	2			1.1	16.9
16	F	6	V	4/30/2012	16:30	2			1.1	16.8
16	F	7	A	4/30/2012	17:30	3			1.1	16.4
16	F	7	V	4/30/2012	17:30	3			1.1	16.5
16	F	8	A	4/30/2012	18:30	4			1.1	16.3
16	F	8	V	4/30/2012	18:30	4			1.1	17.1
23	F	0	A	9/22/2014	10:20	0			1.0	0.007
23	F		A	9/22/2014	10:30	0	1	19	1.0	
23	F	1	A	9/22/2014	10:31	0.02			1.0	17.61
23	F	2	A	9/22/2014	10:35	0.08			1.0	17.48
23	F	3	A	9/22/2014	10:45	0.25			1.0	17.61
23	F	4	A	9/22/2014	11:00	0.5			1.0	17.33
23	F	5	A	9/22/2014	11:30	1			1.0	17.2
23	F	6	A	9/22/2014	12:30	2			1.0	17.16
23	F	7	A	9/22/2014	13:30	3			1.0	17.12
23	F	8	A	9/22/2014	14:30	4			1.0	17.33
23	F	9	A	9/22/2014	18:30	8			1.0	17.37
23	F	10	A	9/22/2014	22:30	12			1.0	17.61
23	F	11	A	9/23/2014	10:30	24			1.0	17.28
23	F	12	A	9/24/2014	10:30	48			1.0	17.37
23	F	13	A	9/25/2014	10:30	72			1.0	17.18
24	F		A	9/22/2014	10:50	0	1	18	1.0	

24	F	1	A	9/22/2014	10:51	0.02			1.0	19.05
24	F	2	A	9/22/2014	10:55	0.08			1.0	18.01
24	F	3	A	9/22/2014	11:05	0.25			1.0	18.49
24	F	4	A	9/22/2014	11:20	0.5			1.0	18.51
24	F	5	A	9/22/2014	11:50	1			1.0	18.79
24	F	6	A	9/22/2014	12:50	2			1.0	18.04
24	F	7	A	9/22/2014	13:50	3			1.0	18.63
24	F	8	A	9/22/2014	14:50	4			1.0	18.33
24	F	9	A	9/22/2014	18:50	8			1.0	17.78
24	F	10	A	9/22/2014	22:50	12			1.0	17.49
24	F	11	A	9/23/2014	10:50	24			1.0	17.59
24	F	12	A	9/24/2014	10:50	48			1.0	17.32
24	F	13	A	9/25/2014	10:50	72			1.0	17.59
25	F	0	A	9/22/2014	11:10	0			1.0	0.004
25	F		A	9/22/2014	11:10	0	1	17	1.0	
25	F	1	A	9/22/2014	11:11	0.02			1.0	17.75
25	F	2	A	9/22/2014	11:15	0.08			1.0	17.29
25	F	3	A	9/22/2014	11:25	0.25			1.0	17.7
25	F	4	A	9/22/2014	11:40	0.5			1.0	17.64
25	F	5	A	9/22/2014	12:10	1			1.0	18.07
25	F	6	A	9/22/2014	13:10	2			1.0	17.94
25	F	7	A	9/22/2014	14:10	3			1.0	16.91
25	F	8	A	9/22/2014	15:10	4			1.0	18.22
25	F	9	A	9/22/2014	19:10	8			1.0	17.88
25	F	10	A	9/22/2014	23:10	12			1.0	17.01
25	F	11	A	9/23/2014	11:10	24			1.0	17.47
25	F	12	A	9/24/2014	11:10	48			1.0	17.87
25	F	13	A	9/25/2014	11:10	72			1.0	17.44
101	F			4/25/2012	16:52	0	1	5		
101	F	1	C	4/25/2012	16:54	0.02			1.1	337

101	F	5	C	4/25/2012	17:54	1			1.1	311
101	F	6	C	4/25/2012	18:53	2			1.1	298
101	F	7	C	4/25/2012	19:53	3			1.1	299
101	F	8	C	4/25/2012	20:53	4			1.1	314
102	F			4/30/2012	16:22	0	1	5		
102	F	1	C	4/30/2012	16:26	0.02			1.1	260
102	F	5	C	4/30/2012	17:26	1			1.1	205
102	F	6	C	4/30/2012	18:25	2			1.1	249
102	F	7	C	4/30/2012	19:31	3			1.1	250
102	F	8	C	4/30/2012	20:33	4			1.1	237
103	F			4/30/2012	17:56	0	1	5		
103	F	1	C	4/30/2012	17:59	0.02			1.0	256
103	F	5	C	4/30/2012	19:01	1			1.0	260
103	F	6	C	4/30/2012	20:03	2			1.0	275
103	F	7	C	4/30/2012	21:12	3			1.0	262
103	F	8	C	4/30/2012	22:08	4			1.0	264
104	F			4/25/2012	14:43	0	1	0.1		
104	F	1	C	4/25/2012	14:44	0.02			1.0	14.6
104	F	5	C	4/25/2012	15:43	1			1.0	14.3
104	F	6	C	4/25/2012	16:43	2			1.0	14.7
104	F	7	C	4/25/2012	17:43	3			1.0	15
104	F	8	C	4/25/2012	18:43	4			1.0	15.7
105	F		C	9/22/2014	10:22	0	1	0.6	1.0	
105	F	1	C	9/22/2014	10:31	0.02			1.0	18.73
105	F	2	C	9/22/2014	10:35	0.08			1.0	17.9
105	F	3	C	9/22/2014	10:45	0.25			1.0	19.04
105	F	4	C	9/22/2014	11:00	0.5			1.0	19.71
105	F	5	C	9/22/2014	11:30	1			1.0	19.74
105	F	6	C	9/22/2014	12:30	2			1.0	18.62
105	F	7	C	9/22/2014	13:30	3			1.0	19.01

105	F	8	C	9/22/2014	14:30	4			1.0	19.83
105	F	9	C	9/22/2014	18:30	8			1.0	19.68
105	F	10	C	9/22/2014	22:30	12			1.0	18.88
105	F	11	C	9/23/2014	10:30	24			1.0	19.24
105	F	12	C	9/24/2014	10:30	48			1.0	19.34
105	F	13	C	9/25/2014	10:30	72			1.0	19.71
106	F		C	9/22/2014	10:43	0	1	0.6	1.0	
106	F	1	C	9/22/2014	10:51	0.02			1.0	20.59
106	F	2	C	9/22/2014	10:55	0.08			1.0	19.82
106	F	3	C	9/22/2014	11:05	0.25			1.0	20.07
106	F	4	C	9/22/2014	11:20	0.5			1.0	20.55
106	F	5	C	9/22/2014	11:50	1			1.0	18.99
106	F	6	C	9/22/2014	12:50	2			1.0	19.9
106	F	7	C	9/22/2014	13:50	3			1.0	19.39
106	F	8	C	9/22/2014	14:50	4			1.0	20.08
106	F	9	C	9/22/2014	18:50	8			1.0	19.46
106	F	10	C	9/22/2014	22:50	12			1.0	19.71
106	F	11	C	9/23/2014	10:50	24			1.0	20.61
106	F	12	C	9/24/2014	10:50	48			1.0	20.18
106	F	13	C	9/25/2014	10:50	72			1.0	20.03
107	F		C	9/22/2014	11:03	0	1	0.6	1.0	
107	F	1	C	9/22/2014	11:11	0.02			1.0	18.95
107	F	2	C	9/22/2014	11:15	0.08			1.0	18.92
107	F	3	C	9/22/2014	11:25	0.25			1.0	18.78
107	F	4	C	9/22/2014	11:40	0.5			1.0	18.09
107	F	5	C	9/22/2014	12:10	1			1.0	19.76
107	F	6	C	9/22/2014	13:10	2			1.0	19.4
107	F	7	C	9/22/2014	14:10	3			1.0	17.69
107	F	8	C	9/22/2014	15:10	4			1.0	19.51
107	F	9	C	9/22/2014	19:10	8			1.0	18.93

107	F	10	C	9/22/2014	23:10	12			1.0	19.12
107	F	11	C	9/23/2014	11:10	24			1.0	18.78
107	F	12	C	9/24/2014	11:10	48			1.0	19.42
107	F	13	C	9/25/2014	11:10	72			1.0	19.23
151	F	1	H	9/22/2014	10:31	0.02			1.0	3.419
151	F	5	H	9/22/2014	11:30	1			1.0	3.927
151	F	11	H	9/23/2014	10:30	24			1.0	14.88
151	F	13	H	9/25/2014	10:30	72			1.0	14.64
152	F	1	H	9/22/2014	10:51	0.02			1.0	0.501
152	F	5	H	9/22/2014	11:50	1			1.0	5.229
152	F	11	H	9/23/2014	10:50	24			1.0	14.04
152	F	13	H	9/25/2014	10:50	72			1.0	14.03
6	M	0	V	8/13/2012	14:13				1.0	0
6	M			8/13/2012	14:17	0	1	13	1.0	
6	M	1	V	8/13/2012	14:18	0.02			1.0	10.06
6	M	1	A	8/13/2012	14:18	0.02			1.0	11.35
6	M	2	V	8/13/2012	14:22	0.08			1.0	11.29
6	M	2	A	8/13/2012	14:22	0.08			1.0	11.77
6	M	3	A	8/13/2012	14:32	0.25			1.0	10.54
6	M	3	V	8/13/2012	14:32	0.25			1.0	10.69
6	M	4	V	8/13/2012	14:47	0.5			1.0	10.69
6	M	4	A	8/13/2012	14:47	0.5			1.0	10.78
6	M	5	A	8/13/2012	15:17	1			1.0	10.99
6	M	5	V	8/13/2012	15:17	1			1.0	11.14
6	M	6	V	8/13/2012	16:17	2			1.0	10.05
6	M	6	A	8/13/2012	16:17	2			1.0	10.13
6	M	7	V	8/13/2012	17:17	3			1.0	10.14
6	M	7	A	8/13/2012	17:17	3			1.0	9.91
6	M	8	A	8/13/2012	18:17	4			1.0	10.54
6	M	8	V	8/13/2012	18:17	4			1.0	10.57

7	M			8/13/2012	14:53	0	1	13	1.0	
7	M	0	V	8/13/2012	14:48				1.0	0
7	M	1	V	8/13/2012	14:54	0.02			1.0	9.76
7	M	1	A	8/13/2012	14:54	0.02			1.0	10.92
7	M	2	A	8/13/2012	14:58	0.08			1.0	10.2
7	M	2	V	8/13/2012	14:58	0.08			1.0	9.41
7	M	3	A	8/13/2012	15:08	0.25			1.0	8.69
7	M	3	V	8/13/2012	15:08	0.25			1.0	8.46
7	M	4	V	8/13/2012	15:23	0.5			1.0	7.83
7	M	4	A	8/13/2012	15:23	0.5			1.0	7.47
7	M	5	V	8/13/2012	15:53	1			1.0	7.25
7	M	5	A	8/13/2012	15:53	1			1.0	7.22
7	M	6	A	8/13/2012	16:53	2			1.0	5.01
7	M	6	V	8/13/2012	16:53	2			1.0	5.61
7	M	7	A	8/13/2012	17:53	3			1.0	4.53
7	M	7	V	8/13/2012	17:53	3			1.0	4.35
7	M	8	A	8/13/2012	18:53	4			1.0	4.71
7	M	8	V	8/13/2012	18:53	4			1.0	4.68
8	M	0	V	8/16/2012	13:31				1.0	0
8	M			8/16/2012	13:36		1	12	1.0	
8	M	1	V	8/16/2012	13:37	0.02			1.0	17.44
8	M	1	A	8/16/2012	13:37	0.02			1.0	17.82
8	M	2	A	8/16/2012	13:41	0.08			1.0	16.5
8	M	2	V	8/16/2012	13:41	0.08			1.0	16.58
8	M	3	V	8/16/2012	13:51	0.25			1.0	17.52
8	M	3	A	8/16/2012	13:51	0.25			1.0	18.11
8	M	4	V	8/16/2012	14:06	0.5			1.0	16.41
8	M	4	A	8/16/2012	14:06	0.5			1.0	18.97
8	M	5	V	8/16/2012	14:36	1			1.0	16.68
8	M	5	A	8/16/2012	14:36	1			1.0	18.12

8	M	6	A	8/16/2012	15:36	2			1.0	16.54
8	M	6	V	8/16/2012	15:36	2			1.0	17.98
8	M	7	A	8/16/2012	16:36	3			1.0	16.56
8	M	7	V	8/16/2012	16:36	3			1.0	17.12
8	M	8	A	8/16/2012	17:36	4			1.0	16.24
8	M	8	V	8/16/2012	17:36	4			1.0	16.7
17	M			3/28/2013	15:15		1	8	1.0	
17	M	0	V	3/28/2013	15:13				1.0	0
17	M	1	A	3/28/2013	15:16	0.02			1.0	10.2
17	M	1	V	3/28/2013	15:16	0.02			1.0	10.49
17	M	2	V	3/28/2013	15:20	0.08			1.0	10.33
17	M	2	A	3/28/2013	15:20	0.08			1.0	10.33
17	M	3	A	3/28/2013	15:30	0.25			1.0	10.34
17	M	3	V	3/28/2013	15:30	0.25			1.0	10.41
17	M	4	A	3/28/2013	15:45	0.5			1.0	11.04
17	M	4	V	3/28/2013	15:45	0.5			1.0	9.91
17	M	5	A	3/28/2013	16:15	1			1.0	8.93
17	M	5	V	3/28/2013	16:15	1			1.0	9.94
17	M	6	V	3/28/2013	17:15	2			1.0	10.15
17	M	6	A	3/28/2013	17:15	2			1.0	9.99
17	M	7	V	3/28/2013	18:15	3			1.0	10.34
17	M	7	A	3/28/2013	18:15	3			1.0	9.33
17	M	8	A	3/28/2013	19:15	4			1.0	10.01
17	M	8	V	3/28/2013	19:15	4			1.0	9.56
18	M	0	V	6/17/2014	10:00				1.0	0
18	M			6/17/2014	10:02		1	1.2		
18	M	1	A	6/17/2014	10:03	0.02			1.0	16.68
18	M	1	V	6/17/2014	10:03	0.02			1.0	17.55
18	M	2	V	6/17/2014	10:08	0.08			1.0	15.92
18	M	2	A	6/17/2014	10:08	0.08			1.0	14.84

18	M	3	A	6/17/2014	10:18	0.25			1.0	13.31
18	M	3	V	6/17/2014	10:18	0.25			1.0	13.17
18	M	4	V	6/17/2014	10:32	0.5			1.0	10.19
18	M	4	A	6/17/2014	10:32	0.5			1.0	10.57
18	M	5	V	6/17/2014	11:02	1			1.0	7.76
18	M	5	A	6/17/2014	11:02	1			1.0	7.85
18	M	6	V	6/17/2014	12:02	2			1.0	5.32
18	M	6	A	6/17/2014	12:02	2			1.0	5.44
18	M	7	V	6/17/2014	13:02	3			1.0	3.89
18	M	7	A	6/17/2014	13:02	3			1.0	4.1
18	M	8	A	6/17/2014	14:02	4			1.0	3.48
18	M	8	V	6/17/2014	14:02	4			1.0	3.31
18	M	9	V	6/17/2014	18:02	8			1.0	2.37
18	M	9	A	6/17/2014	18:02	8			1.0	2.11
18	M	10	A	6/17/2014	22:02	12			1.0	1.85
18	M	10	V	6/17/2014	22:02	12			1.0	1.39
18	M	11	V	6/18/2014	10:02	24			1.0	0.63
18	M	11	A	6/18/2014	10:02	24			1.0	0.62
18	M	12	A	6/19/2014	10:04	48			1.0	0.56
18	M	12	V	6/19/2014	10:04	48			1.0	0.58
18	M	13	A	6/20/2014	10:02	72			1.0	0.74
18	M	13	V	6/20/2014	10:02	72			1.0	0.62
19	M			6/17/2014	11:17	0	1	1.2		
19	M	1	V	6/17/2014	11:18	0.02			1.0	19.94
19	M	1	A	6/17/2014	11:18	0.02			1.0	21.7
19	M	2	A	6/17/2014	11:22	0.08			1.0	19.29
19	M	2	V	6/17/2014	11:22	0.08			1.0	18.5
19	M	3	V	6/17/2014	11:32	0.25			1.0	15.73
19	M	3	A	6/17/2014	11:32	0.25			1.0	15.99
19	M	4	A	6/17/2014	11:47	0.5			1.0	13.84

19	M	4	V	6/17/2014	11:47	0.5			1.0	13.22
19	M	5	A	6/17/2014	12:17	1			1.0	10.68
19	M	5	V	6/17/2014	12:17	1			1.0	10.37
19	M	6	A	6/17/2014	13:17	2			1.0	7.05
19	M	6	V	6/17/2014	13:17	2			1.0	7.02
19	M	7	A	6/17/2014	14:17	3			1.0	5.05
19	M	7	V	6/17/2014	14:17	3			1.0	3.61
19	M	8	V	6/17/2014	15:17	4			1.0	2.97
19	M	8	A	6/17/2014	15:17	4			1.0	2.61
19	M	9	V	6/17/2014	19:17	8			1.0	1.6
19	M	9	A	6/17/2014	19:17	8			1.0	1.61
19	M	10	V	6/17/2014	23:17	12			1.0	0.93
19	M	10	A	6/17/2014	23:17	12			1.0	1.04
19	M	11	V	6/18/2014	11:17	24			1.0	0.71
19	M	11	A	6/18/2014	11:17	24			1.0	0.67
19	M			6/18/2014	11:20	24	2	1.2		
20	M			9/11/2014	14:30		1	1.2		
20	M	1	A	9/11/2014	14:31	0.02			1.0	15.45
20	M	2	A	9/11/2014	14:35	0.08			1.0	16.61
20	M	3	A	9/11/2014	14:45	0.25			1.0	15.42
20	M	4	A	9/11/2014	15:00	0.5			1.0	14.35
20	M	5	A	9/11/2014	15:30	1			1.0	13.08
20	M	6	A	9/11/2014	16:30	2			1.0	11.64
20	M	7	A	9/11/2014	17:30	3			1.0	10.47
20	M	8	A	9/11/2014	18:30	4			1.0	10.19
20	M	9	A	9/11/2014	22:30	8			1.0	7.55
20	M	10	A	9/12/2014	2:30	12			1.0	7.92
20	M	11	A	9/12/2014	14:30	24			1.0	8.14
20	M	12	A	9/13/2014	14:30	48			1.0	6.76
20	M	13	A	9/14/2014	14:30	72			1.0	4.89

21	M	0	A	9/11/2014	15:34	0.02			1.0	0
21	M			9/11/2014	15:35		1	1.2		
21	M	1	A	9/11/2014	15:36	0.02			1.0	16.68
21	M	2	A	9/11/2014	15:40	0.08			1.0	17.23
21	M	3	A	9/11/2014	15:48	0.25			1.0	17.45
21	M	4	A	9/11/2014	16:05	0.5			1.0	17.47
21	M	5	A	9/11/2014	16:35	1			1.0	17.1
21	M	6	A	9/11/2014	17:35	2			1.0	17.24
21	M	7	A	9/11/2014	18:35	3			1.0	16.72
21	M	8	A	9/11/2014	19:35	4			1.0	16.25
21	M	9	A	9/11/2014	23:35	8			1.0	14.73
21	M	10	A	9/12/2014	3:35	12			1.0	13.1
21	M	11	A	9/12/2014	15:35	24			1.0	8.07
21	M	12	A	9/13/2014	15:35	48			1.0	5.02
21	M	13	A	9/14/2014	15:35	72			1.0	4.16
22	M			9/11/2014	16:00		1	1.2		
22	M	1	A	9/11/2014	16:01	0.02			1.0	17.25
22	M	2	A	9/11/2014	16:05	0.08			1.0	17.97
22	M	3	A	9/11/2014	16:15	0.25			1.0	18.24
22	M	4	A	9/11/2014	16:30	0.5			1.0	18
22	M	5	A	9/11/2014	17:00	1			1.0	16.96
22	M	6	A	9/11/2014	18:00	2			1.0	16.57
22	M	7	A	9/11/2014	19:00	3			1.0	15.6
22	M	8	A	9/11/2014	20:00	4			1.0	14.31
22	M	9	A	9/12/2014	0:00	8			1.0	12.55
22	M	10	A	9/12/2014	4:00	12			1.0	10.15
22	M	11	A	9/12/2014	16:00	24			1.0	6.36
22	M	12	A	9/13/2014	16:04	48			1.0	3.64
22	M	13	A	9/14/2014	16:00	72			1.0	1.35
22	M	0	A	9/11/2014		0.02			1.0	

26	M	0	A	1/26/2015	11:58	0			1.0	0
26	M			1/26/2015	12:00		1	1.2		
26	M	1	A	1/26/2015	12:01	0.02			1.0	20.85
26	M	2	A	1/26/2015	12:05	0.08			1.0	20.63
26	M	3	A	1/26/2015	12:15	0.25			1.0	19.76
26	M	4	A	1/26/2015	12:30	0.5			1.0	18.49
26	M	5	A	1/26/2015	13:00	1			1.0	15.49
26	M	6	A	1/26/2015	14:00	2			1.0	15.14
26	M	7	A	1/26/2015	15:00	3			1.0	13.39
26	M	8	A	1/26/2015	16:00	4			1.0	12.56
26	M	9	A	1/26/2015	20:00	8			1.0	11.52
26	M	10	A	1/27/2015	0:00	12			1.0	5.24
26	M	11	A	1/27/2015	12:00	24			1.0	4.39
26	M	12	A	1/28/2015	12:00	48			1.0	5.29
26	M	13	A	1/29/2015	12:00	72			1.0	4.34
27	M	0	A	1/26/2015	12:19	0			1.0	0
27	M			1/26/2015	12:20		1	1.2		
27	M	1	A	1/26/2015	12:21	0.02			1.0	16.96
27	M	2	A	1/26/2015	12:25	0.08			1.0	
27	M	3	A	1/26/2015	12:35	0.25			1.0	17.94
27	M	4	A	1/26/2015	12:50	0.5			1.0	17.74
27	M	5	A	1/26/2015	13:20	1			1.0	14.84
27	M	6	A	1/26/2015	14:20	2			1.0	11.87
27	M	7	A	1/26/2015	15:20	3			1.0	11.71
27	M	8	A	1/26/2015	16:20	4			1.0	8.98
27	M	9	A	1/26/2015	20:20	8			1.0	9.65
27	M	10	A	1/27/2015	0:20	12			1.0	6
27	M	11	A	1/27/2015	12:20	24			1.0	6.15
27	M	12	A	1/28/2015	12:20	48			1.0	6.79
27	M	13	A	1/29/2015	12:20	72			1.0	5.32

28	M	0	A	1/26/2015	12:49	0			1.0	0
28	M			1/26/2015	12:50		1	1.2		
28	M	1	A	1/26/2015	12:51	0.02			1.0	19.4
28	M	2	A	1/26/2015	12:55	0.08			1.0	18.91
28	M	3	A	1/26/2015	13:05	0.25			1.0	17.29
28	M	4	A	1/26/2015	13:20	0.5			1.0	16.08
28	M	5	A	1/26/2015	13:50	1			1.0	15.1
28	M	6	A	1/26/2015	14:50	2			1.0	13.49
28	M	7	A	1/26/2015	15:50	3			1.0	11.78
28	M	8	A	1/26/2015	16:50	4			1.0	11.33
28	M	9	A	1/26/2015	20:50	8			1.0	8.98
28	M	10	A	1/27/2015	0:50	12			1.0	9.11
28	M	11	A	1/27/2015	12:50	24			1.0	4.09
28	M	12	A	1/28/2015	12:50	48			1.0	4.61
28	M	13	A	1/29/2015	12:50	72			1.0	5.38
29	M			2/2/2015	9:30		1	1.2		
29	M	0	A	2/2/2015	8:15	0			1.0	
29	M	1	A	2/2/2015	9:31	0.02			1.0	20.71
29	M	2	A	2/2/2015	9:35	0.08			1.0	20.21
29	M	3	A	2/2/2015	9:45	0.25			1.0	18.41
29	M	4	A	2/2/2015	10:00	0.5			1.0	17.11
29	M	5	A	2/2/2015	10:30	1			1.0	14.2
29	M	6	A	2/2/2015	11:30	2			1.0	13.39
29	M	7	A	2/2/2015	12:30	3			1.0	11.68
29	M	8	A	2/2/2015	13:30	4			1.0	10.41
29	M	9	A	2/2/2015	17:30	8			1.0	7.84
29	M	10	A	2/2/2015	21:30	12			1.0	6.27
29	M	11	A	2/3/2015	9:30	24			1.0	3.92
29	M	12	A	2/4/2015	9:30	48			1.0	3.35
30	M	0	A	2/2/2015	8:15	0			1.0	0

30	M			2/2/2015	9:50		1	1.2		
30	M	1	A	2/2/2015	9:51	0.02			1.0	18.07
30	M	2	A	2/2/2015	9:55	0.08			1.0	18.08
30	M	3	A	2/2/2015	10:05	0.25			1.0	17.25
30	M	4	A	2/2/2015	10:20	0.5			1.0	15.85
30	M	5	A	2/2/2015	10:50	1			1.0	14.43
30	M	6	A	2/2/2015	11:50	2			1.0	12.83
30	M	7	A	2/2/2015	12:50	3			1.0	11.25
30	M	8	A	2/2/2015	13:50	4			1.0	10.67
30	M	9	A	2/2/2015	17:50	8			1.0	8.65
30	M	10	A	2/2/2015	21:50	12			1.0	
30	M	11	A	2/3/2015	9:50	24			1.0	6.41
30	M	12	A	2/4/2015	9:50	48			1.0	5.05
30	M	13	A	2/5/2015	9:50	72			1.0	4.42
31	M			2/2/2015	10:20		1	1.2		
31	M	0	A	2/2/2015	8:15	0			1.0	0
31	M	1	A	2/2/2015	10:21	0.02			1.0	10.31
31	M	2	A	2/2/2015	10:25	0.08			1.0	12.53
31	M	3	A	2/2/2015	10:35	0.25			1.0	9.99
31	M	4	A	2/2/2015	10:50	0.5			1.0	8.89
31	M	5	A	2/2/2015	11:20	1			1.0	5.5
31	M	6	A	2/2/2015	12:20	2			1.0	5.21
31	M	7	A	2/2/2015	13:20	3			1.0	4.75
31	M	8	A	2/2/2015	14:20	4			1.0	4.14
31	M	9	A	2/2/2015	18:20	8			1.0	3.3
31	M	10	A	2/2/2015	22:20	12			1.0	2.75
31	M	11	A	2/3/2015	10:20	24			1.0	4.28
31	M	12	A	2/4/2015	10:20	48			1.0	3.6
31	M	13	A	2/5/2015	10:20	72			1.0	4.23
201	M	1	C	8/13/2012	14:18	0.02			1.0	12.54

201	M	5	C	8/13/2012	15:17	1	1.0	12.74
201	M	6	C	8/13/2012	16:17	2	1.0	11.83
201	M	7	C	8/13/2012	17:17	3	1.0	11.4
201	M	8	C	8/13/2012	18:17	4	1.0	11.93
202	M	1	C	9/11/2014	14:31	0.02	1.0	57.6
202	M	2	C	9/11/2014	14:35	0.08	1.0	58.85
202	M	3	C	9/11/2014	14:45	0.25	1.0	57.37
202	M	4	C	9/11/2014	15:00	0.5	1.0	55.72
202	M	5	C	9/11/2014	15:30	1	1.0	55.17
202	M	6	C	9/11/2014	16:30	2	1.0	55.34
202	M	7	C	9/11/2014	17:30	3	1.0	53.64
202	M	8	C	9/11/2014	18:30	4	1.0	52.64
202	M	9	C	9/11/2014	22:30	8	1.0	38.76
202	M	10	C	9/12/2014	2:30	12	1.0	38.1
202	M	11	C	9/12/2014	14:30	24	1.0	33.56
202	M	12	C	9/13/2014	14:30	48	1.0	18.8
202	M	13	C	9/14/2014	14:30	72	1.0	19.44
203	M	1	C	9/11/2014	15:36	0.02	1.0	67.01
203	M	2	C	9/11/2014	15:40	0.08	1.0	65.65
203	M	3	C	9/11/2014	15:48	0.25	1.0	67.25
203	M	4	C	9/11/2014	16:05	0.5	1.0	66.28
203	M	5	C	9/11/2014	16:35	1	1.0	68.35
203	M	6	C	9/11/2014	17:35	2	1.0	67
203	M	7	C	9/11/2014	18:35	3	1.0	63.7
203	M	8	C	9/11/2014	19:35	4	1.0	61.62
203	M	9	C	9/11/2014	23:35	8	1.0	53.13
203	M	10	C	9/12/2014	3:35	12	1.0	46.91
203	M	11	C	9/12/2014	15:35	24	1.0	33.12
203	M	12	C	9/13/2014	15:35	48	1.0	18.42
203	M	13	C	9/14/2014	15:35	72	1.0	10.52

204	M	1	C	1/26/2015	12:01	0.02	1.0	36.75
204	M	2	C	1/26/2015	12:05	0.08	1.0	35.96
204	M	3	C	1/26/2015	12:15	0.25	1.0	35.05
204	M	4	C	1/26/2015	12:30	0.5	1.0	35.17
204	M	5	C	1/26/2015	13:00	1	1.0	35.56
204	M	6	C	1/26/2015	14:00	2	1.0	36.23
204	M	7	C	1/26/2015	15:00	3	1.0	32.08
204	M	8	C	1/26/2015	16:00	4	1.0	31.26
204	M	9	C	1/26/2015	20:00	8	1.0	28.29
204	M	10	C	1/27/2015	0:00	12	1.0	26.42
204	M	11	C	1/27/2015	12:00	24	1.0	23.01
204	M	12	C	1/28/2015	12:00	48	1.0	20.35
204	M	13	C	1/29/2015	12:00	72	1.0	17.17
251	M	1	H	9/11/2014	14:33	0.02	1.0	0.07
251	M	5	H	9/11/2014	15:30	1	1.0	0.06
251	M	6	H	9/11/2014	16:30	2	1.0	0.21
251	M	11	H	9/13/2014	14:30	24	1.0	0.16
251	M	13	H	9/14/2014	14:30	72	1.0	0.34

Define

circuit	Circuit number
drug	B – amphotericin B deoxycholate F – fluconazole M - micafungin
samp	sample number
site	A – arterial C – control H - hemofiltrate V- venous
date	MM/DD/YYY
time	HH:MM
nom_time	Nominal sampling time (h)
dose_no	Done number
amt	Amount of dose (mg)
flow	ECMO flow rate (l/min)
dv	Concentration (mg/L)

APPENDIX 2

Fluconazole data

ORDN	ID	ECMO	WT	PNA	GA	RACE	SEX	SCRE	ALBE	ASTE	ALTE	HMFLTRE
1	1	0	3.48	19	36	0	0	1.2	2.3	82	32	0
2	1	0	3.48	19	36	0	0	1.2	2.3	82	32	0
3	1	0	3.48	19	36	0	0	1.2	2.3	82	32	0
4	1	0	3.48	19	36	0	0	1.2	2.3	82	32	0
5	1	0	3.48	19	36	0	0	0.9	2.3	39	27	0
6	1	0	3.48	19	36	0	0	0.9	2.3	39	27	0
7	1	0	3.48	19	36	0	0	0.9	2.3	39	27	0
8	1	0	3.48	19	36	0	0	0.9	2.3	39	27	0
9	1	0	3.48	19	36	0	0	0.9	2.3	39	27	0
10	1	0	3.48	19	36	0	0	0.9	2.3	39	27	0
11	1	0	3.48	19	36	0	0	0.9	2.3	29	16	0
12	1	0	3.48	19	36	0	0	0.9	2.3	29	16	0
13	1	0	3.48	19	36	0	0	0.8	2.3	29	16	0
14	1	0	3.48	19	36	0	0	0.8	2.3	29	16	0
15	1	0	3.48	19	36	0	0	0.8	2.3	29	16	0
16	1	0	3.48	19	36	0	0	0.8	2.3	29	16	0
17	2	0	3.00	14	39	0	1	0.5	2.0	35	79	0
18	2	0	3.00	14	39	0	1	0.5	2.0	35	79	0
19	2	0	3.00	14	39	0	1	0.5	2.0	35	79	0
20	2	0	3.00	14	39	0	1	0.5	2.0	35	79	0
21	2	0	3.00	14	39	0	1	0.4	2.0	35	79	0
22	2	0	3.00	14	39	0	1	0.4	2.0	35	79	0
23	2	0	3.00	14	39	0	1	0.4	2.0	35	79	0
24	2	0	3.00	14	39	0	1	0.3	2.0	35	79	0

25	2	0	3.00	14	39	0	1	0.3	2.0	35	79	0
26	2	0	3.00	14	39	0	1	0.3	2.0	35	79	0
27	2	0	3.00	14	39	0	1	0.3	2.0	35	79	0
28	2	0	3.00	14	39	0	1	0.3	2.0	35	79	0
29	3	0	1.00	5	28	0	1	0.7	2.7	16	5	0
30	3	0	1.00	5	28	0	1	0.7	2.7	16	5	0
31	3	0	1.00	5	28	0	1	0.7	2.7	16	5	0
32	3	0	1.00	5	28	0	1	0.7	2.7	16	5	0
33	3	0	1.00	5	28	0	1	0.7	2.7	16	5	0
34	4	0	2.69	13	37	0	0	1.3	2.2	25	10	0
35	4	0	2.69	13	37	0	0	1.3	2.2	25	10	0
36	4	0	2.69	13	37	0	0	1.3	2.2	25	10	0
37	4	0	2.69	13	37	0	0	1.3	2.2	25	10	0
38	4	0	2.69	13	37	0	0	1.3	2.4	12	8	0
39	4	0	2.69	13	37	0	0	1.3	2.4	12	8	0
40	4	0	2.69	13	37	0	0	1.3	2.4	12	8	0
41	4	0	2.69	13	37	0	0	0.8	2.4	12	8	0
42	4	0	2.69	13	37	0	0	1.0	2.0	12	8	0
43	4	0	2.69	13	37	0	0	1.0	2.0	12	8	0
44	4	0	2.69	13	37	0	0	1.0	2.0	12	8	0
45	4	0	2.69	13	37	0	0	1.0	2.0	12	8	0
46	4	0	2.69	13	37	0	0	1.0	2.0	12	8	0
47	4	0	2.69	13	37	0	0	0.7	2.0	12	8	0
48	4	0	2.69	13	37	0	0	0.8	2.8	12	8	0
49	4	0	2.69	13	37	0	0	0.8	2.8	12	8	0
50	4	0	2.69	13	37	0	0	0.8	2.8	12	8	0
51	4	0	2.69	13	37	0	0	0.8	2.8	12	8	0
52	5	0	2.83	55	33	1	0	0.3	2.7	50	65	0
53	5	0	2.83	55	33	1	0	0.3	2.7	50	65	0

54	5	0	2.83	55	33	1	0	0.3	2.7	50	65	0
55	5	0	2.83	55	33	1	0	0.3	2.7	50	65	0
56	5	0	2.83	55	33	1	0	0.4	2.7	50	65	0
57	5	0	2.83	55	33	1	0	0.4	2.7	50	65	0
58	5	0	2.83	55	33	1	0	0.4	2.7	50	65	0
59	5	0	2.83	55	33	1	0	0.4	2.4	62	69	0
60	5	0	2.83	55	33	1	0	0.4	2.4	62	69	0
61	5	0	2.83	55	33	1	0	0.4	2.4	62	69	0
62	5	0	2.83	55	33	1	0	0.4	2.4	62	69	0
63	5	0	2.83	55	33	1	0	0.4	2.4	62	69	0
64	5	0	2.83	55	33	1	0	0.4	2.8	53	71	0
65	5	0	2.83	55	33	1	0	0.4	2.8	53	71	0
66	5	0	2.83	55	33	1	0	0.4	2.8	53	71	0
67	5	0	2.83	55	33	1	0	0.4	2.8	53	71	0
68	6	0	8.00	262	34	1	0	0.4	3.1	26	21	0
69	6	0	8.00	262	34	1	0	0.4	3.1	26	21	0
70	6	0	8.00	262	34	1	0	0.4	3.1	26	21	0
71	6	0	8.00	262	34	1	0	0.4	3.1	26	21	0
72	6	0	8.00	262	34	1	0	0.5	3.1	26	21	0
73	6	0	8.00	262	34	1	0	0.5	3.1	26	21	0
74	6	0	8.00	262	34	1	0	0.5	3.1	26	21	0
75	6	0	8.00	262	34	1	0	0.6	3.1	20	21	0
76	6	0	8.00	262	34	1	0	0.6	3.1	20	21	0
77	6	0	8.00	262	34	1	0	0.6	3.1	20	21	0
78	6	0	8.00	262	34	1	0	0.6	3.1	20	21	0
79	6	0	8.00	262	34	1	0	0.6	3.1	20	21	0
80	6	0	8.00	262	34	1	0	0.6	3.1	20	21	0
81	6	0	8.00	262	34	1	0	0.6	3.1	20	21	0
82	6	0	8.00	262	34	1	0	0.6	3.1	20	21	0

83	7	0	2.06	6	34	1	1	1.0	2.0	18	9	0
84	7	0	2.06	6	34	1	1	1.0	2.0	18	9	0
85	7	0	2.06	6	34	1	1	1.0	2.0	18	9	0
86	7	0	2.06	6	34	1	1	1.0	2.0	18	9	0
87	7	0	2.06	6	34	1	1	1.0	2.0	18	9	0
88	7	0	2.06	6	34	1	1	1.0	2.0	18	9	0
89	7	0	2.06	6	34	1	1	1.0	2.0	18	9	0
90	7	0	2.06	6	34	1	1	0.8	2.0	18	9	0
91	7	0	2.06	6	34	1	1	0.8	2.0	18	9	0
92	7	0	2.06	6	34	1	1	0.8	2.0	18	9	0
93	7	0	2.06	6	34	1	1	0.6	2.2	15	8	0
94	7	0	2.06	6	34	1	1	0.6	2.2	15	8	0
95	7	0	2.06	6	34	1	1	0.6	2.2	15	8	0
96	7	0	2.06	6	34	1	1	0.6	2.2	15	8	0
97	8	0	7.16	257	39	1	0	0.2	2.8	35	16	0
98	8	0	7.16	257	39	1	0	0.2	2.8	35	16	0
99	8	0	7.16	257	39	1	0	0.2	2.8	35	16	0
100	8	0	7.16	257	39	1	0	0.2	2.8	35	16	0
101	8	0	7.16	257	39	1	0	0.2	2.8	35	16	0
102	8	0	7.16	257	39	1	0	0.2	2.8	35	16	0
103	8	0	7.16	257	39	1	0	0.2	2.8	27	12	0
104	8	0	7.16	257	39	1	0	0.2	2.8	27	12	0
105	8	0	7.16	257	39	1	0	0.2	2.8	27	12	0
106	8	0	7.16	257	39	1	0	0.2	2.8	27	12	0
107	8	0	7.16	257	39	1	0	0.2	2.8	27	12	0
108	8	0	7.16	257	39	1	0	0.2	2.8	27	12	0
109	8	0	7.16	257	39	1	0	0.2	2.8	27	12	0
110	8	0	7.16	257	39	1	0	0.2	2.8	27	12	0
111	9	0	1.88	155	24	1	1	1.3	1.1	159	126	0

112	9	0	1.88	155	24	1	1	1.3	1.1	159	126	0
113	9	0	1.88	155	24	1	1	1.3	1.1	159	126	0
114	9	0	1.88	155	24	1	1	1.3	1.1	159	126	0
115	9	0	1.88	155	24	1	1	1.3	1.1	159	126	0
116	9	0	1.88	155	24	1	1	1.3	1.1	159	126	0
117	9	0	1.88	155	24	1	1	1.3	1.1	159	126	0
118	9	0	1.88	155	24	1	1	1.3	1.1	159	126	0
119	9	0	1.88	155	24	1	1	1.3	1.1	159	126	0
120	9	0	1.88	155	24	1	1	1.3	1.1	159	126	0
121	9	0	1.88	155	24	1	1	1.3	1.1	159	126	0
122	9	0	1.88	155	24	1	1	1.3	1.1	159	126	0
123	9	0	1.88	155	24	1	1	1.3	1.1	159	126	0
124	10	0	4.30	59	37	0	1	0.2	2.7	35	19	0
125	10	0	4.30	59	37	0	1	0.2	2.7	35	19	0
126	10	0	4.30	59	37	0	1	0.2	2.7	35	19	0
127	10	0	4.30	59	37	0	1	0.2	2.7	35	19	0
128	10	0	4.30	59	37	0	1	0.2	2.7	35	19	0
129	10	0	4.30	59	37	0	1	0.2	2.7	35	19	0
130	10	0	4.30	59	37	0	1	0.2	2.7	35	19	0
131	10	0	4.30	59	37	0	1	0.2	2.7	35	19	0
132	10	0	4.30	59	37	0	1	0.2	2.7	35	19	0
133	10	0	4.30	59	37	0	1	0.2	2.7	35	19	0
134	10	0	4.30	59	37	0	1	0.2	2.7	35	19	0
135	10	0	4.30	59	37	0	1	0.2	2.7	35	19	0
136	10	0	4.30	59	37	0	1	0.2	2.7	35	19	0
137	11	0	2.93	18	38	1	1	0.2	2.7	16	11	0
138	11	0	2.93	18	38	1	1	0.2	2.7	16	11	0
139	11	0	2.93	18	38	1	1	0.2	2.7	16	11	0
140	11	0	2.93	18	38	1	1	0.2	2.7	16	11	0

141	11	0	2.93	18	38	1	1	0.2	2.7	16	11	0
142	11	0	2.93	18	38	1	1	0.2	2.7	16	11	0
143	11	0	2.93	18	38	1	1	0.2	2.7	16	11	0
144	11	0	2.93	18	38	1	1	0.2	2.7	16	11	0
145	11	0	2.93	18	38	1	1	0.2	2.7	16	11	0
146	11	0	2.93	18	38	1	1	0.2	2.7	16	11	0
147	11	0	2.93	18	38	1	1	0.2	2.7	16	11	0
148	11	0	2.93	18	38	1	1	0.2	2.7	16	11	0
149	12	0	4.59	36	39	1	0	0.5	3.1	24	14	0
150	12	0	4.59	36	39	1	0	0.5	3.1	24	14	0
151	12	0	4.59	36	39	1	0	0.5	3.1	24	14	0
152	12	0	4.59	36	39	1	0	0.5	3.1	24	14	0
153	12	0	4.59	36	39	1	0	0.5	3.1	24	14	0
154	12	0	4.59	36	39	1	0	0.5	3.1	24	14	0
155	12	0	4.59	36	39	1	0	0.5	3.1	24	14	0
156	12	0	4.59	36	39	1	0	0.5	3.1	24	14	0
157	12	0	4.59	36	39	1	0	0.5	3.1	24	14	0
158	12	0	4.59	36	39	1	0	0.5	3.1	24	14	0
159	12	0	4.59	36	39	1	0	0.5	3.1	24	14	0
160	13	1	3.11	14	38	1	1	0.8	1.7	22	10	1
161	13	1	3.11	14	38	1	1	0.8	1.7	22	10	1
162	13	1	3.11	14	38	1	1	0.8	1.7	22	10	1
163	13	1	3.11	14	38	1	1	0.8	1.7	22	10	1
164	13	1	3.11	14	38	1	1	1.1	2.6	32	9	1
165	13	1	3.11	14	38	1	1	1.1	2.6	32	9	1
166	13	1	3.11	14	38	1	1	1.1	2.6	32	9	1
167	13	1	3.11	14	38	1	1	1.6	2.6	32	9	1
168	13	1	3.11	14	38	1	1	1.6	2.6	32	9	1
169	13	1	3.11	14	38	1	1	1.6	2.6	32	9	1

170	13	1	3.11	14	38	1	1	1.6	2.6	32	9	1
171	14	0	7.13	64	40	0	1	0.4	2.7	35	19	0
172	14	0	7.14	64	40	0	1	0.1	2.7	35	19	0
173	14	0	7.14	64	40	0	1	0.4	2.7	35	19	0
174	15	0	2.96	9	37	0	1	0.1	2.7	35	19	0
175	15	0	2.90	9	37	0	1	0.1	2.7	35	19	0
176	15	0	2.90	9	37	0	1	0.1	2.7	35	19	0
177	15	0	2.90	9	37	0	1	0.1	2.7	35	19	0
178	15	0	2.90	9	37	0	1	0.1	2.7	35	19	0
179	15	0	2.86	9	37	0	1	0.1	2.7	35	19	0
180	15	0	2.86	9	37	0	1	0.1	2.7	35	19	0
181	15	0	2.86	9	37	0	1	0.1	2.7	35	19	0
182	15	0	3.10	9	37	0	1	0.1	2.7	35	19	0
183	15	0	3.10	9	37	0	1	0.1	2.7	35	19	0
184	15	0	2.93	9	37	0	1	0.5	2.7	35	19	0
185	15	0	3.04	9	37	0	1	0.1	2.7	35	19	0
186	15	0	2.97	9	37	0	1	0.1	2.7	35	19	0
187	15	0	3.02	9	37	0	1	0.1	2.7	35	19	0
188	15	0	3.02	9	37	0	1	0.1	2.7	35	19	0
189	15	0	3.33	9	37	0	1	0.1	2.7	35	19	0
190	15	0	3.33	9	37	0	1	0.1	2.7	35	19	0
191	15	0	3.27	9	37	0	1	0.1	2.7	35	19	0
192	15	0	3.46	9	37	0	1	0.1	2.7	35	19	0
193	15	0	3.50	9	37	0	1	0.1	2.7	35	19	0
194	15	0	3.53	9	37	0	1	0.1	2.7	35	19	0
195	15	0	3.56	9	37	0	1	0.1	2.7	35	19	0
196	15	0	3.56	9	37	0	1	0.1	2.7	35	19	0
197	16	0	2.30	25	36	1	1	0.1	2.7	35	19	0
198	16	0	2.30	25	36	1	1	0.1	2.7	35	19	0

199	16	0	2.30	25	36	1	1	0.1	2.7	35	19	0
200	16	0	2.30	25	36	1	1	0.1	2.7	35	19	0
201	16	0	2.30	25	36	1	1	0.1	2.7	35	19	0
202	16	0	2.30	25	36	1	1	0.1	2.7	35	19	0
203	16	0	2.30	25	36	1	1	0.1	2.7	35	19	0
204	16	0	2.15	25	36	1	1	0.1	2.7	35	19	0
205	16	0	2.26	25	36	1	1	0.1	2.7	35	19	0
206	16	0	2.28	25	36	1	1	0.1	2.7	35	19	0
207	16	0	2.55	25	36	1	1	0.1	2.7	35	19	0
208	16	0	2.22	25	36	1	1	0.1	2.7	35	19	0
209	16	0	2.53	25	36	1	1	0.1	2.7	35	19	0
210	16	0	2.40	25	36	1	1	0.1	2.7	35	19	0
211	16	0	2.51	25	36	1	1	0.1	2.7	35	19	0
212	16	0	2.51	25	36	1	1	0.1	2.7	35	19	0
213	16	0	2.51	25	36	1	1	0.1	2.7	35	19	0
214	16	0	2.51	25	36	1	1	0.1	2.7	35	19	0
215	16	0	2.59	25	36	1	1	0.1	2.7	35	19	0
216	16	0	2.59	25	36	1	1	0.1	2.7	35	19	0
217	16	0	2.59	25	36	1	1	0.1	2.7	35	19	0
218	16	0	2.72	25	36	1	1	0.1	2.7	35	19	0
219	16	0	2.72	25	36	1	1	0.1	2.7	35	19	0
220	16	0	2.97	25	36	1	1	0.1	2.7	35	19	0
221	16	0	2.80	25	36	1	1	0.6	2.7	35	19	0
222	16	0	2.75	25	36	1	1	0.1	2.7	35	19	0
223	16	0	2.94	25	36	1	1	0.1	2.7	35	19	0
224	16	0	2.94	25	36	1	1	0.1	2.7	35	19	0
225	16	0	2.89	25	36	1	1	0.1	2.7	35	19	0
226	16	0	2.89	25	36	1	1	0.1	2.7	35	19	0
227	16	0	2.89	25	36	1	1	0.1	2.7	35	19	0

228	16	0	2.89	25	36	1	1	0.1	2.7	35	19	0
229	16	0	3.16	25	36	1	1	0.4	2.7	35	19	0
230	16	0	3.36	25	36	1	1	0.1	2.7	35	19	0
231	16	0	3.39	25	36	1	1	0.4	2.7	35	19	0
232	16	0	3.39	25	36	1	1	0.4	2.7	35	19	0
233	16	0	3.65	25	36	1	1	0.1	2.7	35	19	0
234	16	0	3.67	25	36	1	1	0.1	2.7	35	19	0
235	16	0	3.17	25	36	1	1	0.1	2.7	35	19	0
236	16	0	3.17	25	36	1	1	0.1	2.7	35	19	0
237	16	0	3.15	25	36	1	1	0.4	2.7	35	19	0
238	16	0	3.29	25	36	1	1	0.4	2.7	35	19	0
239	16	0	3.29	25	36	1	1	0.1	2.7	35	19	0
240	17	0	3.18	6	39	0	1	0.7	2.7	35	19	0
241	17	0	3.18	6	39	0	1	0.7	2.7	35	19	0
242	17	0	3.18	6	39	0	1	0.7	2.7	35	19	0
243	17	0	3.18	6	39	0	1	0.7	2.7	35	19	0
244	17	0	3.41	6	39	0	1	0.1	2.7	35	19	0
245	17	0	3.50	6	39	0	1	0.6	2.7	35	19	0
246	17	0	3.50	6	39	0	1	0.6	2.7	35	19	0
247	17	0	3.80	6	39	0	1	0.4	2.7	35	19	0
248	17	0	4.38	6	39	0	1	0.1	2.7	35	19	0
249	17	0	4.38	6	39	0	1	0.1	2.7	35	19	0
250	18	0	3.55	78	36	2	1	0.1	2.7	35	19	0
251	18	0	3.35	78	36	2	1	0.1	2.7	35	19	0
252	18	0	3.35	78	36	2	1	0.1	2.7	35	19	0
253	18	0	3.55	78	36	2	1	0.1	2.7	35	19	0
254	18	0	3.55	78	36	2	1	0.1	2.7	35	19	0
255	18	0	3.88	78	36	2	1	0.1	2.7	35	19	0
256	18	0	3.88	78	36	2	1	0.1	2.7	35	19	0

257	18	0	3.89	78	36	2	1	0.1	2.7	35	19	0
258	18	0	3.89	78	36	2	1	0.1	2.7	35	19	0
259	18	0	3.89	78	36	2	1	0.1	2.7	35	19	0
260	18	0	3.89	78	36	2	1	0.1	2.7	35	19	0
261	18	0	3.89	78	36	2	1	0.1	2.7	35	19	0
262	19	0	3.39	16	38	2	1	0.1	2.7	35	19	0
263	19	0	3.38	16	38	2	1	0.1	2.7	35	19	0
264	19	0	3.31	16	38	2	1	0.1	2.7	35	19	0
265	19	0	3.32	16	38	2	1	0.1	2.7	35	19	0
266	19	0	3.21	16	38	2	1	0.1	2.7	35	19	0
267	19	0	3.12	16	38	2	1	0.1	2.7	35	19	0
268	19	0	3.19	16	38	2	1	0.1	2.7	35	19	0
269	19	0	3.19	16	38	2	1	0.1	2.7	35	19	0
270	20	0	3.89	20	39	0	1	0.1	2.7	35	19	0
271	20	0	3.87	20	39	0	1	0.1	2.7	35	19	0
272	20	0	3.79	20	39	0	1	0.1	2.7	35	19	0
273	20	0	3.70	20	39	0	1	0.1	2.7	35	19	0
274	20	0	3.68	20	39	0	1	0.1	2.7	35	19	0
275	20	0	3.68	20	39	0	1	0.1	2.7	35	19	0
276	20	0	3.68	20	39	0	1	0.1	2.7	35	19	0
277	20	0	3.68	20	39	0	1	0.1	2.7	35	19	0
278	20	0	3.68	20	39	0	1	0.1	2.7	35	19	0
279	20	0	3.58	20	39	0	1	0.1	2.7	35	19	0
280	20	0	3.58	20	39	0	1	0.1	2.7	35	19	0
281	20	0	3.50	20	39	0	1	0.1	2.7	35	19	0
282	20	0	3.50	20	39	0	1	0.1	2.7	35	19	0
283	20	0	3.53	20	39	0	1	0.1	2.7	35	19	0
284	20	0	3.43	20	39	0	1	0.3	2.7	35	19	0
285	20	0	3.43	20	39	0	1	0.3	2.7	35	19	0

286	20	0	3.48	20	39	0	1	0.1	2.7	35	19	0
287	20	0	3.32	20	39	0	1	0.1	2.7	35	19	0
288	20	0	3.38	20	39	0	1	0.1	2.7	35	19	0
289	20	0	3.30	20	39	0	1	0.1	2.7	35	19	0
290	20	0	3.26	20	39	0	1	0.1	2.7	35	19	0
291	20	0	3.46	20	39	0	1	0.1	2.7	35	19	0
292	20	0	3.48	20	39	0	1	0.3	2.7	35	19	0
293	20	0	3.48	20	39	0	1	0.3	2.7	35	19	0
294	21	0	3.91	40	37	0	1	0.1	2.7	35	19	0
295	21	0	3.91	40	37	0	1	0.1	2.7	35	19	0
296	21	0	3.91	40	37	0	1	0.1	2.7	35	19	0
297	21	0	3.62	40	37	0	1	0.3	2.7	35	19	0
298	21	0	3.62	40	37	0	1	0.3	2.7	35	19	0
299	22	0	2.23	4	38	2	0	0.1	2.7	35	19	0
300	22	0	2.23	4	38	2	0	0.9	2.7	35	19	0
301	22	0	2.35	4	38	2	0	0.7	2.7	35	19	0
302	22	0	2.35	4	38	2	0	0.7	2.7	35	19	0
303	22	0	2.35	4	38	2	0	0.7	2.7	35	19	0
304	22	0	2.35	4	38	2	0	0.7	2.7	35	19	0
305	22	0	2.35	4	38	2	0	0.7	2.7	35	19	0
306	22	0	2.35	4	38	2	0	0.7	2.7	35	19	0
307	22	0	2.35	4	38	2	0	0.5	2.7	35	19	0
308	22	0	2.35	4	38	2	0	0.5	2.7	35	19	0
309	22	0	2.37	4	38	2	0	0.5	2.7	35	19	0
310	22	0	2.37	4	38	2	0	0.5	2.7	35	19	0
311	22	0	2.36	4	38	2	0	0.4	2.7	35	19	0
312	22	0	2.36	4	38	2	0	0.4	2.7	35	19	0
313	22	0	2.25	4	38	2	0	0.4	2.7	35	19	0
314	22	0	2.21	4	38	2	0	0.1	2.7	35	19	0

315	22	0	2.21	4	38	2	0	0.1	2.7	35	19	0
316	22	0	2.20	4	38	2	0	0.4	2.7	35	19	0
317	22	0	2.22	4	38	2	0	0.1	2.7	35	19	0
318	23	1	3.16	24	38	1	0	0.6	4.0	113	38	1
319	23	1	3.16	24	38	1	0	0.6	4.0	113	38	1
320	23	1	3.16	24	38	1	0	0.6	4.0	113	38	1
321	23	1	3.16	24	38	1	0	0.6	4.0	113	38	1
322	23	1	3.16	24	38	1	0	0.6	4.0	113	38	1
323	23	1	3.16	24	38	1	0	0.6	4.0	131	44	1
324	23	1	3.16	24	38	1	0	0.6	4.0	131	44	1
325	23	1	3.16	24	38	1	0	0.6	4.0	131	44	1
326	23	1	3.16	24	38	1	0	0.4	4.0	155	58	1
327	23	1	3.16	24	38	1	0	0.4	4.0	155	58	1
328	23	1	3.16	24	38	1	0	0.4	4.0	155	58	1
329	23	1	3.16	24	38	1	0	0.4	4.0	155	58	1
330	23	1	3.16	24	38	1	0	0.6	4.0	208	79	1
331	23	1	3.16	24	38	1	0	0.6	4.0	208	79	1
332	23	1	3.16	24	38	1	0	0.6	4.0	208	79	1
333	23	1	3.16	24	38	1	0	0.6	4.0	208	79	1
334	23	1	3.16	24	38	1	0	0.6	4.0	208	79	1
335	23	1	3.16	24	38	1	0	0.6	4.0	208	79	1
336	23	1	3.16	24	38	1	0	0.6	4.0	208	79	1
337	23	1	3.16	24	38	1	0	0.6	4.0	208	79	1
338	23	1	3.16	24	38	1	0	0.6	4.0	208	79	1
339	23	1	3.16	24	38	1	0	0.6	4.0	208	79	1
340	23	1	3.16	24	38	1	0	0.5	4.0	192	80	1
341	23	1	3.16	24	38	1	0	0.6	4.0	208	79	1
342	23	1	3.16	24	38	1	0	0.5	4.0	192	80	1
343	23	1	3.16	24	38	1	0	0.5	4.0	192	80	1

344	23	1	3.16	24	38	1	0	0.5	4.0	192	80	1
345	23	1	3.16	24	38	1	0	0.5	4.0	198	90	1
346	23	1	3.16	24	38	1	0	0.5	4.0	198	90	1
347	23	1	3.16	24	38	1	0	0.5	4.0	198	90	1
348	24	1	3.40	20	40	0	1	0.4	1.2	452	62	1
349	24	1	3.40	20	40	0	1	0.4	1.2	452	62	1
350	24	1	3.40	20	40	0	1	0.4	1.2	452	62	1
351	24	1	3.40	20	40	0	1	0.4	1.2	452	62	1
352	24	1	3.40	20	40	0	1	0.4	1.2	452	62	1
353	24	1	3.40	20	40	0	1	0.4	1.4	452	45	1
354	24	1	3.40	20	40	0	1	0.4	1.4	452	45	1
355	24	1	3.40	20	40	0	1	0.4	1.4	452	45	1
356	24	1	3.40	20	40	0	1	0.4	1.4	452	45	1
357	24	1	3.40	20	40	0	1	0.4	1.4	452	45	1
358	24	1	3.40	20	40	0	1	0.4	1.6	452	43	1
359	24	1	3.40	20	40	0	1	0.4	1.6	452	43	1
360	24	1	3.40	20	40	0	1	0.4	1.6	452	43	1
361	24	1	3.40	20	40	0	1	0.6	1.6	452	80	1
362	24	1	3.40	20	40	0	1	0.9	1.6	455	80	1
363	24	1	3.40	20	40	0	1	0.5	1.8	781	103	1
364	24	1	3.40	20	40	0	1	0.7	2.2	781	103	1
365	24	1	3.40	20	40	0	1	0.8	2.2	1602	164	1
366	24	1	3.40	20	40	0	1	1.2	1.9	1386	156	1
367	24	1	3.40	20	40	0	1	1.5	2.2	996	145	1
368	24	1	3.40	20	40	0	1	1.5	2.2	996	145	1
369	24	1	3.40	20	40	0	1	1.5	2.2	996	145	1
370	24	1	3.40	20	40	0	1	1.5	2.2	996	145	1
371	24	1	3.40	20	40	0	1	1.5	2.2	996	145	1
372	24	1	3.40	20	40	0	1	1.5	2.2	996	145	1

373	24	1	3.40	20	40	0	1	1.5	2.2	996	145	1
374	24	1	3.40	20	40	0	1	1.5	2.2	996	145	1
375	24	1	3.40	20	40	0	1	1.5	2.2	996	145	1
376	24	1	3.40	20	40	0	1	1.5	2.2	996	145	1
377	24	1	3.40	20	40	0	1	1.7	2.2	870	155	1
378	24	1	3.40	20	40	0	1	1.7	2.2	870	155	1
379	24	1	3.40	20	40	0	1	1.7	2.2	870	155	1
380	24	1	3.40	20	40	0	1	2.2	2.6	731	149	1
381	24	1	3.40	20	40	0	1	2.2	2.6	731	149	1
382	24	1	3.40	20	40	0	1	2.2	2.6	731	149	1
383	24	1	3.40	20	40	0	1	2.3	2.6	409	107	1
384	24	1	3.40	20	40	0	1	2.7	2.6	284	105	1
385	24	1	3.40	20	40	0	1	2.8	2.6	284	105	1
386	24	1	3.40	20	40	0	1	3.2	3.0	175	93	1
387	24	1	3.40	20	40	0	1	3.2	3.0	175	93	1
388	24	1	3.40	20	40	0	1	3.2	3.0	175	93	1
389	25	1	7.00	165	39	1	1	0.3	3.5	51	18	0
390	25	1	7.00	165	39	1	1	0.3	3.5	51	18	0
391	25	1	7.00	165	39	1	1	0.3	3.5	51	18	0
392	25	1	7.00	165	39	1	1	0.2	3.5	34	14	0
393	25	1	7.00	165	39	1	1	0.2	3.5	34	14	0
394	25	1	7.00	165	39	1	1	0.2	3.5	34	14	0
395	25	1	7.00	165	39	1	1	0.2	3.5	34	14	0
396	25	1	7.00	165	39	1	1	0.2	3.5	34	14	0
397	25	1	7.00	165	39	1	1	0.2	3.5	34	14	0
398	25	1	7.00	165	39	1	1	0.2	3.5	34	14	0
399	25	1	7.00	165	39	1	1	0.2	3.5	34	14	0
400	25	1	7.00	165	39	1	1	0.2	3.5	30	14	0
401	25	1	7.00	165	39	1	1	0.2	3.5	30	14	0

402	25	1	7.00	165	39	1	1	0.2	3.5	30	14	0
403	25	1	7.00	165	39	1	1	0.2	3.5	30	14	0
404	25	1	7.00	165	39	1	1	0.3	3.5	36	14	0
405	25	1	7.00	165	39	1	1	0.3	3.5	36	14	0
406	25	1	7.00	165	39	1	1	0.1	3.5	15	9	0
407	25	1	7.00	165	39	1	1	0.3	3.5	24	11	0
408	25	1	7.00	165	39	1	1	0.3	3.5	24	11	0
409	25	1	7.00	165	39	1	1	0.3	3.5	24	11	0
410	26	1	2.01	18	38	0	1	0.9	2.2	23	14	0
411	26	1	2.01	18	38	0	1	0.9	2.2	23	14	0
412	26	1	2.01	18	38	0	1	0.9	2.2	23	14	0
413	26	1	2.01	18	38	0	1	0.9	2.2	23	14	0
414	26	1	2.01	18	38	0	1	0.9	2.2	23	14	0
415	26	1	2.01	18	38	0	1	0.9	2.2	23	14	0
416	26	1	2.01	18	38	0	1	0.9	2.2	23	14	0
417	26	1	2.01	18	38	0	1	0.9	2.2	23	14	0
418	26	1	2.01	18	38	0	1	0.9	2.2	23	14	0
419	26	1	2.01	18	38	0	1	0.9	2.2	23	14	0
420	26	1	2.01	18	38	0	1	0.9	2.2	23	14	0
421	26	1	2.01	18	38	0	1	0.9	2.2	23	14	0
422	26	1	2.01	18	38	0	1	0.8	2.2	23	14	0
423	26	1	2.01	18	38	0	1	0.8	2.2	23	14	0
424	26	1	2.01	18	38	0	1	0.8	2.2	23	14	0
425	26	1	2.01	18	38	0	1	0.8	2.2	23	14	0
426	26	1	2.01	18	38	0	1	0.7	2.2	23	14	0
427	26	1	2.01	18	38	0	1	0.7	2.2	23	14	0
428	27	1	2.44	32	34	0	1	0.7	2.1	59	10	0
429	27	1	2.44	32	34	0	1	0.7	2.1	59	10	0
430	27	1	2.44	32	34	0	1	0.7	2.1	59	10	0

431	27	1	2.44	32	34	0	1	0.7	2.1	59	10	0
432	27	1	2.44	32	34	0	1	0.7	2.1	59	10	0
433	27	1	2.44	32	34	0	1	0.7	2.1	59	10	0
434	27	1	2.44	32	34	0	1	0.7	2.1	59	10	0
435	27	1	2.44	32	34	0	1	0.7	2.1	59	10	0
436	27	1	2.44	32	34	0	1	0.7	2.1	59	10	0
437	27	1	2.44	32	34	0	1	0.7	2.1	59	10	0
438	27	1	2.44	32	34	0	1	0.7	2.1	73	33	0
439	27	1	2.44	32	34	0	1	0.7	2.1	73	33	0
440	27	1	2.44	32	34	0	1	0.7	2.1	73	33	0
441	28	1	2.70	1	36	0	0	1.0	1.9	39	12	0
442	28	1	2.70	1	36	0	0	1.0	2.4	42	5	0
443	28	1	2.70	1	36	0	0	1.0	2.4	42	5	0
444	28	1	2.70	1	36	0	0	1.0	2.4	42	5	0
445	28	1	2.70	1	36	0	0	1.0	2.4	42	5	0
446	28	1	2.70	1	36	0	0	1.0	2.4	42	5	0
447	28	1	2.70	1	36	0	0	1.0	2.4	42	5	0
448	28	1	2.70	1	36	0	0	1.0	2.4	42	5	0
449	28	1	2.70	1	36	0	0	1.0	2.4	42	5	0
450	28	1	2.70	1	36	0	0	1.0	2.4	42	5	0
451	28	1	2.70	1	36	0	0	1.0	2.4	42	5	0
452	28	1	2.70	1	36	0	0	0.9	2.8	42	5	0
453	28	1	2.70	1	36	0	0	0.9	2.8	42	5	0
454	28	1	2.70	1	36	0	0	0.9	2.8	42	5	0
455	28	1	2.70	1	36	0	0	0.8	2.5	85	11	0
456	28	1	2.70	1	36	0	0	0.9	2.5	85	11	0
457	28	1	2.70	1	36	0	0	0.9	2.2	112	15	0
458	28	1	2.70	1	36	0	0	0.9	2.2	112	15	0
459	28	1	2.70	1	36	0	0	0.9	2.2	35	9	0

460	28	1	2.70	1	36	0	0	0.9	2.2	35	9	0
461	28	1	2.70	1	36	0	0	0.9	2.2	35	9	0
462	28	1	2.70	1	36	0	0	0.9	2.2	35	9	0
463	28	1	2.70	1	36	0	0	0.9	2.2	35	9	0
464	28	1	2.70	1	36	0	0	0.9	2.2	35	9	0
465	28	1	2.70	1	36	0	0	0.9	2.2	35	9	0
466	28	1	2.70	1	36	0	0	0.9	2.2	35	9	0
467	28	1	2.70	1	36	0	0	0.9	2.2	35	9	0
468	28	1	2.70	1	36	0	0	0.9	2.2	35	9	0
469	28	1	2.70	1	36	0	0	0.8	3.0	35	9	0
470	28	1	2.70	1	36	0	0	0.8	3.0	35	9	0
471	28	1	2.70	1	36	0	0	0.8	3.0	35	9	0
472	28	1	2.70	1	36	0	0	0.8	2.6	35	9	0
473	28	1	2.70	1	36	0	0	0.8	2.6	35	9	0
474	28	1	2.70	1	36	0	0	0.8	2.6	35	9	0
475	29	1	3.20	7	38	2	0	0.5	2.0	31	15	0
476	29	1	3.20	7	38	2	0	0.5	2.0	31	15	0
477	29	1	3.20	7	38	2	0	0.5	2.0	31	15	0
478	29	1	3.20	7	38	2	0	0.5	2.0	31	15	0
479	29	1	3.20	7	38	2	0	0.5	2.0	31	15	0
480	29	1	3.20	7	38	2	0	0.5	2.0	31	15	0
481	29	1	3.20	7	38	2	0	0.5	2.7	31	15	0
482	29	1	3.20	7	38	2	0	0.5	2.7	31	15	0
483	29	1	3.20	7	38	2	0	0.5	2.7	31	15	0
484	29	1	3.20	7	38	2	0	0.6	2.7	31	15	0
485	29	1	3.20	7	38	2	0	0.6	2.7	31	15	0
486	29	1	3.20	7	38	2	0	0.6	2.7	31	15	0
487	29	1	3.20	7	38	2	0	0.6	2.7	25	16	0
488	29	1	3.20	7	38	2	0	0.6	2.7	25	16	0

489	29	1	3.20	7	38	2	0	0.5	2.7	25	16	0
490	29	1	3.20	7	38	2	0	0.5	2.7	25	14	0
491	29	1	3.20	7	38	2	0	0.5	2.7	25	14	0
492	29	1	3.20	7	38	2	0	0.5	2.7	25	14	0
493	29	1	3.20	7	38	2	0	0.5	2.7	25	14	0
494	29	1	3.20	7	38	2	0	0.5	2.7	25	14	0
495	29	1	3.20	7	38	2	0	0.5	2.7	25	14	0
496	29	1	3.20	7	38	2	0	0.5	2.7	25	14	0
497	29	1	3.20	7	38	2	0	0.5	2.7	25	14	0
498	29	1	3.20	7	38	2	0	0.5	2.7	25	14	0
499	29	1	3.20	7	38	2	0	0.5	2.7	25	14	0
500	29	1	3.20	7	38	2	0	0.5	2.7	25	14	0
501	29	1	3.20	7	38	2	0	0.6	2.7	25	14	0
502	29	1	3.20	7	38	2	0	0.6	2.7	25	14	0
503	29	1	3.20	7	38	2	0	0.6	2.7	25	14	0
504	29	1	3.20	7	38	2	0	0.6	2.7	25	14	0
505	29	1	3.20	7	38	2	0	0.6	2.7	25	14	0
506	29	1	3.20	7	38	2	0	0.6	2.7	25	14	0
507	29	1	3.20	7	38	2	0	0.4	2.7	25	14	0
508	29	1	3.20	7	38	2	0	0.4	2.7	25	14	0
509	29	1	3.20	7	38	2	0	0.4	2.7	25	14	0
510	29	1	3.20	7	38	2	0	0.5	2.7	25	14	0
511	29	1	3.20	7	38	2	0	0.4	2.7	19	14	0
512	29	1	3.20	7	38	2	0	0.4	2.7	19	14	0
513	29	1	3.20	7	38	2	0	0.4	2.7	19	14	0
514	30	1	12.50	1072	40	1	1	0.6	2.3	111	17	0
515	30	1	12.50	1072	40	1	1	0.6	2.3	111	17	0
516	30	1	12.50	1072	40	1	1	0.6	2.3	111	17	0
517	30	1	12.50	1072	40	1	1	0.6	2.3	111	17	0

518	30	1	12.50	1072	40	1	1	0.6	2.3	111	17	0
519	30	1	12.50	1072	40	1	1	0.6	2.3	111	17	0
520	30	1	12.50	1072	40	1	1	0.4	2.3	111	17	0
521	30	1	12.50	1072	40	1	1	0.6	2.3	111	17	0
522	30	1	12.50	1072	40	1	1	0.4	2.3	111	17	0
523	30	1	12.50	1072	40	1	1	0.4	2.3	111	17	0
524	30	1	12.50	1072	40	1	1	0.4	2.3	111	17	0
525	30	1	12.50	1072	40	1	1	0.7	2.3	111	17	0
526	30	1	12.50	1072	40	1	1	0.7	2.3	111	17	0
527	31	1	6.22	113	37	1	1	0.6	2.9	59	25	0
528	31	1	6.22	113	37	1	1	0.6	2.9	59	25	0
529	31	1	6.22	113	37	1	1	0.6	2.9	59	25	0
530	31	1	6.22	113	37	1	1	0.6	2.9	59	25	0
531	31	1	6.22	113	37	1	1	0.6	2.9	59	25	0
532	31	1	6.22	113	37	1	1	0.4	2.9	59	25	0
533	31	1	6.22	113	37	1	1	0.4	2.9	59	25	0
534	31	1	6.22	113	37	1	1	0.4	2.9	59	25	0
535	31	1	6.22	113	37	1	1	0.4	2.9	59	25	0
536	31	1	6.22	113	37	1	1	0.4	2.9	59	25	0
537	31	1	6.22	113	37	1	1	0.6	2.9	35	24	0
538	31	1	6.22	113	37	1	1	0.7	3.6	32	23	0
539	31	1	6.22	113	37	1	1	0.7	3.6	32	23	0
540	31	1	6.22	113	37	1	1	0.7	3.6	32	23	0
541	31	1	6.22	113	37	1	1	0.7	3.6	32	23	0
542	31	1	6.22	113	37	1	1	0.7	3.6	32	23	0
543	32	1	2.52	96	30	0	1	0.3	2.9	31	14	0
544	32	1	2.52	96	30	0	1	0.3	2.9	31	14	0
545	32	1	2.52	96	30	0	1	0.3	2.9	31	14	0
546	32	1	2.52	96	30	0	1	0.3	2.9	31	14	0

547	32	1	2.52	96	30	0	1	0.3	2.9	31	14	0
548	32	1	2.52	96	30	0	1	0.3	2.9	31	14	0
549	32	1	2.52	96	30	0	1	0.3	2.9	31	14	0
550	32	1	2.52	96	30	0	1	0.2	2.9	31	14	0
551	32	1	2.52	96	30	0	1	0.2	2.9	31	14	0
552	32	1	2.52	96	30	0	1	0.2	2.9	31	14	0
553	32	1	2.52	96	30	0	1	0.2	2.9	31	14	0
554	32	1	2.52	96	30	0	1	0.2	2.9	31	14	0
555	32	1	2.52	96	30	0	1	0.2	2.9	31	14	0
556	32	1	2.52	96	30	0	1	0.2	2.9	31	14	0
557	32	1	2.52	96	30	0	1	0.2	2.9	31	14	0
558	32	1	2.52	96	30	0	1	0.2	2.9	31	14	0
559	32	1	2.52	96	30	0	1	0.2	2.9	31	14	0
560	32	1	2.52	96	30	0	1	0.2	2.9	31	14	0
561	32	1	2.52	96	30	0	1	0.2	2.9	31	14	0
562	32	1	2.52	96	30	0	1	0.2	2.9	31	14	0
563	32	1	2.52	96	30	0	1	0.2	2.9	31	14	0
564	32	1	2.52	96	30	0	1	0.2	2.9	31	14	0
565	32	1	2.52	96	30	0	1	0.2	2.9	31	14	0
566	32	1	2.52	96	30	0	1	0.2	2.9	31	14	0
567	32	1	2.52	96	30	0	1	0.2	2.9	31	14	0
568	32	1	2.52	96	30	0	1	0.2	2.9	31	14	0
569	32	1	2.52	96	30	0	1	0.2	2.9	31	14	0
570	32	1	2.52	96	30	0	1	0.2	2.9	31	14	0
571	32	1	2.52	96	30	0	1	0.2	2.9	31	14	0
572	32	1	2.52	96	30	0	1	0.2	2.9	31	14	0
573	32	1	2.52	96	30	0	1	0.3	3.7	46	23	0
574	32	1	2.52	96	30	0	1	0.3	3.7	46	23	0
575	32	1	2.52	96	30	0	1	0.3	3.7	46	23	0

576	33	1	22.00	2084	40	1	0	0.4	2.8	46	34	0
577	33	1	22.00	2084	40	1	0	0.4	2.8	46	34	0
578	33	1	22.00	2084	40	1	0	0.4	2.8	46	34	0
579	33	1	22.00	2084	40	1	0	0.4	2.8	46	34	0
580	33	1	22.00	2084	40	1	0	0.4	2.8	46	34	0
581	33	1	22.00	2084	40	1	0	0.4	2.8	46	34	0
582	33	1	22.00	2084	40	1	0	0.4	2.8	46	34	0
583	33	1	22.00	2084	40	1	0	0.4	2.8	89	64	0
584	33	1	22.00	2084	40	1	0	0.4	2.8	89	64	0
585	33	1	22.00	2084	40	1	0	0.4	2.8	89	64	0
586	33	1	22.00	2084	40	1	0	0.5	2.8	42	56	0
587	33	1	22.00	2084	40	1	0	0.5	2.8	42	56	0
588	33	1	22.00	2084	40	1	0	0.5	2.8	42	56	0
589	33	1	22.00	2084	40	1	0	0.5	2.8	42	56	0
590	33	1	22.00	2084	40	1	0	0.5	2.8	23	28	0
591	33	1	22.00	2084	40	1	0	0.6	2.8	23	28	0
592	33	1	22.00	2084	40	1	0	0.5	2.8	23	28	0
593	33	1	22.00	2084	40	1	0	0.6	2.8	23	28	0
594	33	1	22.00	2084	40	1	0	0.6	3.1	77	57	0
595	33	1	22.00	2084	40	1	0	0.6	3.1	77	57	0
596	33	1	22.00	2084	40	1	0	0.6	3.1	77	57	0
597	34	1	3.32	18	40	0	1	0.1	2.9	34	17	0
598	34	1	3.32	18	40	0	1	0.1	2.9	34	17	0
599	34	1	3.32	18	40	0	1	0.1	2.9	34	17	0
600	34	1	3.32	18	40	0	1	0.1	2.9	34	17	0
601	34	1	3.32	18	40	0	1	0.1	2.9	34	17	0
602	34	1	3.32	18	40	0	1	0.1	2.9	34	17	0
603	34	1	3.32	18	40	0	1	0.1	2.9	34	17	0
604	34	1	3.32	18	40	0	1	0.1	2.9	34	17	0

605	34	1	3.32	18	40	0	1	0.1	2.9	34	17	0
606	34	1	3.32	18	40	0	1	0.1	2.9	34	17	0
607	34	1	3.32	18	40	0	1	0.1	2.9	29	15	0
608	34	1	3.32	18	40	0	1	0.1	2.9	29	15	0
609	34	1	3.32	18	40	0	1	0.1	2.9	29	15	0
610	34	1	3.32	18	40	0	1	0.1	2.9	29	14	0
611	34	1	3.32	18	40	0	1	0.1	2.9	29	14	0
612	34	1	3.32	18	40	0	1	0.1	2.9	29	14	0
613	34	1	3.32	18	40	0	1	0.1	2.9	29	14	0
614	34	1	3.32	18	40	0	1	0.1	2.9	29	14	0
615	34	1	3.32	18	40	0	1	0.1	2.9	29	14	0
616	34	1	3.32	18	40	0	1	0.1	2.9	29	14	0
617	34	1	3.32	18	40	0	1	0.1	2.9	29	14	0
618	34	1	3.32	18	40	0	1	0.1	2.9	29	14	0
619	34	1	3.32	18	40	0	1	0.1	2.9	29	14	0
620	34	1	3.32	18	40	0	1	0.1	2.9	29	14	0
621	34	1	3.32	18	40	0	1	0.1	2.9	29	14	0
622	34	1	3.32	18	40	0	1	0.1	2.9	29	14	0
623	34	1	3.32	18	40	0	1	0.1	2.9	29	14	0
624	34	1	3.32	18	40	0	1	0.1	2.9	23	13	0
625	34	1	3.32	18	40	0	1	0.1	2.9	23	13	0
626	34	1	3.32	18	40	0	1	0.1	2.9	23	13	0
627	34	1	3.32	18	40	0	1	1.0	2.9	23	13	0
628	34	1	3.32	18	40	0	1	1.0	2.9	23	13	0
629	34	1	3.32	18	40	0	1	1.0	2.9	23	13	0
630	34	1	3.32	18	40	0	1	0.1	2.9	23	13	0
631	34	1	3.32	18	40	0	1	0.2	2.9	23	13	0
632	34	1	3.32	18	40	0	1	0.2	2.9	23	13	0
633	34	1	3.32	18	40	0	1	0.1	2.9	23	13	0

634	34	1	3.32	18	40	0	1	0.2	2.9	23	13	0
635	34	1	3.32	18	40	0	1	0.2	2.9	23	13	0
636	34	1	3.32	18	40	0	1	0.2	2.9	23	13	0
637	34	1	3.32	18	40	0	1	0.2	2.9	23	13	0
638	34	1	3.32	18	40	0	1	0.2	2.9	23	13	0
639	34	1	3.32	18	40	0	1	0.2	2.9	23	13	0
640	34	1	3.32	18	40	0	1	0.2	2.9	23	13	0
641	36	1	3.90	7	41	2	1	0.6	0.8	68	69	1
642	36	1	3.90	7	41	2	1	0.6	0.8	68	69	1
643	36	1	3.90	7	41	2	1	0.6	0.8	68	69	1
644	36	1	3.90	7	41	2	1	0.6	0.8	68	69	1
645	36	1	3.90	7	41	2	1	0.6	0.8	68	69	1
646	36	1	3.90	7	41	2	1	0.6	0.8	68	69	1
647	36	1	3.90	7	41	2	1	0.6	0.8	68	69	1
648	36	1	3.90	7	41	2	1	1.0	0.8	68	69	1
649	36	1	3.90	7	41	2	1	1.0	0.8	68	69	1
650	36	1	3.90	7	41	2	1	1.0	0.8	68	69	1
651	36	1	3.90	7	41	2	1	1.2	2.5	54	51	1
652	36	1	3.90	7	41	2	1	1.2	2.5	54	51	1
653	36	1	3.90	7	41	2	1	1.2	2.5	54	51	1
654	36	1	3.90	7	41	2	1	1.4	2.5	54	51	1
655	36	1	3.90	7	41	2	1	1.5	1.9	44	28	1
656	36	1	3.90	7	41	2	1	1.6	3.1	44	28	1
657	36	1	3.90	7	41	2	1	2.0	3.1	44	28	1
658	36	1	3.90	7	41	2	1	1.8	3.1	36	19	1
659	36	1	3.90	7	41	2	1	1.8	3.1	36	19	1
660	36	1	3.90	7	41	2	1	1.8	3.1	36	19	1
661	36	1	3.90	7	41	2	1	1.8	3.1	36	19	1
662	36	1	3.90	7	41	2	1	1.8	3.1	36	19	1

663	36	1	3.90	7	41	2	1	1.8	3.1	36	19	1
664	36	1	3.90	7	41	2	1	1.8	3.1	36	19	1
665	36	1	3.90	7	41	2	1	1.8	3.1	36	19	1
666	36	1	3.90	7	41	2	1	1.8	3.1	36	19	1
667	36	1	3.90	7	41	2	1	1.8	3.1	36	19	1
668	36	1	3.90	7	41	2	1	1.6	3.1	36	19	1
669	36	1	3.90	7	41	2	1	1.6	3.1	36	19	1
670	36	1	3.90	7	41	2	1	1.6	3.1	36	19	1
671	36	1	3.90	7	41	2	1	1.3	3.1	36	19	1
672	36	1	3.90	7	41	2	1	1.3	3.1	36	19	1
673	36	1	3.90	7	41	2	1	1.3	3.1	36	19	1
674	36	1	3.90	7	41	2	1	1.3	3.1	36	19	1
675	36	1	3.90	7	41	2	1	1.2	3.1	36	19	1
676	36	1	3.90	7	41	2	1	1.3	3.1	36	19	1
677	36	1	3.90	7	41	2	1	1.3	3.1	36	19	1
678	36	1	3.90	7	41	2	1	1.6	2.2	38	10	1
679	36	1	3.90	7	41	2	1	1.6	2.2	38	10	1
680	36	1	3.90	7	41	2	1	1.9	2.2	33	8	1
681	36	1	3.90	7	41	2	1	2.1	2.2	33	8	1
682	36	1	3.90	7	41	2	1	1.8	2.2	33	8	1
683	36	1	3.90	7	41	2	1	1.3	2.2	33	8	1
684	36	1	3.90	7	41	2	1	1.0	2.2	33	8	1
685	36	1	3.90	7	41	2	1	0.8	2.2	38	9	1
686	36	1	3.90	7	41	2	1	0.8	2.2	38	9	1
687	37	1	37.00	4160	40	1	1	0.9	2.3	102	117	0
688	37	1	37.00	4160	40	1	1	1.2	3.0	94	91	0
689	37	1	37.00	4160	40	1	1	1.2	3.0	94	91	0
690	37	1	37.00	4160	40	1	1	1.2	3.0	94	91	0
691	37	1	37.00	4160	40	1	1	1.2	3.0	94	91	0

692	37	1	37.00	4160	40	1	1	1.1	3.0	94	91	0
693	37	1	37.00	4160	40	1	1	1.2	3.0	94	91	0
694	37	1	37.00	4160	40	1	1	1.1	3.0	94	91	0
695	37	1	37.00	4160	40	1	1	1.1	3.0	94	91	0
696	37	1	37.00	4160	40	1	1	1.1	3.0	94	91	0
697	37	1	37.00	4160	40	1	1	1.1	3.0	94	91	0
698	37	1	37.00	4160	40	1	1	1.1	3.0	94	91	0
699	37	1	37.00	4160	40	1	1	1.1	3.0	94	91	0
700	37	1	37.00	4160	40	1	1	1.1	3.0	94	91	0
701	37	1	37.00	4160	40	1	1	1.1	3.0	94	91	0
702	37	1	37.00	4160	40	1	1	1.1	3.0	94	91	0
703	37	1	37.00	4160	40	1	1	1.1	3.0	94	91	0
704	37	1	37.00	4160	40	1	1	1.1	3.0	94	91	0
705	37	1	37.00	4160	40	1	1	1.1	3.0	94	91	0
706	37	1	37.00	4160	40	1	1	1.1	3.0	94	91	0
707	37	1	37.00	4160	40	1	1	1.1	3.0	94	91	0
708	37	1	37.00	4160	40	1	1	1.1	3.0	94	91	0
709	37	1	37.00	4160	40	1	1	1.1	3.0	94	91	0
710	37	1	37.00	4160	40	1	1	1.1	3.0	94	91	0
711	37	1	37.00	4160	40	1	1	1.1	3.0	94	91	0
712	37	1	37.00	4160	40	1	1	1.1	3.0	94	91	0
713	37	1	37.00	4160	40	1	1	1.1	3.0	94	91	0
714	37	1	37.00	4160	40	1	1	0.6	2.8	50	46	0
715	37	1	37.00	4160	40	1	1	1.1	3.0	94	91	0
716	38	1	77.00	6498	40	1	0	0.5	2.4	31	37	0
717	38	1	77.00	6498	40	1	0	0.5	2.4	31	37	0
718	38	1	77.00	6498	40	1	0	0.5	2.4	31	37	0
719	38	1	77.00	6498	40	1	0	0.5	2.4	31	37	0
720	38	1	77.00	6498	40	1	0	0.5	2.4	31	37	0

721	38	1	77.00	6498	40	1	0	0.5	2.4	31	37	0
722	38	1	77.00	6498	40	1	0	0.5	2.4	31	37	0
723	38	1	77.00	6498	40	1	0	0.6	3.0	31	37	0
724	38	1	77.00	6498	40	1	0	0.6	3.0	31	37	0
725	38	1	77.00	6498	40	1	0	0.7	3.0	31	37	0
726	38	1	77.00	6498	40	1	0	0.7	3.0	31	37	0
727	38	1	77.00	6498	40	1	0	0.7	3.0	31	37	0
728	38	1	77.00	6498	40	1	0	0.7	3.0	31	37	0
729	38	1	77.00	6498	40	1	0	0.7	3.0	31	37	0
730	38	1	77.00	6498	40	1	0	0.7	3.0	31	37	0
731	38	1	77.00	6498	40	1	0	0.7	3.0	31	37	0
732	38	1	77.00	6498	40	1	0	0.6	3.0	31	37	0
733	38	1	77.00	6498	40	1	0	0.7	3.0	31	37	0
734	38	1	77.00	6498	40	1	0	0.6	3.0	31	37	0
735	38	1	77.00	6498	40	1	0	0.6	3.0	31	37	0
736	38	1	77.00	6498	40	1	0	0.5	3.0	31	37	0
737	38	1	77.00	6498	40	1	0	0.5	3.0	31	37	0
738	38	1	77.00	6498	40	1	0	0.5	3.0	31	37	0
739	38	1	77.00	6498	40	1	0	0.5	3.0	31	37	0
740	38	1	77.00	6498	40	1	0	0.5	3.0	31	37	0
741	38	1	77.00	6498	40	1	0	0.5	3.0	31	37	0
742	38	1	77.00	6498	40	1	0	0.5	3.0	31	37	0
743	38	1	77.00	6498	40	1	0	0.5	3.0	31	37	0
744	38	1	77.00	6498	40	1	0	0.4	2.6	42	61	0
745	38	1	77.00	6498	40	1	0	0.4	2.6	42	61	0
746	38	1	77.00	6498	40	1	0	0.4	2.6	42	61	0
747	38	1	77.00	6498	40	1	0	0.4	2.6	42	61	0
748	38	1	77.00	6498	40	1	0	0.4	2.6	42	61	0
749	38	1	77.00	6498	40	1	0	0.4	2.6	42	61	0

750	39	1	4.20	131	31	0	1	1.2	2.5	1238	411	1
751	39	1	4.20	131	31	0	1	1.2	2.5	1238	411	1
752	39	1	4.20	131	31	0	1	1.2	2.5	1238	411	1
753	39	1	4.20	131	31	0	1	1.2	2.5	1238	411	1
754	39	1	4.20	131	31	0	1	1.2	2.5	1238	411	1
755	39	1	4.20	131	31	0	1	1.2	2.5	1238	411	1
756	39	1	4.20	131	31	0	1	1.2	2.5	1238	411	1
757	39	1	4.20	131	31	0	1	1.6	2.1	731	262	1
758	39	1	4.20	131	31	0	1	1.6	2.1	731	262	1
759	39	1	4.20	131	31	0	1	1.6	2.1	731	262	1
760	39	1	4.20	131	31	0	1	1.7	2.4	354	193	1
761	39	1	4.20	131	31	0	1	1.7	2.4	354	193	1
762	39	1	4.20	131	31	0	1	1.7	2.4	354	193	1
763	39	1	4.20	131	31	0	1	1.5	2.1	170	129	1
764	39	1	4.20	131	31	0	1	1.6	2.5	115	91	1
765	39	1	4.20	131	31	0	1	1.6	2.5	115	91	1
766	39	1	4.20	131	31	0	1	1.7	2.7	99	68	1
767	39	1	4.20	131	31	0	1	1.7	2.7	99	68	1
768	39	1	4.20	131	31	0	1	1.7	2.7	99	68	1
769	39	1	4.20	131	31	0	1	1.7	2.6	69	47	1
770	39	1	4.20	131	31	0	1	1.7	2.6	69	47	1
771	39	1	4.20	131	31	0	1	1.8	3.3	92	66	1
772	39	1	4.20	131	31	0	1	1.8	3.3	92	66	1
773	39	1	4.20	131	31	0	1	1.8	3.3	92	66	1
774	39	1	4.20	131	31	0	1	1.8	3.3	92	66	1
775	39	1	4.20	131	31	0	1	1.8	3.3	92	66	1
776	39	1	4.20	131	31	0	1	1.8	3.3	92	66	1
777	39	1	4.20	131	31	0	1	1.8	3.3	92	66	1
778	39	1	4.20	131	31	0	1	1.8	3.3	92	66	1

779	39	1	4.20	131	31	0	1	1.8	3.3	92	66	1
780	39	1	4.20	131	31	0	1	1.8	3.3	92	66	1
781	39	1	4.20	131	31	0	1	2.0	2.9	92	62	1
782	39	1	4.20	131	31	0	1	2.0	2.9	92	62	1
783	39	1	4.20	131	31	0	1	2.0	2.9	92	62	1
784	39	1	4.20	131	31	0	1	1.7	3.4	91	55	1
785	39	1	4.20	131	31	0	1	1.7	3.4	91	55	1
786	39	1	4.20	131	31	0	1	1.7	3.4	91	55	1
787	39	1	4.20	131	31	0	1	1.3	3.2	81	54	1
788	39	1	4.20	131	31	0	1	1.1	3.3	68	44	1
789	39	1	4.20	131	31	0	1	1.3	3.2	81	54	1
790	39	1	4.20	131	31	0	1	1.0	3.2	60	39	1
791	39	1	4.20	131	31	0	1	1.0	3.2	60	39	1
792	39	1	4.20	131	31	0	1	0.9	3.0	55	34	1
793	39	1	4.20	131	31	0	1	0.9	3.0	55	34	1
794	39	1	4.20	131	31	0	1	0.9	3.0	64	33	1
795	39	1	4.20	131	31	0	1	0.9	3.0	64	33	1
796	39	1	4.20	131	31	0	1	0.9	3.0	64	33	1
797	39	1	4.20	131	31	0	1	0.9	3.0	64	33	1
798	39	1	4.20	131	31	0	1	0.9	3.0	64	33	1
799	39	1	4.20	131	31	0	1	1.1	3.1	38	29	1
800	40	1	5.60	125	38	1	0	0.4	3.7	35	14	0
801	40	1	5.60	125	38	1	0	0.4	3.7	35	14	0
802	40	1	5.60	125	38	1	0	0.4	3.7	35	14	0
803	40	1	5.60	125	38	1	0	0.4	3.7	35	14	0
804	40	1	5.60	125	38	1	0	0.4	3.7	35	14	0
805	40	1	5.60	125	38	1	0	0.4	3.7	35	14	0
806	40	1	5.60	125	38	1	0	0.4	3.7	35	14	0
807	40	1	5.60	125	38	1	0	0.4	3.7	35	14	0

808	40	1	5.60	125	38	1	0	0.4	3.7	35	14	0
809	40	1	5.60	125	38	1	0	0.5	3.7	37	14	0
810	40	1	5.60	125	38	1	0	0.9	3.7	28	13	0
811	40	1	5.60	125	38	1	0	0.9	3.7	28	13	0
812	40	1	5.60	125	38	1	0	0.9	3.7	28	13	0
813	40	1	5.60	125	38	1	0	0.6	3.9	28	13	0
814	40	1	5.60	125	38	1	0	0.6	4.0	30	13	0
815	40	1	5.60	125	38	1	0	0.6	4.0	30	13	0
816	40	1	5.60	125	38	1	0	0.6	4.0	30	13	0
817	40	1	5.60	125	38	1	0	0.6	4.0	30	13	0
818	40	1	5.60	125	38	1	0	0.6	4.0	30	13	0
819	40	1	5.60	125	38	1	0	0.6	4.0	30	13	0
820	40	1	5.60	125	38	1	0	0.6	4.0	30	13	0
821	40	1	5.60	125	38	1	0	0.6	4.0	30	13	0
822	40	1	5.60	125	38	1	0	0.6	4.0	30	13	0
823	40	1	5.60	125	38	1	0	0.6	4.0	30	13	0
824	40	1	5.60	125	38	1	0	0.6	4.0	30	13	0
825	40	1	5.60	125	38	1	0	0.6	4.0	30	13	0
826	40	1	5.60	125	38	1	0	0.6	4.0	30	13	0
827	40	1	5.60	125	38	1	0	0.6	4.0	30	13	0
828	40	1	5.60	125	38	1	0	0.6	4.0	30	13	0
829	40	1	5.60	125	38	1	0	0.6	4.0	30	13	0
830	40	1	5.60	125	38	1	0	0.5	3.6	30	12	0
831	40	1	5.60	125	38	1	0	0.5	3.6	30	12	0
832	40	1	5.60	125	38	1	0	0.5	3.6	30	12	0
833	41	1	10.00	392	40	1	1	0.2	2.2	29	11	0
834	41	1	10.00	392	40	1	1	0.2	2.2	29	11	0
835	41	1	10.00	392	40	1	1	0.2	2.2	29	11	0
836	41	1	10.00	392	40	1	1	0.2	2.2	29	11	0

837	41	1	10.00	392	40	1	1	0.2	2.2	29	11	0
838	41	1	10.00	392	40	1	1	0.2	2.2	29	11	0
839	41	1	10.00	392	40	1	1	0.3	2.2	29	11	0
840	41	1	10.00	392	40	1	1	0.3	2.2	29	11	0
841	41	1	10.00	392	40	1	1	0.3	2.2	29	11	0
842	41	1	10.00	392	40	1	1	0.3	2.2	29	11	0
843	41	1	10.00	392	40	1	1	0.3	2.2	29	11	0
844	41	1	10.00	392	40	1	1	0.5	2.2	29	11	0
845	41	1	10.00	392	40	1	1	0.5	2.2	29	11	0
846	41	1	10.00	392	40	1	1	0.5	2.2	29	11	0
847	41	1	10.00	392	40	1	1	0.3	2.2	29	11	0
848	41	1	10.00	392	40	1	1	0.6	2.5	37	26	0
849	41	1	10.00	392	40	1	1	0.5	2.5	37	26	0
850	41	1	10.00	392	40	1	1	0.5	2.5	37	26	0
851	41	1	10.00	392	40	1	1	0.5	2.5	37	26	0
852	41	1	10.00	392	40	1	1	0.5	2.5	37	26	0
853	41	1	10.00	392	40	1	1	0.5	2.5	37	26	0
854	41	1	10.00	392	40	1	1	0.4	2.9	25	17	0
855	41	1	10.00	392	40	1	1	0.4	2.9	25	17	0
856	41	1	10.00	392	40	1	1	0.4	2.9	25	17	0
857	41	1	10.00	392	40	1	1	0.4	2.9	25	17	0
858	41	1	10.00	392	40	1	1	0.4	2.9	25	17	0
859	41	1	10.00	392	40	1	1	0.4	2.9	25	17	0
860	41	1	10.00	392	40	1	1	0.4	2.9	25	17	0
861	41	1	10.00	392	40	1	1	0.4	2.9	25	17	0
862	41	1	10.00	392	40	1	1	0.4	2.9	25	17	0
863	41	1	10.00	392	40	1	1	0.4	2.9	25	17	0
864	41	1	10.00	392	40	1	1	0.4	2.9	25	17	0
865	41	1	10.00	392	40	1	1	0.4	2.9	25	17	0

866	41	1	10.00	392	40	1	1	0.4	2.9	25	17	0
867	41	1	10.00	392	40	1	1	0.4	2.9	25	17	0
868	41	1	10.00	392	40	1	1	0.3	2.9	25	17	0
869	41	1	10.00	392	40	1	1	0.3	2.9	25	17	0
870	41	1	10.00	392	40	1	1	0.3	2.9	25	17	0
871	42	1	15.00	938	40	0	0	0.4	2.8	46	33	0
872	42	1	15.00	938	40	0	0	0.4	2.8	46	33	0
873	42	1	15.00	938	40	0	0	0.4	2.8	46	33	0
874	42	1	15.00	938	40	0	0	0.4	2.8	46	33	0
875	42	1	15.00	938	40	0	0	0.4	2.8	46	33	0
876	42	1	15.00	938	40	0	0	0.4	2.8	46	33	0
877	42	1	15.00	938	40	0	0	0.4	2.8	46	33	0
878	42	1	15.00	938	40	0	0	0.5	2.8	46	33	0
879	42	1	15.00	938	40	0	0	0.5	2.8	46	33	0
880	42	1	15.00	938	40	0	0	0.5	2.8	46	33	0
881	42	1	15.00	938	40	0	0	0.5	2.8	46	33	0
882	42	1	15.00	938	40	0	0	0.5	2.8	46	33	0
883	42	1	15.00	938	40	0	0	0.5	2.7	46	33	0
884	42	1	15.00	938	40	0	0	0.5	2.7	46	33	0
885	42	1	15.00	938	40	0	0	0.4	2.7	46	33	0
886	42	1	15.00	938	40	0	0	0.3	2.7	46	33	0
887	42	1	15.00	938	40	0	0	0.3	2.7	46	33	0
888	42	1	15.00	938	40	0	0	0.3	2.7	46	33	0
889	42	1	15.00	938	40	0	0	0.3	2.7	46	33	0
890	42	1	15.00	938	40	0	0	0.3	2.7	46	33	0
891	42	1	15.00	938	40	0	0	0.3	2.7	46	33	0
892	42	1	15.00	938	40	0	0	0.3	2.7	46	33	0
893	42	1	15.00	938	40	0	0	0.3	2.4	24	27	0
894	42	1	15.00	938	40	0	0	0.3	2.4	24	27	0

895	42	1	15.00	938	40	0	0	0.3	2.4	24	27	0
896	42	1	15.00	938	40	0	0	0.3	2.4	24	27	0
897	42	1	15.00	938	40	0	0	0.3	2.4	24	27	0
898	42	1	15.00	938	40	0	0	0.3	2.4	24	27	0
899	42	1	15.00	938	40	0	0	0.3	2.4	24	27	0
900	42	1	15.00	938	40	0	0	0.3	2.4	24	27	0
901	42	1	15.00	938	40	0	0	0.3	2.4	24	27	0
902	42	1	15.00	938	40	0	0	0.3	2.4	24	27	0
903	42	1	15.00	938	40	0	0	0.3	2.4	24	27	0
904	43	1	10.00	391	40	0	1	0.2	3.1	23	15	0
905	43	1	10.00	391	40	0	1	0.2	3.1	23	15	0
906	43	1	10.00	391	40	0	1	0.2	3.1	23	15	0
907	43	1	10.00	391	40	0	1	0.2	3.1	23	15	0
908	43	1	10.00	391	40	0	1	0.2	3.1	23	15	0
909	43	1	10.00	391	40	0	1	0.2	3.1	23	15	0
910	43	1	10.00	391	40	0	1	0.2	3.1	23	15	0
911	43	1	10.00	391	40	0	1	0.3	3.1	23	15	0
912	43	1	10.00	391	40	0	1	0.3	3.1	23	15	0
913	43	1	10.00	391	40	0	1	0.3	3.1	23	15	0
914	43	1	10.00	391	40	0	1	0.3	3.1	23	15	0
915	43	1	10.00	391	40	0	1	0.3	3.1	23	15	0
916	43	1	10.00	391	40	0	1	0.3	3.1	23	15	0
917	43	1	10.00	391	40	0	1	0.3	3.1	23	15	0
918	43	1	10.00	391	40	0	1	0.2	3.1	23	15	0
919	43	1	10.00	391	40	0	1	0.3	3.1	23	15	0
920	43	1	10.00	391	40	0	1	0.2	3.1	23	15	0
921	43	1	10.00	391	40	0	1	0.2	3.1	23	15	0
922	43	1	10.00	391	40	0	1	0.2	3.3	23	15	0
923	43	1	10.00	391	40	0	1	0.2	3.3	23	15	0

CVVHDE	SCAVENGE	TAFD	TALD	AMT	DUR	RATE	DV	EVID
0		0.00	0.00	87.0	2.0	43.5		1
0	0	2.12	2.10				25.2	0
0	0	4.37	4.35				20.4	0
0	0	8.42	8.40				22.2	0
0		16.97	16.95					2
0	0	20.03	20.02				20.5	0
0		23.97	0.00	40.0	1.0	40.0		1
0	0	44.80	20.83				26.0	0
0		48.55	0.00	40.0	1.0	40.0		1
0	0	53.05	4.50				31.3	0
0		60.38	11.84					2
0		72.07	0.00	40.0	1.0	40.0		1
0		88.97	16.90					2
0	0	92.97	20.90				34.5	0
0		96.03	0.00	40.0	1.0	40.0		1
0	0	98.97	2.94				39.0	0
0		0.00	0.00	75.0	2.0	37.5		1
0	0	2.10	2.11				24.6	0
0	0	4.25	4.26				22.3	0
0	0	8.42	8.43				21.4	0
0		16.08	16.09					2
0	0	23.33	23.34				17.2	0
0		24.08	0.00	35.0	1.0	35.0		1
0		40.08	15.99					2
0	0	46.42	22.32				18.5	0
0		48.08	0.00	35.0	1.0	35.0		1
0		64.08	16.00					2
0	0	71.08	23.00				19.6	0

0		0.00	0.00	26.5	2.5	10.6		1
0	0	2.83	2.84				10.6	0
0	0	4.75	4.76				26.4	0
0	1	14.50	14.51				26.7	0
0	0	26.00	26.01				21.2	0
0		0.00	0.00	67.5	2.0	33.8		1
0	0	2.33	2.32				20.8	0
0	0	4.17	4.15				15.3	0
0	0	11.92	11.90				15.1	0
0		12.67	12.65					2
0	0	20.67	20.65				14.2	0
0		22.67	0.00	30.0	1.0	30.0		1
0		36.67	14.00					2
0		36.67	14.00					2
0		47.42	0.00	30.0	1.0	28.6		1
0	0	47.42	24.75				16.6	0
0	0	51.17	3.74				23.8	0
0		68.17	0.00	30.0	1.0	30.0		1
0		84.67	16.49					2
0		84.67	16.49					2
0	0	92.67	24.49				24.4	0
0		92.67	0.00	30.0	1.0	30.0		1
0	0	97.67	4.99				28.0	0
0		0.00	0.00	70.0	2.0	35.0		1
0	0	2.17	2.17				29.7	0
0	0	5.97	5.97				24.2	0
0	0	8.32	8.32				23.2	0
0		17.25	17.26					2
0	0	21.17	21.17				18.2	0

0		23.25	0.00	30.0	1.0	30.0		1
0		41.25	17.99					2
0	0	47.25	23.99				16.0	0
0		47.25	0.00	30.0	1.0	30.0		1
0	0	51.33	4.08				19.2	0
0		71.75	0.00	30.0	1.0	30.0		1
0		89.25	17.49					2
0	0	95.92	24.16				15.3	0
0		96.33	0.00	30.0	1.0	30.0		1
0	0	100.58	4.25				26.8	0
0		0.00	0.00	212.5	2.0	106.3		1
0	0	2.00	2.01				36.9	0
0	0	4.50	4.51				34.0	0
0	0	10.50	10.51				25.8	0
0		17.75	17.76					2
0	0	21.75	21.76				27.8	0
0		23.75	0.00	100.0	1.0	100.0		1
0		41.75	18.02					2
0	0	45.75	22.02				32.4	0
0		47.75	0.00	100.0	1.0	100.0		1
0	0	53.75	5.99				42.4	0
0		71.75	0.00	100.0	1.0	100.0		1
0	0	93.75	21.99				37.1	0
0		95.75	0.00	100.0	1.0	100.0		1
0	0	98.75	3.00				46.8	0
0		0.00	0.00	48.5	2.0	24.3		1
0	0	2.67	2.68				26.2	0
0	0	4.33	4.34				26.0	0
0	0	10.42	10.43				22.2	0

0		0	22.92	22.93			17.7	0
0			23.75	0.00	24.0	1.0	24.0	1
0		1	34.17	10.40			17.8	0
0			38.25	14.49				2
0			47.25	0.00	24.0	1.0	24.0	1
0			71.25	0.00	24.0	1.0	24.0	1
0			86.25	15.01				2
0		0	92.83	21.59			9.5	0
0			95.25	0.00	24.0	1.0	24.0	1
0		0	101.83	6.60			30.9	0
0			0.00	0.00	175.0	2.0	87.5	1
0		0	2.58	2.58			27.3	0
0		0	4.50	4.49			23.7	0
0		0	10.00	9.99			18.3	0
0		0	23.00	22.99			11.3	0
0			24.00	0.00	80.0	2.0	40.0	1
0			41.58	17.58				2
0		0	46.25	22.25			15.3	0
0			48.00	0.00	80.0	1.0	80.0	1
0		0	51.75	3.76			24.6	0
0			73.25	0.00	80.0	2.0	40.0	1
0		0	93.28	20.02			8.1	0
0			96.00	0.00	80.0	1.0	80.0	1
0		0	101.50	5.48			20.8	0
0			0.00	0.00	43.0	2.0	21.5	1
0		0	2.67	2.67			32.7	0
0		0	7.50	7.50			29.1	0
0			10.00	10.00				2
0		0	11.50	11.50			23.2	0

0		23.00	0.00	21.0	1.0	21.0		1
0	0	31.92	8.91				42.8	0
0	1	31.92	8.91				39.4	0
0	0	38.50	15.49				37.5	0
0	1	38.50	15.49				20.3	0
0	1	41.83	18.82				34.7	0
0		47.00	0.00	21.0	1.0	21.0		1
0	1	51.83	4.83				47.2	0
0		0.00	0.00	75.0	2.0	37.5		1
0	1	6.25	6.23				17.6	0
0	0	7.00	6.98				13.6	0
0	1	11.00	10.98				12.8	0
0		15.00	0.00	35.0	1.0	35.0		1
0	0	35.50	20.48				19.0	0
0		40.50	0.00	35.0	1.0	35.0		1
0	0	42.50	2.00				22.9	0
0	0	44.50	4.00				22.6	0
0		63.00	0.00	35.0	1.0	35.0		1
0	0	83.00	20.00				24.6	0
0		85.00	0.00	35.0	1.0	35.0		1
0	0	88.00	3.01				26.5	0
0		0.00	0.00	38.7	2.0	19.4		1
0	0	2.63	2.63				12.9	0
0	0	4.13	4.13				10.7	0
0	0	13.55	13.55				9.0	0
0	0	19.63	19.63				6.9	0
0	0	23.13	23.13				8.1	0
0		23.88	0.00	35.0	1.0	35.0		1
0	0	43.88	20.00				10.9	0

0		49.05	0.00	35.0	1.0	35.0		1
0	0	51.13	2.09				20.5	0
0		72.88	0.00	35.0	1.0	35.0		1
0	0	93.72	20.82				17.4	0
0		0.00	0.00	115.0	2.0	57.5		1
0	0	2.08	2.09				33.3	0
0	0	4.25	4.26				32.1	0
0		6.42	6.43					2
0	0	8.33	8.34				29.2	0
0	0	18.85	18.86				21.3	0
0		23.08	0.00	55.0	1.0	55.0		1
0		46.42	0.00	55.0	1.0	55.0		1
0	1	57.17	10.75				26.3	0
0		70.42	0.00	55.0	1.0	55.0		1
0	0	91.75	21.34				18.1	0
0		0.00	0.00	80.0	2.0	40.0		1
0	0	2.42	2.41				18.0	0
0	0	6.42	6.41				17.7	0
0	0	11.92	11.91				14.8	0
0		16.92	16.91					2
0	0	22.92	22.91				11.3	0
0		23.92	0.00	40.0	1.0	40.0		1
0		40.92	16.99					2
0	0	46.75	22.82				22.0	0
0		47.92	0.00	40.0	1.0	40.0		1
0	0	54.92	6.99				25.9	0
0		0.00	0.00	85.0	2.0	42.5		1
0		24.08	0.00	85.0	2.0	42.5		1
0	1	47.10	23.02				14.4	0

0		0.00	0.00	8.7	2.0	4.3		1
0	0	22.33	22.33				1.9	0
0		22.67	0.00	8.7	2.2	4.0		1
0	0	25.00	2.33				4.3	0
0	0	27.92	5.25				4.5	0
0	0	34.83	12.16				3.4	0
0	0	46.50	23.83				3.1	0
0		46.67	0.00	8.7	2.0	4.3		1
0	0	70.33	23.66				3.3	0
0		70.42	0.00	8.7	2.0	4.3		1
0		94.33	0.00	8.7	2.0	4.3		1
0		119.33	0.00	8.7	2.0	4.3		1
0		143.33	0.00	8.7	2.0	4.3		1
0	0	166.33	23.00				3.7	0
0		166.50	0.00	8.7	2.0	4.3		1
0		190.33	0.00	8.7	2.0	4.3		1
0		214.33	0.00	8.7	2.0	4.3		1
0		238.33	0.00	8.7	2.0	4.3		1
0		262.83	0.00	8.7	2.2	4.0		1
0		286.33	0.00	8.7	2.2	4.0		1
0		310.33	0.00	8.7	2.2	4.0		1
0		334.17	0.00	8.7	2.2	4.0		1
0	1	353.83	19.66				2.3	0
0		0.00	0.00	7.0	1.0	7.0		1
0		23.50	0.00	7.0	1.0	7.0		1
0		47.00	0.00	7.0	1.0	7.0		1
0		72.17	0.00	7.0	1.0	7.0		1
0		95.17	0.00	7.0	1.0	7.0		1
0		119.83	0.00	7.0	1.0	7.0		1

0		143.25	0.00	7.0	1.0	7.0		1
0		167.50	0.00	7.0	1.0	7.0		1
0		191.75	0.00	7.0	1.0	7.0		1
0		215.50	0.00	7.0	1.0	7.0		1
0		239.50	0.00	7.0	1.0	7.0		1
0		263.50	0.00	7.0	1.0	7.0		1
0		287.50	0.00	7.0	1.0	7.0		1
0		311.50	0.00	7.0	2.5	2.8		1
0	1	328.33	16.83				6.7	0
0		336.17	0.00	7.0	2.6	2.7		1
0	0	338.83	2.66				7.8	0
0	0	341.75	5.58				7.6	0
0	0	348.75	12.58				6.2	0
0	0	359.50	23.33				5.5	0
0		360.50	0.00	7.0	1.7	4.2		1
0	0	383.92	23.42				5.6	0
0		384.08	0.00	7.0	2.0	3.5		1
0		408.17	0.00	7.0	1.2	5.8		1
0		431.70	0.00	7.0	1.1	6.2		1
0		456.00	0.00	7.0	2.0	3.5		1
0	0	479.50	23.50				4.7	0
0		480.33	0.00	7.0	1.0	7.0		1
0		503.75	0.00	7.0	1.0	7.0		1
0		527.67	0.00	7.0	2.0	3.5		1
0		553.00	0.00	7.0	2.0	3.4		1
0		576.33	0.00	7.0	1.3	5.6		1
0		599.00	0.00	7.0	1.5	4.7		1
0		624.08	0.00	7.0	1.2	6.0		1
0	0	647.50	23.42				4.4	0

0		647.58	0.00	7.0	2.2	3.2		1
0		671.50	0.00	7.0	2.1	3.4		1
0		695.57	0.00	7.0	2.0	3.5		1
0		719.00	0.00	7.0	1.8	4.0		1
0		743.25	0.00	7.0	1.2	6.0		1
0		767.75	0.00	7.0	2.0	3.5		1
0		791.67	0.00	7.0	2.0	3.5		1
0	0	815.50	23.83				3.8	0
0		0.00	0.00	17.0	2.0	8.5		1
0	0	2.00	2.00				9.8	0
0	0	3.00	3.00				9.0	0
0	0	8.00	8.00				8.5	0
0	0	23.00	23.00				6.7	0
0	0	47.00	47.00				5.5	0
0		47.75	0.00	17.0	2.0	8.5		1
0		96.00	0.00	17.0	2.2	7.8		1
0	0	143.00	47.00				1.8	0
0		143.50	0.00	17.0	2.0	8.5		1
0		0.00	0.00	22.0	2.0	11.0		1
0	1	7.83	7.83				5.5	0
0		24.00	0.00	22.0	2.0	11.0		1
0	1	32.25	8.25				6.8	0
0		48.00	0.00	22.0	2.0	11.0		1
0	1	56.50	8.50				6.2	0
0		72.00	0.00	22.0	2.0	11.0		1
0	1	79.17	7.17				6.1	0
0		95.75	0.00	22.0	2.0	11.0		1
0	1	127.67	31.92				2.9	0
0	1	148.83	53.08				1.4	0

0	1	176.00	80.25				0.9	0
0		0.00	0.00	18.0	1.0	18.0		1
0		20.67	0.00	18.0	1.0	18.0		1
0		44.50	0.00	18.0	1.0	18.0		1
0		68.67	0.00	18.0	1.0	18.0		1
0		92.50	0.00	18.0	1.0	18.0		1
0		116.50	0.00	18.0	1.0	18.0		1
0		140.58	0.00	18.0	2.0	9.0		1
0	0	154.67	14.09				7.4	0
0		0.00	0.00	40.0	1.0	40.0		1
0		24.00	0.00	40.0	1.0	40.0		1
0		48.83	0.00	40.0	1.0	40.0		1
0		72.50	0.00	40.0	2.0	20.0		1
0	0	95.75	23.25				6.9	0
0		96.25	0.00	40.0	1.0	40.0		1
0	0	97.00	0.75				15.3	0
0	0	98.00	1.75				14.1	0
0	0	102.98	6.73				13.2	0
0	0	119.75	23.50				7.4	0
0		120.00	0.00	40.0	1.0	40.0		1
0	0	143.75	23.75				7.4	0
0		144.00	0.00	40.0	2.0	20.0		1
0		168.00	0.00	40.0	2.0	20.0		1
0	0	191.75	23.75				8.6	0
0		192.00	0.00	40.0	2.0	20.0		1
0		216.00	0.00	40.0	2.0	20.0		1
0		240.00	0.00	40.0	2.0	20.0		1
0		264.25	0.00	40.0	2.0	20.0		1
0		288.00	0.00	40.0	2.0	20.0		1

0		312.25	0.00	40.0	2.0	20.0		1
0		336.00	0.00	40.0	2.0	20.0		1
0	0	359.75	23.75				9.7	0
0		360.08	0.00	40.0	2.0	20.0		1
0		0.00	0.00	42.0	1.0	42.0		1
0		23.42	0.00	21.0	1.0	21.0		1
0		47.33	0.00	21.0	1.0	21.0		1
0		71.25	0.00	21.0	1.0	21.0		1
0	0	71.87	0.62				13.1	0
0		0.00	0.00	6.0	1.0	6.0		1
0	1	44.25	44.25				1.8	0
0	1	66.95	66.95				1.3	0
0	0	71.25	71.25				1.0	0
0		71.50	0.00	6.0	1.0	6.0		1
0	0	72.75	1.25				4.0	0
0	0	75.75	4.25				3.5	0
0	0	82.75	11.25				3.1	0
0	1	90.25	18.75				2.5	0
0	0	97.50	26.00				2.2	0
0	1	114.00	42.50				1.3	0
0	0	121.75	50.25				1.2	0
0	1	139.50	68.00				0.7	0
0		144.00	0.00	6.0	0.5	12.0		1
0	1	161.50	17.50				2.4	0
0	0	239.00	95.00				0.3	0
0		240.00	0.00	6.0	0.5	12.0		1
0	1	284.07	44.07				0.8	0
0		312.00	0.00	6.0	0.5	12.0		1
0		0.00	0.00	37.9	1.0	37.9		1

0		24.00	0.00	37.9	1.0	37.9		1
0		48.00	0.00	37.9	1.0	37.9		1
0		72.00	0.00	37.9	1.0	37.9		1
0		72.75	0.76					2
0		95.93	23.95					2
0		96.00	0.00	37.9	1.0	37.9		1
0		120.00	0.00	37.9	1.0	37.9		1
0		120.25	0.24					2
0	0	144.00	23.99				16.8	0
0	0	144.00	23.99				14.9	0
0		144.50	0.00	37.9	1.0	37.9		1
0		145.12	0.60					2
0	0	146.00	1.49				24.7	0
0	0	146.00	1.49				24.2	0
0	0	150.00	5.49				24.1	0
0	0	150.00	5.49				20.6	0
0	0	152.00	7.49				22.5	0
0	0	152.00	7.49				15.8	0
0		169.08	24.57					2
0	0	169.75	25.24				16.1	0
0	0	169.75	25.24				16.2	0
0		192.00	47.49					2
0	0	192.00	47.49				13.5	0
0	0	192.00	47.49				13.0	0
0	0	209.67	65.15				11.3	0
0	0	209.83	65.32				11.2	0
0		217.50	72.99					2
0	0	234.75	90.24				8.6	0
0	0	234.75	90.24				8.3	0

0		0.00	0.00	85.0	2.0	42.5		1
0	0	2.00	2.01				16.0	0
0	0	2.00	2.01				21.3	0
0	0	5.83	5.84				14.1	0
0	0	5.83	5.84				16.9	0
0	0	13.50	13.51				14.4	0
0	0	13.50	13.51				13.2	0
0		13.50	13.51					2
0	0	26.08	26.09				6.1	0
0	0	26.08	26.09				11.8	0
0		38.00	38.01					2
0	0	49.83	49.84				8.1	0
0	0	49.83	49.84				8.1	0
0		62.00	62.01					2
0		68.08	68.09					2
0		74.92	74.92					2
0		85.92	85.92					2
0		110.17	110.17					2
0		134.00	134.01					2
0		158.00	158.01					2
0	0	164.67	164.67				3.8	0
0	0	164.67	164.67				3.7	0
0		168.00	0.00	85.0	2.0	42.5		1
0	0	170.33	2.35				21.6	0
0	0	170.33	2.35				21.8	0
0	0	173.75	5.77				15.2	0
0	0	173.75	5.77				19.7	0
0	0	182.05	14.07				13.0	0
0	0	182.05	14.07				17.0	0

0		183.08	15.10					2
0	0	194.08	26.10				15.0	0
0	0	194.08	26.10				15.1	0
0		206.33	38.35					2
0	0	216.17	48.18				14.1	0
0	0	216.17	48.18				13.9	0
0		229.67	61.68					2
0		254.33	86.35					2
0		277.33	109.35					2
0		301.00	133.02					2
0	0	315.25	147.27				9.4	0
0	0	315.25	147.27				9.5	0
0		0.00	0.00	84.0	1.0	84.0		1
0	0	1.25	1.26				14.2	0
0	0	1.25	1.26				14.3	0
0		2.18	2.19					2
0	0	5.25	5.26				10.9	0
0	0	5.25	5.26				9.8	0
0	0	9.33	9.34				9.4	0
0	0	9.33	9.34				9.8	0
0	0	22.75	22.76				6.7	0
0	0	22.75	22.76				6.7	0
0		23.75	0.00	84.0	1.0	84.0		1
0		26.62	2.85					2
0	0	47.00	23.23				8.0	0
0	0	47.00	23.23				7.5	0
0		47.75	0.00	84.0	1.0	84.0		1
0		51.00	3.24					2
0		71.75	0.00	84.0	1.0	84.0		1

0		74.75	3.00					2
0		98.92	27.16					2
0	0	117.25	45.50				4.6	0
0	0	117.25	45.50				3.3	0
0		0.00	0.00	50.3	2.0	25.1		1
0	0	2.25	2.24				17.1	0
0	0	2.42	2.41				20.3	0
0	0	4.25	4.24				14.9	0
0	0	4.25	4.24				18.6	0
0	0	10.25	10.24				7.0	0
0	0	10.25	10.24				17.3	0
0	0	28.50	28.49				12.9	0
0	0	28.50	28.49				12.9	0
0	0	52.33	52.32				10.4	0
0	0	52.33	52.32				11.6	0
0		63.92	63.91					2
0		87.83	87.82					2
0	0	95.08	95.07				4.8	0
0	0	95.08	95.07				5.1	0
0	0	102.33	102.32				3.9	0
0		111.83	111.82					2
0	0	120.33	120.32				3.8	0
0		0.00	0.00	61.0	2.0	30.5		1
0	0	2.25	2.25				15.7	0
0	0	2.25	2.25				15.7	0
0	0	6.00	6.00				15.1	0
0	0	6.00	6.00				14.3	0
0	0	8.00	8.00				14.5	0
0	0	8.00	8.00				13.7	0

0		14.00	14.00					2
0	0	26.00	26.00				12.2	0
0	0	26.00	26.00				12.1	0
0		37.00	37.00					2
0	0	49.92	49.92				9.1	0
0	0	49.92	49.92				9.9	0
0		0.00	0.00	67.5	2.0	33.8		1
0		1.50	1.48					2
0	0	2.58	2.57				22.2	0
0	0	2.58	2.57				21.0	0
0	0	6.00	5.98				14.7	0
0	0	6.00	5.98				13.0	0
0	0	8.00	7.98				18.2	0
0	0	8.00	7.98				15.2	0
0		13.25	13.23					2
0	0	26.00	25.98				15.3	0
0	0	26.00	25.98				13.4	0
0		38.00	37.98					2
0	0	46.00	45.98				12.6	0
0	0	46.08	46.07				12.4	0
0		66.50	66.48					2
0		85.83	85.82					2
0		109.83	109.82					2
0		134.17	134.15					2
0		157.50	157.48					2
0	0	164.00	163.98				1.3	0
0	0	164.25	164.23				1.6	0
0		164.42	0.00	67.5	2.0	33.8		1
0	0	166.50	2.10				16.7	0

0	0	166.50	2.10				18.5	0
0	0	170.50	6.10				15.3	0
0	0	170.50	6.10				17.7	0
0	0	174.08	9.68				13.5	0
0	0	174.08	9.68				16.5	0
0		181.75	17.35					2
0	0	188.00	23.60				14.1	0
0	0	188.00	23.60				13.8	0
0		205.50	41.10					2
0	0	211.83	47.43				9.3	0
0	0	212.00	47.60				8.7	0
0		0.00	0.00	80.0	2.0	40.0		1
0	0	2.17	2.16				18.3	0
0	0	4.08	4.08				14.4	0
0	0	4.08	4.08				15.3	0
0	0	8.08	8.08				15.8	0
0	0	8.08	8.08				13.2	0
0		18.92	18.91					2
0	0	25.83	25.83				11.0	0
0	0	25.83	25.83				12.3	0
0		42.83	42.83					2
0	0	49.80	49.79				9.1	0
0	0	49.80	49.79				6.8	0
0		67.58	67.58					2
0		91.58	91.58					2
0		115.58	115.58					2
0		151.83	151.83					2
0		163.67	163.66					2
0	0	163.83	163.83				2.1	0

0	0	163.83	163.83				2.2	0
0		167.83	0.00	80.0	2.0	40.0		1
0	0	170.17	2.35				13.9	0
0	0	170.17	2.35				19.2	0
0	0	171.83	4.02				15.6	0
0	0	171.83	4.02				16.7	0
0	0	175.83	8.02				15.1	0
0	0	175.83	8.02				16.1	0
0		187.58	19.77					2
0	0	193.92	26.10				13.0	0
0	0	193.92	26.10				11.8	0
0		210.83	43.02					2
0	0	217.92	50.10				11.6	0
0	0	217.92	50.10				11.2	0
0		235.58	67.77					2
0		259.57	91.75					2
0		283.58	115.77					2
0		307.67	139.85					2
0		331.33	163.52					2
0	0	417.17	249.35				1.0	0
0	0	420.00	252.18				0.9	0
0		0.00	0.00	312.5	2.0	156.3		1
0	0	2.00	2.01				23.8	0
0	0	2.00	2.01				22.2	0
0	0	3.75	3.76				20.6	0
0	0	3.92	3.92				22.8	0
0	0	11.75	11.76				17.9	0
0		11.75	11.76					2
0	0	11.75	11.76				18.0	0

0		0	21.00	21.01			18.5	0
0		0	23.75	23.76			17.6	0
0		0	27.67	27.67			15.2	0
0			34.92	34.92				2
0		0	59.33	59.34			11.3	0
0			0.00	0.00	155.5	2.0	77.8	1
0		0	2.75	2.77			22.6	0
0		0	2.75	2.77			16.9	0
0		0	4.00	4.02			20.7	0
0		0	4.00	4.02			22.0	0
0			9.33	9.35				2
0		0	9.50	9.52			21.6	0
0		0	9.50	9.52			20.8	0
0		0	25.50	25.52			16.8	0
0		0	25.50	25.52			17.0	0
0			32.50	32.52				2
0			39.75	39.77				2
0		0	40.75	40.77			12.7	0
0		0	40.75	40.77			14.0	0
0		0	51.50	51.52			12.4	0
0		0	51.50	51.52			11.9	0
0			0.00	0.00	63.0	2.0	31.5	1
0		0	2.00	1.99			18.9	0
0		0	2.00	1.99			17.8	0
0		0	4.00	3.99			14.4	0
0		0	4.00	3.99			16.8	0
0		0	8.00	7.99			14.5	0
0		0	8.00	7.99			14.8	0
0			19.33	19.32				2

0	0	25.83	25.82				8.6	0
0	0	25.83	25.82				7.8	0
0		43.83	43.82					2
0	0	50.00	49.99				3.7	0
0	0	50.00	49.99				3.5	0
0		68.00	67.99					2
0		90.08	90.07					2
0		114.33	114.32					2
0		140.00	139.99					2
0	0	163.58	163.57				0.3	0
0	0	163.58	163.57				0.2	0
0		163.58	163.57					2
0		168.50	0.00	63.0	2.0	31.5		1
0	0	170.50	1.99				17.8	0
0	0	170.50	1.99				17.2	0
0	0	173.00	4.49				16.7	0
0	0	173.50	4.99				16.8	0
0	0	176.00	7.49				14.6	0
0	0	176.00	7.49				15.7	0
0		187.50	18.99					2
0	0	194.00	25.49				10.3	0
0	0	194.00	25.49				9.8	0
0		212.08	43.57					2
0	0	218.25	49.74				5.5	0
0	0	218.25	49.74				5.3	0
0		0.00	0.00	550.0	2.0	275.0		1
0	0	2.00	2.00				25.1	0
0	0	2.00	2.00				24.0	0
0	0	6.25	6.25				19.2	0

0		0	6.25	6.25			17.7	0
0		0	10.25	10.25			17.9	0
0		0	10.25	10.25			15.4	0
0			18.42	18.42				2
0		0	26.00	26.00			13.0	0
0		0	26.00	26.00			13.5	0
0			42.50	42.50				2
0		0	50.25	50.25			8.0	0
0		0	50.25	50.25			8.6	0
0			66.00	66.00				2
0			69.70	69.70				2
0			89.58	89.59				2
0			113.50	113.50				2
0			138.00	138.00				2
0			162.00	162.00				2
0		0	166.42	166.42			0.6	0
0		0	166.42	166.42			0.6	0
0			0.00	0.00	83.0	2.0	41.5	1
0		0	2.08	2.07			16.5	0
0		0	2.08	2.07			10.8	0
0		0	3.92	3.91			16.6	0
0		0	3.92	3.91			9.8	0
0		0	7.92	7.91			11.4	0
0		0	7.92	7.91			15.5	0
0			19.67	19.66				2
0		0	25.92	25.91			11.3	0
0		0	25.92	25.91			8.9	0
0			43.67	43.66				2
0		0	49.92	49.91				0

0	0	49.92	49.91				6.8	0
0		67.92	67.91					2
0		91.83	91.82					2
0		115.92	115.91					2
0		139.83	139.82					2
0		163.13	163.12					2
0	0	167.92	167.91				0.2	0
0		167.92	0.00	83.0	2.0	41.5		1
0	0	167.92	167.91				0.1	0
0	0	169.92	1.99				18.0	0
0	0	169.92	1.99				16.7	0
0	0	171.92	3.99				16.8	0
0	0	171.92	3.99				17.5	0
0	0	176.00	8.07				16.3	0
0	0	176.00	8.07				15.3	0
0		187.92	19.99					2
0	0	194.00	26.07				11.4	0
0	0	194.00	26.07				10.8	0
0		211.77	43.84					2
0	0	217.00	49.07				6.4	0
0	0	217.92	49.99				4.9	0
0		235.33	67.41					2
0		259.83	91.91					2
0		283.67	115.74					2
0		307.67	139.74					2
0		331.67	163.74					2
0	0	335.92	167.99				0.4	0
0	0	335.92	167.99				0.3	0
0	0	342.50	174.57				0.3	0

0		0	343.92	175.99			0.2	0
0		0	349.42	181.49			0.3	0
0		0	353.42	185.49			0.2	0
1			0.00	0.00	97.5	2.0	48.8	1
1		0	2.00	2.02			17.0	0
1		0	2.00	2.02			13.7	0
1		0	5.50	5.52			14.5	0
1		0	5.50	5.52			16.5	0
1		0	12.17	12.18			15.7	0
1		0	12.17	12.18			15.2	0
1			18.08	18.10				2
1		0	23.83	23.85			13.1	0
1		0	23.83	23.85			10.8	0
1			41.23	41.25				2
1		0	48.00	48.02			11.3	0
1		0	48.00	48.02			12.4	0
1			65.50	65.52				2
1			89.92	89.93				2
1			114.00	114.02				2
1			137.75	137.77				2
1			161.75	161.77				2
1		0	161.75	161.77			6.7	0
1		0	161.75	161.77			5.4	0
1			166.75	0.00	97.5	2.0	48.8	1
1		0	169.00	2.26			19.2	0
1		0	169.00	2.26			16.9	0
1		0	171.00	4.26			14.4	0
1		0	171.00	4.26			17.9	0
1		0	174.00	7.26			15.9	0

1		0	174.00	7.26				19.2	0
1			185.83	19.10					2
1		0	192.00	25.26				17.7	0
1		0	192.00	25.26				17.4	0
1			209.87	43.13					2
1		0	215.83	49.10				14.0	0
1		0	215.83	49.10				14.5	0
1			233.50	66.76					2
1			257.50	90.76					2
1			282.08	115.35					2
1			306.08	139.35					2
1			330.00	163.26					2
1			334.00	0.00	97.5	2.0	48.8		1
1			354.00	20.00					2
1			378.17	44.17					2
1			401.42	67.42					2
1			425.83	91.84					2
1			449.92	115.92					2
1			473.75	139.75					2
1		0	510.50	176.50				6.1	0
0			0.00	0.00	444.0	1.0	444.0		1
0			13.75	13.74					2
0		1	13.75	13.74				12.6	0
0		1	21.00	20.99				10.9	0
0			24.00	0.00	222.0	1.0	222.0		1
0			37.33	13.33					2
0		1	37.33	13.33				16.3	0
0		1	45.00	21.00				16.2	0
0			48.00	0.00	222.0	1.0	222.0		1

0		1	55.13	7.14			16.7	0
0		1	59.95	11.96			15.2	0
0		1	60.78	12.79			15.6	0
0			60.78	12.79				2
0		1	64.58	16.59			14.3	0
0		1	68.67	20.67			12.7	0
0			72.00	0.00	222.0	1.0	222.0	1
0		0	72.00	24.01			14.7	0
0		0	72.00	24.01			14.2	0
0		1	73.50	1.51			17.0	0
0		0	73.50	1.51			23.6	0
0		0	73.50	1.51			22.8	0
0		0	76.00	4.01			22.0	0
0		0	76.00	4.01			19.8	0
0		0	80.00	8.01			20.9	0
0		0	80.00	8.01			19.6	0
0		0	91.67	19.68			14.9	0
0		0	91.67	19.68			12.9	0
0		0	94.00	22.01			11.9	0
0		0	94.00	22.01			12.3	0
0			0.00	0.00	800.0	4.0	200.0	1
0		0	4.00	4.02			11.7	0
0		0	7.92	7.93			11.5	0
0		0	14.00	14.02			11.5	0
0		0	23.33	23.35			6.9	0
0			24.00	0.00	400.0	2.0	200.0	1
0		1	26.42	2.40			11.7	0
0			26.42	2.40				2
0		1	38.00	13.99			13.2	0

0		38.00	13.99					2
0	0	43.75	19.74				10.3	0
0		48.00	0.00	400.0	2.0	200.0		1
0	1	62.53	14.53				14.6	0
0		62.53	14.53					2
0	1	75.33	27.33				11.2	0
0		76.00	0.00	400.0	2.0	200.0		1
0		85.92	9.91					2
0	1	85.92	9.91				17.2	0
0		96.00	0.00	400.0	2.0	200.0		1
0	1	98.25	2.26				20.1	0
0		110.00	14.01					2
0	1	110.00	14.01				15.1	0
0	1	119.92	23.92				11.2	0
0		120.00	0.00	400.0	2.0	200.0		1
0	1	122.63	2.65				15.6	0
0	0	143.58	23.60				9.9	0
0		144.00	0.00	400.0	2.0	200.0		1
0	0	146.33	2.32				19.2	0
0		146.50	2.48					2
0	0	150.25	6.23				14.3	0
0		158.00	13.98					2
0	0	158.00	13.98				13.3	0
0	0	164.08	20.07				12.0	0
0	0	191.33	47.32				10.8	0
1		0.00	0.00	105.0	2.0	52.5		1
1	0	2.33	2.35				20.1	0
1	0	2.33	2.35				21.2	0
1	0	5.25	5.27				18.3	0

1		0	5.25	5.27			18.4	0
1		0	11.00	11.02			15.8	0
1		0	11.00	11.02			14.7	0
1			16.00	16.02				2
1		0	23.00	23.02			13.4	0
1		0	23.00	23.02			16.2	0
1			40.08	40.10				2
1		0	47.00	47.02			13.1	0
1		0	47.00	47.02			13.0	0
1			65.17	65.18				2
1			88.67	88.68				2
1		1	112.42	112.43			9.3	0
1			112.42	112.43				2
1		1	122.08	122.10			8.2	0
1		1	130.33	130.35			7.4	0
1			136.67	136.68				2
1		1	149.00	149.02			7.0	0
1			160.50	160.52				2
1		0	162.50	162.52			6.4	0
1		0	162.50	162.52			5.2	0
1			166.50	0.00	105.0	2.0	52.5	1
1		0	169.00	2.48			7.2	0
1		0	169.00	2.48			7.9	0
1		0	173.08	6.57			15.9	0
1		0	173.08	6.57			16.2	0
1		0	179.17	12.65			17.9	0
1		0	179.17	12.65			15.6	0
1			184.00	17.48				2
1		0	191.00	24.48			17.8	0

1		0	191.00	24.48			17.3	0
1			207.92	41.40				2
1		0	215.00	48.48			14.7	0
1		0	215.00	48.48			14.7	0
1			232.98	66.47				2
1			256.50	89.98				2
1		1	256.50	89.98			10.8	0
1			280.83	114.32				2
1		1	280.83	114.32			8.3	0
1			304.25	137.73				2
1		1	304.25	137.73			9.1	0
1		1	328.83	162.32			6.4	0
1			328.83	162.32				2
1			334.00	0.00	105.0	2.0	52.5	1
1		1	337.00	3.00			19.2	0
1		1	340.00	6.00			21.6	0
1		1	352.17	18.17			21.5	0
0			0.00	0.00	140.0	3.3	43.1	1
0		0	3.25	3.25			25.9	0
0		0	3.25	3.25			21.7	0
0		0	6.00	6.00			25.2	0
0		0	6.00	6.00			22.3	0
0		0	12.17	12.17			19.4	0
0		0	12.17	12.17			23.2	0
0		0	26.00	26.00			16.8	0
0		0	26.00	26.00			17.8	0
0			28.58	28.59				2
0			42.17	42.17				2
0		0	54.00	54.00			12.3	0

0	0	54.00	54.00				14.0	0
0		70.92	70.92					2
0		89.50	89.50					2
0		113.17	113.17					2
0		137.92	137.92					2
0		161.25	161.25					2
0	0	168.00	168.00				6.0	0
0	0	168.00	168.00				6.0	0
0		168.17	0.00	140.0	2.1	67.3		1
0	0	170.25	2.08				29.4	0
0	0	170.25	2.08				16.2	0
0	0	174.00	5.83				23.1	0
0	0	174.00	5.83				22.7	0
0	0	180.08	11.91				23.7	0
0	0	180.08	11.91				23.2	0
0		185.67	17.50					2
0	0	197.00	28.83				17.4	0
0	0	197.00	28.83				17.3	0
0		209.42	41.25					2
0	0	215.83	47.66				13.3	0
0	0	215.83	47.66				13.5	0
0		0.00	0.00	250.0	2.3	111.1		1
0		2.08	2.09					2
0	0	2.28	2.29				21.2	0
0	0	2.28	2.29				21.8	0
0	0	5.58	5.59				15.7	0
0	0	5.58	5.59				17.7	0
0		13.42	13.42					2
0	0	13.58	13.59				16.3	0

0		0	13.58	13.59			12.7	0
0		0	25.48	25.49			13.0	0
0		0	25.48	25.49			10.9	0
0			37.58	37.59				2
0		0	49.42	49.42			9.0	0
0		0	49.42	49.42			9.2	0
0			61.58	61.59				2
0			97.92	97.92				2
0			109.33	109.34				2
0		1	127.42	127.42			29.0	0
0			131.92	0.00	250.0	2.0	125.0	1
0			133.50	1.60				2
0			154.92	0.00	120.0	1.0	120.0	1
0			157.33	2.42				2
0		0	179.33	24.42			16.4	0
0		0	179.33	24.42			18.5	0
0			179.42	0.00	120.0	1.0	120.0	1
0		0	180.50	1.08			29.1	0
0		0	180.50	1.08			31.8	0
0			180.58	1.17				2
0		0	183.42	4.00			31.0	0
0		0	183.42	4.00			26.8	0
0		0	187.42	8.00			23.3	0
0		0	187.42	8.00			26.8	0
0		0	203.42	24.00			18.6	0
0		0	203.42	24.00			18.5	0
0			203.42	0.00	120.0	1.0	120.0	1
0			205.58	2.17				2
0		0	227.42	24.01			16.2	0

0	0	227.42	24.01				18.2	0
0		0.00	0.00	375.0	2.1	180.3		1
0	0	2.17	2.16				18.4	0
0	0	2.17	2.16				13.2	0
0	0	3.92	3.91				16.7	0
0	0	3.92	3.91				16.3	0
0	0	7.92	7.91				15.7	0
0	0	7.92	7.91				15.5	0
0		19.83	19.83					2
0	0	25.92	25.91				11.3	0
0	0	25.92	25.91				10.8	0
0	0	49.92	49.91				7.3	0
0	0	49.92	49.91				8.6	0
0		55.92	55.91					2
0		68.17	68.16					2
0		92.00	92.00					2
0		115.92	115.91					2
0		138.92	138.91					2
0	0	167.88	167.88				0.8	0
0	0	167.92	167.91				0.5	0
0		168.17	0.00	375.0	2.1	176.1		1
0	0	170.38	2.21				19.7	0
0	0	170.38	2.21				5.1	0
0		170.42	2.24					2
0	0	172.12	3.94				14.3	0
0	0	172.12	3.94				19.1	0
0	0	175.88	7.71				16.2	0
0	0	175.92	7.74				13.5	0
0		187.67	19.49					2

0	0	193.92	25.74				9.5	0
0	0	193.92	25.74				8.2	0
0		211.67	43.49					2
0	0	212.17	43.99				6.1	0
0	0	212.17	43.99				5.5	0
0		0.00	0.00	250.0	2.1	120.2		1
0	0	2.17	2.18				17.6	0
0	0	2.17	2.18				20.5	0
0	0	4.08	4.10				14.2	0
0	0	4.08	4.10				16.4	0
0	0	7.58	7.60				16.8	0
0	0	7.58	7.60				16.0	0
0		20.08	20.10					2
0	0	25.58	25.60				10.7	0
0	0	25.58	25.60				9.9	0
0		43.58	43.60					2
0	0	49.58	49.60				4.2	0
0	0	49.58	49.60				4.0	0
0	1	55.42	55.43				3.1	0
0		67.92	67.93					2
0	1	67.92	67.93				2.6	0
0		77.58	0.00	120.0	1.0	120.0		1
0	1	79.58	2.01				14.5	0
0		91.28	13.71					2
0	0	98.08	20.51				8.8	0

Define

ORDN	Unique number for each record
ID	Subject ID
ECMO	1 = ECMO support 0 = No ECMO support
WT	Weight (kg)
PNA	Postnatal age (days)
GA	Gestational age (weeks)
RACE	0 = White 1 = Black 2 = Other
SEX	0 = Female 1 = Male
SCRE	Serum creatinine
ALBE	Serum albumin
ASTE	Serum aspartate aminotransferase
ALTE	Serum alanine aminotransferase
HMFLTRE	0 = No hemofilter support 1 = Hemofilter support
CVVHDE	0 = No continuous venovenous hemodialysis support 1 = Continuous venovenous hemodialysis support
SCAVENGE	0 = timed sample 1 = scavenge sample
TAFD	Time after first dose (h)
TALD	Time after last dose (h)

AMT	Amount (mg)
DUR	Duration of infusion (h)
RATE	Rate of infusion (mg/h)
DV	Concentration (mg/L)
EVID	0 = Concentration record 1 = Dosing record 2 = Lab record

APPENDIX 3

Micafungin data

id	wt	pna	ga	race	sex	scr	alb	ast	alt	tafd	Tald	amt	rate	dv
1	3.30	2	39	black	0					0.00				
1	3.30	0	39	black	0					0.00				
1	3.30	4	39	black	0					0.00				0.00
1	3.30	4	39	black	0	0.3				0.00				
1	3.30	4	39	black	0					0.00				0.00
1	3.30	1	39	black	0		2.5	29	9	0.00				
1	3.30	4	39	black	0					0.01		13.2	13.2	
1	3.30	4	39	black	0					1.09	1.08			4.81
1	3.30	4	39	black	0					1.09	1.08			4.70
1	3.30	4	39	black	0					2.01	2.00			3.66
1	3.30	4	39	black	0					2.01	2.00			3.56
1	3.30	5	39	black	0					3.09	3.08			3.63
1	3.30	5	39	black	0					3.09	3.08			4.25
1	3.30	5	39	black	0					10.76	10.75			3.51
1	3.30	5	39	black	0					10.76	10.75			3.49
1	3.30	5	39	black	0					13.01	13.00			2.96
1	3.30	5	39	black	0					13.01	13.00			3.20
1	3.30	5	39	black	0					23.84	23.83			1.82
1	3.30	5	39	black	0					23.84	23.83			1.63
1	3.30	5	39	black	0					24.01	24.00	13.2	13.2	
1	3.30	6	39	black	0					48.01	24.00	13.2	13.2	
1	3.30	7	39	black	0					71.92	23.92			2.17
1	3.30	7	39	black	0					71.92	23.92			2.43
1	3.30	7	39	black	0					72.01	24.00	13.2	13.2	

1	3.30	7	39	black	0				73.17	1.17			6.39
1	3.30	7	39	black	0				73.17	1.17			3.95
1	3.30	7	39	black	0				74.09	2.08			5.34
1	3.30	7	39	black	0				74.09	2.08			1.43
1	3.30	8	39	black	0				75.09	3.08			3.17
1	3.30	8	39	black	0				75.09	3.08			5.05
1	3.30	8	39	black	0				83.01	11.00			5.22
1	3.30	8	39	black	0				83.01	11.00			5.25
1	3.30	8	39	black	0				84.84	12.83			5.57
1	3.30	8	39	black	0				84.84	12.83			5.27
1	3.30	8	39	black	0				96.66	24.65			2.01
1	3.30	8	39	black	0				96.66	24.65			3.03
1	3.30	8	39	black	0				96.67	24.67	13.2	13.2	
1	3.30	9	39	black	0				121.01	24.33	13.2	13.2	
1	3.30	10	39	black	0				144.01	23.00	13.2	13.2	
1		11	39	black	0		3.7	30	14	151.01			
1		11	39	black	0	0.3				158.26			
1	3.30	11	39	black	0				168.01	24.00	13.2	13.2	
1		11	39	black	0				169.26				
1		12	39	black	0				174.92				
1		15	39	black	0								
2	85.60	6024	37	White	0				0.00				
2	85.60	6024	37	White	0				0.00		150.0	150.0	
2	85.60	6025	37	White	0		2.5	27	42	12.00			
2	85.60	6025	37	White	0				24.00	24.00	150.0	150.0	
2	85.60	6026	37	White	0	0.4				36.00			
2	85.60	6026	37	White	0				48.09				
2	85.60	6026	37	White	0				48.19	24.18			2.04
2	85.60	6026	37	White	0				48.34	24.33	150.0	128.2	

2	85.60	6026	37	White	0					49.59	1.25			10.09
2	85.60	6026	37	White	0					53.00	4.67			6.98
2	85.60	6027	37	White	0					59.00	10.67			4.19
2	85.60	6027	37	White	0	0.5	2.3	19	25	59.75				
2	85.60	6027	37	White	0					62.00	13.67			3.52
2	85.60	6027	37	White	0					71.92				
2	85.60	6027	37	White	0					71.92	23.58			2.17
2	85.60	6027	37	White	0					72.00	23.67	150.0	150.0	
2	85.60	6028	37	White	0					96.00	24.00	150.0	150.0	
2	85.60	6029	37	White	0					120.17	24.17			2.40
2	85.60	6029	37	White	0					120.37	24.37	150.0	150.0	
2	85.60	6029	37	White	0					121.50	1.13			13.79
2	85.60	6029	37	White	0					122.50	2.13			10.18
2	85.60	6029	37	White	0					123.92	3.55			9.84
2	85.60	6030	37	White	0					130.00	9.63			6.70
2	85.60	6030	37	White	0					134.17	13.80			4.56
2	85.60	6030	37	White	0					144.17	23.80			2.62
2	85.60	6030	37	White	0					144.19	23.82	150.0	150.0	
2	85.60	6031	37	White	0					168.00	23.82	150.0	150.0	
2	85.60	6033	37	White	0					204.00				
2	85.60	6033	37	White	0	0.4				215.84				
2	85.60	6034	37	White	0		2.1	120	177	245.00				
2	85.60	6043	37	White	0		2.1	62	113	443.50				
2	85.60	6426	37	White	0			41	42	9642.50				
3	9.60	575	37	White	1	0.2	3.5	210	479	0.00				
3	9.60	574	37	White	1					0.00				
3	9.60	575	37	White	1					0.00		39.0	39.0	
3	9.60	574	37	White	1					0.00				
3	9.60	575	37	White	1					1.16	1.17			7.47

3	9.60	575	37	White	1			1.16	1.17		8.93
3	9.60	575	37	White	1			2.04	2.05		5.36
3	9.60	575	37	White	1			2.08	2.08		6.25
3	9.60	575	37	White	1			3.13	3.13		5.84
3	9.60	575	37	White	1			3.13	3.13		5.72
3	9.60	575	37	White	1			10.96	10.97		3.32
3	9.60	575	37	White	1			10.98	10.98		2.92
3	9.60	575	37	White	1			13.04	13.05		2.57
3	9.60	575	37	White	1			13.04	13.05		3.67
3	9.60	576	37	White	1			23.91	23.92		1.76
3	9.60	576	37	White	1			29.49	29.50	39.0	39.0
3	9.60	577	37	White	1			55.08	25.58	39.0	39.0
3	9.60	578	37	White	1			78.99	23.92		2.90
3	9.60	578	37	White	1			78.99	23.92		3.53
3	9.60	578	37	White	1	0.2		78.99			
3	9.60	578	37	White	1			79.16	24.08	39.0	39.0
3	9.60	578	37	White	1			80.16	1.00		17.02
3	9.60	578	37	White	1			80.16	1.00		14.26
3	9.60	578	37	White	1			81.24	2.08		14.91
3	9.60	578	37	White	1			81.24	2.08		8.94
3	9.60	578	37	White	1			84.91	5.75		11.66
3	9.60	578	37	White	1			84.91	5.75		12.45
3	9.60	579	37	White	1			88.08	8.92		8.89
3	9.60	579	37	White	1			88.08	8.92		6.47
3	9.60	579	37	White	1			91.49	12.33		6.77
3	9.60	579	37	White	1			91.49	12.33		6.94
3	9.60	579	37	White	1			103.11	23.95		4.03
3	9.60	579	37	White	1			103.19	24.03		2.94
3	9.60	579	37	White	1			103.56	24.40	39.0	39.0

3	9.60	580	37	White	1					115.58				
3	9.60	580	37	White	1					126.99	23.43	39.0	39.0	
3	9.60	581	37	White	1		3.9	45	72	138.36				
3	9.60	581	37	White	1	0.1				150.83				
3	9.60	581	37	White	1					152.33	25.33	39.0	33.3	
4	3.90	124	27	black	0					0.00				
4	3.90	124	27	black	0	0.2				0.00				
4	3.90	124	27	black	0					0.00				0.00
4	3.90	122	27	black	0		2.7	40	17	0.00				
4	3.90	124	27	black	0					0.00				
4	3.90	122	27	black	0					0.00				
4	3.90	124	27	black	0					0.01		15.6	15.6	
4	3.90	124	27	black	0					1.51	1.50			8.87
4	3.90	124	27	black	0					1.51	1.50			5.09
4	3.90	124	27	black	0					2.76	2.75			5.22
4	3.90	124	27	black	0					2.76	2.75			6.57
4	3.90	124	27	black	0					5.10	5.08			5.38
4	3.90	124	27	black	0					5.10	5.08			5.20
4	3.90	125	27	black	0					11.21	11.20			3.30
4	3.90	125	27	black	0					11.21	11.20			3.20
4	3.90	125	27	black	0					11.35				
4	3.90	125	27	black	0					13.10	13.08			3.14
4	3.90	125	27	black	0					13.10	13.08			2.84
4	3.90	125	27	black	0	0.2				22.60				
4	3.90	125	27	black	0					23.65	23.63			1.52
4	3.90	125	27	black	0					23.65	23.63			1.44
4	3.90	125	27	black	0					24.50	24.48	15.6	15.6	
4	3.90	126	27	black	0					48.01	23.52	15.6	13.3	
4	3.90	127	27	black	0	0.2				58.35				

4	3.90	127	27	black	0				59.23				
4	3.90	127	27	black	0				70.43	22.42			1.88
4	3.90	127	27	black	0				70.43	22.42			1.92
4	3.90	127	27	black	0				72.01	24.00	15.6	15.6	
4	3.90	127	27	black	0				73.43	1.42			8.80
4	3.90	127	27	black	0				73.43	1.42			7.68
4	3.90	127	27	black	0				74.51	2.50			7.01
4	3.90	127	27	black	0				74.51	2.50			7.10
4	3.90	127	27	black	0				77.10	5.08			6.00
4	3.90	127	27	black	0				77.10	5.08			4.27
4	3.90	128	27	black	0	0.2			82.93				
4	3.90	128	27	black	0				82.98	10.97			3.63
4	3.90	128	27	black	0				82.98	10.97			3.12
4	3.90	128	27	black	0				85.13	13.12			2.89
4	3.90	128	27	black	0				85.13	13.12			3.51
4	3.90	128	27	black	0				95.10	23.08			2.29
4	3.90	128	27	black	0				95.10	23.08			2.13
4	3.90	128	27	black	0				96.01	24.00	15.6	15.6	
4	3.90	129	27	black	0				120.30	24.28	15.6	15.6	
4	3.90	130	27	black	0	0.3			130.68				
4	3.90	136	27	black	0	0.2			274.83				
4	3.90						76	31	8987.11				
4	3.90	126	27	black	0								
4		122											
4	3.90	130	27	black	0								
4	3.90	131	27	black	0								
5	2.94	10	39	black	1				0.00				
5	2.94	1	39	black	1		48	9	0.00				
5	2.94	1	39	black	1		32	5	0.00				

5	2.94	7	39	black	1		3.6	0.00				
5	2.94	1	39	black	1			0.00				
5	2.94	11	39	black	1			0.00		23.6	23.5	
5	2.94	12	39	black	1	0.6		11.08				
5	2.94	12	39	black	1			11.38				
5	2.94	12	39	black	1			22.83	22.83			5.05
5	2.94	12	39	black	1			22.83	22.83			4.47
5	2.94	12	39	black	1			23.75	23.75	23.6	23.5	
5	2.94	12	39	black	1			25.03	1.28			16.88
5	2.94	12	39	black	1			25.10	1.35			20.64
5	2.94	12	39	black	1			26.37	2.62			14.43
5	2.94	12	39	black	1			26.37	2.62			12.91
5	2.94	12	39	black	1			28.75	5.00			12.53
5	2.94	12	39	black	1			28.75	5.00			12.86
5	2.94	13	39	black	1	0.5		34.83				
5	2.94	13	39	black	1			34.83	11.08			8.10
5	2.94	13	39	black	1			34.83	11.08			7.19
5	2.94	13	39	black	1			40.75	17.00			5.57
5	2.94	13	39	black	1			40.83	17.08			7.23
5	2.94	13	39	black	1			46.73	22.98			5.21
5	2.94	13	39	black	1			46.73	22.98			4.51
5	2.94	13	39	black	1			47.78	24.03	23.6	23.5	
5	2.94	14	39	black	1	0.4		66.62				
5	2.94	14	39	black	1			71.68	23.90	23.6	23.5	
5	2.94	15	39	black	1	0.4		83.00				
5	2.94	15	39	black	1			94.82	23.13			5.60
5	2.94	15	39	black	1			94.92	23.23			4.19
5	2.94	15	39	black	1			96.13	24.45	23.6	23.5	
5	2.94	15	39	black	1			97.33	1.20			16.72

5	2.94	15	39	black	1				97.33	1.20			14.92
5	2.94	15	39	black	1				98.38	2.25			9.95
5	2.94	15	39	black	1				98.40	2.27			11.09
5	2.94	15	39	black	1				101.23	5.10			7.18
5	2.94	15	39	black	1				101.23	5.10			9.40
5	2.94	16	39	black	1	0.5			106.75				
5	2.94	16	39	black	1				106.92	10.78			8.53
5	2.94	16	39	black	1				106.92	10.78			7.37
5	2.94	16	39	black	1				112.88	16.75			6.19
5	2.94	16	39	black	1				112.88	16.75			5.33
5	2.94	16	39	black	1				118.73	22.60			4.42
5	2.94	16	39	black	1				118.73	22.60			4.28
5	2.94	16	39	black	1				119.87	23.73	23.6	23.5	
5	2.94	17	39	black	1				130.75				
5	2.94	8	39	black	1								
5	2.94	14	39	black	1								
6	3.47	6	39	White	1				0.00				0.00
6	3.47	4	39	White	1				0.00				
6	3.47	6	39	White	1				0.00				0.00
6	3.47	6	39	White	1				0.00				
6	3.47	4	39	White	1				0.00				
6	3.47	5	39	White	1		2.3	103	25	0.00				
6	3.47	6	39	White	1	1.2				0.00				
6	3.47	6	39	White	1				0.01		13.9	13.9	
6	3.47	6	39	White	1				1.34	1.33			6.13
6	3.47	6	39	White	1				1.34	1.33			5.10
6	3.47	6	39	White	1				2.76	2.75			4.99
6	3.47	6	39	White	1				2.76	2.75			3.67
6	3.47	6	39	White	1				5.38	5.37			0.44

6	3.47	6	39	White	1					5.46	5.45			3.88
6	3.47	6	39	White	1					11.43	11.42			0.99
6	3.47	6	39	White	1					11.43	11.42			2.67
6	3.47	7	39	White	1			148	41	17.18				
6	3.47	7	39	White	1					17.43	17.42			1.69
6	3.47	7	39	White	1					17.43	17.42			1.11
6	3.47	7	39	White	1					23.18	23.17			0.88
6	3.47	7	39	White	1					23.21	23.20			1.84
6	3.47	7	39	White	1					23.71	23.70	13.9	13.9	
6	3.47	7	39	White	1	1.5				29.84				
6	3.47	8	39	White	1					48.93	25.22	13.9	13.9	
6	3.47	9	39	White	1	1.6				65.68				
6	3.47	9	39	White	1					71.16	22.23			2.37
6	3.47	9	39	White	1					71.21	22.28			2.28
6	3.47	9	39	White	1					72.83	23.90	13.9	13.9	
6	3.47	9	39	White	1					73.68				
6	3.47	10	39	White	1					89.18				
6	3.47	11	39	White	1		3.3	15	22	113.68				
7	2.90	2	39	black	1			59	17	0.00				
7	2.90	6	39	black	1					0.00				0.00
7	2.90	6	39	black	1					0.00				0.00
7	2.90	1	39	black	1		2.5			0.00				
7	2.90	6	39	black	1					0.00		11.6	11.6	
7	2.90	6	39	black	1	0.6				0.00				
7	2.90	7	39	black	1					1.13	1.15			7.74
7	2.90	7	39	black	1					1.13	1.15			7.81
7	2.90	7	39	black	1					2.00	2.02			5.50
7	2.90	7	39	black	1					2.00	2.02			5.57
7	2.90	7	39	black	1					4.98	5.00			4.03

7	2.90	7	39	black	1					4.98	5.00			3.98
7	2.90	7	39	black	1					10.82	10.83			2.66
7	2.90	7	39	black	1					10.82	10.83			3.02
7	2.90	7	39	black	1					16.97	16.98			2.25
7	2.90	7	39	black	1					16.98	17.00			2.19
7	2.90	7	39	black	1					24.47	24.48	11.6	11.6	
7	2.90	8	39	black	1					29.07				
7	2.90	8	39	black	1					48.90	24.43	11.6	11.6	
7	2.90	9	39	black	1	0.8				61.70				
7	2.90	4	39	black	1									
8	6.20	138		black	0	0.3				0.00				
8	6.20	138		black	0					0.00				0.00
8	6.20	138		black	0					0.00				
8	6.20	135		black	0		3.1	53	27	0.00				
8	6.20	138		black	0					0.01		24.8	24.8	
8	6.20	139		black	0					0.96	0.95			10.23
8	6.20	139		black	0					1.96	1.95			7.69
8	6.20	139		black	0					5.21	5.20			6.50
8	6.20	139		black	0	0.3				5.26				
8	6.20	139		black	0					11.01	11.00			4.32
8	6.20	139		black	0					17.04	17.03			2.74
8	6.20	139		black	0					23.16	23.15			2.22
8	6.20	139		black	0					23.78	23.77	24.8	24.8	
8	6.20	140		black	0	0.2				40.68				
8	6.20	141		black	0					49.06	25.28	24.8	24.8	
8	6.20	141		black	0					53.46				
8	6.20	144		black	0			22	22	136.71				
8	6.20	141		black	0									
8	6.20	134		black	0									

9	65.00	6254		black	0		3.1	96	103	0.00				
9	65.00	6257		black	0	1.1				0.00				
9	65.00	6257		black	0					0.00				
9	65.00	6257		black	0					0.02		100.0	100.0	
9	65.00	6258		black	0	1.3				14.85				
9	65.00	6258		black	0					20.60	20.58			1.41
9	65.00	6258		black	0					23.38	23.37	100.0	100.0	
9	65.00	6258		black	0					24.88	1.50			5.75
9	65.00	6258		black	0					26.88	3.50			5.12
9	65.00	6258		black	0					32.77	9.38			3.71
9	65.00	6259		black	0					38.52	15.13			2.82
9	65.00	6259		black	0					44.52	21.13			2.33
9	65.00	6259		black	0					47.65	24.27	100.0	100.0	
9	65.00	6260		black	0	1.9				63.65				
9	65.00	6261		black	0					86.27				
9	65.00	6265		black	0		3.4	56	42	182.82				
9	65.00	6257		black	0									
10	3.90	111	39	black	0	0.7				0.00				
10	3.90	111	39	black	0					0.00				0.00
10	3.90	109	39	black	0			265	27	0.00				
10	3.90	108	39	black	0		2.5			0.00				
10	3.90	111	39	black	0					0.00				0.00
10	3.90	111	39	black	0	0.5				0.00				
10	3.90	111	39	black	0		2.5			0.00				
10	3.90	111	39	black	0					0.01		15.6	13.3	
10	3.90	112	39	black	0					1.21	1.20			8.66
10	3.90	112	39	black	0					1.21	1.20			5.72
10	3.90	112	39	black	0					2.13	2.12			6.58
10	3.90	112	39	black	0					2.13	2.12			4.65

10	3.90	112	39	black	0			5.08	5.07			4.95
10	3.90	112	39	black	0			5.08	5.07			5.45
10	3.90	112	39	black	0	0.6		5.11				
10	3.90	112	39	black	0			11.01	11.00			2.80
10	3.90	112	39	black	0			11.01	11.00			2.73
10	3.90	112	39	black	0	0.6		14.78				
10	3.90	112	39	black	0			17.46	17.45			1.32
10	3.90	112	39	black	0			17.48	17.47			1.41
10	3.90	112	39	black	0			23.00	22.98			0.94
10	3.90	112	39	black	0			23.01	23.00			1.13
10	3.90	112	39	black	0			24.40	24.38	15.6	15.6	
10	3.90	113	39	black	0			47.28	22.88	15.6	14.4	
10	3.90	114	39	black	0			53.11				
10	3.90	114	39	black	0	0.4		64.91				
10	3.90	114	39	black	0			71.13	23.85			1.97
10	3.90	114	39	black	0			71.15	23.87			1.68
10	3.90	114	39	black	0			72.10	24.82	15.6	15.6	
10	3.90	115	39	black	0			73.25	1.15			11.35
10	3.90	115	39	black	0			73.25	1.15			7.51
10	3.90	115	39	black	0			74.16	2.07			9.93
10	3.90	115	39	black	0			74.16	2.07			6.74
10	3.90	115	39	black	0			77.20				
10	3.90	115	39	black	0			78.10	6.00			6.61
10	3.90	115	39	black	0			78.10	6.00			6.13
10	3.90	115	39	black	0			82.90	10.80			4.94
10	3.90	115	39	black	0			83.11	11.02			4.74
10	3.90	115	39	black	0			88.83	16.73			3.43
10	3.90	115	39	black	0			88.85	16.75			3.36
10	3.90	115	39	black	0	0.4		88.86				

10	3.90	115	39	black	0					95.28	23.18			1.75
10	3.90	115	39	black	0					95.28	23.18			1.84
10								18	13	137.45				
10	3.90	107	39	black	0									
11	3.00	18		White	0					0.00				0.00
11	3.00	16		White	0		2.5	41	16	0.00				
11	3.00	18		White	0					0.00		12.0	12.0	
11	3.00	18		White	0	0.6				0.00				
11	3.00	18		White	0					1.47	1.48			3.59
11	3.00	18		White	0					1.47	1.48			3.40
11	3.00	18		White	0					3.47	3.48			4.33
11	3.00	18		White	0					9.46	9.47			2.57
11	3.00	18		White	0					13.47	13.48			0.00
11	3.00	19		White	0					23.31	23.32			0.89
11	3.00	19		White	0					24.22	24.23	12.0	12.0	
11								24	14	100.39				
12	3.40	46	37	White	1					0.00				0.00
12	3.40	46	37	White	1					0.00		13.6	13.6	
12	3.40	44	37	White	1		2.1			0.00				
12	3.40	46	37	White	1	0.3		77	93	0.00				
12	3.40	46	37	White	1					1.37	1.38			7.37
12	3.40	46	37	White	1					2.35	2.37			5.19
12	3.40	46	37	White	1					4.44	4.45			4.14
12	3.40	46	37	White	1					10.45	10.47			2.18
12	3.40	47	37	White	1					16.05	16.07			1.52
12	3.40	47	37	White	1					22.62	22.63			0.98
12	3.40	47	37	White	1					23.17	23.18	13.6	13.6	
12	3.40	50	37	White	1			20	70	88.29				
13	4.90	187	34	White	0					0.00				

13	4.90	187	34	White	0					0.00				0.00
13	4.90	187	34	White	0	0.6		31	13	0.00				
13	4.90	187	34	White	0					0.01		19.6	19.6	
13	4.90	187	34	White	0					1.21	1.20			9.84
13	4.90	187	34	White	0					2.29	2.28			7.24
13	4.90	187	34	White	0					4.88	4.87			5.88
13							3.8			4.94				
13	4.90	187	34	White	0					11.71	11.70			2.76
13	4.90	188	34	White	0					17.04	17.03			2.06
13	4.90	188	34	White	0					22.79	22.78			1.37
13	4.90	188	34	White	0					23.93	23.92	19.6	19.6	
13	4.90	189	34	White	0					47.96	24.03	19.6	19.6	
13								33	15	52.34				
13										56.38				
14	5.50	74		White	0					0.00				
14	5.50	74		White	0	2.6	3.2	35	79	0.00				
14	5.50	74		White	0					0.00				0.00
14	5.50	74		White	0					0.00		22.0	22.0	
14	5.50	74		White	0					1.60	1.60			7.25
14	5.50	74		White	0					2.60	2.60			6.04
14	5.50	74		White	0					4.90	4.90			4.86
14	5.50	74		White	0					11.26	11.27			3.95
14	5.50	75		White	0					16.93	16.93			3.25
14	5.50	75		White	0					23.01	23.02			2.48
14	5.50	75		White	0					24.01	24.02	22.0	22.0	
14	5.50	76		White	0					47.26	23.25	22.0	22.0	
14	5.50	77		White	0					70.85	23.58			4.13
14	5.50	77		White	0					71.83	24.57	22.0	22.0	
14	5.50	77		White	0					73.43	1.60			12.34

14	5.50	77	White	0					74.26	2.43			10.48
14	5.50	77	White	0					76.93	5.10			9.69
14	5.50	77	White	0					82.91	11.08			7.71
14	5.50	78	White	0					88.93	17.10			5.29
14	5.50	78	White	0					95.18	23.35			2.71
14	5.50	78	White	0					95.75	23.92	22.0	22.0	
14	5.50	79	White	0					118.10	22.35	22.0	22.0	
14	5.50	80	White	0					145.58	27.48	22.0	22.0	
14	5.50	81	White	0	0.6				160.63				
14	5.50	81	White	0					167.03	21.45	22.0	22.0	
14	5.50	82	White	0		5.1	88	31	189.75				

Define

id	Subject ID
wt	Weight (kg)
pna	Postnatal age (days)
ga	Gestational age (weeks)
race	Race
sex	0 = Female 1 = Male
scr	Serum creatinine
alb	Serum albumin
ast	Serum aspartate aminotransferase
alt	Serum alanine aminotransferase
tafd	Time after first dose (h)
tald	Time after last dose (h)
amt	Amount (mg)
rate	Rate of infusion (mg/h)
dv	Concentration (mg/L)

APPENDIX 4

Ex vivo Extraction Calculations

4.1 AUC_{0-24} Calculations for micafungin ex vivo circuits

Circuit	Time	Conc	lnConc	AUC Log	AUC Circuit
18	0.02	16.68	2.81421	0	
18	0.08	14.84	2.697326	0.944525	
18	0.25	13.31	2.588516	2.390392	
18	0.5	10.57	2.35802	2.971854	
18	1	7.85	2.060514	4.571332	
18	2	5.44	1.693779	6.571512	
18	3	4.1	1.410987	4.738464	
18	4	3.48	1.247032	3.781533	
18	8	2.11	0.746688	10.95246	
18	12	1.85	0.615186	7.908606	
18	24	0.62	-0.47804	13.50138	58.33206
19	0.02	21.7	3.077312	0	
19	0.08	19.29	2.959587	1.228282	
19	0.25	15.99	2.771964	2.990034	
19	0.5	13.84	2.627563	3.722284	
19	1	10.68	2.368373	6.095912	
19	2	7.05	1.953028	8.739718	
19	3	5.05	1.619388	5.994497	
19	4	2.61	0.95935	3.696757	
19	8	1.61	0.476234	8.279584	
19	12	1.04	0.039221	5.21723	
19	24	0.67	-0.40048	10.09783	56.06213

20	0.02	15.45	2.737609	0	
20	0.08	16.61	2.810005	0.96138	
20	0.25	15.42	2.735665	2.721297	
20	0.5	14.35	2.66375	3.719647	
20	1	13.08	2.571084	6.852597	
20	2	11.64	2.454447	12.34601	
20	3	10.47	2.348514	11.04467	
20	4	10.19	2.321407	10.32937	
20	8	7.55	2.021548	35.21652	
20	12	7.92	2.069391	30.9341	
20	24	8.14	2.09679	96.35397	210.4796
22	0.02	17.25	2.847812	0	
22	0.08	17.97	2.888704	1.056453	
22	0.25	18.24	2.903617	3.077793	
22	0.5	18	2.890372	4.529934	
22	1	16.96	2.830858	8.737421	
22	2	16.57	2.807594	16.76424	
22	3	15.6	2.747271	16.08012	
22	4	14.31	2.660959	14.94572	
22	8	12.55	2.529721	53.64303	
22	12	10.15	2.317474	45.23033	
22	24	6.36	1.850028	97.2948	261.3599
26	0.02	20.85	3.037354	0	
26	0.08	20.63	3.026746	1.244388	
26	0.25	19.76	2.98366	3.432619	
26	0.5	18.49	2.91723	4.779493	
26	1	15.49	2.740195	8.472882	

26	2	15.14	2.71734	15.31433	
26	3	13.39	2.594508	14.24709	
26	4	12.56	2.530517	12.97057	
26	8	11.52	2.444085	48.13004	
26	12	5.24	1.656321	31.88776	
26	24	4.39	1.479329	57.62964	198.1088
27	0.02	16.96	2.830858	0	
27	0.25	17.94	2.887033	4.012445	
27	0.5	17.74	2.875822	4.459953	
27	1	14.84	2.697326	8.123443	
27	2	11.87	2.474014	13.29978	
27	3	11.71	2.460443	11.78982	
27	4	8.98	2.195	10.28468	
27	8	9.65	2.266958	37.24393	
27	12	6	1.791759	30.72401	
27	24	6.15	1.816452	72.8963	192.8344
28	0.02	19.4	2.965273	0	
28	0.08	18.91	2.939691	1.149237	
28	0.25	17.29	2.850128	3.074945	
28	0.5	16.08	2.777576	4.169421	
28	1	15.1	2.714695	7.792433	
28	2	13.49	2.601949	14.27988	
28	3	11.78	2.466403	12.61569	
28	4	11.33	2.427454	11.55354	
28	8	8.98	2.195	40.43807	
28	12	9.11	2.209373	36.17938	
28	24	4.09	1.408545	75.22217	206.4748

29	0.02	20.71	3.030617	0	
29	0.08	20.21	3.006178	1.227539	
29	0.25	18.41	2.912894	3.280322	
29	0.5	17.11	2.839663	4.438017	
29	1	14.2	2.653242	7.80491	
29	2	13.39	2.594508	13.79104	
29	3	11.68	2.457878	12.51554	
29	4	10.41	2.342767	11.03282	
29	8	7.84	2.059239	36.25744	
29	12	6.27	1.835776	28.10315	
29	24	3.92	1.366092	60.04028	178.491
30	0.02	18.07	2.894253	0	
30	0.08	18.08	2.894806	1.0845	
30	0.25	17.25	2.847812	3.002497	
30	0.5	15.85	2.76317	4.135032	
30	1	14.43	2.669309	7.564447	
30	2	12.83	2.551786	13.61433	
30	3	11.25	2.420368	12.0227	
30	4	10.67	2.367436	10.95744	
30	8	8.65	2.157559	38.49879	
30	24	6.41	1.857859	119.5862	210.466
31	0.02	10.31	2.333114	0	
31	0.08	12.53	2.528126	0.683037	
31	0.25	9.99	2.301585	1.906055	
31	0.5	8.89	2.184927	2.357327	
31	1	5.5	1.704748	3.529934	
31	2	5.21	1.65058	5.353691	

31	3	4.75	1.558145	4.976457	
31	4	4.14	1.420696	4.438015	
31	8	3.3	1.193922	14.81656	
31	12	2.75	1.011601	12.06659	
31	24	4.28	1.453953	41.5054	91.63307

Define

Circuit	Circuit/Control ID
Time	Time (h)
Conc	Concentration (mg/L)
lnConc	Natural log of concentration
AUC log	Logarithmic calculation of AUC for each time interval = (t2-t1) * (C2-C1) / ln (C2 / C1) Where t = time, C = concentration
AUC Circuit	Total AUC for each Circuit at 24h =sum of AUC for each time interval

4.2 Relative decrease in AUC_{0-24} for micafungin circuits

Circuit	Time	Conc	lnConc	AUC Log	AUC Base	AUC Circuit	Relative Decrease in AUC
18	0.02	16.68	2.81421	0			
	0.08	16.67	2.813611	1.00049997			
	0.25	16.66	2.813011	2.833049915			
	0.5	16.65	2.81241	4.163749875			
	1	16.64	2.811809	8.32249975			

	2	16.63	2.811208	16.6349995			
	3	16.62	2.810607	16.6249995			
	4	16.61	2.810005	16.6149995			
	8	16.6	2.809403	66.41999799			
	12	16.59	2.8088	66.37999799			
	24	16.58	2.808197	199.019994	398.0148	58.33205672	0.853442489
19	0.02	21.7	3.077312	0			
	0.08	21.69	3.076851	1.301699977			
	0.25	21.68	3.07639	3.686449935			
	0.5	21.67	3.075929	5.418749904			
	1	21.66	3.075467	10.83249981			
	2	21.65	3.075005	21.65499962			
	3	21.64	3.074543	21.64499961			
	4	21.63	3.074081	21.63499961			
	8	21.62	3.073619	86.49999846			
	12	21.61	3.073156	86.45999846			
	24	21.6	3.072693	259.2599954	518.3944	56.06213081	0.891854287
20	0.02	15.45	2.737609	0			
	0.08	15.44	2.736962	0.926699968			
	0.25	15.43	2.736314	2.623949908			
	0.5	15.42	2.735665	3.856249865			
	1	15.41	2.735017	7.70749973			
	2	15.4	2.734368	15.40499946			
	3	15.39	2.733718	15.39499946			
	4	15.38	2.733068	15.38499946			
	8	15.37	2.732418	61.49999783			
	12	15.36	2.731767	61.45999783			

	24	15.35	2.731115	184.2599935	368.5194	210.4795624	0.428850775
22	0.02	17.25	2.847812	0			
	0.08	17.24	2.847232	1.034699971			
	0.25	17.23	2.846652	2.929949918			
	0.5	17.22	2.846071	4.306249879			
	1	17.21	2.845491	8.607499758			
	2	17.2	2.844909	17.20499952			
	3	17.19	2.844328	17.19499952			
	4	17.18	2.843746	17.18499952			
	8	17.17	2.843164	68.69999806			
	12	17.16	2.842581	68.65999806			
	24	17.15	2.841998	205.8599942	411.6834	261.3598502	0.36514356
26	0.02	20.85	3.037354	0			
	0.08	20.84	3.036874	1.250699976			
	0.25	20.83	3.036394	3.541949932			
	0.5	20.82	3.035914	5.2062499			
	1	20.81	3.035434	10.4074998			
	2	20.8	3.034953	20.8049996			
	3	20.79	3.034472	20.7949996			
	4	20.78	3.033991	20.7849996			
	8	20.77	3.03351	83.0999984			
	12	20.76	3.033028	83.05999839			
	24	20.75	3.032546	249.0599952	498.0114	198.1088135	0.602200236
27	0.02	16.96	2.830858	0			
	0.08	16.95	2.830268	1.017299971			
	0.25	16.94	2.829678	2.880649916			
	0.5	16.93	2.829087	4.233749877			

	1	16.92	2.828496	8.462499754			
	2	16.91	2.827905	16.91499951			
	3	16.9	2.827314	16.90499951			
	4	16.89	2.826722	16.89499951			
	8	16.88	2.826129	67.53999803			
	12	16.87	2.825537	67.49999802			
	24	16.86	2.824944	202.3799941	404.7292	192.8343521	0.523547207
28	0.02	19.4	2.965273	0			
	0.08	19.39	2.964757	1.163699974			
	0.25	19.38	2.964242	3.295449927			
	0.5	19.37	2.963725	4.843749892			
	1	19.36	2.963209	9.682499785			
	2	19.35	2.962692	19.35499957			
	3	19.34	2.962175	19.34499957			
	4	19.33	2.961658	19.33499957			
	8	19.32	2.961141	77.29999828			
	12	19.31	2.960623	77.25999827			
	24	19.3	2.960105	231.6599948	463.2404	206.4747637	0.554281603
29	0.02	20.71	3.030617	0			
	0.08	20.7	3.030134	1.242299976			
	0.25	20.69	3.02965	3.518149932			
	0.5	20.68	3.029167	5.171249899			
	1	20.67	3.028683	10.3374998			
	2	20.66	3.028199	20.6649996			
	3	20.65	3.027715	20.6549996			
	4	20.64	3.027231	20.6449996			
	8	20.63	3.026746	82.53999838			

	12	20.62	3.026261	82.49999838			
	24	20.61	3.025776	247.3799951	494.6542	178.4910445	0.639159946
30	0.02	18.07	2.894253	0			
	0.08	18.06	2.8937	1.083899972			
	0.25	18.05	2.893146	3.069349922			
	0.5	18.04	2.892592	4.511249885			
	1	18.03	2.892037	9.017499769			
	2	18.02	2.891482	18.02499954			
	3	18.01	2.890927	18.01499954			
	4	18	2.890372	18.00499954			
	8	17.99	2.889816	71.97999815			
	12	17.98	2.88926	71.93999815			
	24	17.97	2.888704	215.6999944	431.347	210.4659732	0.512072696
31	0.02	10.31	2.333114	0			
	0.08	10.3	2.332144	0.618299951			
	0.25	10.29	2.331173	1.750149862			
	0.5	10.28	2.3302	2.571249797			
	1	10.27	2.329227	5.137499594			
	2	10.26	2.328253	10.26499919			
	3	10.25	2.327278	10.25499919			
	4	10.24	2.326302	10.24499919			
	8	10.23	2.325325	40.93999674			
	12	10.22	2.324347	40.89999674			
	24	10.21	2.323368	122.5799902	245.2622	91.6330655	0.6263873
						MEAN AUC DECREASE	**0.59969401**

						MEDIAN AUC DECREASE	**0.538914405**

Define

Circuit	Circuit/Control ID
Time	Time (h)
Conc	Concentration (mg/L)
lnConc	Natural log of concentration
AUC log	Logarithmic calculation of AUC for each time interval = (t2-t1) * (C2-C1) / ln (C2 / C1) Where t = time, C = concentration
AUC Base	Total AUC assuming no extraction at 24h =sum of AUC for each time interval
AUC Circuit	Total AUC for each Circuit at 24h =sum of AUC for each time interval (from Appendix 4.1)
Relative Decrease in AUC	Decrease in AUC in circuit relative to AUC if no extraction =(AUC Base – AUC Circuit) / AUC Base)
Circuit	Subject ID
Time	Time (h)
Conc	Concentration (mg/L)
lnConc	Natural log of concentration
AUC log	Logarithmic calculation of AUC for each time interval = (t2-t1) * (C2-C1) / ln (C2 / C1) Where t = time, C = concentration

AUC Circuit	Total AUC for each Circuit at 24h =sum of AUC for each time interval

4.3 AUC_{0-24} Calculations for micafungin ex vivo controls

Circuit	Time	Conc	lnConc	AUC Log	AUC Control
202	0.02	57.6	4.053523	0	
202	0.08	58.85	4.074992	3.493366	
202	0.25	57.37	4.049521	9.878166	
202	0.5	55.72	4.020339	14.13525	
202	1	55.17	4.010419	27.72227	
202	2	55.34	4.013496	55.25496	
202	3	53.64	3.982295	54.48558	
202	4	52.64	3.963476	53.13843	
202	8	38.76	3.657389	181.386	
202	12	38.1	3.640214	153.7162	
202	24	33.56	3.513335	429.3841	982.5944
203	0.02	67.01	4.204842	0	
203	0.08	65.65	4.184338	3.979661	
203	0.25	67.25	4.208417	11.29595	
203	0.5	66.28	4.193888	16.69096	
203	1	68.35	4.224642	33.65485	
203	2	67	4.204693	67.67276	
203	3	63.7	4.154185	65.33611	
203	4	61.62	4.120986	62.65425	
203	8	53.13	3.972742	229.0806	
203	12	46.91	3.848231	199.8219	
203	24	33.12	3.500137	475.3894	1165.577
204	0.02	36.75	3.604138	0	

204	0.08	35.96	3.582407	2.181214	
204	0.25	35.05	3.556776	6.03552	
204	0.5	35.17	3.560193	8.777491	
204	1	35.56	3.571221	17.68232	
204	2	36.23	3.589888	35.89396	
204	3	32.08	3.468233	34.11294	
204	4	31.26	3.442339	31.66823	
204	8	28.29	3.342508	119.0012	
204	12	26.42	3.274121	109.3774	
204	24	23.01	3.135929	296.1089	660.8391

Define

Circuit	Circuit/Control ID
Time	Time (h)
Conc	Concentration (mg/L)
lnConc	Natural log of concentration
AUC log	Logarithmic calculation of AUC for each time interval = (t2-t1) * (C2-C1) / ln (C2 / C1) Where t = time, C = concentration
AUC Control	for each Control at 24h =sum of AUC for each time interval

4.4 Relative decrease in $AUC_{0\text{-}24}$ for micafungin controls

Circuit	Time	Conc	lnConc	AUC Log	AUC Base	AUC Control	Relative Decrease in AUC
202	0.02	57.6	4.053523	0			
202	0.08	57.59	4.053349	3.4557			
202	0.25	57.58	4.053175	9.78945			
202	0.5	57.57	4.053002	14.39375			
202	1	57.56	4.052828	28.7825			
202	2	57.55	4.052654	57.555			
202	3	57.54	4.05248	57.545			
202	4	57.53	4.052307	57.535			
202	8	57.52	4.052133	230.1			
202	12	57.51	4.051959	230.06			
202	24	57.5	4.051785	690.06	1379.276	982.5944	0.287602
203	0.02	67.01	4.204842	0			
203	0.08	67	4.204693	4.0203			
203	0.25	66.99	4.204543	11.38915			
203	0.5	66.98	4.204394	16.74625			
203	1	66.97	4.204245	33.4875			
203	2	66.96	4.204095	66.965			
203	3	66.95	4.203946	66.955			
203	4	66.94	4.203797	66.945			
203	8	66.93	4.203647	267.74			
203	12	66.92	4.203498	267.7			
203	24	66.91	4.203348	802.98	1604.928	1165.577	0.273752
204	0.02	36.75	3.604138	0			

204	0.08	36.74	3.603866	2.2047			
204	0.25	36.73	3.603594	6.24495			
204	0.5	36.72	3.603322	9.18125			
204	1	36.71	3.603049	18.3575			
204	2	36.7	3.602777	36.705			
204	3	36.69	3.602504	36.695			
204	4	36.68	3.602232	36.685			
204	8	36.67	3.601959	146.7			
204	12	36.66	3.601686	146.66			
204	24	36.65	3.601413	439.86	879.2934	660.8391	0.248443
						MEAN AUC DECREASE	0.269932
						MEDIAN AUC DEACREASE	0.248443

Define

Circuit	Circuit/Control ID
Time	Time (h)
Conc	Concentration (mg/L)
lnConc	Natural log of concentration
AUC log	Logarithmic calculation of AUC for each time interval = (t2-t1) * (C2-C1) / ln (C2 / C1) Where t = time, C = concentration
AUC Base	Total AUC assuming no extraction at 24h =sum of AUC for each time interval

AUC Circuit	Total AUC for each Control at 24h =sum of AUC for each time interval (from Appendix 4.1)
Relative Decrease in AUC	Decrease in AUC in control relative to AUC if no extraction =(AUC Base – AUC Control) / AUC Base)